24708

National Research Council Canada
Conseil national de recherches Canada

ASSOCIATE COMMITTEE ON GEOTECHNICAL RESEARCH

WORKSHOP ON ICE SCOURING
15 – 19 FEBRUARY 1982

SPONSORED BY
SNOW AND ICE SUBCOMMITTEE
ASSOCIATE COMMITTEE ON GEOTECHNICAL RESEARCH

EDITOR: R. PILKINGTON

TECHNICAL MEMORANDUM NO. 136

PRICE: $14.00

APRIL 1985

Canada

86-02675/

The Associate Committee on Geotechnical Research is one of about thirty special committees which assist the National Research Council in its work. Formed in 1945 to deal with an urgent wartime problem involving soil and snow, the Committee is now performing its intended task of coordinating Canadian research studies concerned with the physical and mechanical properties of Snow and Ice, Peatlands, Permafrost, Urban Engineering Terrain Problems, Soil and Rock Engineering, and Marine Geotechnical Engineering. The Committee consists of about twenty Canadians appointed as individuals and not as representatives, each for a three-year term. Enquiries will be welcomed and should be addressed to: The Secretary, Associate Committee on Geotechnical Research, c/o Division of Building Research, National Research Council of Canada, Ottawa K1A 0R6.

This publication is one of a series being produced by the Associate Committee on Geotechnical Research of the National Research Council of Canada. It may therefore be reproduced without amendment, provided that the Division is told in advance and that full and due acknowledgment of this publication is always made. No abridgment of this report may be published without the written authority of the Secretary of the ACGR. Extracts may be published for purposes of review only.

****

Le Comité associé de recherches géotechniques est l'un des quelque trente comités spécieux qui assistent le Conseil national de recherches dans ses fonctions. Créé en 1945 pour s'occuper de problèmes ayant trait aux sols et à la neige et urgents par suite de la guerre, le Comité remplit maintenant le rôle qui lui était destiné, celui de coordonner au Canada les recherches portant sur les propriétes physiques et mécaniques du sol canadien. Il s'acquitte de ses fonctions par l'intermédiaire des sous-comités de la neige et de la glace, dus marécages, du pergélisol, des problèmes l'ingénierie urbaine relatifs au terrain et de génie du sol et des roches, et de génie géotechnique marin. Le Comité se compose d'environ vingt canadiens nommés à titre individuel, et répondrons avec plaisir à vos demandes de renseignement. Veuillez les adresser à:

Le Secrétaire,
Comité associé de recherches géotechniques,
a/s Division des recherches sur le batiment,
Conseil national de recherches,
Ottawa K1A 0R6

La présente publication fait partie d'une série réalisée par le Comité associé de recherches géotechniques du Conseil national de recherches. Elle peut donc être reproduite telle quelle à condition que la division en soit prévenue au préalable et que l'on mentionne toujours la présente publication. Il est interdit de publier tout résume du présent publication. Il est interdit de publier tout résume du présent rapport sans le consentement écrit du secrétaire du CARG, seule sont authorisée les extraits cités dans un comptes rendus.

NATIONAL RESEARCH COUNCIL OF CANADA
ASSOCIATE COMMITTEE ON GEOTECHNICAL RESEARCH

WORKSHOP ON ICE SCOURING
15-19 FEBRUARY 1982

SPONSORED BY
SNOW AND ICE SUBCOMMITTEE
ASSOCIATE COMMITTEE ON GEOTECHNICAL RESEARCH

EDITOR: R. PILKINGTON

TECHNICAL MEMORANDUM NO.136

APRIL 1985

ADDENDUM TO T.M. 136

ABSTRACT

ICEBERG "HARROWING" AS OPPOSED TO ICEBERG "PLOUGHING"

Alan Ruffman

This model of iceberg scouring was first presented verbally at the 1st Canadian Conference on Marine Geotechnical Engineering in Calgary April 25-27, 1979. The model is still not widely used, thus it is presented here in a written form in the hope it will become more widely considered. The "harrowing" iceberg is believed to be a rather common mode of iceberg scouring, especially towards the south as bergs become unstable.

Almost from the very beginning of the mapping of ice ridge keel and inceberg scours, the assumption has been made that the ice keel "ploughs" its furrow into the ocean floor. This paper uses published or available Canadian Government data, plus data from wellsi surveys for Eastcan, to demonstrate that a different process also operates with respect to icebergs for which the term "harrowing" can be coined.

Data available since 1975 clearly show icebergs can scour uphill and downhill over topographic highs and through topographic lows. Fully 10 m of elevational change can be demonstrated on sidesca surveys of very small areas and larger surveys of less than 100 per cent coverage indicate more "overscouring" beyond 10 m has been experienced off Labrador.

The simple conversion of a berg's kinetic to potential energy does not adequately explain a berg's ability to scour uphill or to scour into topographic lows. The author invokes a tilting mechanism whereby the berg leans in direction of travel and its keel is lifted to drag over the bottom in a "harrowing" process.

The paper also discusses a number of factors that affect the ability of a berg to harrow, such as season, latitude and age. As well, the author reviews a number of implications of the harrowing process on bottom-mounted installations.

OPENING REMARKS

NRC ICE SCOUR WORKSHOP

MONTEBELLO, QUEBEC

February 15 - 19, 1982

L.W. Gold
Chairman, Associate Committee on Geotechnical Research

On behalf of the Associate Committee on Geotechnical Research and its Subcommittee on Snow and Ice, I wish to welcome you to this Seminar/Workshop on Ice Scour. This subject is a most important one for development of offshore resources, both off the east coast of Canada as well as in the Arctic. One of the challenges for Canadians is to add to the normal scope of ocean engineering that knowledge, technology, techniques and know-how necessary to work effectively and safely in ice-affected waters. A major challenge in this regard is to determine the characteristics of large ice masses such as icebergs, ridges and ice islands, and their effects, particularly on the ocean floor, so that these can be taken into proper consideration in the design, construction and operation of offshore structures and in resource exploration and exploitation activity.

The Associate Committee on Geotechnical Research is one of several committees of the National Research Council of Canada. It was formed in 1945 "to coordinate and stimulate research on the engineering and physical aspects of the terrain of Canada". The Committee was an outgrowth of one that was concerned with the performance of tracked military vehicles during the Second World War. It does most of its work through several Subcommittees that look at various areas of the geotechnical field. At present it has Subcommittees looking at research needs in soil and rock engineering, peatlands, permafrost, urban terrain engineering, marine geotechnical engineering

in addition to snow and ice. These Subcommittees have been very active in sponsoring seminars and workshops and in the preparation of special publications. These are normally published in the Technical Memorandum Series of the ACGR. There are now over 130 publications in this series.

The Snow and Ice Subcommittee was established in 1955. Right from the beginning it concentrated on specific problems associated with these materials and summarized knowledge on them through conferences and seminars. The first two dealt with the bearing strength of ice and the use of air bubbling systems to prevent ice formation. These were followed by symposia on heat exchange at snow and ice surfaces, snow removal and ice control, ice pressures on structures, ice engineering, avalanche hazard forecasting and avalanche control, action of ice on structures, ice jams, thermal regime of river ice, mechanical properties of ice, winter roads, sea ice (with C-CORE at Memorial University) and sea ice ridging and pile up. The Subcommittee has also produced a Manual on Snow Removal and Ice Control in Urban Areas. Its interests are broad and it has dealt with topics of consider national importance.

The newest Subcommittee of the ACGR is looking into problems in marine geotechnical engineering. This group, along with the Canadian Geotechnical Society, was responsible for sponsoring the First Canadian Marine Geotechnical Conference, held in Calgary in 1979. It has now organized the Second Canadian Conference on Marine Geotechnical Engineering, again with the assistance of the Canadian Geotechnical Society. This Conference will be held in the Bedford

Institute of Oceanography in Dartmouth, Nova Scotia, in June 1982. Subjects to be covered include geotechnical investigations, environmental aspects (including ice scour), performance monitoring, sea bed problems, and geotechnical design and construction offshore. The information presented to this Seminar would be of great interest for the Conference. It would be very appropriate if a report on the discussions and conclusions arising from this Seminar/Workshop could be presented to the meeting in Dartmouth.

One of the very encouraging aspects of the activity of the ACGR and its Subcommittees is the extend to which this work is supported by individuals, universities, industry and many others. In the present case, organizing the program, arranging for facilities and registration have been carried out primarily by Roger Pilkington and Beth Weber of Dome Petroleum. I want to say how much we appreciate their efforts. It is a lot of work and on behalf of the ACGR I want to thank them and Dome Petroleum for it.

Through the ages, icebergs have been a source of awe and of fear. They have been simply something to be avoided if possible and to watch from a distance. Recently they have been recognized as potential sources of fresh water. Now we want to place fixed structures in their possible paths. How do we protect these structures from icebergs? How deep must facilities be placed below the ocean floor in order not to be affected by ice scour? What design information can be gleaned from the evidence of past ice scour? These are some of the topics that you will be considering over the next five days. I wish to thank the Subcommittee on Snow and Ice for taking the initiative to organize this Symposium on a subject which is of such importance for present and future offshore activity and facilities in ice-affected waters.

Chairman's Introductory Remarks

The Workshop was divided into two parts. The first two days, Monday and Tuesday, were for submitted papers covering recent work being done in Canada and the United States; the second two days were for specific topics and discussion.

Some of the papers presented at the Workshop have been published elsewhere. Abstracts have been included here for completeness. It should also be pointed out that papers have been reproduced as received from the authors.

I wish to thank all those who took part in this Workshop for their interest and discussions, which, along with the beautiful setting (Chateau Montebello), made a most enjoyable and stimulating week.

Roger Pilkington.

TABLE OF CONTENTS

	Page
Opening Remarks - L.W. Gold	(i)
Chairman's Introductory Remarks - R. Pilkington	(iv)
Table of Contents	(v)
Lake Erie Cable Crossing - Ice Scour Study - J.D. Grass	1
Subaerial Expressions of Relict Ice Scour Signatures in Different Environments on Mainland Canada - J.D. Mollard	11
Predictions of Extreme Keel Depths from Submarine Sonar Data - P. Wadhams	32
Ice Scour Protection Drake F-75 Flowline Bundle - M. Van Ieperen	48
Lake Erie Ice Scour Investigation - G. Comfort, R. Abdelnour, B. Trak, B. Menon and B. Graham	55
Preliminary Results of Submersible Observations on the Labrador Shelf - H.W. Josenhans and J.V. Barrie	100
Submersible Observations of Iceberg Furrows in Glacial Till, Northeast Newfoundland Shelf: and in Sand and Gravel, Grand Banks of Newfoundland - C.F.M. Lewis and G.B. Fader	101
A New Type of Lineation Seen on the Ocean Floor in Landcaster Sound, N.W.T. - Possible Glacial Fluting - A. Ruffman and L. Lee	102
Physical Dimensions of Icebergs in the Labrador Sea - J.D. Miller and I.S. Hotzel	103
Relationships Between Measured Iceberg Dimensions - I.S. Hotzel and J.D. Miller	114
Correlation Between Iceberg Draft and Above Water Dimensions - M. El-Tahan and H.L. Davis	130
Iceberg Dimensions - L.D. Brooks	148
Review of Deep Water Scours in the Davis Strait and its Relevance to Present-Day Activity - J.Y. Guigne, D.I. Ross and H. Westergard	155

Page

Use of Draft Distribution for Evaluating Iceberg Incursion Probability - J. Lewis and P. Benedict 168

Correlation Between an Ice Ridge and Sea Bed Geologic Boundary - P.W. Barnes, C.R. Ross and E. Reimnitz 169

Ice Gouge Characteristics Related to Sea-Ice Zonation, Beaufort Sea, Alaska - P.W. Barnes, E. Reimnitz and D.M. Rearic 185

The Frequency of Ice Scouring on the Northeastern Grand Banks of Newfoundland Using the Interrelationship of Scours and Bedform Migration - C.L. Amos and J.V. Barrie.. 220

Sea Bottom Scouring in the Canadian Beaufort Sea - J. Hnatiuk and B.D. Wright 222

Shore-Zone Ice Scour Statistics: Implications to Coastal Development - J.R. Harper 223

Risk Assessment and Pipeline Trench Depths (Discussion Summary)..... 231

Panel Discussion 245

Ice Scour Workshop - Program (Appendix "A")

List of Participants (Appendix "B")

Lake Erie Cable Crossing - Ice Scour Study

J.D. Grass, Ontario Hydro

Abstract

Ontario Hydro and General Public Utilities of New Jersey are proposing the construction of 5 high voltage transmission cables across the eastern part of Lake Erie. The cable will run from the Nanticoke generating station in Ontario to the Coho Site in Pennsylvania, USA.

Geotechnical investigations along the cable corridor predominantly by barge drilling and gravity sampling techniques have been carried out to determine soil and bedrock characteristics and distributions.

Marine geophysical surveys using side-scan sonar, bottom and subbottom profiling echo sounders have been used to study the lake bottom and subbottom conditions. The geophysical surveys revealed the existence of ice scour on the Canadian and American sides of the corridor in about 13 to 25 m of water. The scours are generally less than 1 m deep up to a maximum of 1.7 m, up to 6 km long and up to 100 m wide.

To protect the cables from ice damage, they are to be buried in trenches up to 3 m deep on the Canadian side and up to 2 m deep on the American side.

Ontario Hydro - General Public Utilities Interconnection Lake Erie Cable Crossing Ice Scour Study

J.D. Grass
Ontario Hydro

Presentation given at
NRC Ice Scour Workshop Montebello, Quebec,
February 15-19, 1982

1.0 INTRODUCTION

Ontario Hydro and General Public Utilities of New Jersey are planning the construction of a high voltage transmission cable system across the eastern basin of Lake Erie. The cables will connect the Nanticoke Generating Station with the presently undeveloped Coho Site located about 20 km west of Erie, Pennsylvania. The area is 105 km long and 4.5 km wide. The corridor comprises a Nanticoke and Coho approach areas and an openwater section (Fig. 1).

The study area was investigated by the Geotechnical Engineering Department of Ontario Hydro to determine the distribution and characteristics of soil and bedrock relative to the design and construction of the cables.

The investigation of the lake bottom was carried out during 1980 and 1981, and involved drilling numberous boreholes from spud leg and floating barges as well as benthos and vibracore sampling. Thermal resistivity (T/R) measurement and soil and rock testing were carried out by the Research Deparment in the laboratory. In-situ T/R measurements were also made.

A major part of the investigations involved the use of marine geophysical equipment specifically the 100 and 500 KHz Klein side scan sonar, the Ocean Research Equipment subbottom profiler and the Krupp-Atlas Deso echo sounder.

During the 1980 survey, complete coverage of the study area was achieved using marine geophysics. Based on these and the other geotechnical data, five cable routes were selected within a 1 km wide corridor. In 1981, the selected cable routes were surveyed in the approach areas. A total of approximately 3500 km of surey lines were run during the 1980-81 investigations.

During the geophysical survey, long, wide, linear gouges were discovered in the soft silty clay sediments in both the Nanticoke and Coho approach areas.

It was apparent that these marks in the sediments were caused by ice scouring the lake bottom and that the security of the cables could possibly be affected by the scouring action of the ice.

2.0 CANADIAN SIDE

On the Canadian side ice scours were found within the corridor and also 6 km west of the corridor south of Nanticoke Shoal (Fig. 2).

The scours are 4.5 to 6 km long and from 10 m to 100 m wide.

They range in depth up to 1.7 m with an average of less than 1 m. The scours are found in water depths ranging from 12 to 25 m. The scour within the cable corridor are less than 0.6 m deep (Fig. 3).

The location and trend of the ice scours appears to be influenced by the Nanticoke Shoal. The scours to the south of the shoal run northwesterly while the scours through the corridor run northeasterly. No scours were found immediately east of the Shoal.

The rock shoal within the corridor may have caused the change in direction of the scours in this area.

It is our opinion that the Nanticoke Shoal provides a place for ice to ground and anchor itself forming a fast ice condition in front of the shoal. Mobile ice moving into the area would be diverted by the fast ice mass resulting in ice moving along the edge of the fast ice producing this scour pattern. A similar condition may occur along the corridor rock shoal.

The age of the scours was also investigated. Fortunately, there is an extensive network of gas pipelines in the area of the corridor which acts as a time benchmark based on their installation dates. Ice damage has occurred to the pipelines since their installation date in 1965. Damage has occurred in the ara of intense scour in the area northeast of the corridor from 1967 to 1971. A diver's report of damage to gaslines in 1970-71 confirms that an ice scour was observed cutting across the damaged pipe. The ice scour must have occurred in the 1970-71 winter period at this location to cause this damage. In the scour area, south of Nanticoke shoal, no gas pipeline damage has occurred since their installation in 1965. These scours must, therefore, have been formed before that date.

The scour record in the lake sediments is believed to be accumulated over maybe 100 to 200 years and with the low energy, sedimentation environment in this area, most of the scours appear fresh and only a few have been partially infilled.

3.0 AMERICAN SIDE

On the American side, ice scour was discovered within the cable corridor and offshore Presque Isle (Fig. 4).

The ice scours are about 4.5 km long and 10 m to 60 m wide. They are less than 0.5 m deep where subbottom profiles of the scours were obtained. The scours were found in 13 to 23 m of water.

The scours were found in soft silty clay sediments. There is a considerable amount of mobile sand in the area which is redistributed during storms. Sand filled scours were found in the corridor during the 1980 survey. In 1981, fresh scours were discovered in the same general area as the sand filled scours. These new scours must have formed during the winter period of 1981.

It is very likely that these new scours will be obliterated by the redistribution of the lake bottom sediments during storms. The side scan sonar record (Fig. 5) shows clearly the side piles and furrows of the ice scour. The soil pile at the end of the scour indicates an easterly ice movement. This direction of ice movement was also indicated in other scours. The ice movement is consistant with the prevailing wind direction in the area.

The scour offshore Presque Isle was discovered by accident during the calibration of the geophysical intruments. These scours appear fresh and were found cutting across dredged spoil piles in an offshore dumping area. The exact date of these scours is not known but their appearance suggests that they are recent.

The scours run in an east-west direction parallel to the shoreline. The location and trend of the scours appear to be related to the limit of the fast ice sheet offshore. This fast ice will be shown on a later slide.

4.0 CABLE PROTECTION

Burial Depth Determination

With such a force to cause major disruption of the lake bottom it became apparent that to protect the cables from ice they would have to be buried. The question was how deep?

To answer this important question, Arctec Canada Ltd. was engaged to determine analytically the maximum depth of scour using Ontario Hydro data. After utilizing various theories, mathematical models, ice-soil interaction scenarios, no analytical method seemed to give even the known scour information let alone a realistic maximum scour depth that could be expected in the area.

Several parameters including angle of ice part, ice stregth, soil ice friction coefficients, etc. were not available and were critical to the calculations.

Ontario Hydro computer analysis carried out numberous calculations from published mathematical models using various ranges and combinations of import parameters, however, no realistic answers were obtained.

We decided to use the known ice scour depths on the Canadian side for a probabilistic analysis since over 170 depth measurements were available. The paucity of data on the American side precluded the probabilistic approach.

The ice scour depths were fitted to a beta distribution and log-normal distribution.[1] The mean value is 0.76 m and standard deviation is 0.33. The plot shows the cumulative probability distirubtion of exceeding a given scour depth (Fig. 6).

Present technology can bury the cables a depth of 3 m. Based on our limited number of data, it appears that the probability of exceeding a scour depth of 3 m is about 0.02% or very remote. The maximum depth of scour in our cable corridor is 0.6 m so the 3 m depth is considered a conservative safe depth of burial.

It has been recommended that the cables be buried to a maximum depth of 3 m on the Canadian side and 2 m on the American side of the corridor. The depth of burial varies from 1 m to 1.5 m in rock and soil, 2 m to 3 m in soft soils in susceptible areas.

5.0 ICE MONITORING PROGRAM

The investigations to date of the lake bottom have been very successful in providing us with valuable geotechnical data for the design and construction of the cables. However, the data that is missing is the ice conditions on the lake during the winter and breakup periods. So an ice monitoring program was prepared to better understand the ice build up on the lake particularly in the cable corridor area and vicinity.

The LANDSAT image taken in March 1979 shows the large ice floes during the breakup period. Particular attention should be paid to the limit of the fast ice on the American side. The ice floes are from 5 km to 15 km in diameter and ridges can be seen on the original image.

An ice monitoring program by helicopter was carried out last winter and is presently being done this winter. Ice thicknesses range from 100 mm to 600 mm and ice ridges heights are less than 1 m up to about 4 m. Iceridging of 10-12 m also were found. These ridges are grounded. Considerable amount of silty clay soil was observed in the ice and sampled within several ridged areas.

1 Harr, M.E., 1977. Mechanics of Particulate Media, A probabilistic Approach.

6.0 FUTURE INVESTIGATIONS

Our investigation of the ice scour are going to continue this May with detailed marine geophysical scanning of two large areas on the Canadian and American sides of the corridor. We hope that this additional work will provide more data on the frequency, location and depth of scour.

Note: Following the Montebello Workshop an ice monitoring flight was made February 26, 1982. A 10-12 m high rumble field grounded in less than 20 m of water was observed in the midlake area about 40 km west of our corridor and 20 km offshore Long Point. The ridge was building as we observed the ice. A super 8 movie of this ridging process was made at that time. Subsequent visits to this huge rubble field has revealed further ridge building under different wind conditions. A movie of all our film footage is presently being put together. Anyone interested in seeing this movie is welcomed to contact the author at 1-416-592-5399.

FIG. 1
Layout Plan

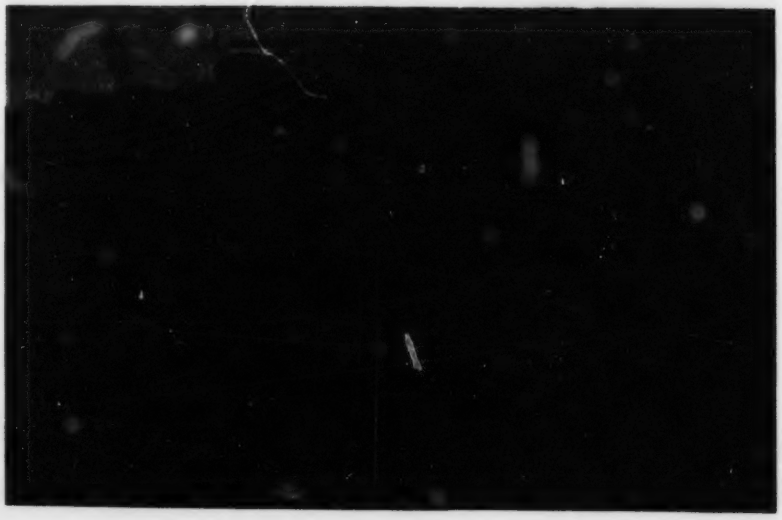

FIG. 2
Ice Scours on Canadian Side of Corridor

FIG. 3
Subbottom Profile Record of Ice Scoured Area on Canadian Side

FIG. 4
Ice Scour on American Side of Corridor

FIG. 5

Side-Scan Sonar Record (100 kHz klein)
of Ice Scour on American Side of Corridor

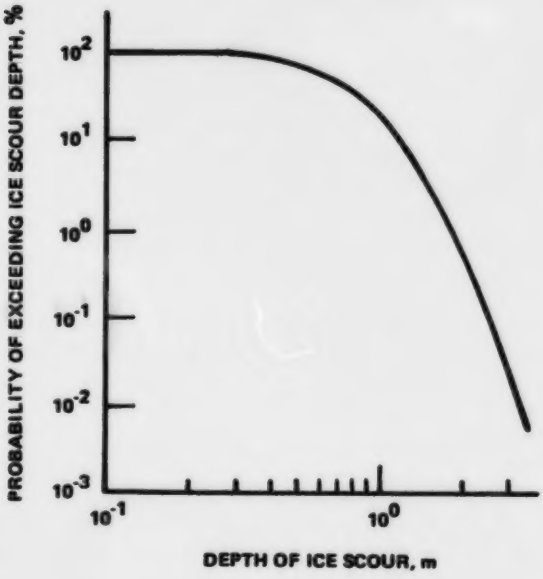

FIG. 6
Cumulative Probability Distribution Based on Log Normal
Distribution of 170 Ice Scour Depths (canadian side only)

DISCUSSION

W. Spring

You mentioned that 170 individual scour depth measurements were used in the probability calculations. How many separate scours were observed to obtain these depths? Did you make any attempt to ensure that the deepest depth in an individual scour was obtained for use in the extreme calculations?

J.D. Grass

The actual number of individual ice scours along which these depth measurements were taken is about 5 to 8.

The maximum depth of scour found on the Canadian side is 1.7 m. Whether this is the deepest scour anywhere in the area is not known. However, if the distribution of the scour depth measurements follows a log normal type distribution, then the extreme scour depths should also fall into this distribution. The probability calculations are geared toward the extreme values projecting into the tail section of the distribution beyond our firm data. The probability of deeper scours is far less than the probability of shallower scours in our study area. Further work is planned this Spring to expand our data and hopefully obtain more of the deeper scour depths.

P. Wadhams

You mentioned ridges of height varying from 1 m to 10 m. Presumably the 10 m ridge must have been grounded.

J.D. Grass

The 10 m high ice ridges are grounded in water depth of approximately 15 m on the American side of the corridor. Other ridges in the vicinity of the corridor on the Canadian side are up to 10 m high and are grounded in about 9 in. of water on Nanticoke Shoal.

NRC WORKSHOP ON ICE SCORING
MONTEBELLO, QUEBEC
FEBRUARY 15 - 19, 1982

SUBAERIAL EXPRESSIONS OF RELICT ICE SCOUR SIGNATURES IN DIFFERENT ENVIRONMENTS ON MAINLAND CANADA

J. D. Mollard, PhD., P. Eng.
President, J D Mollard and Associates Limited
Regina, Saskatchewan, Canada S4P 2G9

Abstract

Relict ice scours formed by the keels of icebergs and the keels of pressure ridges in floe ice can be seen in certain areas of mainland Canada. These ice scour markings are visible locally on areas of former marine submergence, the beds of extinct glacial lakes, and beneath shoal water on the bottom of large modern lakes, which are commonly present-day remnants of much larger glacial lakes. Subaerial expressions of relict ice scour activity can be seen in good quality black and white panchromatic aerial photographs. Topographic and stratigraphic relationships can be examined on the ground. Similar studies on the ocean bottom are difficult and costly.

Although many of the characteristics of relict ice scour furrows are easily appreciated, the origin of apparently related straight, curvilinear, and parabolic microridges are difficult to explain. Where they have been observed in the field, the microridges overlie ice scour trenches that have been filled with buff-colored, calcareous, silt-rich sediments. Typically, the back-sedimented trenches are flanked by dark grey, highly plastic lacustrine clay. Stratigraphy of the silty microridges appears to be very complicated in detail.

Variations in the geographic distribution, geologic occurrence, geometric characteristics and preservation of the ice scours, as well as occurrence of associated microridge features, can be correlated with environmental conditions at the time of their origin, including differences in bottom topography, stratigraphy, and the shearing resistance of sediments in which the ice scour signatures were formed.

Even though ice scour markings are found in several localities and in a variety of environments in mainland Canada, relatively little detailed research has been done on them. One of the reasons for this is that they are often very difficult to identify on the ground. In addition, deep and fresh-appearing natural incisions, man-made ditches, and borrow pits cutting across them are rare.

The diverse surface expressions of ice scours and their relation to the environments in which they occur raise a number of questions. Answers to them may be useful to the oil and gas industry and to governments carrying out ice scour studies in ocean waters located off the coasts of Alaska, eastern Canada, the Beaufort Sea, and in the channels between the Arctic Islands of Canada.

Objectives in presenting this paper

My main objective in preparing this paper was to bring to the attention of investigators of ice scour signatures and processes those localities in mainland Canada where detailed field studies can be made in order to better understand the relation of ice scour occurrence, intensity and maximum depth of scours, and ice scour formation processes to the differing shearing resistance of bottom materials, to differences in bottom topography, and changes in water depth, among other factors.

A number of questions arise. Why are ice scour markings found on the floors or only portions of the floors of extinct glacial lake basins and areas of former marine submergence, and not on others? Why are the ice scour features much better preserved in some localities than in others? Were the ice scours formed by longitudinal ploughing, by a lateral squeezing action, or both? Can one date the age of relict scours from organic material in the partly sedimented trenches? Were the main driving forces largely strong winds or currents? Were seemingly related microridges created as lateral embankments on each side of a furrow? Or does their present-day relief result almost entirely from differential shrinkage and settlement associated with lowering of the water table and the desiccation of silty materials in the backfilled trenches and of highly plastic clay material on their flanks?

Regional distribution and observations of ice scour features on mainland Canada

Localities in mainland Canada where I have observed ice scour features are shown on a small scale location map (Figure 1).

I first noticed the relict ice scour features along the western shore of Great Slave Lake (see, also, Weber, 1958; Noble and Comfort, 1980), on parts of the floor of glacial Lake Agassiz (see, also, Clayton et al, 1965; Horberg, 1951; Nikiforoff, 1952; Wardlow et al, 1964) and on the floor of glacial Lake Whittlesey while carrying out research studies on surficial lineaments and fracture patterns for oil and gas companies in the late 1950s (Mollard, 1957).

Ice scours on the floor of Tyrrell Sea in northeastern Ontario were first observed by the writer in the mid-1960s during the study of hydro sites along northern Ontario rivers flowing into Hudson Bay and James Bay.

The classical ice scour markings found between the Hayes River and Gods River in northeastern Manitoba, north of Spence Bay, Northwest Territories, and west of Lake Mattagami in western Quebec (see, also, Dionne, 1977) were detected while making pipeline route corridor studies east and west of Hudson Bay in the early 1970s.

While aerial reconnaissance examinations of the ice scours were made and boreholes were drilled in vicinity of some of the ice scours, no detailed or systematic study of the ice scours themselves was ever made. Stereograms of several of the ice scour patterns mentioned above appear in a 681 stereogram manual on the aerial photographic interpretation of landforms and surface materials of Canada (Mollard, 1982).

Ice scours on the bottom of Great Slave Lake (Plate 1)

The aerial photograph seen in Plate 1A was taken in 1947. It shows a number of criss-crossing ice scour markings that traverse small islands and channel bottoms as well as land above the present level of Great Slave Lake (see arrows Plate 1A). The effects of river ice erosion and of fluvial erosion, over perhaps hundreds or even thousands of years, have not obliterated the ice scour features. This scene suggests that there is little transport of coarse bedload at the outlet of Great Slave Lake, apparently, and also that very little channel bottom erosion is taking place. Because some of the scours are well preserved and still probably very old, one may expect that a buried pipeline crossing at this location would be safe against the possibility of deep ice scour.

The photograph in Plate 1B shows Moose Point on the north shore of Great Slave Lake, about 40 km ENE of the area shown in Plate 1A. The photograph in Plate 1B was taken in 1948. A number of questions arise when studying this photograph. Were ice scours on the lake bottom caused by the keels of pressure ridges on modern pack ice? Were the relict scours formed on Great Slave Lake when it was much larger than it is today? Or were they formed by icebergs that drifted across glacial Lake McConnell 10,000 or more years ago? Compare ice scour markings on the present lake bottom with their vague extensions above the lake shore. Note also that a pit has been gouged and a semicircular ridge of lake bottom sediment has been dozed up where at one time a piece of ice grounded at 1.

Recent ice grooving in lake bottom sediments on Great Slave Lake has been reported by Weber (1958). Also, pipeline damage caused by ice action on the bed of Great Slave Lake, north of the town of Hay River, has been reported by Noble and Comfort (1980).

Different appearances of ice scour markings in till and in lacustrine muds on the floor of glacial Lake Agassiz (Plate 2)

Quite marked differences in the surface expressions of ice scour features can be seen in places where the topography is almost level but the lake bottom materials consist of relatively hard silty till, east of Lake Manitoba (Plate 2A), and relatively soft lacustrine muds, north of Emerson, Manitoba (Plate 2B). Although there are similarities in the trends of ice scours there are obvious differences in the subaerial patterns, particularly in the width of the scour markings. Are the differences in scour width caused by changes in shearing resistance of the bottom materials, or by large changes in the water depth (i.e. deeper water, larger ice blocks, greater momentum, and thus deeper and wider trenches).

Notice that the ice scour effects as seen in Plate 2B tend in places to produce a reticulate microrelief pattern. That pattern is emphasized by slight differences in the moisture content of the ridges and the swales following overbank flooding of the Red River (lower left, Plate 2B) and subsequent retreat of the floodwaters, and differential drying of the surface soil materials in the spring of 1945. A soft consistency of muddy bottom materials and the effects of longterm river flooding and deposition of suspended sediments have tended to degrade the appearance of the ice scour features in Plate 2B.

Note that the ice scours formed in relatively hard till in the area east of southeastern Lake Manitoba show relatively long and narrow furrows and sharp borders. Ice scours at location 1 may be caused by fragments of drifting pack ice during high stages of modern Lake Manitoba. Ice scours at 2, 3 and 4 are more likely to have been eroded into the floor of a much larger Lake Manitoba, or into the floor of extinct glacial Lake Agassiz. Trends of the scours suggest winds dominantly from the northwest, and probably lake current directions from that direction as well. Note also the curvilinear trace at 5.

Cross-cutting relationships can be used to determine relative age of some of the scours. The relative contributions of longitudinal ploughing and lateral squeezing of material out of the furrows might be determined from close-up examination of deeper and fresher ditch cuts crossing the scour markings. The photograph in Plate 2A was taken in 1958, the photograph in Plate 2B in 1945.

Figure 2 shows the effects of damage to beach and lakeshore property during lake ice breakup on April 12, 1981 (snapshot by Ken Gigliotti, Winnipeg Free Press).

Comparison of ice scours on the floor of glacial Lake Whittlesey, Windsor, Ontario, and glacial Lake Ojibway, Mattagami, Quebec (Plate 3)

Differences in vegetation and land use are emphasized in Plate 3A and Plate 3B, showing small portions of the floors of glacial Lake Whittlesey southeast of Windsor, Ontario (Plate 3A) and glacial Lake Ojibway in southwestern Quebec, west of Lake Mattagami, Quebec (Plate 3B). The aerial photograph in Plate 3A was taken in 1953, the one in Plate 3B in 1972. Note the large difference in the preferred direction of ice scours on glacial Lake Agassiz (Plate 2A) and on glacial Lake Whittlesey (see 1, 2, 3 and 4 on Plate 3A). Surficial deposits in both areas, and also on glacial Lake Ojibway, consist of highly disturbed glaciolacustrine clay containing much ice-rafted material. These sediments are often referred to as "waterlain till." Dionne (1977) states that ice scour furrows reached depths of more than 4 m on glacial Lake Ojibway (see arrows, Plate 3B).

Apparently the direction of prevailing paleowinds and paleocurrents in glacial Lake Whittlesey (Plate 3A) were more or less parallel to the present north and south shorelines of Lake Erie. Notice what appears to be two parallel tracks from the same ice block at 1 in Plate 3A, and changes in direction of furrows at 3 and 4 in Plate 3A.

Ice scours in contrasting bottom topography in areas of postglacial seafloor emergence (Plate 4)

The ice scour markings seen in Plate 4A and 4B are separated by over 1500 kilometres. The landscapes in Plate 4A and Plate 4B are situated below the limit of former marine submergence in early postglacial time. Boreholes drilled in both areas disclosed a patchy veneer of highly disturbed marine silt and clay overlying dense silt-rich till. In both areas the terrain is more undulating than that appearing in Plates 1, 2, and 3. The topography of the area in Plate 4A shows a drumlinoid appearance. Here forces created by winds and currents were sufficient to carry the blocks of ice up and down the sides of the drumlinoid ridges. Notice large differences in the density of ice

scour markings in the area north of Spence Bay, District of Franklin, N W T (see furrows at 1, 2 and 3 in Plate 4A), and in the area north of Red Cross Lake, Manitoba (Plate 4B). The aerial photograph showing the area north of Spence Bay was taken in 1958, that north of Red Cross Lake in 1954.

The ice scour lineaments appearing in Plates 4A and 4B are generally much narrower than those north of Emerson, Manitoba (Plate 2B), suggesting significant differences in the shearing resistance of materials on the former sea and lake bottoms.

Plate 4A shows an area where the offshore water depth reached about 150 m while the ocean water depth in Plate 4B was more likely about 30 m. Some of the scours seen in Plate 4B appear to describe the arcs of circles, e.g. 1-1, 2-2, 3-3, and perhaps at 4-4. Notice as well that present-day creeks in the area shown in Plate 4B follow the furrows created by ice blocks.

Parabolic, curving, and straight microridges southeast and north of Winnipeg, Manitoba (Plate 5)

The photograph in Plate 5A, taken in 1970, and that in Plate 5B, taken in 1979, show parabolic, curved and linear ridges southeast of Winnipeg (see 1, 2, 3 and 4 in Plate 5A) and north of Winnipeg (see 1, 2 and 3 in Plate 5B). Generally the ridges stand out less than 1 m above the surrounding land surface. Material in these long, narrow ridges consists of finely stratified, buff coloured to pale yellowish, highly calcareous silt, silty very fine sand, clayey silt, and silty clay that frequently encloses blocks, lenses,pods, stringers, ribbons and bands of highly plastic dark grey glaciolacustrine clay (see closeup view showing details of the near-surface stratigraphy of two of the microridges in Figures 3 and 4).

The ridges have lengths and widths that are much the same as the ice scour furrows (see also Clayton et al, 1965; Horberg, 1951; Nikiforoff 1952). Commonly the preferred orientations of the silty microridges roughly parallels the dominant direction of the ice scours. At the few places where I examined these ridges in the field I estimated the silty backfill to be 2 m to as much as 5 m thick.

Origin of the microridges is problematic and speculative. Although they were first considered to be fillings of silt in cracks in grounded lake ice, which settled on the lake bottom as a result of rapid draining of glacial Lake Agassiz (Charron, 1964), recent observations suggest that they are more likely to be silt-filled ice scour furrows. The silty ridges may project above the flanking dark grey clay owing to differential settlement resulting from lowering of the water table some 4 m or more, and the drying out and differential shrinkage of silt in the old scours and highly plastic montmorillonitic clay in the area adjoining the ridges. Shrinkage created by desiccation can account for about 1.5 m of ridge projection in the case of one-dimensional (vertical) shrinkage as the water content is reduced from the liquid limit to the shrinkage limit, and about 0.4 m in the case of three dimensional shrinkage.

Similar projections of the silty ridges are indicated by calculations of consolidation resulting from desiccation that causes suction loads. An increase in total pressure of 20 tonnes per m^2 (2 kg/cm^2) in the silt and adjoining clay, for example, will produce a 0.4 m projection of a silt ridge, and an increase of 200 tonnes per m^2 (200 kg/cm^2) will produce a silt ridge projection of about 0.9 m, each of these consolidation cases being possible.

Giant light toned circular ring structures in the black spruce swamp vegetation in areas of ice scour markings on the floor of extinct Tyrrell Sea, northeastern Ontario (Plate 6)

High altitude airphotos show circular and near circular rings, oval rings, and segments of rings in the black spruce swamp vegetation in northeastern Ontario. The anomalous-looking rings are particularly well expressed on the floor of Tyrrell Sea in vicinity of the confluence of the Kenogami, Little Current, and Albany Rivers, especially in places where relict ice scour features are a common occurrence (Plate 6). About 500 rings have been counted. The light toned rings in the vegetation are commonly 100 to 1000 m in diameter and 15 to 30 m in width. Origin of the rings is speculative. Hypotheses to explain them have centered on the effects created by buried diamond pipes and by craters from a large shower of meteorites. In size and outline they closely resemble drained thermokarst lakes and ponds on the Great Plain of the Koukjuak in southwestern Baffin Island. Others have considered them to be anthropogenic effects from Paleo Indian cultures. More likely they are extraordinarily large "fairy rings" produced by the radial growth and death of the mycelium of a fungus. The advancing mycelium exhausts the food supply, and by a packing effect creates an impermeable substrate that causes a slight rise in the water table. This causes black spruce trees in the ring to become stunted and sparse, increasing the albedo from the ground cover in the rings. Wetter conditions in the rings also favors growth of light green coloured tamarack trees there. In time the growth conditions inside the ring return to normal and black spruce trees are regenerated there.

The circular vegetation rings are shown partly for the sake of interest, and partly because they are commonly found in areas criss-crossed by many relict ice scour markings.

References Cited

Charron, J.E. 1964. Surficial deposits and groundwater resources, Emerson area, Manitoba, Geological Survey of Canada Report 64-7.

Clayton, L., Laird, W.M., Klassen, R.W., and Kupsch, W.O. 1965. Intersecting minor lineations on Lake Agassiz Plain. J. Geol., 73 (4), pp. 652-656.

Dionne, J.C. 1977. Relict iceberg furrows on the floor of glacial Lake Ojibway, Quebec and Ontario, Maritime Sediments, vol. 13, p. 1 fig.

Horberg, L. 1951. Intersecting minor ridges and periglacial features in the Lake Agassiz Basin, North Dakota, J. Geol., 59, pp. 1-18.

Mollard, J. D. 1957. Aerial mosaics reveal fracture patterns on surface materials in southern Saskatchewan and Manitoba. Oil in Canada, 9, No. 40, pp. 26-50.

Mollard, J.D. 1982. Landforms and surface materials of Canada: a stereoscopic airphoto atlas and glossary, Regina, J. D. Mollard and Associates Limited, 7th ed., 365 pp., 681 stereograms.

Nikiforoff, C. C. 1952. Origin of microrelief in the Lake Agassiz Basin. Amer. J. Sci., 60, pp. 99-103.

Noble, P., and Comfort, G. 1980. Pipeline damage by ice ridges. National Research Council Workshop on Ice Ridging (in press).

Wardlaw, N.C., Stauffer, M.R., and Hogue, M. 1964. Striations, giant grooves, and superposed drag folds, Interlake area, Manitoba. Can. Jour. Earth Sciences, vol. 6, no. 4, pp. 577-593.

Weber, J.N. 1958. Recent grooving in lake bottom sediments at Great Slave Lake, J. Sed. Petrol., vol. 28, no. 3, pp. 333-341, 10 fig.

MAP SHOWING LOCATIONS OF
RELICT AND MODERN ICE SCORING FEATURES IN MAINLAND CANADA
AND THAT ARE SHOWN IN AIRPHOTOS AND DISCUSSED IN PRESENTATION
TO NRC ICE SCORE WORKSHOP AT MONTEBELLO, QUEBEC
FEBRUARY 15-19, 1982

FIGURE 1

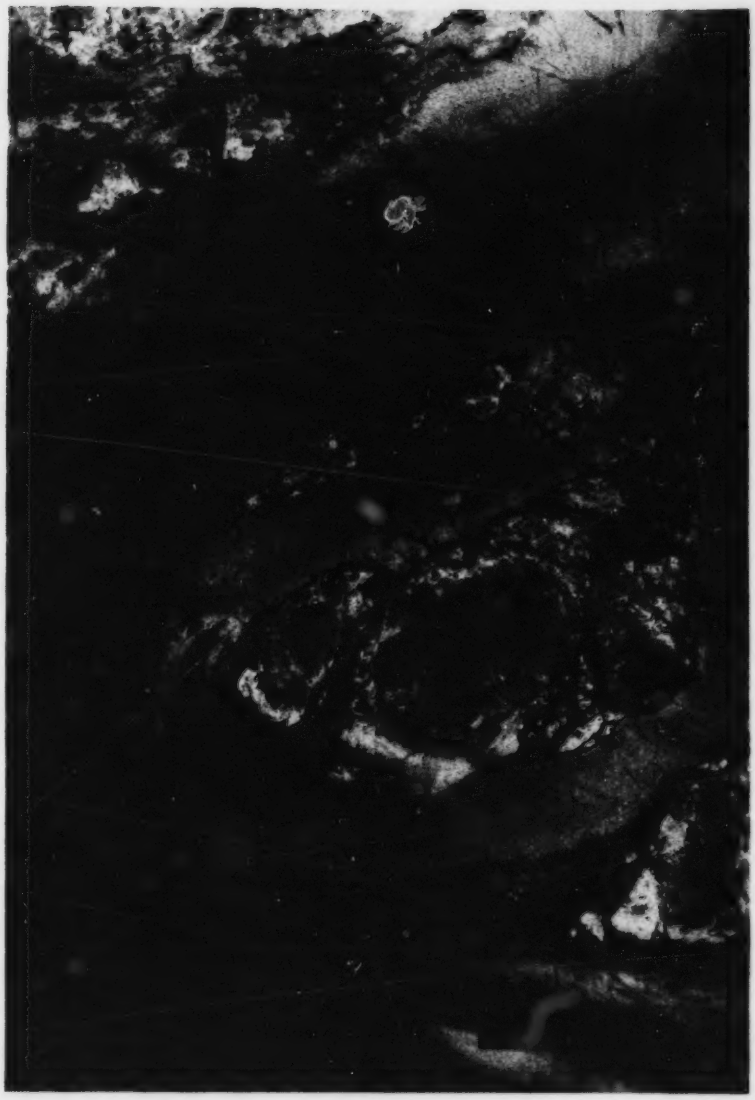

Ice Scours near Big Island at the outlet of Great Slave Lake, Northwest Territories.

PLATE 1A

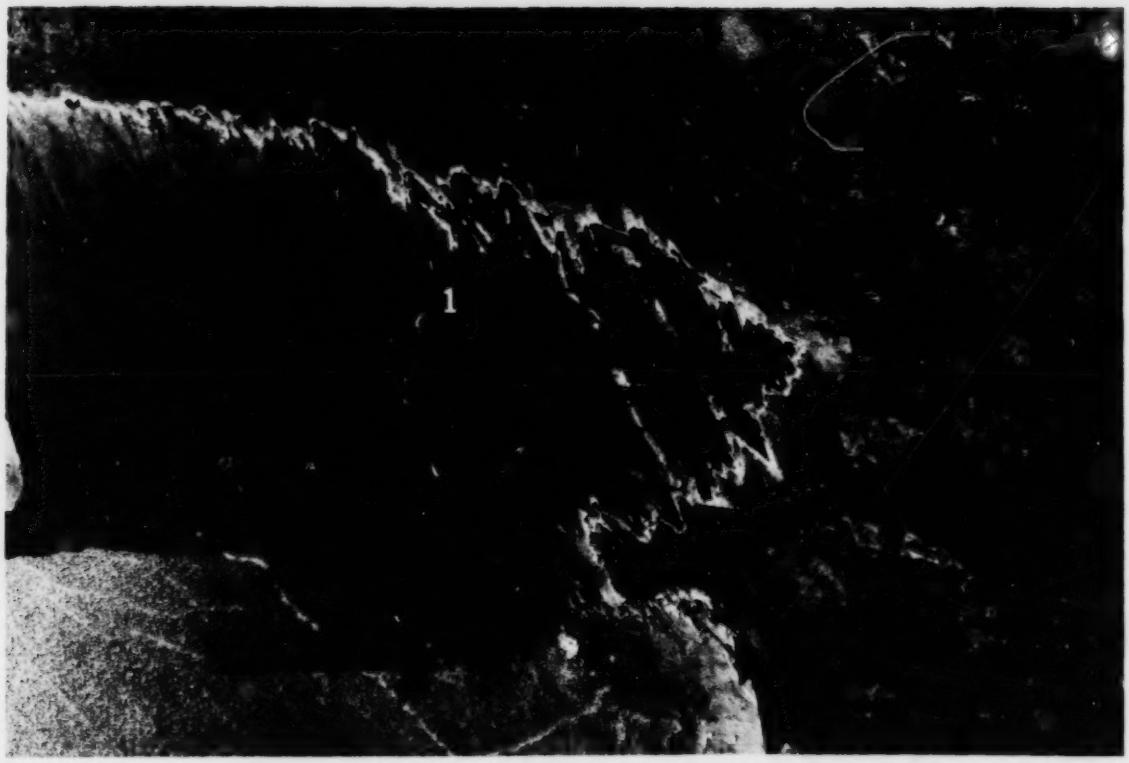

Ice scours, north of Moose Point on Deep Bay, Great Slave Lake, Northwest Territories.

PLATE 1B

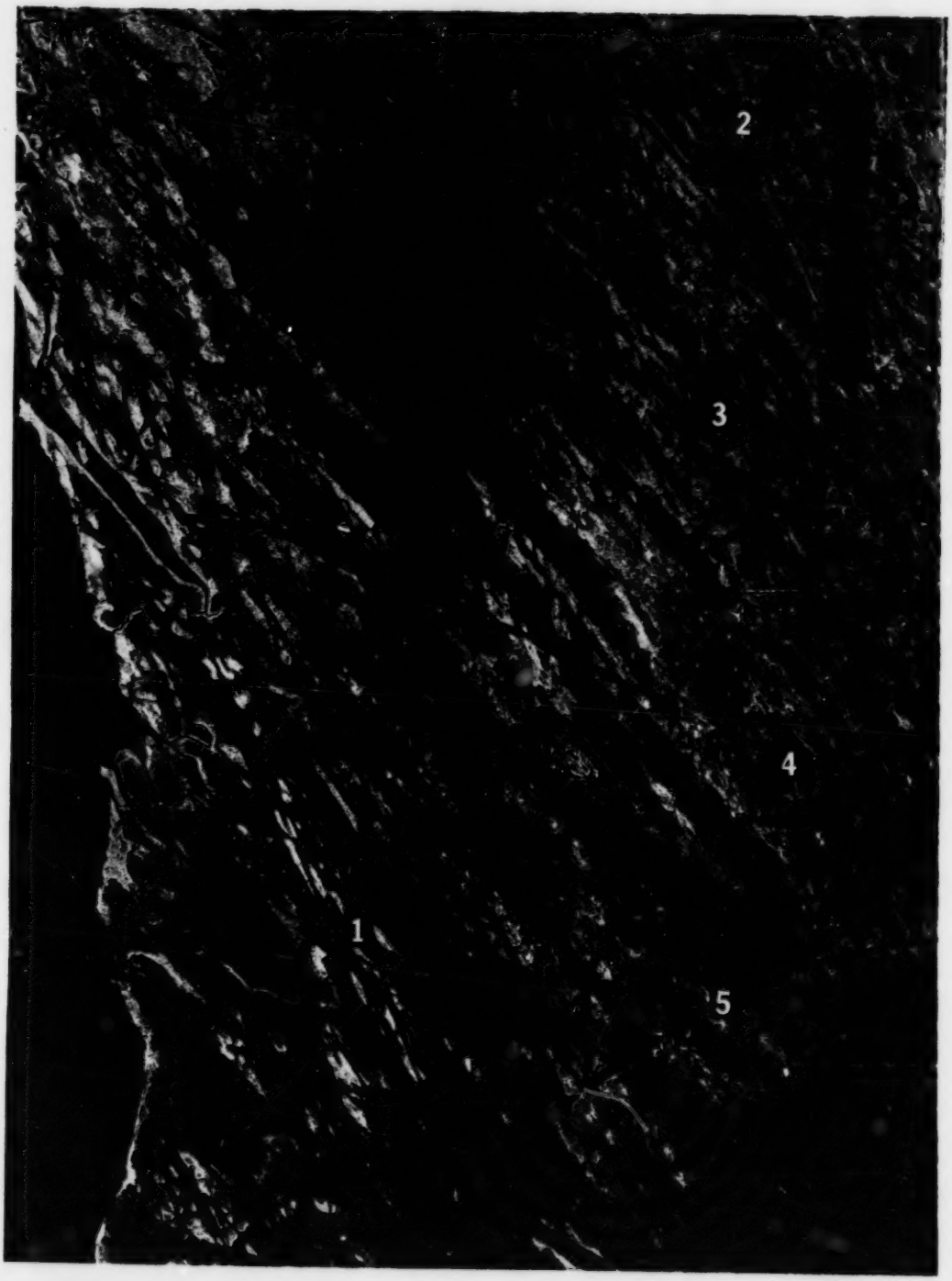

Relict ice scour pattern adjoining the southeast shore of Lake Manitoba, Manitoba.

PLATE 2A

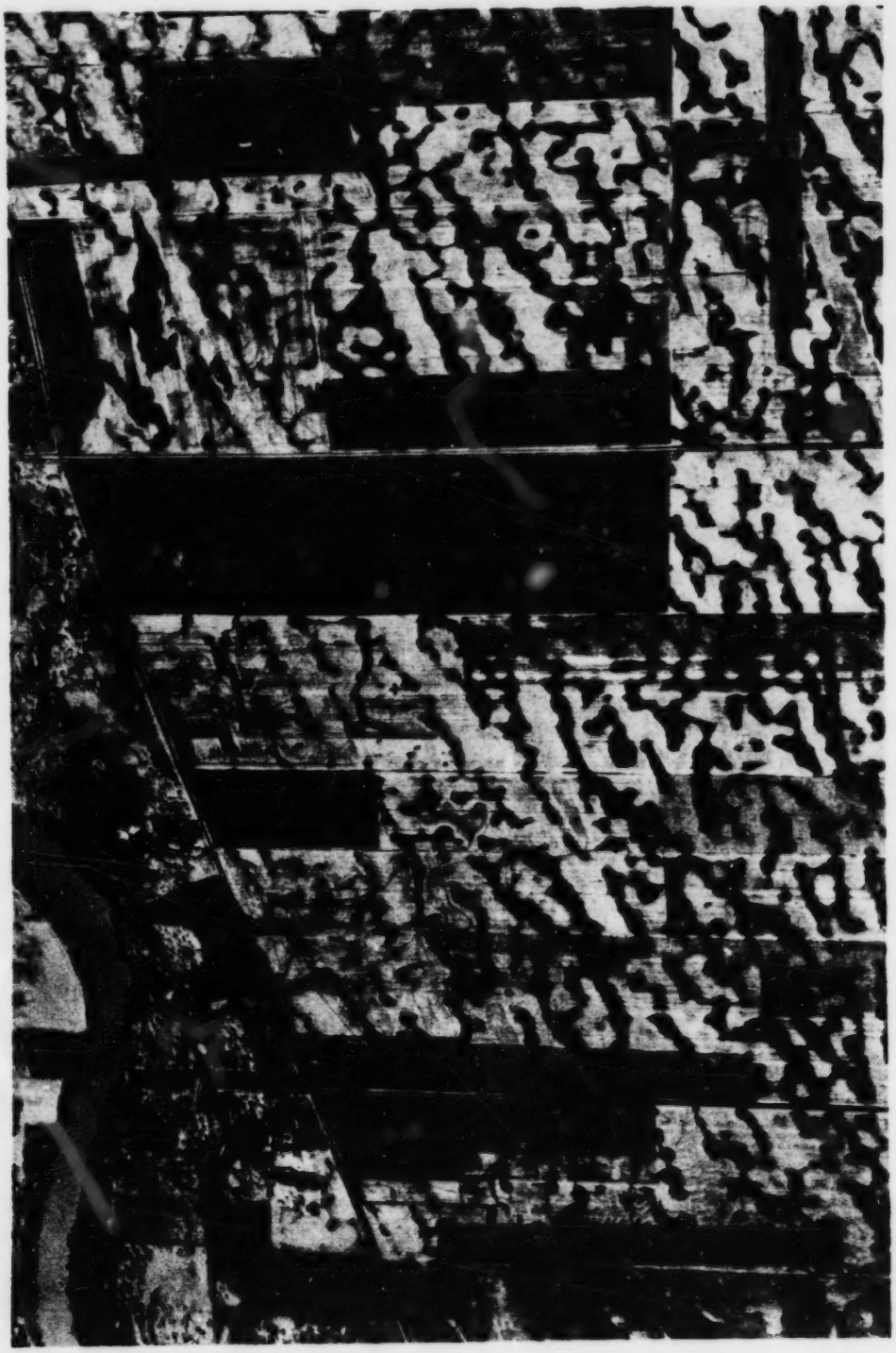

Ice scour lineament pattern north of Emerson, Manitoba.

PLATE 2B

Figure 2 Lake ice damage to cottage at Delta on the southeast shore of Lake Manitoba. Photo taken by Ken Gigliotti April 12, 1981.

Ice scour features southeast of Windsor, Ontario.

PLATE 3A

Ice scour west of Mattagami Lake, Quebec.

PLATE 3B

Ice scour pattern north of Spence Bay, Northwest Territories.

PLATE 4A

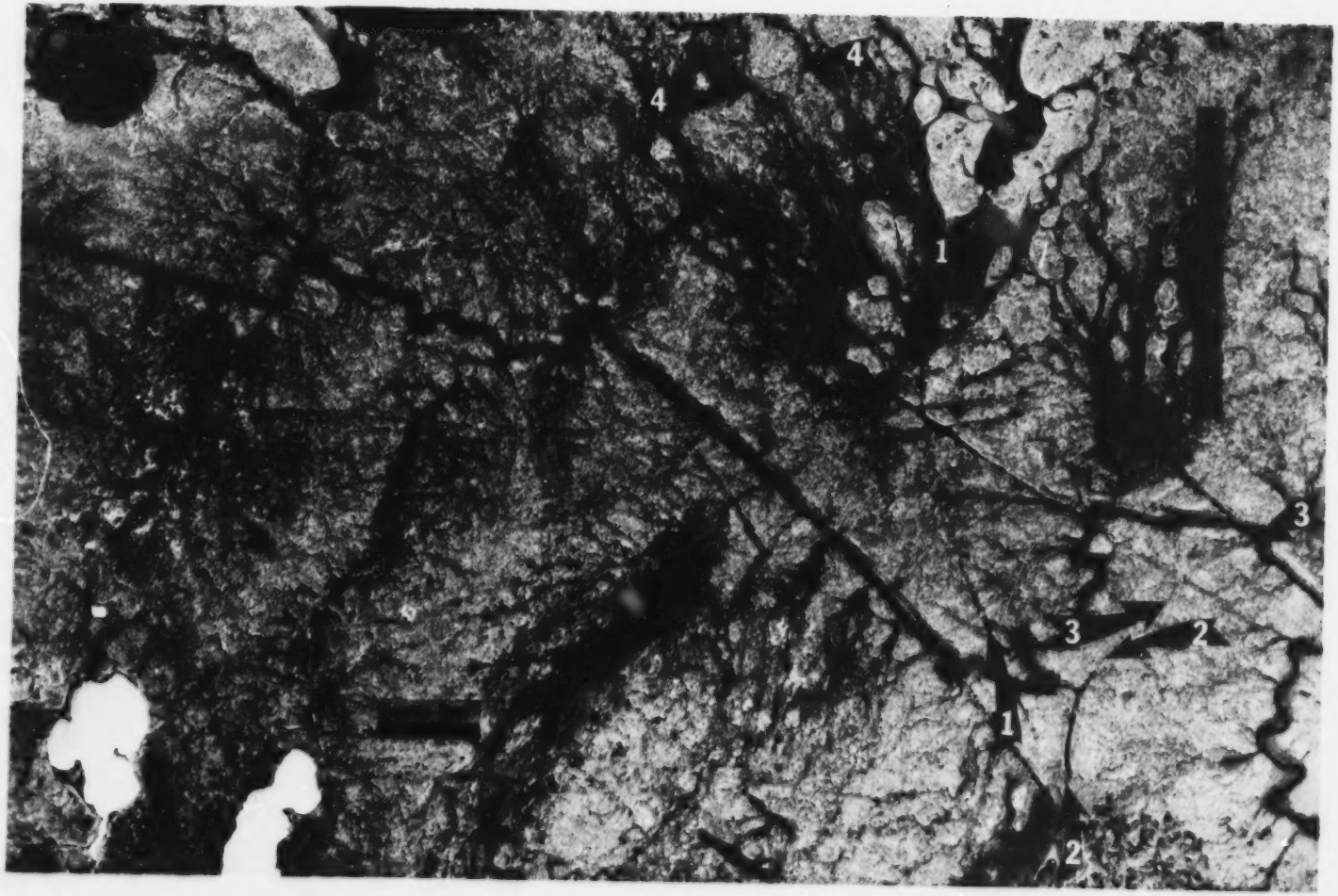

Ice scour features north of Red Cross Lake, east-central Manitoba.

PLATE 4B

Straight, curved, and parabolic microridges southeast of Winnipeg, Manitoba.

PLATE 5A

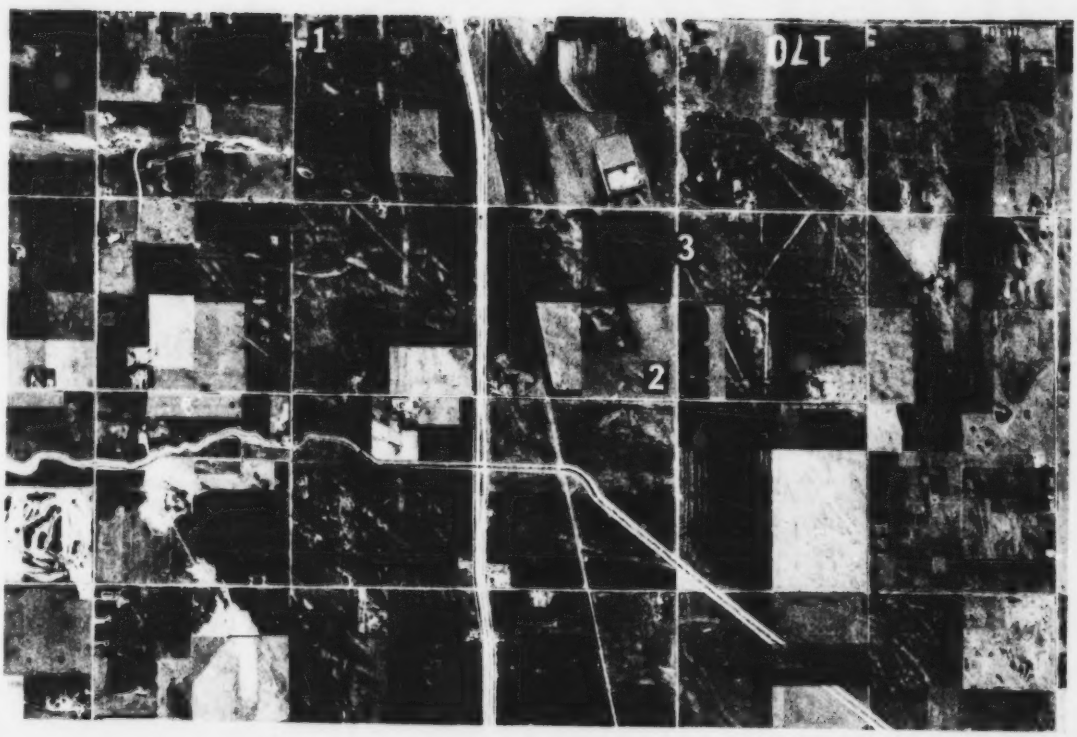

Microridges south of Stony Mountain, Manitoba.

PLATE 5B

Figure 3 Irregular discontinuous layers of calcareous buff-colored silt in dark grey lacustrine clay in microridge near Ile des Chene, Manitoba. The pattern here resembles structures seen in some migmatites in the Canadian Shield.

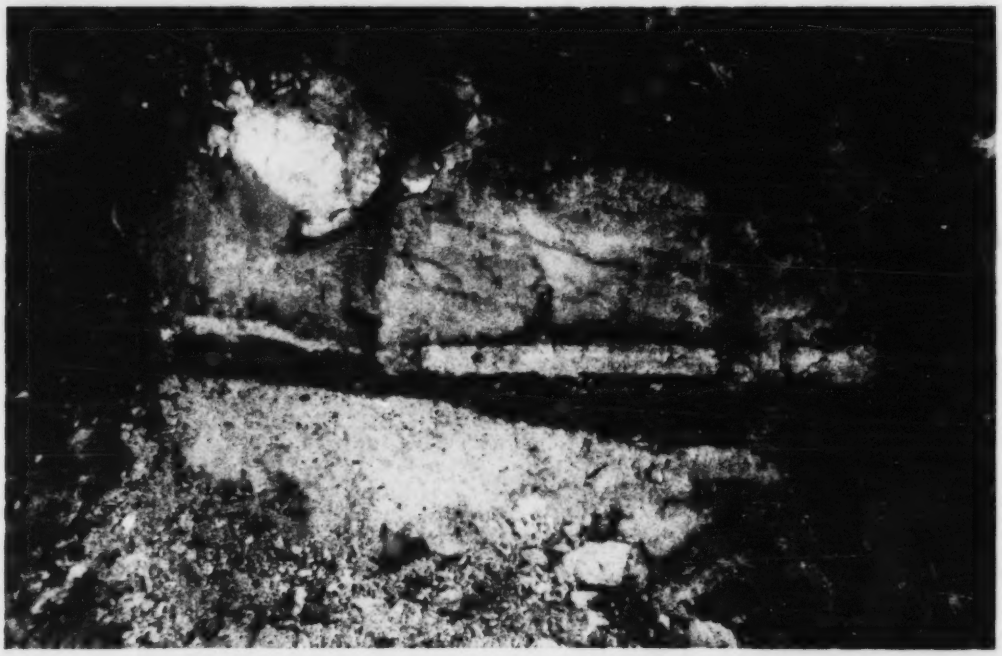

Figure 4 Irregular layering of dark grey lacustrine clay and buff-colored calcareous silt in microridge, west of Stony Mountain, Manitoba.

Circular vegetation rings in an area of relict ice scours on the floor of Tyrrell Sea, James Bay Lowland, Ontario.

PLATE 6

PREDICTIONS OF EXTREME KEEL DEPTHS FROM SUBMARINE SONAR DATA

Peter Wadhams

Scott Polar Research Institute
University of Cambridge, Cambridge CB2 1ER, England

1. INTRODUCTION/ABSTRACT

A fundamental problem in the estimation of return periods for deep keels at a point is that of predicting extreme values from a time series or spatial profile of limited extent. In this paper we examine three techniques of prediction, and compare their performances using a data set in the public domain. We then examine the problem of predicting extreme keel depths along a line, i.e. the probability that a pipeline route will suffer scoring by a keel during a given interval. We propose two ways of attacking this problem, and consider an example of how to predict pipeline burial depths using these statistics.

2. THE DATA SET

The pressure ridge distribution in the Beaufort Sea coastal environment is highly variable, both in time and space. The best way of obtaining data suitable for keel depth prediction at a given location is therefore to employ a bottom-mounted upward-looking sonar at that location to record continuously for a year or more. This gives a time series which is site-specific and which is free of bias due to improper estimation of mean ice drift velocity (a drawback of spatial profiles). It also avoids the problem of estimating how the local bottom topography affects the likelihood of keel scoring at that location, i.e. whether there is a sheltering effect on point A due to keels grounding at a nearby point B and distorting the local ice velocity and deformation fields so as to reduce the likelihood of a grounding at A.

Data obtained by this technique are not as yet in the public domain, so to illustrate various techniques of extreme draft prediction we employ a data set which has already been analysed (Wadhams and Horne, 1980, henceforth WH), a 1400 km submarine sonar profile from the southern Beaufort Sea obtained by U.S.S. "Gurnard" in April 1976. The beamwidth of the sonar (2^{o}) was very small and so this record represents the best quality of all submarine sonar profiles available to date. Figure 1 shows the track of "Gurnard", beginning at the 100 m isobath off Barter Island, and figure 2 shows the division of the track into 50 km sections for WH's statistical analysis.

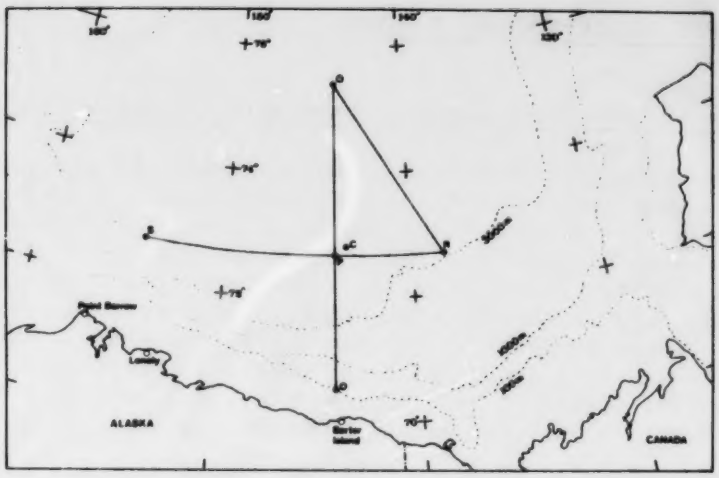

FIGURE 1. Route of U.S.S. "Gurnard", 7-10 April 1976. (After Wadhams and Horne, 1980).

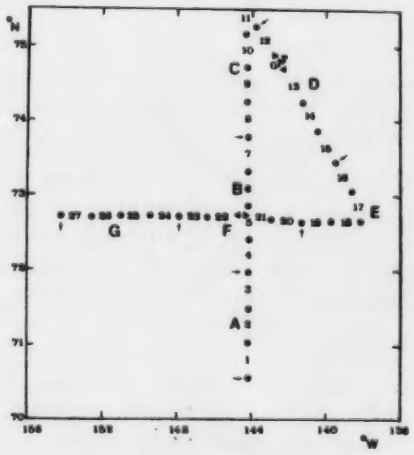

FIGURE 2. Division of track into 50 km sections. (After Wadhams and Horne, 1980).

3. EXTREME DEPTH PREDICTIONS AT A POINT

3.1. Technique 1: Use of the negative exponential distribution

WH defined an independent keel as one in which the troughs (points of minimum draft) on either side of the keel crest (point of maximum draft) each rise at least half way towards the local level ice bottom before beginning to descend again. The 'local level ice bottom' is difficult to find, especially in heavily ridged areas, so it is defined arbitrarily as being a draft of 2.5 m. This is the Rayleigh criterion for ridge definition; it is one of an infinite range of possible empirical criteria, but is the most common in published analyses of sonar and laser profiles (Leppäranta, 1981; Lowry and Wadhams, 1979; Tucker et al, 1979; Wadhams, 1976, 1978, 1980, 1981; Wadhams and Lowry, 1977; Weeks et al, 1980; Williams et al, 1975).

Using this criterion WH found that the number of keels per km of track per metre of draft increment, $n(h)$, was related to the draft h by a simple negative exponential distribution:-

$$n(h)\,dh = B \exp(-b\,h)\,dh \qquad (1)$$

where the parameters B and b can be expressed in terms of the experimentally observed mean keel draft $\bar{h}$, mean number of keels per km μ, and low value cut-off draft h_o:-

$$b = (\bar{h} - h_o)^{-1} \qquad (2)$$

$$B = \mu\, b \exp(b\, h_o) \qquad (3)$$

Table I shows values for μ and $\bar{h}$ for each of the 50 km sections, calculated using 5 m and 9 m for h_o. The fit of the data to this distribution is extremely good, as shown in figure 3.

The negative exponential distribution has been found to fit sail heights as measured by laser profilometers (Leppäranta, 1981; Tucker et al, 1979; Wadhams, 1976, 1980, 1981; Weeks et al, 1980) as well as keel drafts. However, keel drafts measured by a wide beam sonar in the Eurasian Basin (Wadhams, 1981) were found to fit a distribution proposed by Hibler et al (1972), of form

$$n(h) \propto \exp(-\lambda h^2) \qquad (4)$$

although with some deviation towards (1) at extreme depths (figure 4). It is reasonable to conclude that this is due to the effect of beamwidth upon the shape of the under-ice profile and that (1), since it fits narrow-beam data, is an equation of more general validity for ridge keels.

Using (1) we can estimate the total number of keels per year passing a given point and having depths of D or greater, as follows:-

$$N_D = L\int_{h_o}^{\infty} n(h)\,dh = L\,\mu \exp\left[\frac{-(D - h_o)}{(\bar{h} - h_o)}\right] \qquad (5)$$

where L km is the distance drifted per year by the ice cover over that point. If D is the water depth, then N_D is the number of grounding ridges at that site per year, i.e. the number of scoring events. $(1/N_D)$ is the return period in years, T_D, for a keel of depth D or greater.

$$T_D = 1/N_D \qquad (6)$$

TABLE I. Number of keels per km μ and mean keel draft $\bar{h}$ for cut-off drafts h_o of 5 m and 9 m. (After Wadhams and Horne, 1980).

Section	Draft > 5 m		Draft > 9 m		Maximum draft
	No. per km	Mean draft m	No. per km	Mean draft m	m
1	14.77	8.57	5.11	12.15	23.13
2	10.28	8.30	3.07	12.20	28.83
3	8.11	7.69	1.81	11.79	21.64
4	7.41	7.62	1.55	11.75	19.60
5	7.92	7.78	1.90	11.61	22.65
6	5.68	7.57	1.10	12.77	22.65
7	5.49	7.43	0.99	12.06	20.54
8	5.47	7.20	0.91	11.84	20.73
9	8.17	7.39	1.43	11.51	20.09
10	6.40	7.51	1.40	11.34	16.86
11	6.59	7.26	1.24	11.25	22.59
12	7.08	7.65	1.58	11.75	23.65
(Short	6.17	7.78	1.06	13.10	31.12)
13	6.60	7.65	1.49	11.89	20.97
14	6.69	7.68	1.38	12.13	24.93
15	5.46	7.32	0.89	12.11	23.38
16	6.24	7.39	1.13	11.23	18.96
17	7.15	7.79	1.65	12.31	24.84
18	7.46	7.64	1.64	11.40	18.35
19	5.50	7.53	1.11	11.93	26.73
20	7.25	7.50	1.38	11.71	20.36
21	6.98	7.52	1.53	11.98	19.99
22	5.43	7.71	1.37	11.73	19.66
23	7.01	7.65	1.56	12.04	24.48
24	6.36	7.49	1.22	12.01	22.01
25	7.82	7.66	1.78	11.72	22.07
26	8.82	8.25	2.65	12.32	29.23
27	8.72	8.34	2.60	12.69	29.14
Mean of main group (3–25)	6.71 ±0.20	7.55 ±0.03	1.39 ±0.06	11.79 ±0.07	

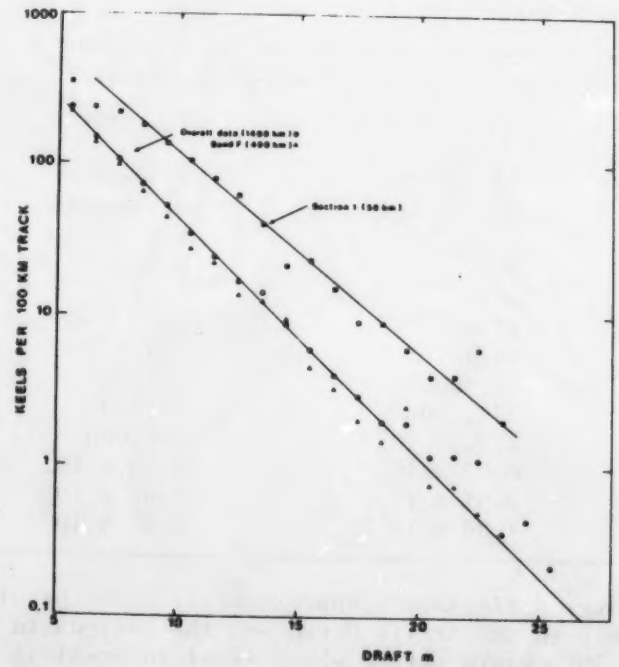

FIGURE 3. Distribution of keel drafts on semilogarithmic plot for overall data (circles), section 1 (squares) and sections 20–25 (triangles). Bin size 1 m. (After Wadhams and Horne, 1980).

In order to calculate T_D from (5) we need to know L. This is a site-specific quantity, but typical values would be 500 km in the transition zone and 1000 km over deep water in the southern Beaufort Sea. The best data come from buoys (NORCOR, 1977; Thorndike and Colony, 1980b, 1981) and the AIDJEX experiment provided a year's data relevant to the central Beaufort Sea (Thorndike and Colony, 1980a; L=2100 km). Having taken a best value for L from available data, we proceed either by taking values for $\bar{h}$ and μ from table I, or by actually plotting out the observed data on semilogarithmic paper as in fig.3 and extrapolating the line of best fit. The results from these procedures will differ slightly since, as fig.3 shows, there is some deviation from a negative exponential at low drafts (e.g. section 1, 5-8 m depth) and at extremely high drafts. The low draft deviation occurs because some features which are not ridges appear in the statistics, e.g. deep floe bottoms. The high draft deviation occurs mainly because of the very small numbers of keels per bin counted at deep draft, making the statistics unreliable. The best procedure is therefore to plot out the data, to ignore the shallow end of the curve if it deviates from a negative exponential, to ignore the very deep end when there are, say, fewer than 10 keels per bin, and to fit the rest of the curve to a negative exponential so as to obtain $\bar{b}$ and B from the gradient and intercept. A quicker procedure is simply to use $\bar{h}$ and μ from the computed statistics for h_o = 9 m, since the higher cut-off removes the low draft deviation.

As an illustration, we use the quick procedure to compute T_D for two cases:-

1. The mean of sections 3-25, putting L = 1000 km, assumed to be typical of the central Beaufort Sea.
2. The mean of sections 1 and 2, putting L = 500 km, assumed to be typical of the transition zone.

The results are shown in table II.

TABLE II. Extreme depth predictions using negative exponential distribution.

D (m)	T_D, case 1	T_D, case 2
25	2.7 months	27 days
30	1.34 years	4.4 months
35	8.02	1.76 years
40	48.1	8.50
45	289	41.1
50	1730	199
55	10,400	959
60	62,300	4,630
65	374,000	22,400
70	2.24×10^6	108,000
80	8.07×10^7	2.52×10^6
90	2.91×10^9	5.87×10^7
100	1.05×10^{11}	1.37×10^9

Note the very large difference - approximately a factor of 10 - between the return periods deep in the Arctic Ocean and the periods in the heavily ridged coastal environment. The return period which is of interest in practice, e.g. the desired interval between scoring events at a sea bottom wellhead, is of order 1000 years. In case 2 this occurs at about 55 m water depth.

3.2. Technique 2: Distances between depth crossings

Technique 1 depends for its success on the fact that the keel drafts follow a particularly simple mathematical distribution, thanks to the high quality of the data. We have already mentioned wide-beam data which follows a different distribution, although tending towards the negative exponential at great depths (fig.4). In future it is likely that extensive wide-beam data from early U.S. Navy cruises to the Beaufort Sea will be declassified. We need a technique to handle such data, since even when bottom detail has been smoothed out by the beamwidth it ought to be possible to manipulate the data so that extreme value predictions are similar to those from good data.

A distribution-free technique, which also avoids the use of an arbitrary ridge-defining criterion, is to look at the statistics of crossings of a given depth horizon by the ice bottom profile. In figure 5, let $X(h)$ be the set of distances between an upward crossing of a depth horizon h and the subsequent downward crossing of the same horizon. The probability density function of $X(h)$ will consist partly of very small values due to the intervals between peaks within a single keel, and partly of large values due to the spacings between keels. The mean value $\bar{X}(h)$, however, should increase monotonically with h except where h is so small that $X(h)$ is just the distribution of lead widths. If $\bar{X}(h)$ is a simple mathematical function of h, then we can extrapolate beyond the range of measured values to obtain $\bar{X}(h)$ at very large h. This is then the return spacing between keels of depth h or larger, and so the return period T_D is simply

$$T_D = \bar{X}(D) \; / \; L \qquad (7)$$

Figure 6 shows the result of computing $\bar{X}(h)$ for the two cases of the whole data set and of sections 1 and 2 alone. The computation was carried out at 2 m intervals starting at h = 4 m. For the overall data, the range from h= 6 m to h = 22 m fits an exponential distribution, while for sections 1 and 2 the fit extends from 4 m to 22 m. From 24 m upwards there are too few values for valid statistics. The fit to an exponential distribution was a likely, but not inevitable, consequence of the keel draft distribution having a negative exponential form. By fitting regression lines to the valid parts of figure 6, we obtain the following predictions for T_D using (7).

TABLE III. Extreme depth predictions using depth crossing technique.

D (m)	T_D, case 1	T_D, case 2
25	1.3 months	22 days
30	8.1 months	3.9 months
35	4.2 years	1.78 years
40	26.2	9.66
45	163	52.5
50	1010	286
55	6280	1550
60	39,100	8450
65	243,000	46,000
70	1.51×10^6	250,000
80	5.84×10^7	7.39×10^6
90	2.26×10^9	2.19×10^8
100	8.74×10^{10}	6.48×10^9

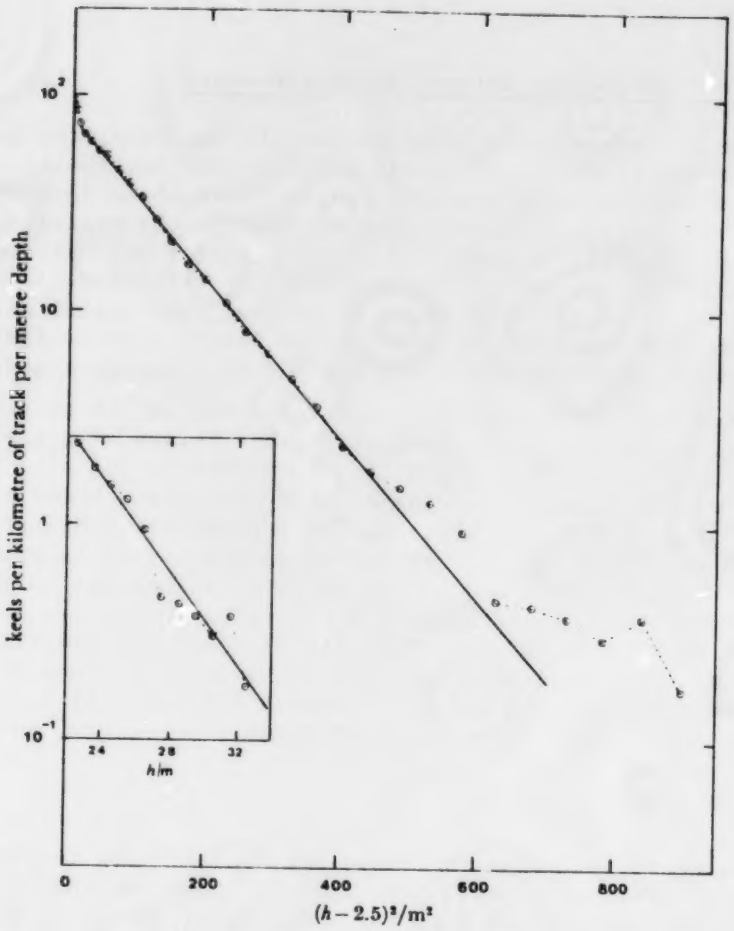

FIGURE 4. Keel draft distribution from 4000 km wide-beam sonar track in Eurasian Basin, showing fit to equation (4). Inset shows deviation towards equation (1) at depths beyond 23 m. (After Wadhams, 1981).

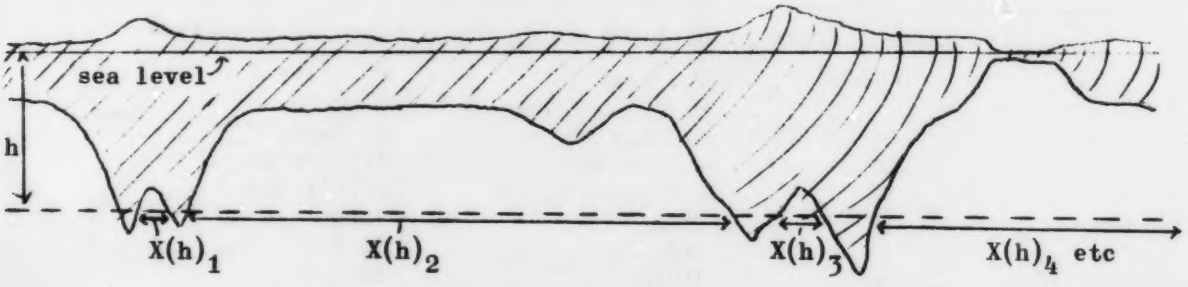

FIGURE 5. The depth crossing technique.

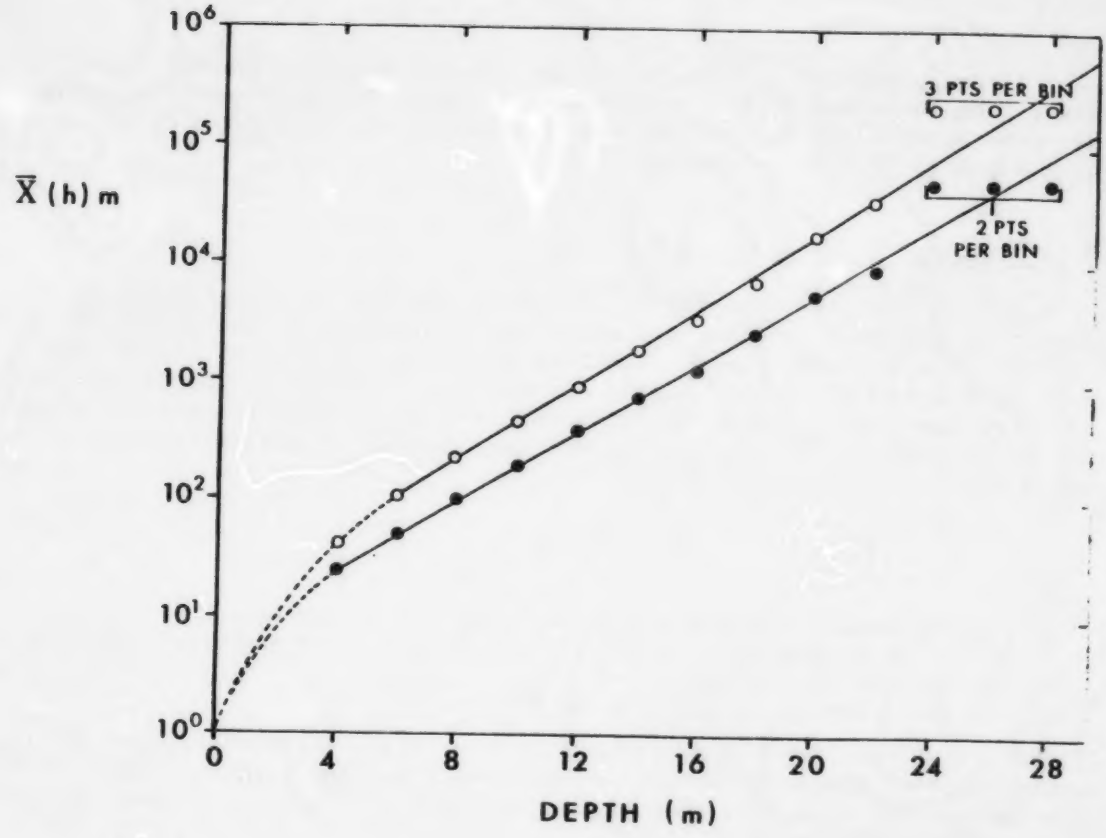

FIGURE 6. $\overline{X}(h)$ plotted against h for the whole data set (open circles) and for sections 1 and 2 only (filled circles).

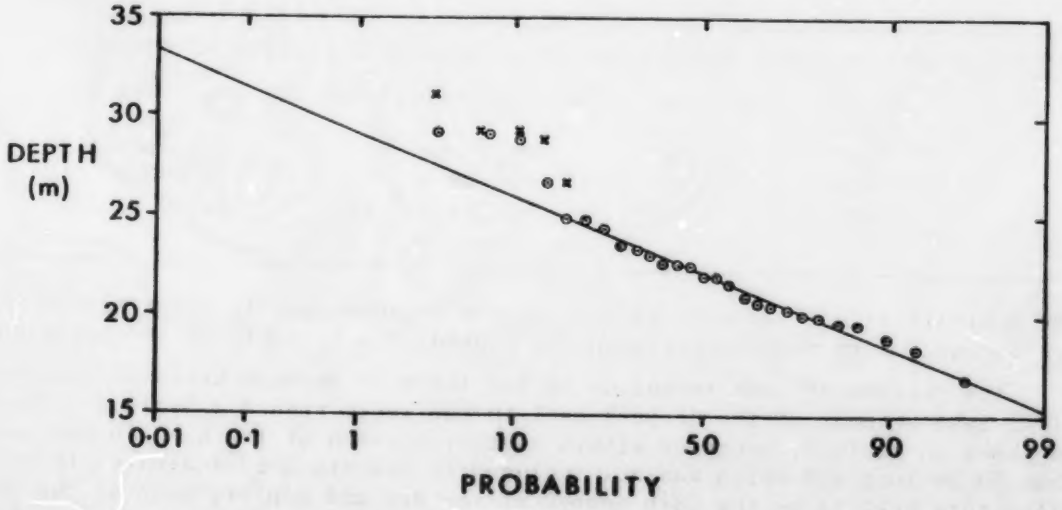

FIGURE 7. Plot of recurrence probability for deepest keel in a 50 km section. Open circles use 27 sections; crosses show effect of including additional very deep keel.

Although the return periods for the central Beaufort Sea are somewhat lower than those obtained from technique 1, those for the coastal environment are remarkably similar. The 1000 year return period, for instance, now occurs at a depth of 53.7 m instead of 55.1 m.

3.3. Technique 3: Probability plotting

A second distribution-free technique of prediction was proposed by Tucker et al (1979) for the interpretation of laser data. The record is divided into uniform sampling intervals of convenient length; in our case a 50 km interval fits the analysis scheme shown in table I. The deepest keel is extracted from each sampling interval, and the resulting keels are ranked in order of depth. The keel depths are then plotted on probability paper using the Weibull plotting formula

$$F = \frac{1}{P(X > x)} = \frac{n + 1}{m} \qquad (8)$$

where

n = total number of depth values involved (27 in our case);
m = rank of a given keel (m = 1 for the deepest keel and m = 27 for the shallowest in the set);
F = return distance in units of 50 km.

Tucker et al found that such a plot fitted a straight line over almost the whole range of the data, with a deviation only for the highest ridges. Such a technique has also been used to predict other extreme events such as floods (Slack et al, 1975).

We have plotted the 27 deepest keels obtained from table I in this way, with results shown in figure 7 (circles). There is a good fit to a straight line for all except the four deepest keels. An extrapolation of this straight line, however, produces the following predictions for return periods, equivalent to case 1 in sections 3.1 and 3.2.

TABLE IV. Extreme depth predictions using probability plotting technique.

D (m)	P(X > x)	F = recurrence interval	T_D, case 1
25	17.5%	285.7 km	3.4 months
30	0.5%	10^4 km	10 years
35	0.0008%	6.25×10^6 km	6,250 years

The analysis is not taken to greater depths because clearly the return periods are becoming very much larger than those predicted by the first two techniques.

The failure of this technique to fit the four deepest keels is even worse if we take account of the deepest keel in the whole record - 31.12 m - which, as shown in table I, occurred within a short stretch of track which was less than 50 km long and which was not included in the standard analysis. If we allow this keel to be the 28th member of the set and replot, most of the data points in fig.7 are shifted only a negligible distance. The four deepest keels, however, are shifted further, and their new positions, together with that of the new deepest keel, are shown as crosses in fig.7. The five keels now show

an enhanced deviation from the extrapolated straight line, and it is clear that this technique is not valid for predicting extreme values. Even Tucker et al found that the highest sails in their records were much higher than the predictions of probability plotting.

3.4. Recommendations

In dealing with a newly acquired data set, the first task should be to apply a ridge-picking criterion and examine the keel draft distribution. If this fits a negative exponential closely, with no significant deviation except at the shallow end or due to shortage of data points per bin, then the negative exponential should be used as the basis for extreme value predictions. If the fit is not good, then technique 2 should be employed in the hope that $\overline{X}(h)$ fits an exponential distribution or other distribution of simple form which can be used as the basis for extrapolation. Technique 3 is not recommended unless the data in the probability plot fit a straight line throughout the depth range, including the greatest depths in the record.

4. EXTREME DEPTH PREDICTIONS ALONG A LINE

4.1. Basic definitions

Having determined N_D or T_D, our next step is to attempt a prediction of the number of scoring events per year along a 1 km line oriented at right angles to the mean ice drift direction. If this number, S_D say, is multiplied by the number of km of pipeline y_D that are to be constructed at this water depth (again, projected at right angles to mean ice drift direction), then we can obtain an estimate of the scoring rate along the whole pipeline as

$$\text{Scoring events per year} = \sum_D S_D \, y_D \qquad (9)$$

The pipeline route is expressed as a sum of as many sections as are required by the varying bottom topography and varying ice conditions. We expect S_D to be linearly dependent on N_D so we can say

$$S_D = N_D \, f \qquad (10)$$

and our problem is to calculate f.

Consider 1 km of pipeline (figure 8) and assume that the ice drift is always at right angles to it. The area of icefield that sweeps past the pipeline in one year is therefore L sq km. At any instant there are, on average, (N_D/L) keels intersecting the pipeline and scoring the bottom if the water depth is D, assuming that keels are statistically isotropic, i.e. randomly oriented.

Now consider the 'annual box' of fig.8 divided into narrow strips as shown of width δx. Each time that the ice moves by δx, (N_D/L) "keel linkages" are transported across the pipeline, where a "keel linkage" is defined as a section of keel, depth greater than D, and projected length δx along the x-axis. Therefore when the whole 'annual box' has drifted across the pipeline, $(N_D/\delta x)$ "keel linkages" have been transported across the pipeline. Now if each keel has an average projected length ℓ' along the x-axis, the number of keels that have been transported is $(N_D/\delta x)/(\ell'/\delta x) = (N_D/\ell')$. Therefore we infer

$$f = 1/\ell' \qquad (11)$$

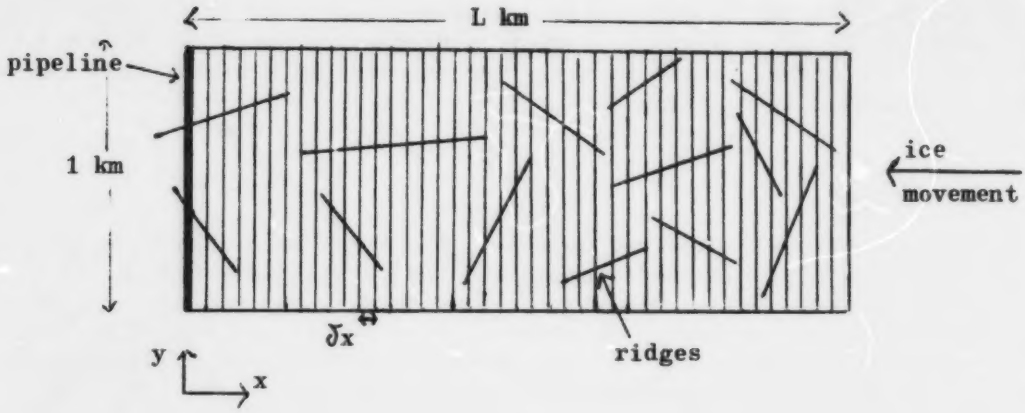

FIGURE 8. The area geometry of pressure ridges.

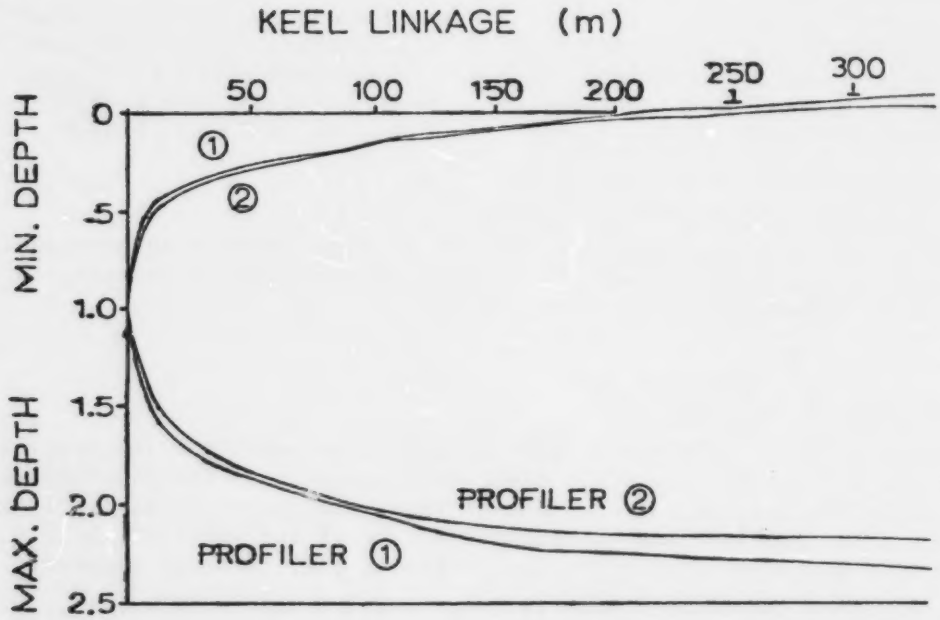

FIGURE 9. Minimum and maximum drafts along a keel crest, expressed as a multiple of the mean draft (5.95 m) and averaged over the length of the profile. (After Wadhams, 1976).

If keels are randomly oriented and of mean length ℓ , then

$$\ell' = \frac{2\ell}{\pi} \int_0^{\pi/2} \cos\theta \, d\theta = 2\ell/\pi \qquad (12)$$

so $$f = \pi / 2\ell \qquad (13)$$

where ℓ is the mean length of a keel in km.

This is not, unfortunately, the overall length of a keel as observable on aerial photographs. Instead, it is the length of a continuous section of keel which is deeper than D, since we have insisted in the analysis that the keels must all score the bottom. This involves us in the problem of longitudinal keel statistics, i.e. how the depth of a keel crest varies with distance along its axis.

4.2. Estimates from keel observations

Field observations of depth variations along the crest of a keel are extremely sparse, because of the difficulty of measurement. The only available sonar profile along a keel crest was obtained by an unmanned submersible in the Beaufort Sea in 1972 and analysed in Wadhams (1976). The keel was a shallow one of mean draft 5.95 m in a floe of draft 2.58 m, so its mean relief was only 3.37 m. Wadhams published a graph of the crest coherence (figure 9), but since the depth variations are almost certainly due to the relief of single ice blocks, the analysis is inappropriate for deeper keels. With deeper keels we expect greater absolute variations in depth along the crest, but smaller relative variations and with a tendency to a longer wavelength of variation. With normal submarine sonar profiles the angles at which ridges are crossed are not known. In fact, models of keels (e.g. Wadhams, 1978) usually assume them to be linear features of triangular cross-section, so that even an oblique crossing by submarine will generate a profile in which genuine along-crest depth variations are convolved with the flattened triangle of the keel cross-section. Valid information cannot therefore be extracted.

There are a few studies in which a keel has been cored and its dimensions examined more extensively than across a single cross-section. For instance, Wright et al (1979) reported that three multi-year keels had lengths of 250 m, 70 m and 70 m. This suggests that we could take 100 m as an order-of-magnitude guess for ℓ , giving an f of 16. Clearly a priority in field observations must be depth measurements along keel crests, by divers or scanning sonar.

4.3. Estimates from score observations

In the absence of direct measurements of keel crest coherence, we can estimate ℓ by looking at the widths of the score marks made by the keels. ℓ is the mean length of a keel section which is continuously deeper than D. In water of depth D, this is exactly the same as the mean width of a score mark, provided the keel which makes the score is oriented at right angles to the direction of scoring.

Figure 10, from Lewis (1977), shows the mean width of score marks as a function of water depth, measured along a one-dimensional sonar line running NW from Kugmallit Bay. The widths are thus projected onto a NW-SE axis, which

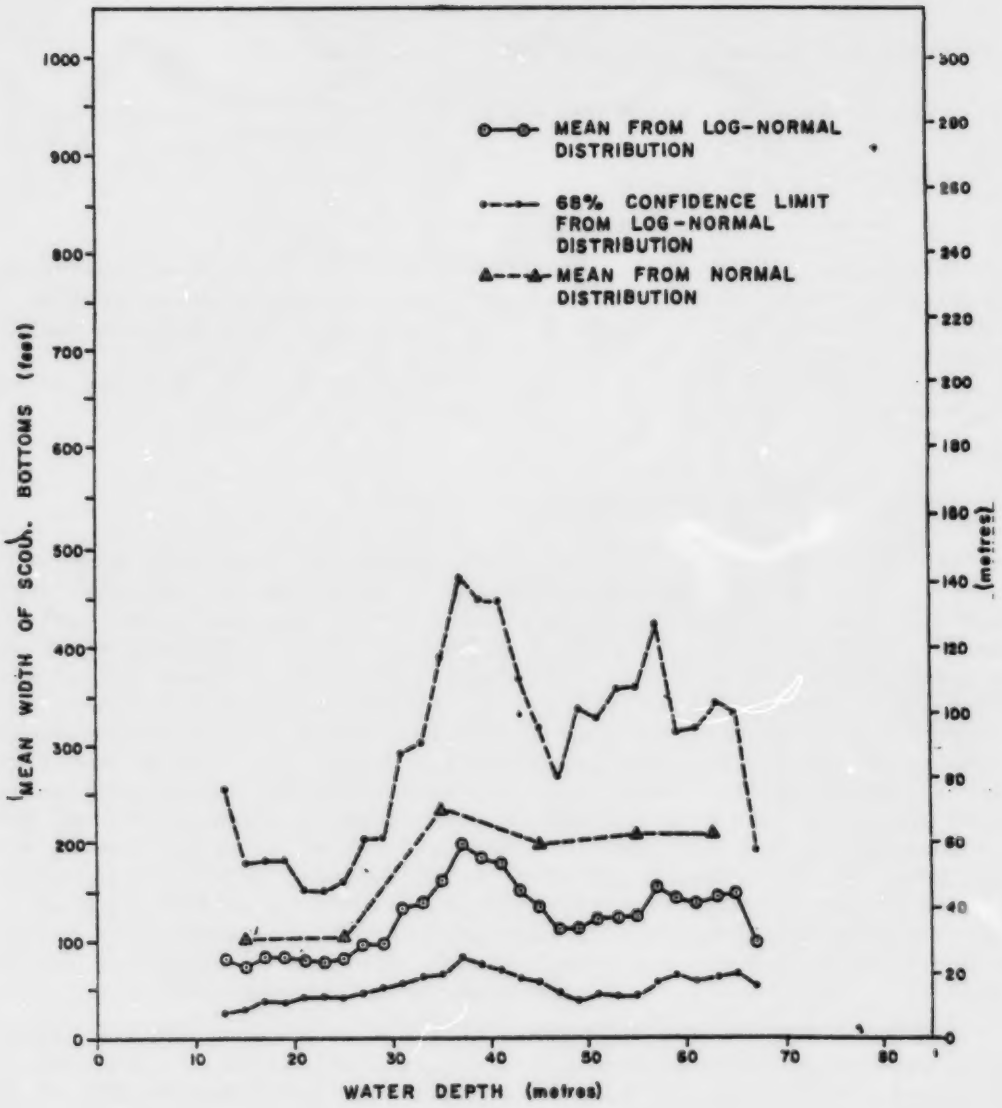

FIGURE 10. Mean score widths as a function of water depth. (After Lewis, 1977). The "mean from normal distribution" has been used as the basis for table V.

lies approximately at right angles to the mean direction of ice drift in that vicinity. Assuming random keel orientation, then (which may not be valid in the nearshore zone), we can identify the mean projected score width with ℓ' in equation (11). This gives us the following values for f.

TABLE V. Predictions of f using mean score widths of Lewis (1977).

Water depth D (m)	ℓ' km	$f = 1/\ell'$
15	0.0302	33.1
25	0.0313	32.0
35	0.0699	14.3
45	0.0595	16.8
55	0.0625	16.0
65	0.0628	15.9

The values do not differ wildly from the guess made in section 4.2. Thus we now have a means of estimating f and hence S_D in equation (10). The numerous sidescan sonar profiles of the Beaufort Sea shelf that are now available, both in and out of the public domain, enable estimates of f to be made in a site-specific sense.

4.4. Application to pipeline burial depths

Finally we consider a case study in which the sonar statistics are applied to the estimation of the depth required to bury a pipeline so that disturbance occurs at only a 1000 year return period. The numbers are intended mainly for illustration, and for any real case will be subject to major revision in the light of field observations.

We assume that we wish to lay a pipeline 76 km long, the distance from the Kopanoar well to shore. We use a result discovered by Lewis (1977) and employed by Pilkington and Marcellus (1981), that the probability that a given score mark extends to a depth d or greater below the undisturbed sea bottom is exp (-k d), where k is a parameter which is site-specific and which can be determined from sonar mosaics of the immediate area. Thus

Scoring events per year per km at depth D = $S_D = N_D$ f from (10);

Return period per km for a score of depth d at water depth D

$$= (S_D\, e^{-k\, d})^{-1} = T, \text{ say} \qquad (14)$$

which gives, using negative exponential distribution of keel drafts, eqn.(5),

$$d = \frac{1}{k} \ln \left[L \mu T\, f \exp \left(-\frac{(D - h_o)}{(\bar{h} - h_o)} \right) \right] \qquad (15)$$

d is then the required depth of burial for the top of the pipe to give a return period T of disturbance per km.

In this case, for a return period of 1000 years and a 76 km pipeline, the return period per km in (15) must be set at 76,000 years. This raises the question of what happens when further pipelines are built. If n pipelines of 76 km are built to the same specifications as the first, the return period for disturbance of one of the pipelines drops to 1000/n years. In selecting a design value for T, then, the engineer must make some estimate of the total number of pipelines that are likely to be constructed during the life of the oilfield.

Using (15) we now calculate d at different water depths using k values from Lewis (1977), f values from section 4.3, reasonable guesses for L, and ice statistics from section 1 of the "Gurnard" profile (h_o = 9 m, $\bar{h}$ = 12.15 m, μ = 5.11 km^{-1}). The results are as follows.

TABLE VI. Burial depths to top of pipeline for 1000 year return period.

Water depth D (m)	k	f	L	Burial depth d (m)
15	3.120	33.1	150	6.24
25	2.129	32.0	400	8.10
35	1.775	14.3	600	7.70
45	1.142	16.8	800	9.59
55	1.148	16.0	1000	6.92
65	0.725	15.9	1200	6.83

The required burial depths lie in the range 6.2 to 9.6 m. It is significant that the required burial depth is high even at the extreme water depth of 65 m where the scoring frequency is very low. This is because those scores which do occur tend to be very deep ones, hence the low k value. The low k then compensates for the high D in (15). This prediction could be revised downwards if some of the scores at great water depths, contributing to the low k, could be shown to be archaic.

ACKNOWLEDGEMENTS

I am indebted to Roger Pilkington and Bob Marcellus for useful discussions which helped in the formulation of section 4, and to Donald Gaver and Pat Jacobs (U.S. Naval Postgraduate School, Monterey) for useful discussions on section 3.2. I thank Rob Massom for diagrams and Ruth Weintraub for computing.

REFERENCES

Hibler, W.D. III, W.F. Weeks and S.J. Mock (1972). Statistical aspects of sea-ice ridge distributions. J. Geophys. Res., 77(30), 5954-5970.

Leppäranta, M. (1981). Statistical features of sea ice ridging in the Gulf of Bothnia. Winter Navigation Res. Bd., Helsinki, Tech. Rept. 32.

Lewis, C.F.M. (1977). Bottom scour by sea ice in the southern Beaufort Sea. Dept. of Fisheries & Envt, Ottawa; Beaufort Sea Project Tech. Rept. 23.

Lowry, R.T. and P. Wadhams (1979). On the statistical distribution of pressure ridges in sea ice. J. Geophys. Res., 84, 2487-2494.

NORCOR (1977). Probable behaviour and fate of a winter oil spill in the Beaufort Sea. Rept. EPS 4-EC-77-5 by NORCOR Engng & Res. Ltd., Yellowknife, to Envtl. Protection Service, Dept.of Fisheries & Envt., Ottawa.

Pilkington, G.R. and R.W. Marcellus (1981). Methods of determining pipeline trench depths in the Canadian Beaufort Sea. Proc. 6th Intl. Conf. on Port & Ocean Engng under Arctic Conditions, Quebec, Aug 1981.

Slack, J.R., J.R. Wallis and N.C. Matalas (1975). On the value of information to flood frequency analysis. Water Resources Res., 11, 629-647.

Thorndike, A.S. and R. Colony (1980a). Large-scale ice motion in the Beaufort Sea during AIDJEX, April 1975 - April 1976. In Sea Ice Processes and Models (R.S. Pritchard ed.), Univ. Washington Press, Seattle, 249-260.

_____(1980b). Arctic Ocean Buoy Program. Data report, 19 January 1979 - 31 December 1979. Polar Science Center, Univ. Washington.

_____(1981). Arctic Ocean Buoy Program. Data report, 1 January 1980 - 31 December 1980. Polar Science Center, Univ. Washington.

Tucker, W.B.III, W.F. Weeks and M. Frank (1979). Sea ice ridging over the Alaskan continental shelf. J. Geophys. Res., 84, 4885-4897.

Wadhams, P. (1976). Sea ice topography in the Beaufort Sea and its effect on oil containment. AIDJEX Bull., 33, 1-52.

_____(1978). Characteristics of deep pressure ridges in the Arctic Ocean. Proc. 4th Intl. Conf. on Port & Ocean Engng Under Arctic Conditions, (D.B. Muggeridge, ed.), Memorial Univ., St. John's, 1, 544-555.

_____(1980). A comparison of sonar and laser profiles along corresponding tracks in the Arctic Ocean. In Sea Ice Processes and Models (R.S. Pritchard, ed.), Univ. Washington Press, Seattle, 283-299.

_____(1981). Sea-ice topography of the Arctic Ocean in the region 70°W to 25°E. Phil. Trans. Roy. Soc., Lond.,A302(1464), 45-85.

Wadhams, P. and R.J. Horne (1980). An analysis of ice profiles obtained by submarine sonar in the Beaufort Sea. J. Glaciol., 25(93), 401-424.

Wadhams, P. and R.T. Lowry (1977). A joint topside-bottomside remote sensing experiment on Arctic sea ice. Proc. 4th Can. Symp. Remote Sensing, Quebec, May 1977. Can. Remote Sensing Soc., Ottawa, 407-423.

Weeks, W.F., W.B. Tucker III, M. Frank and S. Fungcharoen (1980). Characterization of the surface roughness and floe geometry of the sea ice over the continental shelves of the Beaufort and Chukchi Seas. In Sea Ice Processes and Models (R.S. Pritchard, ed.), Univ. Washington Press, Seattle, 300-312.

Williams, E., C.W.M. Swithinbank and G. de Q. Robin (1975). A submarine sonar study of Arctic pack ice. J. Glaciol., 15, 349-362.

Wright, B., J. Hnatiuk and A. Kovacs (1979). Multi year pressure ridges in the Canadian Beaufort Sea. Proc. 5th Intl. Conf. on Port & Ocean Engng Under Arctic Condns, Univ. Trondheim, 1, 107-126.

ICE SCOUR PROTECTION DRAKE F-76 FLOWLINE BUNDLE

Maarten Van Ieperen
Panarctic Oils Ltd., Calgary

Introduction

Drake F-76 is the first producing subsea gas well in the High Arctic. Jointly undertaken by Panarctic Oils Ltd., Petro-Canada and Nova (An Alberta Corporation), the project was successfully completed on April 23, 1978. It involved the design of a rig to drill from an artificial ice platform; the design and installation of a flowline bundle and its connection with a subsea Christmas tree; and finally the design of an ice scour protection system. In accordance with the theme of this conference, my paper will concentrate on aspects of the ice scour protection system of the pipeline only. The technical details of the project have been reported by Hood (1) and others (2).

Environmental Conditions

Drake F-76 is located in the Canadian Archipelago about 1200 m off Sabine Peninsula, Melville Island (Figure 1). Situated in a small bay, it is relatively well protected from ice scour. Most of the time, however, the ice in the area is landfast. The probability that at Drake F-76 the ice breaks up in summer is about 50%. The probability of ice break-up decreases with increasing latitude to about 20% in the upper Western Sverdrup Basin. The maximum ice thickness of first year ice in the area is about 2.4 metres. Because of summer ablation of the ice cover, second and multi-year ice reaches an equilibrium

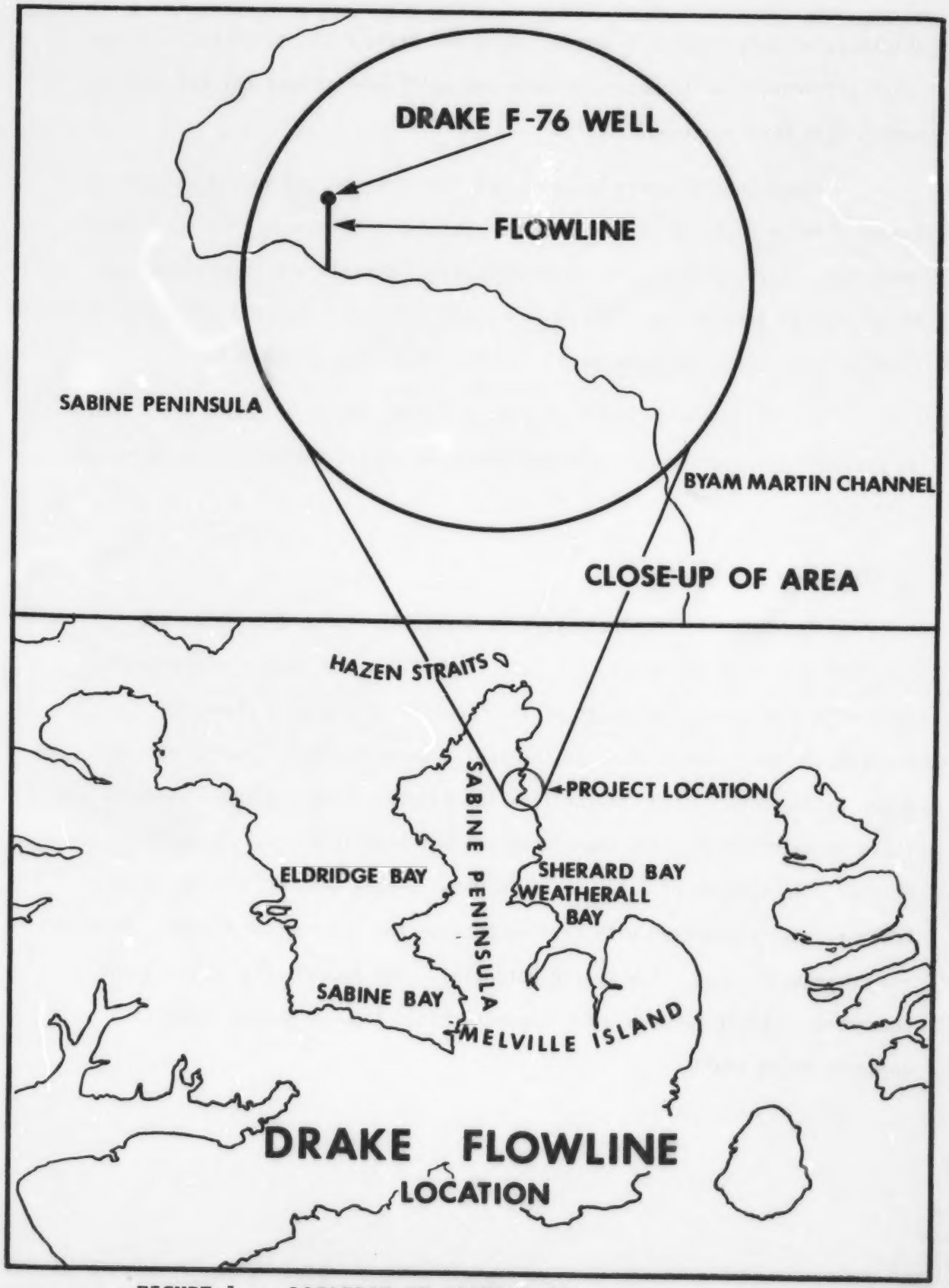

FIGURE 1. LOCATION OF DRAKE F-76

thickness of only about 2.5 metres. North of Drake F-76, multi-year ice may reach a thickness of 10 metres or more and multi-year ridges thicker than 40 metres have been observed.

About once in every 10 years the ice cover in the entire Western Sverdrup Basin disintegrates. When this happens ice islands from the Arctic Ocean may enter. At the time of calving they typically are about 50 metres thick, but as some melting takes place their thickness in the Sverdrup Basin is usually less. Very few have been sighted in Byam Martin Channel.

The predominant wind direction at Drake F-76 is offshore which tends to prevent the entering of ice floes from Byam Martin Channel. The currents are very weak.

Flowline Bundle Protection

The lack of ice statistics, in particular those describing the occurrence of extreme events, has made it difficult to determine the optimum cost effective protection depth of the flowline bundle at Drake F-76. To investigate the scour history in the area a side scan sonar survey was conducted prior to the construction of the flowline bundle. Some ice scour evidence was found in water depths less than 20 metres but none in depths greater than 20 metres. The absence of scour marks in water depths greater than 20 metres, however, was interpreted with caution because the sea bottom is highly plastic and consequently has a low mosaic potential. The probability of ice scour occurring at Drake F-76 in water depths greater than 20 metres, however, appeared to be small.

After careful consideration of the above factors the following ice scour protection system was chosen:

The flowline bundle was placed in a trench 1.5 metres deep, which started at the shoreline and ended where the water depth was 20 metres as illustrated in Figure 2 (a deeper trench was impossible because of the softness of the soil). For additional protection of this portion of the flowline bundle a refrigeration system was designed to enable the freezing of the backfill of the trench, should this be required. Tests showed that the unconfined compressive strength of the frozen backfill and the natural bottom soil would be 600 kPa at -10°, which is many times greater than the strength of the sea bottom material. Finally, to provide additional protection to this section of the flowline bundle passing through the high risk scour zone in the very shallow water area, an ice berm was constructed to a water depth of 5 metres. This berm protects the flowline bundle over a horizontal distance of about 100 metres.

Present Status

Although Drake F-76 is at present not operative, the condition of the flowlines, ice berm and refrigeration system appears to be excellent. The system has been monitored regularly and so far no ice scour damage has been detected. This indicates that the ice scour protection system, barring freak events, is adequate.

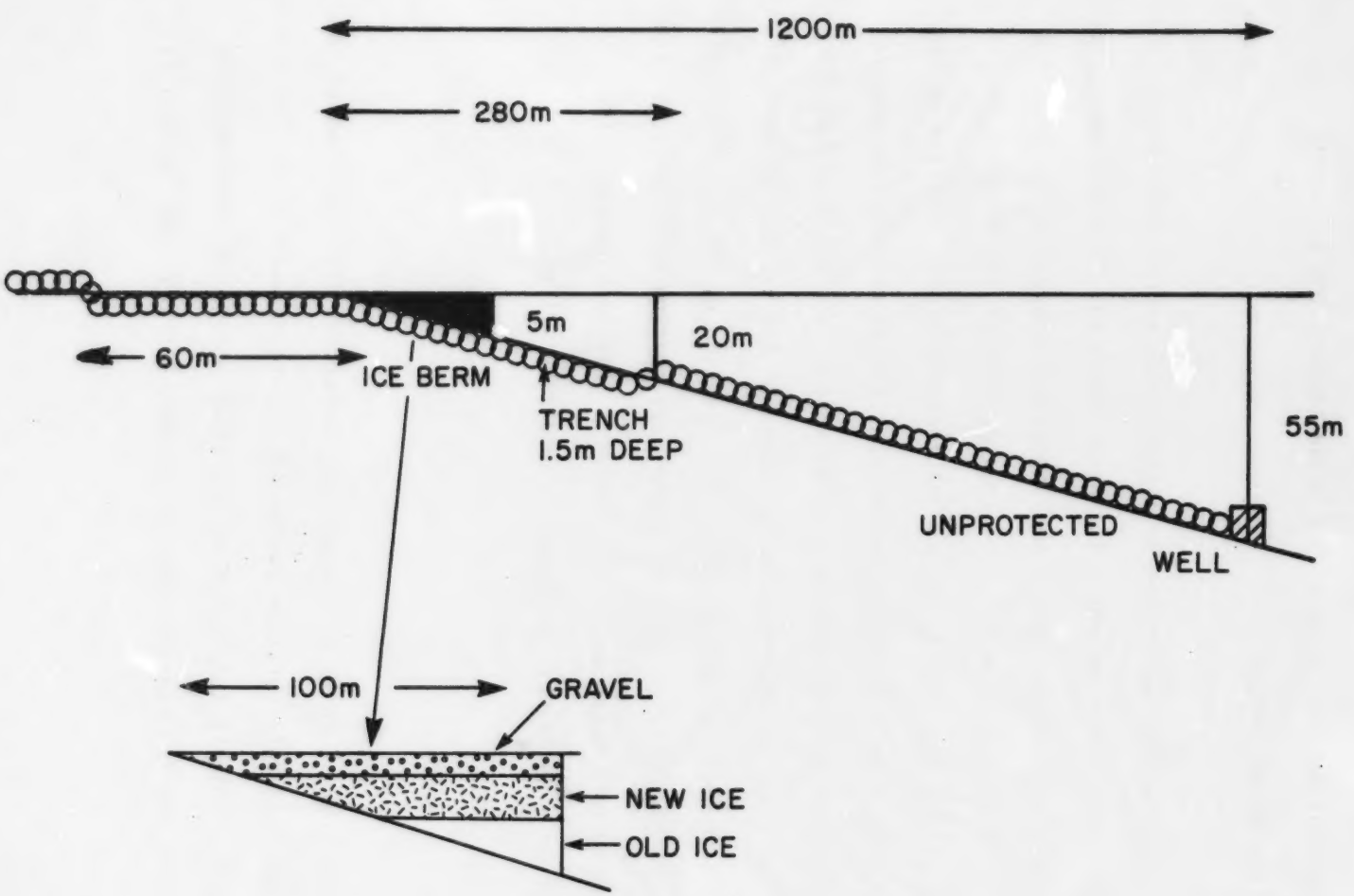

Figure 2 DETAILS OF FLOWLINE PROTECTION

Q: What is the radius of the freezing zone of the refrigertion system?

A: The refrigeration system is normally switched off. The radius will depend on the time the system is active, I imagine exponentially.

Q: Is the refrigeration system shut off at present?

A: Yes. It is much too costly to keep it on all the time. The costs of running the system is relatively small, but having permanent personnel on site is too expensive.

Q: Will you be putting the refrigeration system on when Drake F-76 becomes operational?

A: Only if there is a real scour danger to the pipeline. Most of the time the pipeline is naturally protected by the landfast ice in the area.

REFERENCES

1. Hood, G.L., D.N. Masterson, G.S. Watts (1979) Installation of a Subsea Completion in the Canadian Arctic Islands. Paper presented at the 30th Annual Technical Meeting of the Petroleum Society of CIM in Banff, May 8 - 11, 1979.

2. Palmer, A.C. et al. (1979) Design and Operation of an Underwater Pipeline Trenching Plough. Géotechnique 29, No.3, 305-322.

LAKE ERIE
ICE SCOUR
INVESTIGATION

G. Comfort
R. Abdelnour
B. Trak
B. Menon
B. Graham

Submitted at:

NRC WORKSHOP ON ICE SCORING

Held at MONTEBELLO, Quebec

G. Comfort, R. Abdelnour, B. Menon and B. Graham are employed at ARCTEC CANADA LIMITED. B. Trak is a professor at Ottawa University.

ACKNOWLEDGEMENT

The authors wish to thank Ontario Hydro, who funded the original work, and supplied the field data on lakebed soil properties and scours, for permission to publish this paper.

1.0 INTRODUCTION

Ontario Hydro is planning the construction of a high voltage submarine cable which will cross Lake Erie between the Canadian north shore near the city of Nanticoke, Ontario and the U.S. south shore near Girard, Pennsylvania. Figure 1 shows the general location of the proposed submarine corridor.

Lakebottom surveys by Ontario Hydro (1980, 1981) have verified the presence of several scours along specific reaches of the proposed corridor (see Figure 1). Ice scours up to 1.7 m deep were found in the Nanticoke approach area in 9 m to 22 m of water; lesser ice scours (ie. up to 0.6 m depth) were found on the Coho side in 15 m to 23 m of water.

This paper describes analytical work which was undertaken to estimate the maximum probable scour depth. Two analytical approaches were used to determine a safe burial depth in an attempt to verify conclusions drawn from the available field measurements of ice scour:

- Analytical models based on considerations of kinetic energy and work done in soil deformation were exercised for a range of input parameters to provide a comparison with the available field ice scour measurements.

- The limiting scour depth, (based on consideration of the limited flexural strength of the ridge), was predicted.

The objective of this work was to determine a safe burial depth for the submarine cable.

2.0 BASELINE ENVIRONMENTAL DATA

Baseline environmental data is required for an assessment of the severity of the ice scour problem in Lake Erie. An extensive literature review revealed a great paucity of environmental data for Lake Erie. Nevertheless, sufficient information was gathered to provide quantification of critical parameters which allowed ice scour estimates to be made.

The following environmental data is of interest:

- typical ice mass/soil interaction scenarios
- ice thickness
- floe size
- ice ridge size and composition
- ice mass drift rate, wind speed and current speed
- lakebed soil properties.

As well, field data on ice scours is required for corroboration of the analytical predictions.

2.1 Ice Mass/Soil Interaction Scenarios

Information on the ice regime in Lake Erie was obtained from an analysis of satellite imagery and aerial photos.

Plates 1 and 2 show typical ice conditions that may be expected over the proposed cable corridor.

The Lake Erie ice cover typically starts to form in late December and persists until March. A solid ice cover is never formed over Lake Erie. Rather, the ice cover is highly dynamic and may be characterized by broken ice floes which drift subject to the forces of winds and currents. Since the prevailing winds are westerly, ice floes typically

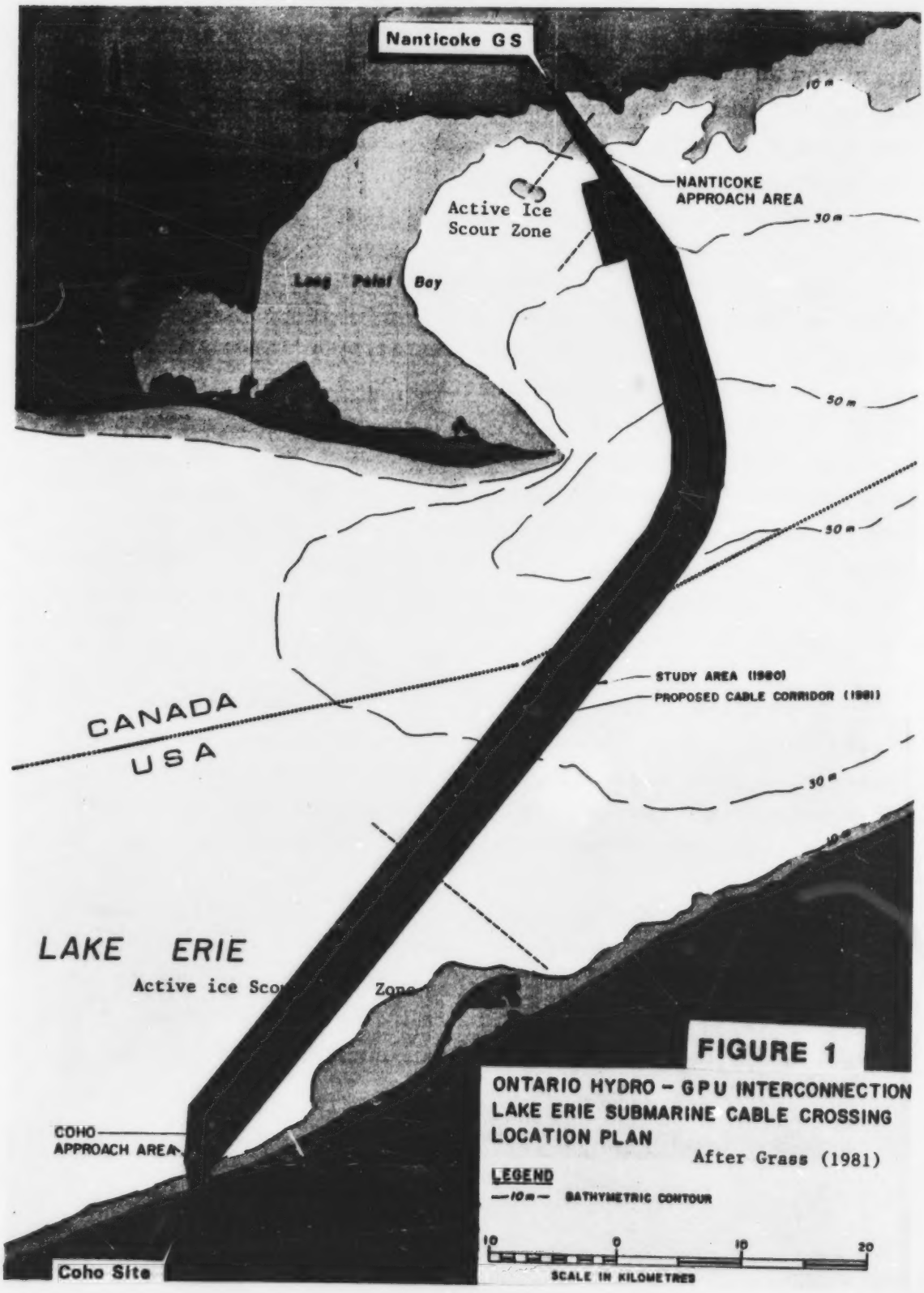
Nanticoke GS
10 m
NANTICOKE
APPROACH AREA
Active Ice
Scour Zone
30 m
Long Point Bay
50 m
50 m
STUDY AREA (1980)
PROPOSED CABLE CORRIDOR (1981)
CANADA
USA
30 m
LAKE ERIE
Active ice Scou
Zone
COHO
APPROACH AREA
Coho Site
FIGURE 1
ONTARIO HYDRO - GPU INTERCONNECTION
LAKE ERIE SUBMARINE CABLE CROSSING
LOCATION PLAN
After Grass (1981)
LEGEND
—10m— BATHYMETRIC CONTOUR
10 0 10 20
SCALE IN KILOMETRES

become packed into the eastern end of Lake Erie and consequently the ice cover in the area from Erie, Pennsylvania to Nanticoke to Port Colborne, Ontario, frequently has much higher ice concentrations than the western end of the lake. The ice concentration in the eastern end of the lake typically reaches a maximum value of 9+/10.

The ice cover is continually broken into floes (by the wind and the current) and as the floes are packed together, ice pressure ridges are formed. Relatively large ridges may form in Lake Erie although most ridges are relatively small (i.e. the sail height is typically less than 1 m). The largest ridge reported in the literature occurred in 1971 near Port Colborne with a sail height on the order of 5 to 6 m, (Anonymous 1971). The breadth of the ridge that may form is also highly variable, depending upon the conditions of formation. Ridge breadths may range from a few metres to hundreds of metres.

Immediately after formation, the ridges consist of a relatively highly porous accumulation of ice blocks with weak interblock bonds. Ridges in Lake Erie typically remain unconsolidated throughout the winter due to the dynamic nature of the ice cover and the southern location.

There are many possible soil/ice interaction scenarios. However, for this project, we were interested in constructing a worst case scenario. This was felt to be the case where a large ridge and ice floe drifted in a direction perpendicular to the lake bottom isobaths.

PLATE 1

ICE CONDITIONS IN LAKE ERIE: MARCH 1981

NOTE: PHOTO COURTESY OF J. GRASS, ONTARIO HYDRO (1981)

PLATE 2

ICE CONDITIONS IN LAKE ERIE: MARCH 1981

NOTE: PHOTO COURTESY OF J. GRASS, ONTARIO HYDRO, (1981)

2.2 Ice Environmental Data

Table 1 summarizes the ice environmental data which were gathered and used during this study.

For all measured parameters, (ie. ice thickness, floe size, ridge height and breadth, wind speed and current speed), the observed frequency distribution was compared to the normal, lognormal, and the Gumbel extreme value distributions. The theoretical distribution which provided the best degree of fit was used to describe the distribution of the individual parameters in subsequent analyses.

(i) Ice Thickness

Ice thicknesses measured in the harbour at Erie, Pennsylvania over the 1967 to 1976 period, have provided data on the ice thickness to be expected in the cable corridor.

Level ice thicknesses offshore can be expected to be typically less than those measured in the harbour as the ice cover dynamics (ie. the continual opening and closing of leads within the ice pack) will create areas of thinner ice. Nevertheless, the measured values give a reasonable upper limit of ice thickness.

(ii) Ice Floe Size

Data on ice floe size was obtained from aerial photography and satellite imagery.

Aerial photographs are sometimes taken by the Atmospheric Environment Services (AES) during routine ice reconnaissance flights. Unfortunately, aerial photos for only the 1977 ice year were available from AES. The aerial photographs had a 70 mm negative size and provided imagery

TABLE 1

ENVIRONMENTAL CONDITION SUMMARY

PARAMETER	EXCEEDANCE PROBABILITY				STATISTICAL DISTRIBUTION USED
	0.5	0.10	0.01	0.01	
Floe diameter (km)	1.5	5.5	16.0	38.0	Lognormal
Floe thickness (m)	0.35	0.5	0.8	1.0	Lognormal
Windspeed (kmh)	88.0	125.0	170.0	215.0	Gumbel
Current speed (m/sec)	0.075	0.18	0.33	0.52	Gumbel
Ice drift rate (m/sec)	0.33	0.55	0.85	1.15	Calculated using(2.6)
Ridge sail height(m)	0.7	1.2	2.0	2.7	Gumbel
Ridge sail breadth(m)	23.0	90.0	280.0	650.0	Lognormal
Ridge keel breadth (m) for Coho Area for[1]:					
0 - 13m W.D.	70.0	120.0	280.0	570.0	Calculated using(2.2)
13 - 13.5m W.D.	70.0	120.0	280.0	570.0	
13.5-18m W.D.	90.0	140.0	290.0	590.0	
18 - 20m W.D.	100.0	150.0	300.0	600.0	
20 - 24m W.D.	112.0	160.0	320.0	610.0	
Ridge keel breadth (m) for Nanticoke Area for[1]:					
9 - 13m W.D.	80.0	120.0	280.0	570.0	Calculated using(2.2)
13 - 21m W.D.	100.0	150.0	310.0	600.0	
21 - 24m W.D.	110.0	160.0	320.0	610.0	
Ridge unit wt (MN/m) for Coho Area for[1,2]:					
0 - 13m W.D.	1.73	6.78	21.10	49.60	Calculated using(2.4)
13 - 13.5m W.D.	1.80	7.04	21.92	51.51	
13.5-18m W.D.	2.40	9.39	29.22	68.67	
18 - 20m W.D.	2.67	10.44	32.47	76.30	
20 - 24m W.D.	3.20	12.52	38.96	91.57	
Ridge unit wt.(MN/m) for Nanticoke Area for[1,2]:					
9 - 13m W.D.	1.73	6.78	21.10	49.60	Calculated using(2.4)
13 - 21m W.D.	2.80	10.96	34.09	80.12	
21 - 24m W.D.	3.20	12.52	38.96	91.57	

NOTES:

1. Ridge keel breadths and unit weights were calculated for the maximum water depth of the range indicated.
2. Ridge sail breadth was taken as the value which would initiate grounding at the maximum water depth of the range indicated. (This was taken as the maximum water depth ÷ 4.6 - see equation 2.1).

at scales ranging from 1: 5000 to 1: 35000.

Imagery from the LANDSAT series of satellites was also used to provide data on ice floe size. This imagery has been collected since 1972 and is at 1: 1,000,000 scale. Nominally, successive images are provided from each satellite at 18 day intervals; however, cloud conditions in winter severely limited the number of usable images. In total, three mosaics were obtained (ie. Feb. 18, 1974, March 21-22, 1979) which provided good data on ice floe size.

(iii) Ridge Size

As previously mentioned, little information on ice conditions was available for Lake Erie. No data on ridge keel depth, ridge keel breadth or ridge mass specific to Lake Erie was available. However, data on ridge sail height and ridge sail breadth was found. Data on ridge geometries measured in other locations for fresh ice or brackish ice (ie. Gulf of Bothnia, Lake Melville, Port Colborne, Great Slave Lake) was used to relate the keel depth, keel breadth and the ridge area to the ridge sail height and/or sail breadth.

Data on ridge sail height was obtained from analysis of laser profilometer records collected during AES ice reconnaissance missions. Laser profilometer records from a total of two flights for the area of interst (ie. March 12, 1979 and February 11, 1978) was available from AES.

Data on ridge sail width was obtained from analysis of the previously-mentioned 1977 AES aerial photos.

A total of 16 first-year ridge profiles were obtained from the literature. In addition, 19 spot measurements of keel depth and sail height were available. Table 2 lists

the ridge data obtained as well as providing the sources of the data.

After a number of parameter groupings, the following best fit predictors were obtained:

1. Ridge Keel Depth = 4.6 x Ridge Sail Height. [2.1]

2. Ridge Keel Breadth = 18 x Ridge Sail Height + 0.8 x Ridge Sail Breadth. [2.2]

3. Ridge Total Area = 6.0 x Ridge Sail Height x Ridge Sail Breadth. [2.3]

4. Ridge Weight/Unit Length = (1-n) ($\ell_i g$) Ridge Area. [2.4]

where n = ridge sail and keel porosity (taken as 0.5)

$\ell_i g$ = weight density of ice (taken as 9000 N/m^3)

(iv) Ice Drift Rate

Since no measurements of ice drift rate for Lake Erie were available from the literature and it was not possible to establish drift rates from successive satellite images, it was decided to estimate the ice drift rate from available current speed and wind speed data.

The drift rate and direction of an ice floe is dependent upon the magnitude and direction of the wind drag and current drag forces as well as the magnitude of the Coriolis

TABLE 2 RIDGE GEOMETRY DATA

SOURCE	SAIL HT (M)	SAIL BREADTH (M)	MEAN SAIL ANGLE (°)	EQUIV. SAIL AREA (M)	KEEL DEPTH (M)	KEEL BREADTH (M)	MEAN KEEL ANGLE (°)	KEEL AREA (M)	COMMENTS
Lake Melville, Lab.:	2.2	9.4	25	9.5	10.7	47.0	25	71.7	Ridge Geometry
1974 Nemac (1973)	0.8	3.7	24	4.0	3.8	53.0	8	28.9	Interpolated
	0.8	28.3	3	5.8	3.2	53.0	7	23.0	
	1.0	3.7	29	6.5	3.6	43.0	10	41.0	Sail Porosity: 40-50%
	1.1	6.4	19	3.8	5.7	36.6	17	24.4	Keel Porosity: 20-30%
Lake Melville, Lab.:	1.0	7.6	15	14.3	2.4	35.1	8	53.5	
Anon. (1973)	1.5	6.1	26	21.4	4.0	42.7	11	101.5	
	1.2	6.7	20	35.4	9.5	41.2	25	198.4	
Gulf of Bothnia:	1.3	12.0	12	7.9	0.8	16.0	6	8.5	Sail Porosity: 36-43%
Keinonen (1977)	1.1	7.5	16	5.9	0.5	17.5	3	9.1	
Gulf of Bothnia	3.4	13.8	26	46.3	28.0	42.0	53	803.7	
Palosuo (1974)	1.5	15.3	11	29.3	7.0	32.0	24	92.0	
	1.8	10.0	19	12.5	14.0	46.1	31	328.1	
	1.4	9.4	17	10.5	14.0	40.3	35	231.0	
Gulf of Bothnia:	1.1	35.0	3	4.8	6.0	46.3	15	41.8	Ridge Geometry
Palosuo (1971)	1.1	66.0	1	7.8	7.3	67.0	12	95.2	Interpolated
Port Colborne, Anon ('77)	3.5				5.8				
" Anon ('78)	3.0				4.0				
" Anon ('79)	1.8				2.7	15.0			
" Anon ('79)	1.2				1.5	30.0			
" Anon ('80)	1.5				3.4	150.0			
Gulf of Bothnia:	0.8				8.0				
Palosuo (1974)	0.4				0.9				
	0.4				0.9				
	0.7				6.0				
	1.2				8.0				
	2.6				20.0				
	0.8				6.5				
	0.7				2.0				
	1.8				14.0				
	1.4				14.0				
	2.7				15.0				
	1.7				10.0				
Great Slave Lake:	3.1				6.7		Mean Keel		
Comfort (1980)							Angle:		
							16°±13°		

1. Equiv. Sail Area = $A_I + A_S \frac{pice - psnow}{pice}$

where A_I = Area of ice in sail

A_S = Area of snow in sail

pice = Ice Density (taken as 0.9 g/cc)

psnow = Snow Density (taken as 0.3 g/cc)

force which always acts perpendicularly to the direction of floe motion.

Analyses of the sensitivity of the ice floe drift rate to the Coriolis force were conducted. It was found that, for the range of ice floe masses, windspeeds and current speeds considered, the inclusion of the Coriolis force term typically increased the predicted ice drift rate by less than 5%. This is not significant within the precision of the analysis conducted. Consequently the Coriolis force term was neglected and the ice drift rate was calculated by balancing the wind drag and current drag forces acting on the floe.

The wind and current were assumed to be colinear and to drive the ice floe perpendicular to the shore. This is the condition that will cause maximum scour and will result in a conservative analysis.

The ice drift rate resulting from the combination of a given windspeed and current speed at steady state can be estimated from the equation of motion. This may be written as:

$$\frac{1}{2}\rho_A \, C_{DA} \, A \, V_W^2 + \frac{1}{2}\rho_W \, C_{DW} \, A_C \quad V_I - V_C \, (V_I - V_C) = 0 \qquad [2.5]$$

where ρ_A, ρ_W = mass density of air and water respectively

C_{DA}, C_{DW} = drag coefficient for air and water respectively

V_W = windspeed

V_C = current speed

V_I = ice drift rate

A = area over which drag forces act.

Since windspeed and current speed are assumed to be colinear and skin friction drag is dominant for the case considered, equation 2.5 may be rewritten to provide the following more expedient predictor of ice drift rate:

$$V_I = V_C + \sqrt{\frac{\rho_A C_{DA}}{\rho_W C_{DW}}} \; V_W \qquad [2.6]$$

2.3 Wind and Current Environmental Conditions

(i) Windspeed Data

Relatively longterm windspeed and direction data (ie. approximately 10 years of record), is available for the Nanticoke, Long Point, Port Colborne and Simcoe locations.

The annual maximum windspeed condition was used to describe winds at the site since it appeared probable that the annual maximum windspeed was likely to both occur during the winter and to blow for a sufficient time period to allow steady state drift conditions to be reached.

Data on the time of occurrence for the annual maximum windspeed at Nanticoke were not immediately available. However, since the mean monthly windspeed for Nanticoke peaked during the December to April period, it was felt to be reasonable to assume that the maximum annual windspeed would also occur during this time period.

Analyses of floe motions indicated short transient periods. The worst case considered, which was a 25 km diameter floe acted upon by a 30 km h wind and a 10 cm/s current, required approximately 5 minutes to reach steady state conditions.

As no data on the annual maximum wind speed was immediately available for Nanticoke, this parameter was estimated by increasing annual maximum windspeeds at Simcoe by 40%. (This was the mean ratio for the December to April period of mean monthly windspeeds at Nanticoke and Simcoe.)

(ii) Wind Drag Force and Energy

The wind drag force was estimated using the standard fluid drag expression as follows:

$$F_{dw} = 1/2\ \rho_A A \left(C_{D_{FA}} \cdot A_F + C_{D_{RA}} \cdot A_{RS} \right) Vw^2 \qquad [2.7]$$

where $C_{D_{FA}}$ = air drag coefficient for smooth floe

A_F = horizontal area of floe

$C_{D_{RA}}$ = air drag coefficient for ridge

A_{RS} = cross sectional surface area of ridge sail.

The work done by the wind drag force during scouring may be estimated as:

$$F_{dw} \cdot L \qquad [2.8]$$

where L = length of scour.

(iii) Current Speed Data

Currents in the proposed cable corridor were measured by Faroqui (1981) for a total of approximately three months during the summer and fall of 1980 near the Coho approach area two metres above the bed. It is difficult to draw general conclusions regarding currents with the relatively small data base that is available. Nevertheless, the

available data does provide some understanding of the current regime and has been used in subsequent ice scour depth predictions.

(iv) Current Drag Force and Energy

The current drag force was estimated using the following relation:

$$F_{dc} = \frac{1}{2}\ell_w \left(C_{D_{FW}} A_F + C_{D_{RW}} \cdot A_{RK} \right) \left| V_I - V_C \right| \left(V_I - V_C \right) \qquad [2.9]$$

where $C_{D_{FW}}$ = water drag coefficient for smooth floe

$C_{D_{RW}}$ = water drag coefficient for ridge

During the scouring process the current drag force varies from zero, or negative (depending on the relative magnitudes of floe velocity and current velocity) at the commencement of scouring, to a maximum value at the end of scouring. Based upon our experience of studying ship-ice ramming scenarios, it is reasonable to assume that the deceleration of the floe will vary linearly during the grounding process from zero to a maximum value. Consequently, the work done by the current drag force during grounding may be expressed as:

$$\frac{F_{dw} \cdot L}{28} \qquad [2.10]$$

(v) Considerations on the Choice of Drag Coefficients

Based on measurements of wind and current drag stress on ice sheets, Michel (1978) suggests the following drag coefficient values:

HEIGHT (or depth) OF MEASUREMENT (m)	C_d	NATURE OF SURFACE
10 (air)	.0019	smooth snow-covered surface
10 (air)	.0052	gently rolling hummocked
10 (air)	.0066	rafted
0.5 (water)	.010	smooth
0.5 (water)	.040	rough
0.5 (water)	.094	very rough

It was decided to adopt wind and current skin friction drag coefficients of 0.005 and 0.05 respectively.

2.4 Soil Properties

Geotechnical investigations, Cheng (1980; 1981), were undertaken to determine the properties of the sediments comprising the lake bottom.

The approach areas were divided into regions for subsequent analyses of similar bed slope and soil properties. Figures 2 and 3 show the regions that were selected, as well as soil properties and bed slope used for each section.

The geotechnical activities included offshore boreholes, (over 600), in the shallow water approaches and lake bottom sediment gravity sampling over the remainder of the

FIGURE 2

SOIL PROFILE FOR LAKE ERIE, OHIO, USA

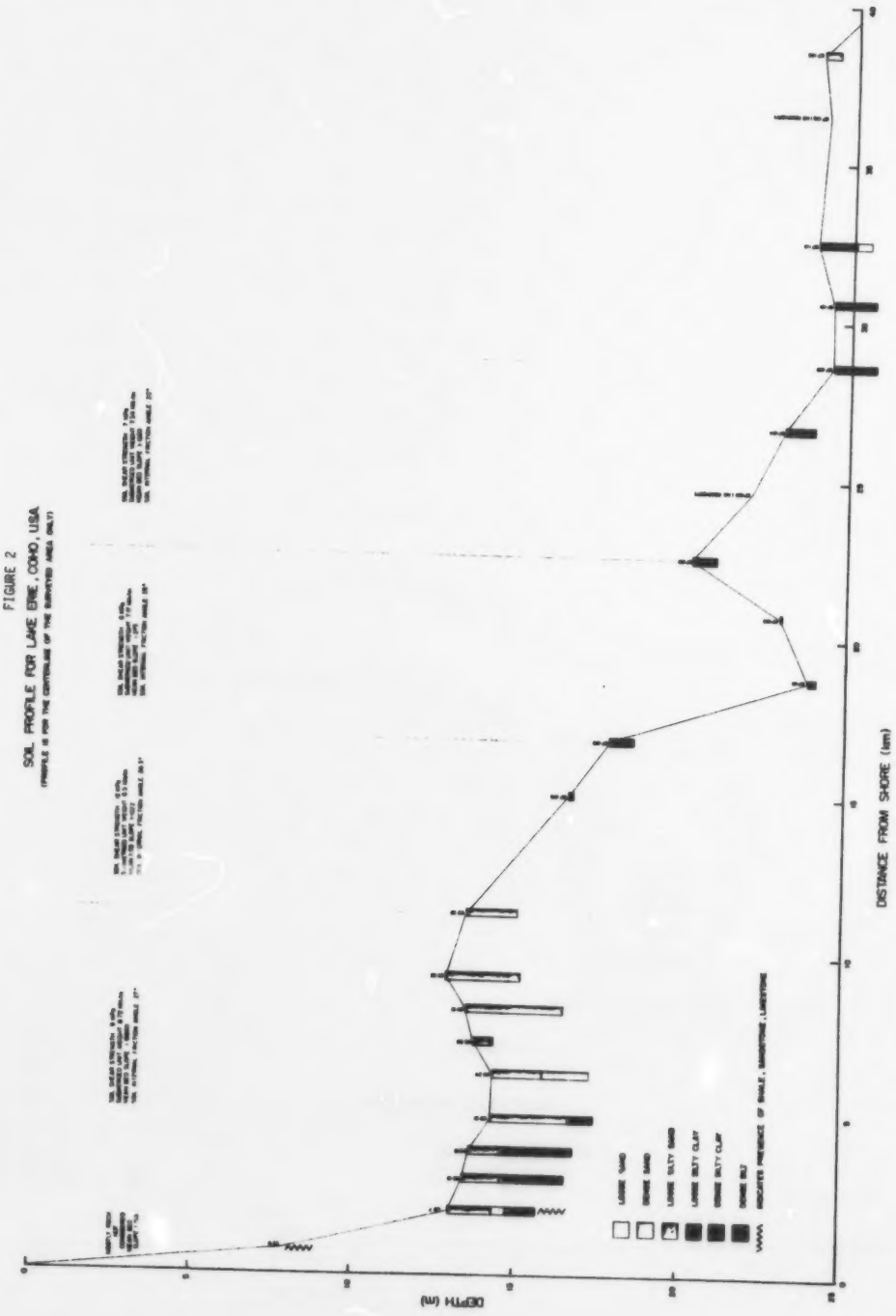

Figure 3

SOIL PROFILE FOR LAKE ERIE, NANTICOKE, CANADA

(PROFILE IS FOR THE CENTERLINE OF THE SURVEYED AREA ONLY)

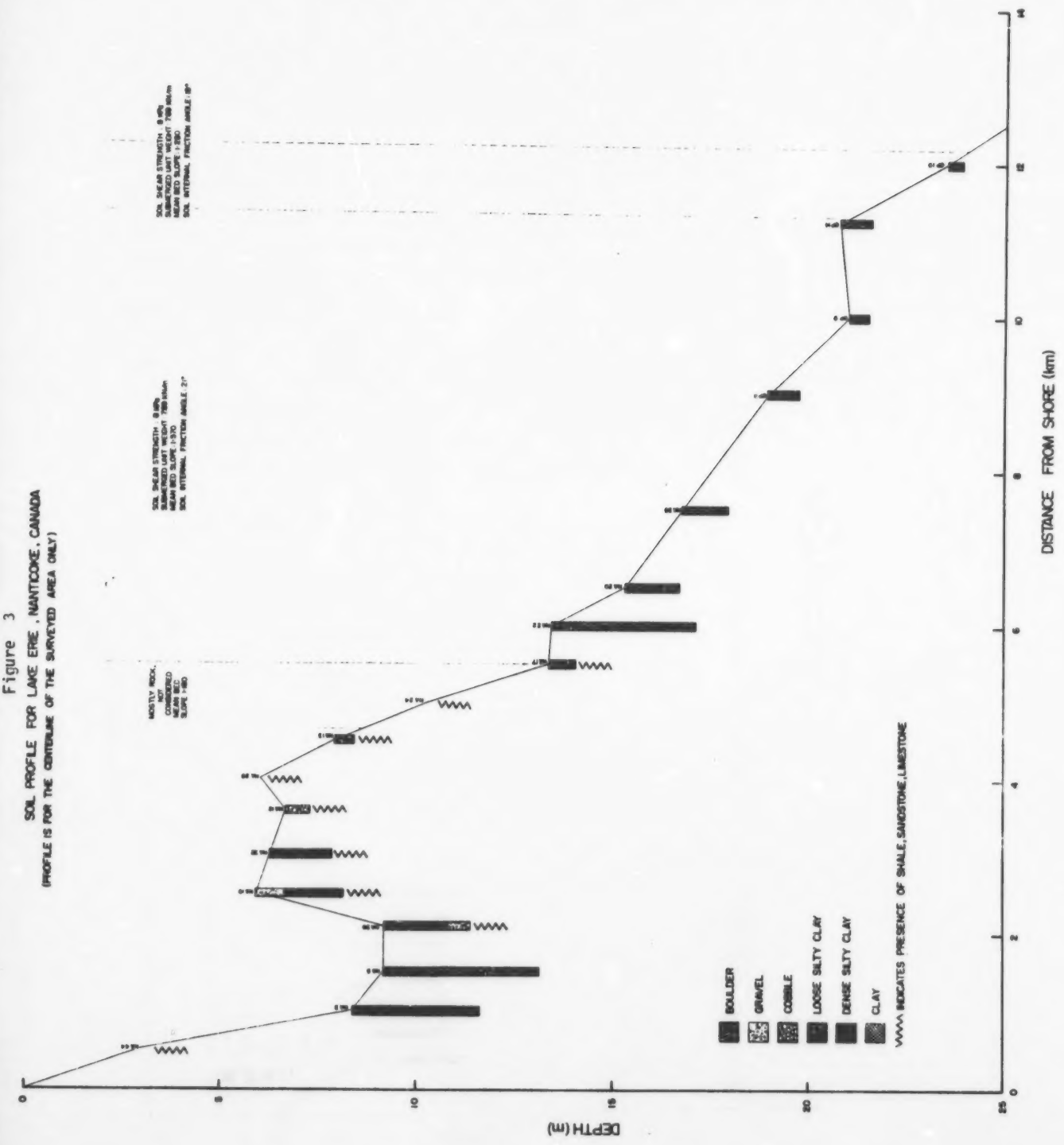

corridor. Geophysical data were used to complete the stratigraphy and provide a broad overview. Disturbed soil samples were recovered using benthos-gravity coring and vibracoring equipment. The maximum depth of sampling was 2.8 m. Laboratory tests were done on each sample.

According to sieve analyses, all soft sediments found in areas where ice scouring is active can be described as clayey silt with a trace of find sand. In some samples in the open area the clay content is higher, whereas, in the Coho approach areas, the soil can be described as silt with some clay and sand.

All samples analyzed in the lab have a natural water content higher than the liquid limit, indicating the presence of a sensitive material. It is known that sensitive materials lose part of their shear strength upon remolding.

In the Nanticoke approach area, the soil has low plasticity and the average natural water content is slightly higher than 30%. Laboratory vane tests on disturbed samples indicated low shear strength values, varying between 5 and 11 kPa. The average unit weight of the soil samples is about 1800 kg/m^3. The silty clay is apparently of low sensitivity.

The geotechnical properties of the sediments in the Coho approach area were not well known (at the time). No shear strength evaluation was provided but it is probable that the shear strength of these sediments is approximately the same as the values obtained for similar sediments in the Nanticoke approach and mid-lake areas. The average unit weight of the samples in the Coho area is about 2200 kg/m^3 and the natural water content is quite erratic, ranging from 12.8 to 42.0%.

It is difficult to evaluate the in-situ shear strength of the soft sediments. The shear strength values given by laboratory vane tests on remolded samples of sensitive materials are typically lower than those determined by in-situ tests. Field vane tests have recently been performed along the proposed cable corridor; preliminary reports (Grass, 1981), indicate shear strength values of the same order as those obtained from the laboratory vane tests (ie. 5 to 10 kPa). Consequently, the laboratory shear strength values used during subsequent analyses can be taken to be representative of the field values.

2.5 Observed Scours

Ice scours were found in the soft sediments in the Nanticoke and Coho approach areas during geotechnical investigations carried out by Ontario Hydro during the 1980 and 1981 summers (Gheng/Grass, 1980; 1981).

Individual lakebed scours were observed to extend approximately 0.1 to 7.5 km in length and were highly variable in both breadth and depth over their length, reflecting differences in both lakebed properties (eg. bed slope, soil type and strength) and ice ridge mechanical properties.

The following table summarizes the scour data that was collected.

REGION	NO. OF INDIV. SCOURS		MEAN SCOUR DEPTH & STD. DEV. (M)		EXTREME SCOUR DEPTH (M)	MEAN SCOUR BREADTH & STD. DEV. (M)		EXTREME SCOUR BREADTH (M)
	1980	1981	Max. Depth Per Indiv. Scour	All Meas.		Max. Brdth Per Indiv Scour	All Meas.	
NANTI-COKE	7	10	1.23±0.3	0.96±0.4	1.7	76±38	46±32	140
COHO	No Data	5	0.3 ±0.1	0.27±0.1	0.4	29±22	-	60

NOTES: 1. Above scour data is for all regions of approach areas where scours were observed. Water depths ranged from 9 to 24 m. Figures 2 and 3 show lakebed properties for these areas.

2. Scour breadths were only measured in the 1981 survey.

The available scour depth and breadth measurements have been related to known probabilistic distribution, (ie. normal, lognormal and Gumbel extreme value), to gain an understanding of the maximum scour depth and breadth that is probable. The Gumbel extreme value distribution provided the best degree of fit (see Figure 4).

FIGURE 4

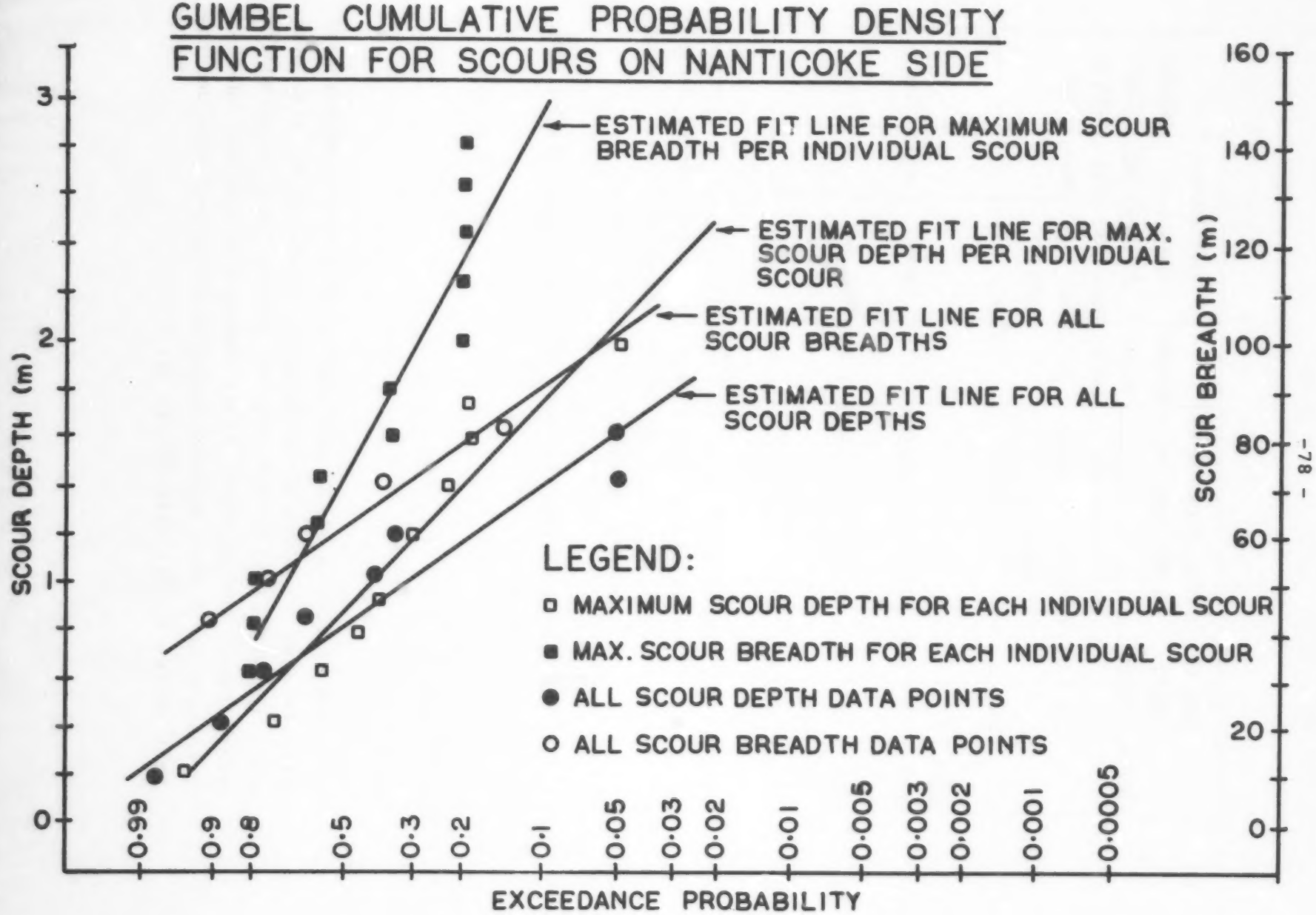
GUMBEL CUMULATIVE PROBABILITY DENSITY FUNCTION FOR SCOURS ON NANTICOKE SIDE
ESTIMATED FIT LINE FOR MAXIMUM SCOUR BREADTH PER INDIVIDUAL SCOUR
ESTIMATED FIT LINE FOR MAX. SCOUR DEPTH PER INDIVIDUAL SCOUR
ESTIMATED FIT LINE FOR ALL SCOUR BREADTHS
ESTIMATED FIT LINE FOR ALL SCOUR DEPTHS
LEGEND:
MAXIMUM SCOUR DEPTH FOR EACH INDIVIDUAL SCOUR
MAX. SCOUR BREADTH FOR EACH INDIVIDUAL SCOUR
ALL SCOUR DEPTH DATA POINTS
ALL SCOUR BREADTH DATA POINTS
SCOUR DEPTH (m)
SCOUR BREADTH (m)
EXCEEDANCE PROBABILITY
0
1
2
3
20
60
80
100
120
140
160
0·99
0·9
0·8
0·5
0·3
0·2
0·1
0·05
0·03
0·02
0·01
0·005
0·003
0·002
0·001
0·0005

SCOUR DEPTH PREDICTIONS

3.1 Theoretical Energy Models

3.1.1 Background

Chari (1979) proposed a theoretical model to describe ice gouging of seafloor sediments by an iceberg. The model estimates the scour depth by balancing the kinetic energy of the drifting berg, along with the work done by current and wind drag forces during scouring, with the work done in deforming the soil. The seabottom sediments have low strength in relation to the iceberg so that soil failure is the critical criterion during the interaction.

Chari assumes that in the process of scouring, the iceberg scoops out a series of soil wedges and the resistance to the iceberg movement is primarily the frontal resistance on the scouring face. The failure model is therefore of Coulomb type: a planar failure surface inclined at an angle 0 to the horizontal ($\theta = \pi/4 + \phi/2$, where ϕ is the angle of internal friction of the soil).

In the calculations, it is assumed that the surcharge material does not contribute any shear resistance as it is remolded and would not have settled for sufficient time to regain its strength before being moved again by the iceberg. It is also assumed that the soil strength is independent of the strain rate; is the same in all directions; and is equal to the 'undrained' strength.

The passive soil resistance to the moving iceberg is determined by limit equilibrium analysis, resolving forces along the X and Y axes. In these calculations, the shear strength at both faces of the wedge are added to the shear strength along the inclined face, whereas the forces due to

friction along the sides and the bottom of the iceberg are neglected. It is also assumed that the shear strength is completely mobilized at failure.

Chari's model may be expressed by the following relation, for the case of ϕ equal to zero:

$$F_{WD}L + \frac{F_{CD}L}{28} + \frac{MV^2}{2} = \gamma' \frac{(H+D)^2}{6} BL + \tau DLB + \frac{\sqrt{2}}{3} \tau D^2 L \qquad [3.1]$$

where
- M = mass of iceberg
- V = drift rate of iceberg
- γ' = submerged unit weight of sediment
- H = surcharge height
- D = scour depth
- B = breadth of scour
- L = length of scour
- τ = soil shear strength
- F_C = current drag force
- F_W = wind drag force

In an attempt to improve Chari's analysis, Pilkington (1975) proposed a second theoretical model based also on energy considerations. The basic differences are the determination of the surcharge height and of the inclusion of the side friction. Pilkington (1975) assumed that the surcharge material would be deposited at the bed slope angle. This fixes the H/D ratio at $\sqrt{2}$.

The following relation results from the theoretical model proposed by Pilkington:

$$F_{WD}L + \frac{F_{CD}L}{28} + \frac{MV^2}{2}$$
$$= L^2B\,(1+\sqrt{2})\,\tan\alpha \left[\frac{(1+\sqrt{2})L\tan\alpha}{6} + \tau\right] + \frac{\mu\gamma'\tan^2\alpha L^4}{12} \qquad (3.2)$$

where
- α = bed slope
- μ = ice-soil friction coefficient

Although neither of these models describes the case being considered, they were both exercised for a range of input parameters. The results obtained from these models provide upper limit estimates of the maximum scour depth since it will be limited by the flexural and shear strength of the ridge creating the scour.

3.1.2 Scour Depths Predicted By Theoretical Energy Models

Both the Pilkington and Chari models were exercised for a range of environmental input parameters at the 0.5, 0.1 and 0.01 exceedance probability level. (See Table 1 for values). In addition, the ice-soil friction factor, (for the Pilkington model), was varied from zero to tan ϕ.

The ridge size used was governed by the minimum ridge keel depth necessary to inititate scouring at the deepest water depth over the range of water depths considered.

Pilkington (1975) suggested that the hydrodynamic added mass of the ice was significant in some cases and should be included in equations 3.1 and 3.2. Since calculations showed that the added mass of the ice floe/ridge system would be less than 10% of the mass of ice floe itself, this term was neglected. Tables 3 and 4 summarize the scour depths predicted by the two models.

Table 5 lists the maximum predicted scour depths for the two models for the range of environmental inputs considered. As would be expected, the deepest scours were predicted to occur for the combination of the highest drift rate, windspeed, current speed, ice floe diameter and ice thickness (ie. the 0.01 exceedance probability level conditions) and for the narrowest ridge keel (ie. the 0.5 exceedance probability level condition).

TABLE 3

PREDICTED SCOUR DEPTH: NANTICOKE APPROACH AREA

		Water Depth Range (M)	Bed Slope	Exceedance Probability Level of All Individual Environmental Inputs (See table 1):					
				0.5		0.1		0.01	
				Theoretical Model		Theoretical Model		Theoretical Model	
				Pilkington	CHARI	Pilkington	CHARI	Pilkington	CHARI
Soil Shear Strength : Measured Values (ie. ~10kpa)	Ice-soil Friction Factor:0	9-13	1:187	0.4	0.6	2.5	3.1	7.9	8.8
		13-21	1:569	0.3	0.4	2.0	2.5	7.0	7.6
		21-24	1:292	0.3	0.5	2.2	2.6	7.3	7.9
	Ice-soil Friction Factor: Tan ϕ	9-13	1:187	0.4	-	2.4	-	7.6	-
		13-21	1:569	0.3	-	1.9	-	6.3	-
		21-24	1:292	0.3	-	2.1	-	6.8	-

Notes: 1. Predicted scour depths in metres

2. Predicted scour depth values for Chari model are obtained for $H/D = \sqrt{2}$

TABLE 4

PREDICTED SCOUR DEPTH: COHO APPROACH AREA

		Water Depth Ranges (M)	Bed Slope	Exceedance Probability Level of All Individual Environmental Inputs (See table 1)					
				0.5		0.1		0.01	
				Theoretical Model		Theoretical Model		Theoretical Model	
				Pilkington	Chari	Pilkington	Chari	Pilkington	Chari
Soil Shear Strength Measured Values (ie. ~10 kPa)	Ice-soil Friction Factor: 0	0-13	1:154	0.5	0.7	2.6	3.1	7.9	8.5
		13-13.5	1:18483	0.2	0.3	1.8	2.4	6.5	7.2
		13.5-18	1:1222	0.2	0.3	1.7	2.4	6.9	7.9
		18-20	1:375	0.4	0.5	2.4	2.9	7.8	8.3
		20-24	1:1500	0.2	0.3	1.9	2.4	6.9	7.5
	Ice-soil Friction Factor = Tan ϕ	0-13	1:154	0.5	-	2.5	-	7.4	-
		13-13.5	1:18483	0.1	-	0.9	-	2.5	-
		13.5-18	1:1222	0.2	-	1.5	-	5.3	-
		18-20	1:375	0.4	-	2.3	-	7.0	-
		20-24	1:1500	0.2	-	1.6	-	5.3	-

Notes: 1. Predicted scour depths in metres

2. Predicted scour depth values for Chari model are obtained for $H/D = \sqrt{2}$

TABLE 5

MAXIMUM PREDICTED SCOUR DEPTHS

Approach Area	Theoretical Model	Water Depth Range (M)	Bed Slope	Ice - Soil Friction Factor: 0	Ice - Soil Friction Factor: Tan ϕ	Comments
Nanticoke	Pilkington	9-13	1:187	16.1	12.7	1. Predicted scour depths in metres.
		13-21	1:569	12.6	8.6	2. For range of environmental inputs considered, (ie. exceedance probability levels of 0.5,0.1 and 0.01), the maximum scour depth always occurred at the following conditions:
		21-24	1:292	12.2	9.6	
	Chari	9-13	1:187	20.1	-	
		13-21	1:569	15.8	-	
		21-24	1:292	15.3	-	
Coho	Pilkington	0-13	1:154	15.4	11.2	° floe thickness: 0.01 exc. prob.
		13-13.5	1:18483	14.0	2.7	° floe diameter : 0.01 exc. prob.
		13.5-18	1:1222	13.8	6.8	° ridge keel breadth: 0.5 exc. prob. and mass
		18-20	1:375	13.9	9.5	° ice drift rate, : 0.01 exc. prob. windspeed and current speed
		20-24	1:1500	12.2	6.4	
	Chari	0-13	1:154	19.0	-	3. The H/D ratio for the Chari model was varied from 1.0 to 2.0. The maximum scour depth always occurred for H/D equal to 1.0.
		13-13.5	1:18483	17.6	-	
		13.5-18	1:1222	17.7	-	
		18-20	1:375	17.3	-	
		20-24	1:1500	15.4	-	

3.2 The Limiting Scour Depth

In the previous section, scour depths have been calculated by balancing the available kinetic energy of the drifting ice mass, as well the work done by wind drag and current drag forces during scouring, against the work done in deforming the lake bottom sediments. However, it is felt that this treatment is not realistic, for the case of ridges in Lake Erie, since shear and flexural failures of the scouring ridge will limit the force applied to the lake bottom.

Upon contact with the lake bottom, the keel of the ridge will probably be sheared, (since the bottom part of the keel consists of unconsolidated ice blocks), to an angle which conforms with the lakebed. The vertical force which is applied to the ridge which will increase and eventually result in a flexural failure. Figure 5 depicts the interaction scenario pictorially.

The vertical force (P_V) applied to the ridge keel is related to the ice-soil friction factor (μ) and the angle between the lakebed and the ridge (α) as follows:

$$P_V = \left(\frac{\cos\alpha - \mu \sin\alpha}{\sin\alpha + \mu \cos\alpha} \right) P_H \qquad [3.5]$$

where P_H = horizontal force applied to lakebottom.

Figure 6 shows the relationship graphically.

FIGURE 5

INTERACTION SCENARIO CONSIDERED

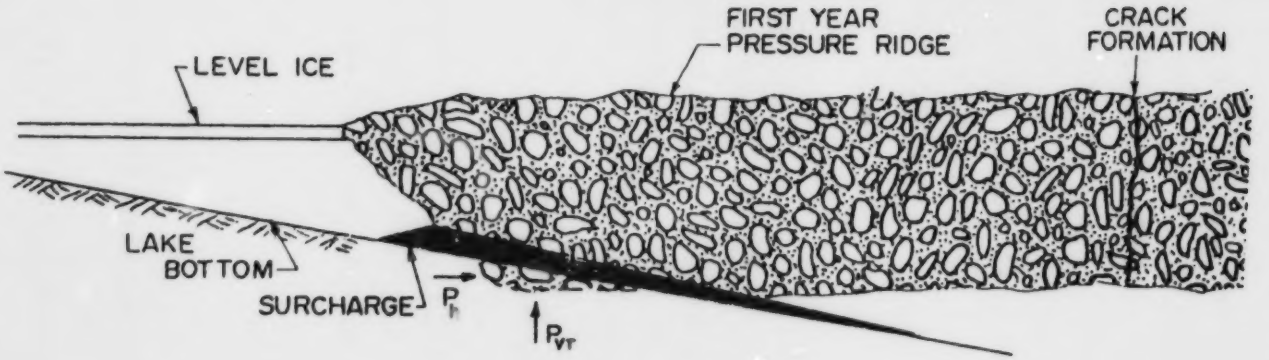

SOIL RESULTANT FORCE ON VERTICAL
AND SLOPED KEEL SHAPE

FIGURE 6

EFFECT OF KEEL SHAPE ON
THE RATIO OF THE UPLIFTING
FORCE TO THE HORIZONTAL FORCE

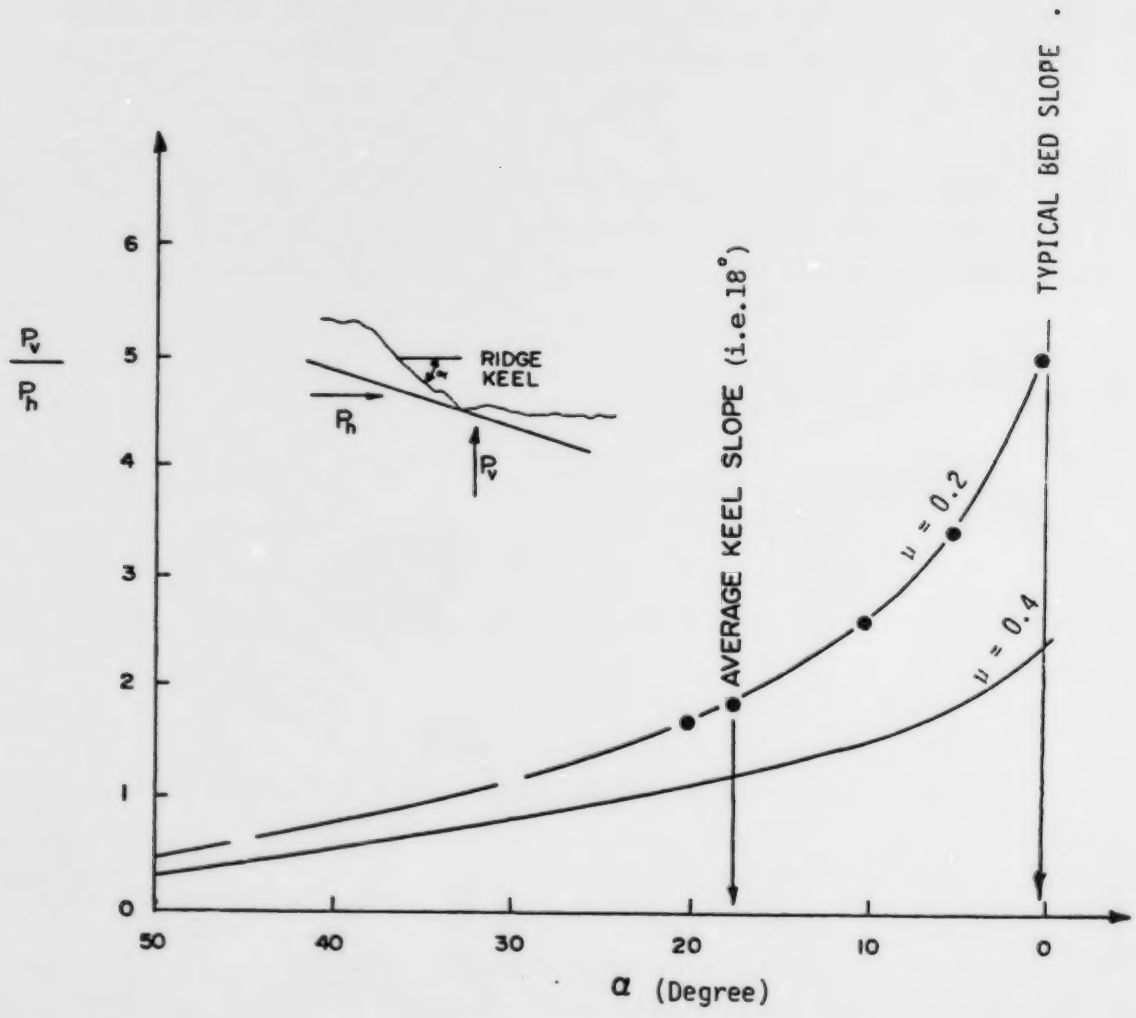

Little model or full scale data is available for corroboration of Figure 6. In reduced scale scouring experiments, Abdelnour (1981) reported that the horizontal and vertical forces were approximately equal for a 63° slope. Croasdale (1981) reported a vertical force to horizontal force ratio of 0.17 for a vertically-faced ice island. Consequently, it is probable that Figure 6 represents a pessimistic view. However, in the absence of extensive field or model scale data, we have elected to use Figure 6 since it produces conservative results.

The flexural strength of the ridge may be estimated from Hetenyi's (1946) analysis of vertical lifting forces applied to a semi-infinite beam on its free end as follows:

$$P_V = \frac{\lambda M}{e^{-\lambda x} \sin \lambda x} \qquad [3.6]$$

where $$\lambda = \sqrt[4]{\frac{\rho_w g}{E H^3}} \qquad [3.7]$$

$$M = \frac{\sigma B H^3}{24} \text{ (for a triangular keel shape)} \qquad [3.8]$$

σ = ridge flexural strength

B = ridge breadth (taken as 3.5 times the ridge depth)

H = ridge depth

$\rho_w g$ = weight density of water (taken as 10,000 N/m^3)

E = ridge modulus of elasticity (taken as 5000 times the ridge flexural strength which is typical of field measurements of ice mechanical properties).

NOTE: Ice sheet is poorly bonded to ridge and it is assumed that it tears away during the interaction.

By substituting equations (3.7) and (3.8) in equation (3.6) and giving a value to λx of 0.8 (ie. the dimensionless location of the maximum moment - Nevel (1965)), the following expression is obtained:

$$P_V = 0.129\ \sigma\ BH^2 \sqrt[4]{\frac{\ell_w g}{EH^3}} \qquad [3.9]$$

On the other hand, the horizontal scouring force predicted by Chari (1979) is given as follows for cohesive poorly-drained sediments:

$$P_H = \frac{\gamma'(H+D)^2\ B}{6} + CDB + \sqrt{\frac{2}{3}}\ C\ D^2 \qquad [3.10]$$

where γ' = submerged weight density of soil
D = scour depth
B = scour breadth (taken as 3.5 times the scour depth)
C = soil cohesion (soil internal angle of friction taken as 0°, since it is assumed that pore-water pressures will not have had sufficient time to dissipate during the interaction)
H = height of surcharged material.

Equations [3.10], [3.9] and [3.5] were solved to estimate the probable scour depth for the following range of input parameters:

Water Depth: 15 m; 20 m; 25 m
Ice-soil Friction Coefficient: 0.2; 0.4; 0.6
Ice Ridge-lakebed Angle: 0.1°; 30°, 45°
Ice Ridge Flexural Strength: 0.1 MPa; 0.2 MPa
Soil Cohesion: 10 kPa; 50 kPa
Soil Submerged Unit Weight Density: 6500 KN/m^3
(ie. the minimum submerged soil unit weight in the study area)
Ratio of Surcharge Height to Scour Depth (H/D): 1.0; 1.414; 2.0.

Figures 7, 8 and 9 show the results of this analysis graphically.

The following discussion provides some insight into the selection of the values of the various parameters.

- "WATER DEPTH" The scour depth is related to the water depth since this governs the size of the ridge which is responsible for creating the scour. Deeper scours are predicted for deeper water depths; on the other hand, these events are of lower probability than those in shallower water.

- "ICE-SOIL FRICTION COEFFICIENT" Unfortunately, little data is available to guide the selection of the ice-soil friction coefficient. However, based on a knowledge of typical ice-ice friction coefficients (ie. 0.1 to 0.2) and soil to soil friction coefficients (ie. tan ϕ for granular soils), it is felt that the probable value will be encompassed by the range considered.

FIGURE 7

ICE SCOUR DEPTH PREDICTION SUMMARY

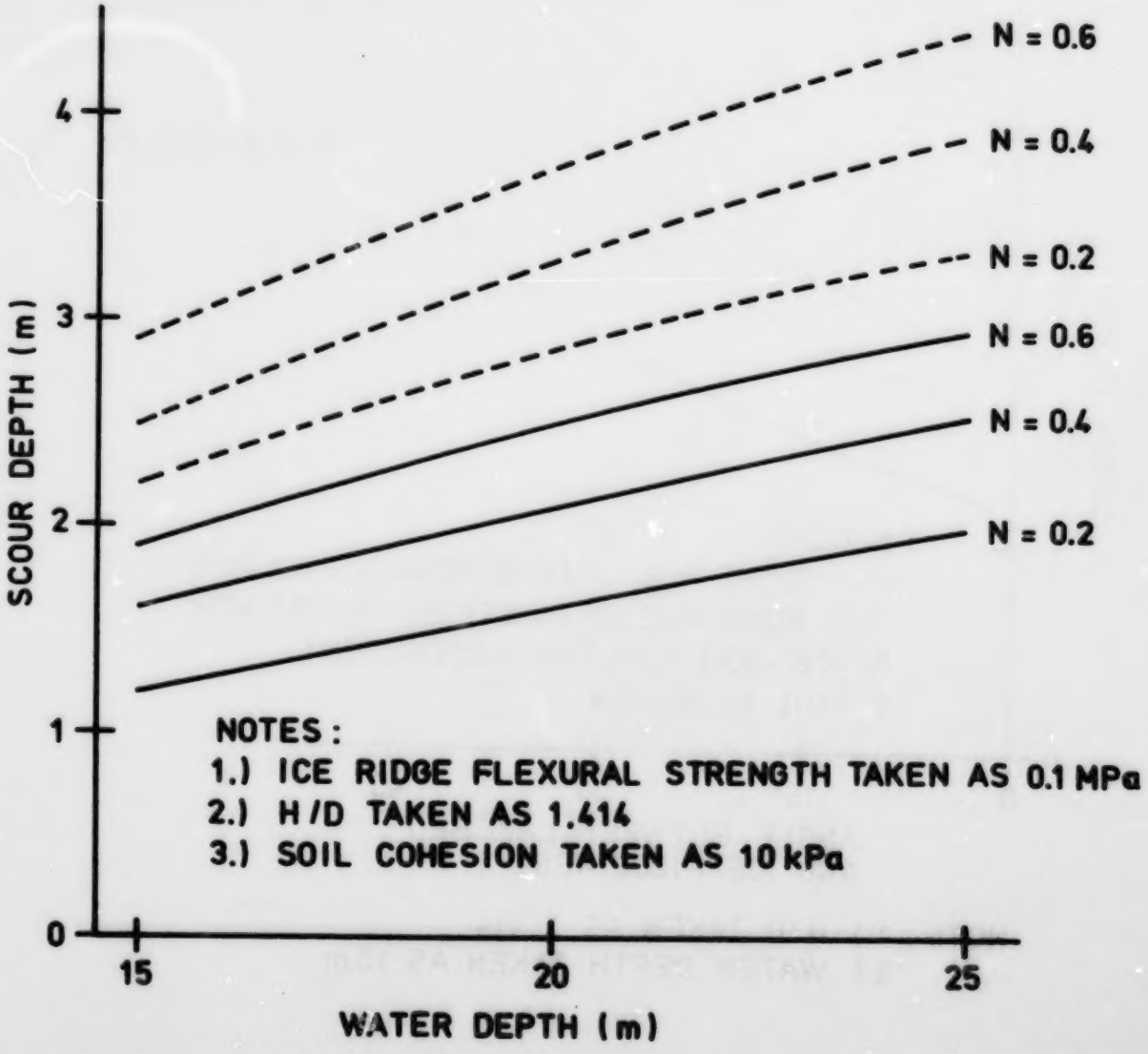

FIGURE 8

SENSITIVITY OF PREDICTED SCOUR DEPTH TO RIDGE FLEXURAL STRENGTH AND SOIL COHESION

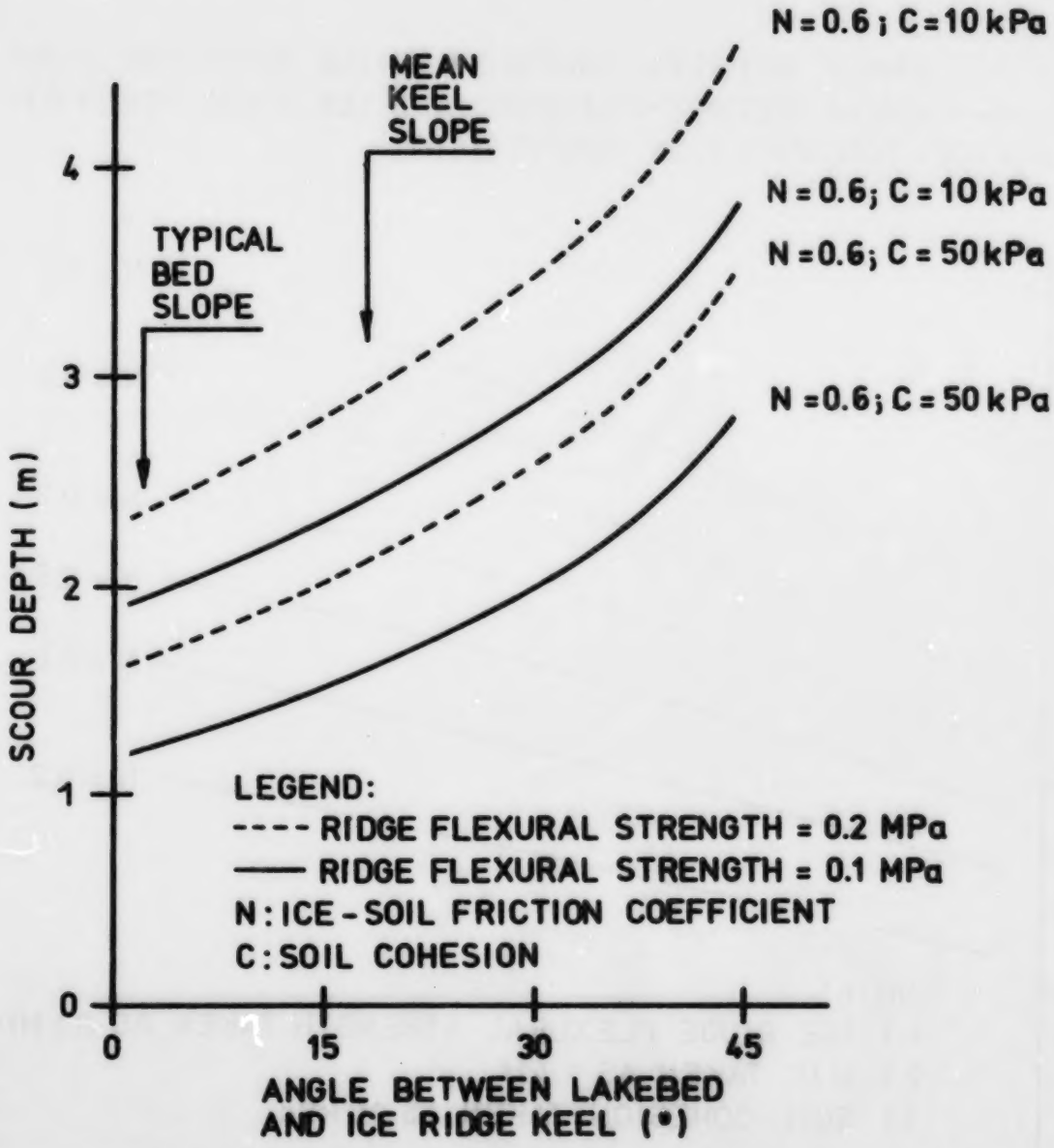

NOTE: 1.) H/D TAKEN AS 1.414
2.) WATER DEPTH TAKEN AS 15 m

FIGURE 9

ICE SCOUR DEPTH SENSITIVITY ANALYSIS

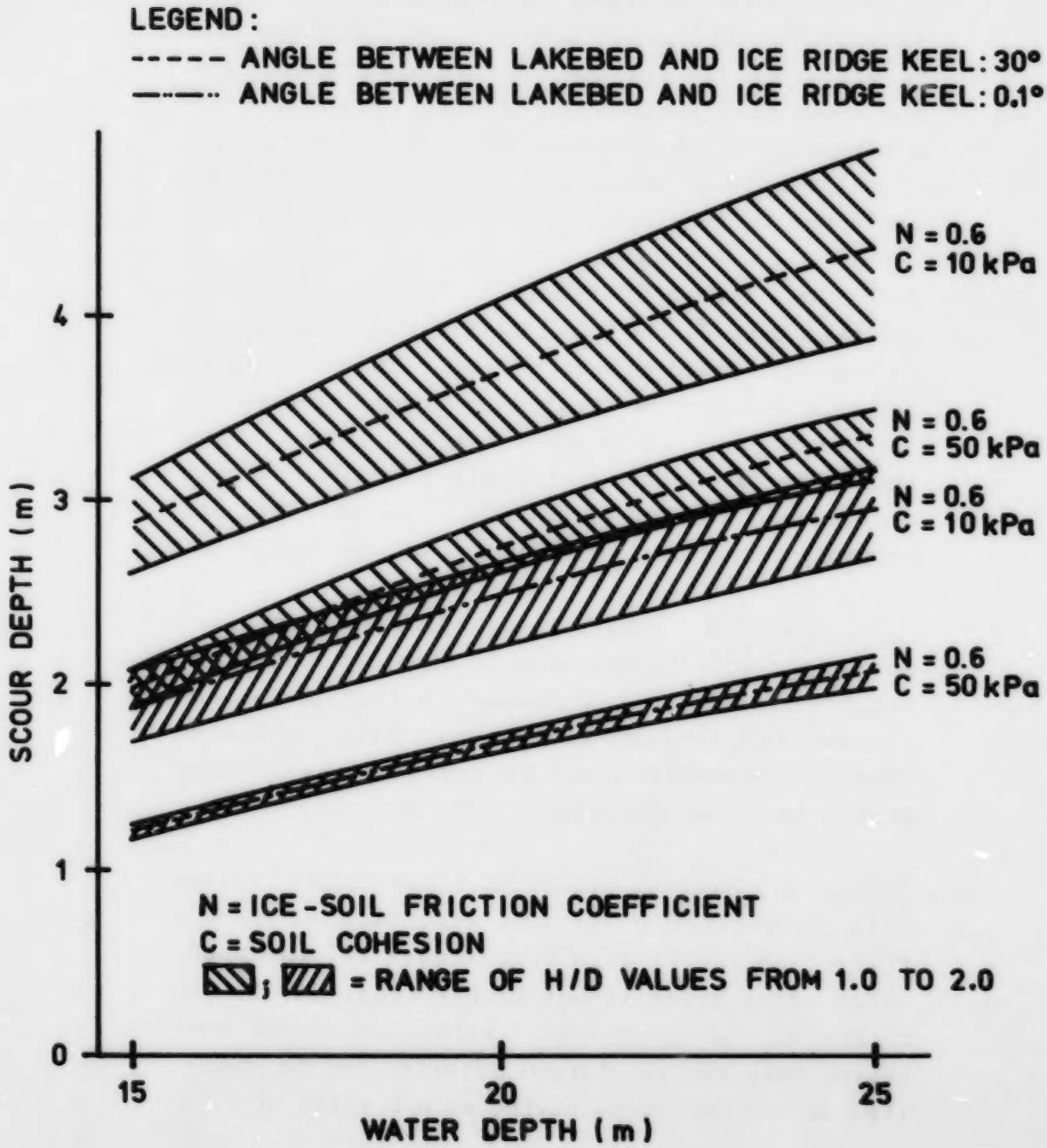

- "ICE RIDGE KEEL-LAKEBED ANGLE" The angle between the ridge keel and the lakebed is a critical parameter as it governs the vertical force which is applied to the ridge. It is most probable that this angle will range between the bed slope (ie. 0.0031° to 0.37° for the submarine corridor) and the mean keel slope (ie. 18°) for the fresh ice and brackish ice ridges considered - see Section 2). The curves shown in Figure 13 for the 30° angle may be considered a practical upper limit.

- "ICE RIDGE FLEXURAL STRENGTH" There is unfortunately no data on the apparent flexural strength of an unconsolidated pressure ridge. However, keeping in mind that the flexural strength of lake ice (ie. fresh ice) is between 500 and 1000 kPa, we feel that the range of ridge flexural strengths considered (ie. 100 to 200 kPa), is realistic and probably represents the high end of the spectrum.

- "SOIL COHESION" The soil cohesion is a critical parameter affecting the soil shear strength and the scour depth. As discussed in Section 2, laboratory and in-situ field tests have indicated that the probable shear strength of the lakebed sediments is on the order of 10 kPa.

- "RATIO OF SURCHARGE HEIGHT TO SCOUR DEPTH" Little data is available for the selection of an H/D ratio. As can be seen from Figure 10, the predicted scour depth is not highly sensitive to the choice of this parameter. Pilkington (1975) suggested that the surcharged material may be deposited at the bed slope giving an H/D ratio of $\sqrt{2}$.

4.0 SUMMARY AND DISCUSSION OF PROBABLE SCOUR DEPTH PREDICTIONS

Three approaches have been used to evaluate the probable scour depth in the submarine cable corridor.

If we assume that no refill has occurred and that the scours made remain intact, then scour depth estimates based on field measurements should be accurate. Unfortunately, lake bottom scours do change over time, due to the effects of many factors such as currents, wave action, and subsequent ice action. Field observations over a two year period have confirmed this for the American side while there appears to have been little change for the Canadian side over time. This reduces the reliability of this method and suggests an analytical approach for verification.

The theories available to study the scouring problem have been developed for conditions that are not completely applicable to our case. Two assumptions have been made by Chari's and Pilkington's theoretical work: firstly, that the ridge keel is much stronger than the soil and secondly, that the ice mass has a prismatic shape with no uplifting or deformation of its face during the interaction. These assumptions are justified for an iceberg; however they result in the prediction of very high scour depths since energy dissipation is done entirely by scouring rather than deforming or failing the ridge. This is felt to be unjustified for a first-year ridge and consequently we feel that these models are overly pessimistic for the case being considered.

A simple limited scour depth approach has been developed which considers the effect of the limited strength of the ridge on the scour created. This theory assumes that uplifting of the ridge will occur due to the vertical defor-

mation of the ridge. The vertical deflection of the ridge will generate flexural failure and consequently limit the scour depth. This approach shows better correlation with the observed scour depths; however, the parameters used for these calculations have not yet been investigated and any probabilistic approach to this method is still far from being understood. Further field and laboratory investigations are required to verify the accuracy of the limiting scour depth approach. Further improvements to this model could be effected by incorporating the limited shear strength of the ridge into the calculation of the limiting scour depth.

Ontario Hydro is presently considering the adoption of a 3 m burial depth for the cable (Grass, 1981). Both the field measurements and the scours predicted by the limiting scour depth approach verify the selection of 3 m as a safe burial depth.

5.0 REFERENCES

[1] ABDELNOUR, R., LAPP, D., HAIDER S., SHINDE V. and WRIGHT B., 1981, "Model Tests of Sea Scouring", POAC Symposium, Quebec City.

[2] ANONYMOUS, 1971 to 1980, "Navigation Season Extension Studies", Gulf of St. Lawrence to Great Lakes for Winters 1971 to 1980 Inclusive, St. Lawrence Seaway Authority, Transport Canada.

[3] ANONYMOUS, 1973, "Lake Melville Ice Research", Ocean Engineering Group, Memorial University, St. John's.

[4] CHARI, T. 1979, "Geotechnical Aspects of Iceberg Scours on Ocean Floors", Canadian Geotechnical Journal, Vol. 16.

[5] CHENG, K.L., GRASS, J.D., and JOHNSTON, O.A., 1980, "GPU Interconnection Lake Erie Marine Cable Crossing Geotechnical Investigation 1980 Program", Ontario Hydro Report No. S1169, Toronto.

[6] CHENG, K.L., GRASS, J.D., and JOHNSTON, O.A., 1981, "GPU Interconnection Lake Erie Marine Cable Crossing Geotechnical Investigation 1981 Program", Ontario Hydro Report No. S1425, Toronto.

[7] COMFORT, G., 1980, "Hay River Water Intake Line Damage" ARCTEC CANADA LIMITED, Report No. 598, submitted to Government of Northwest Territories.

[8] CROASDALE K.R. and MARCELLUS, R.W., 1981, "Ice Forces on Large Marine Structures", IAHR Symposium on Ice Problems, Quebec City.

[9] FAROQUI, R., 1981, "Lake Erie Cable Crossing: Summary of 1980 Hydrologic Investigations, Interval Report 81346", submitted to Ontario Hydro, Toronto (proprietary).

[10] GRASS, J.D. 1980, "GPU Interconnection Lake Erie Submarine Cable Crossing Ice Scour Study", Report No. 80463, Ontario Hydro, Toronto.

[11] GRASS, J., 1981, Ontario Hydro, Personal Communication.

[12] GRASS, J.D., 1981, "GPU Interconnection Lake Erie Submarine Cable Crossing Ice Scour Study, Report No. 81317" (Supplementary to Report No. 80463), Ontario Hydro, Toronto.

[13] HETENYI M., 1946, "Beams on Elastic Foundations", the University of Michigan Press, Ann Harbour, Michigan.

[14] KEINONEN, A., 1977, "Measurements of Physical Characteristics of Ridges on April 14 and 15, 1977", Winter Navigation Research Board, Finland and Sweden.

[15] MICHEL, B., 1980, "Ice Mechanics", Laval University Press, Laval, Quebec.

[16] NEMAC, A.O. and MILLS, D.A. et al, 1973, "Lake Melville Ice Investigation", Labrador, POAC '73, University of Iceland.

[17] NEVEL, D.E., 1965, "A Semi-Infinite Plate on an Elastic Foundation, Research Report 136, U.S. Army Material Command, Cold Regions Research and Engineering Laboratory, Hanover, New Hampshire.

[18] PALOSUO, E., 1974, "The Formation and Structure of Ice Ridges in the Baltic", University of Helsinki Research Report No. 12, Finland.

[19] PALOSUO, E., 1971, "Ice Ridges in a Coastal Area of Finland, POAC '71. Trondheim, Norway.

[20] PILKINGTON, R., and IYER, H., 1975, "An Analytical Study of Ice Scour on the Sea Bottom", APOA Project 69.

PRELIMINARY RESULTS OF SUBMERSIBLE OBSERVATIONS ON THE LABRADOR SHELF

H.W. Josenhans and J.V. Barrie
Atlantic Geoscience Centre, Dartmouth

(From Scientific and Technical Notes in Current Research, Part B, Geological Survey of Canada Paper 82-1B)

ABSTRACT

Iceberg scour marks are the most dominant surface features on the Labrador Shelf and have until recently been described only on the basis of acoustic data. Regional acoustic mapping and sediment sampling on the Labrador Shelf as well as a detailed study on Makkovik Bank in the area of the Bjarni wells (Lewis and Barrie, 1980) have increased our understanding of the frequency and morphological characteristics of iceberg scour marks but lack detailed definition that can only be obtained by submersible observations. Side-scan sonar and high resolution Huntec profiles suggest a relationship between iceberg scour mark morphology and sediment properties that warrants more detailed investigation by submersible. Also submersible observations of the local seabed dynamics are necessary to determine the degradation rate of scour marks in order to ultimately establish their recurrence interval. In October 1981 the use of the Pisces IV manned submersible provided visual and photographic documentation of the seabed within the Bjarni area and provided a vehicle for precise surficial sampling in iceberg-scoured terrain and over areas of bedrock outcrop. Our three main objectives were to: 1) investigate areas of the seafloor that have been actively disrupted by the grounding keels of icebergs and to note the degradation of these scour marks by the superimposed current regime and benthic biological activity; 2) provide ground truth for the acoustic data and note the modern sedimentary environment in terms of erosion or deposition; and 3) describe and sample a section of Tertiary (?) outcrop.

ABSTRACT

Submersible Observations of Iceberg Furrows in Glacial Till, Northeast Newfoundland Shelf: and in Sand and Gravel, Grand Banks of Newfoundland

C.F.M. Lewis and G.B. Fader
Atlantic Geoscience Centre
Geological Survey of Canada
Bedford Institute of Oceanography

Observations from the research submersible PISCES IV of relic iceberg furrows in glacial till on the Northeast Newfoundland Shelf in water depths of 180 m, show that the troughs of the furrows are very flat and consist of well-sorted, angular, cobble-sized clasts. Large boulders are compressed into the substrate. Furrows are abundant, virtually saturating the seabed surface. Most furrows are less than 100 m in width, their shoulders or berms marked by linear ridges of exposed boulders projecting one to five metres above the adjacent furrow troughs. The berms slope more steeply inward toward the troughs than outward. A conspicuous paucity of sediment in the troughs of the furrows indicates that little deposition of sediment by ice rafting or other mechanisms has taken place since the furrows were formed.

Observations of iceberg furrows in water depths of 80 m on the Grand Banks of Newfoundland in the Hibernia discovery area across a sand and gravel seabed show that the furrows are less numerous and much less well defined, even though they are inferred to be younger. The icebergs appear to have broken through a gravel lag exposing underlying pebbly sand which has subsequently been developed into small sand waves, or mega ripples. The berms of the furrows are approximately 0.5 m or less in height. A furrow was observed which continued for 50 m and terminated in a circular depression "iceberg pit", formed as the iceberg ceased to move in a linear direction. These observations are documented with video recordings.

A NEW TYPE OF LINEATION SEEN ON THE OCEAN FLOOR IN LANCASTER SOUND, N.W.T. - POSSIBLE GLACIAL FLUTING

Alan Ruffman
Geomarine Associates
Halifax, Nova Scotia

and

Loring Lee
Petro Canada Exploration Inc.
Calgary, Alberta

ABSTRACT

A series of three site surveys in Lancaster Sound and related regional reconnaissance work in 1979 used side scan sonar in depths up to 1000 m. The side scan sonar was touchy to handle on the 750 m Byam Martin site and careful ship handling and side scan reruns had to be employed to ensure coverage. Precise digitization of the bathymetry with detailed adjustments along with assembly of the sidescan sonograms revealed a linear series of low subtle ridges and troughs trending across the whole area.

The site was relatively close to the axis of Lancaster Sound and the ridges trend subparallel to the axis and to the expected flow lines of the glacial tongues that travelled eastward down the Sound, till they eventually calved or lifted to form an ice shelf in Baffin Bay. The ridges have in the order of 2 to 4 m of relief and a lateral wavelength of up to 500 m. The features are masked with a veneer of recent pelagic muds and are occasionally marked by small unexplained mounds. The linear features are believed to be glacial fluting carved beneath the sole of the Lancaster Sound glacial tongue; the exact age is not known though we presume a Pleistocene age.

The existence of glacial fluting out to depths of 750 m suggests glacial deposits such as tills or moraines could be found out to these depths and could floor much of Lancaster Sound.

PHYSICAL DIMENSIONS OF ICEBERGS IN THE LABRADOR SEA

J. D. Miller
Senior Environmental Analyst - Ice
Petro-Canada Exploration Inc.

I. S. Hotzel
Environmental Analyst - Ice
Petro-Canada Exploration Inc.

1. INTRODUCTION

The concerns of ice scour are the focus of this workshop and although this paper does not address the scouring process directly, it does provide information useful in defining the characteristics of one of the ice scour agents, the icebergs themselves. Although icebergs provide many interesting avenues of study, such as their sources, drift or deterioration, it is the intent here to provide summary data on the physical dimensions of the icebergs found in the Labrador Sea region. It is felt that the provision of these data to scour researchers will aid in the development of improved modelling efforts as well as increasing the overall understanding of the phenomenon.

2. THE DATA

The data was collected by the Labrador Group of Companies in support of exploratory drilling activity in the Labrador Sea region during the period 1973 to 1978. Within these years the data are restricted to the July through October period most favoured for drilling. Of these months the largest numbers of observations were made in August (49%) followed by September (26%), July (19%), and October (6%). The frequency of observations noted here is not comparable with the frequency of occurrence of icebergs as the data are biased by the scope and extent of the drilling program. Regionally, the data were taken from wellsites located between 52° N and 60° N lying on the offshore banks (Saglek, Nain, Makkovik, and Hamilton), as shown in figure one. A summary of the descriptive statistics for the iceberg dimensions is presented in Table One; values are presented for the mean, median, mode, maximum, minimum, range, standard deviation and the number of observations.

3. DATA PRESENTATION

3.1 ICEBERG TYPE

Categorizing the often complex shapes of icebergs into a simple and universal classification scheme is a difficult task that has not been fully mastered. During the period of measurement, several differing classifications were employed and these have been reduced to five common forms: pinnacle, drydock, domed, blocky and tabular. The tabular iceberg is regarded as having undergone a minimum of degradation and erosion whereas the other forms bear witness to such activity in varying degrees.

The pinnacle was the most commonly observed form (36%) followed by tabular (29%), domed (16%), drydock (15%) and blocky (4%) icebergs. If one simplifies this to a binary classification composed only of tabular and nontabular forms, the data suggest that the latter occur more than twice as often as the degradationally immature form (71% versus 29%).

3.2 ICEBERG LENGTH

The above water length of the iceberg is defined as the longest horizontal dimension of the iceberg at the water plane. Measurement techniques involve sextant determinations in the early years which were later replaced by measurements from photographic documentation. The median iceberg length is 94m with 550m representing the larges iceberg measured.

The skewness of the data is immediately apparent in the histogram and and again in the displacement of the measurements of central tendency (mean, mode and median). The frequency distribution for iceberg length is provided in both graph and table form in figure two. While a variety of distributions may be fitted to the data, none are presented here as the choice of what constitutes an acceptable and appropriate fit is dependant, to some level, on the particular application.

3.4 ICEBERG HEIGHT

Iceberg height is the distance from the water line to the highest point of the iceberg. Originally measured with a sextant its determination has been replaced by the use of scaled photographic measurements. The maximum height recorded in this period was 103 metres with a median value of 23.5 metres. The frequency distribution histogram for iceberg height is presented in figure four.

3.5 ICEBERG DRAFT

The distribution of iceberg draft is one of the more interesting from the point of view of scour phenomena. The currently favoured measurement technique is the vertical deployment of a side scan sonar which provides a line profile of the underwater portion of the iceberg and an estimate of the maximum draft. Figure five presents the data in histogram format, from which may be deduced a median value of 89 metres and a maximum value of 202 metres. The upper value corresponds closely to a maximum estimated draft of 230 metres and a maximum measured draft of 187 metres, obtained during four years of offshore drilling near West Greenland.

3.6 ICEBERG MASS

The mass of an iceberg as presented here is not the true mass. Rather, it is an inferred estimate of the true mass based on some model employing dimensional and shape information. A rather large sampling of mass estimation techniques has been used to date and the results that the majority (78%) lie below 2 million tons. The maximum estimated masses are of the order 30 million tons whereas the median iceberg mass is 390,000 tons and the modal mass 50,000 tons.

4. FUNCTIONAL RELATIONSHIPS

The quantitative documentation of iceberg dimensions can be a dangerous, time consuming and expensive task. It many cases it may be possible to obtain one or more of the above water dimensions from visual or photographic information. When this information is coupled with a suitable functional relationship it may be possible to infer, to a first approximation, the dimensions of other variables such as draft.

To define potential relationships a simple regression of the logarithmically transformed values was undertaken; the defining variable was taken as the length, reflecting the relative ease with which it may be measured, and this was regressed against the draft, height, width and mass measurements. A regression was also made of draft versus mass. These relationships were defined for each of the iceberg type classifications (tabular, domed, pinnacle, blocky and drydock) as well as for all iceberg types combined. The functional relationships are presented for power function format ($Y=ax^b$) in Table Two which also includes the correlation coefficient and the number of observations. As an example, the relationship between length and height for all iceberg types has the form:

$$H = 0.402L^{0.89}$$

The correlation coefficient is 0.83 and 230 data pairs were used to define the relation.

In employing these relationships one should note their strength, the size of the data set and review the applicability of such a mathematical form which uniquely defines a dependant y-value from a specified input and is defined from a variance minimizing model.

5. SUMMARY

The data is presented here so that it may be employed in scientific and engineering investigations requiring realistic input data. The format allows its use in a variety of applications from statistical analysis through simulation studies. It is our intent to upgrade and distribute the data as more measurements are made available. It is hoped to enhance the level of scientific study of iceberg related phenomena through the provision of a realistic source data.

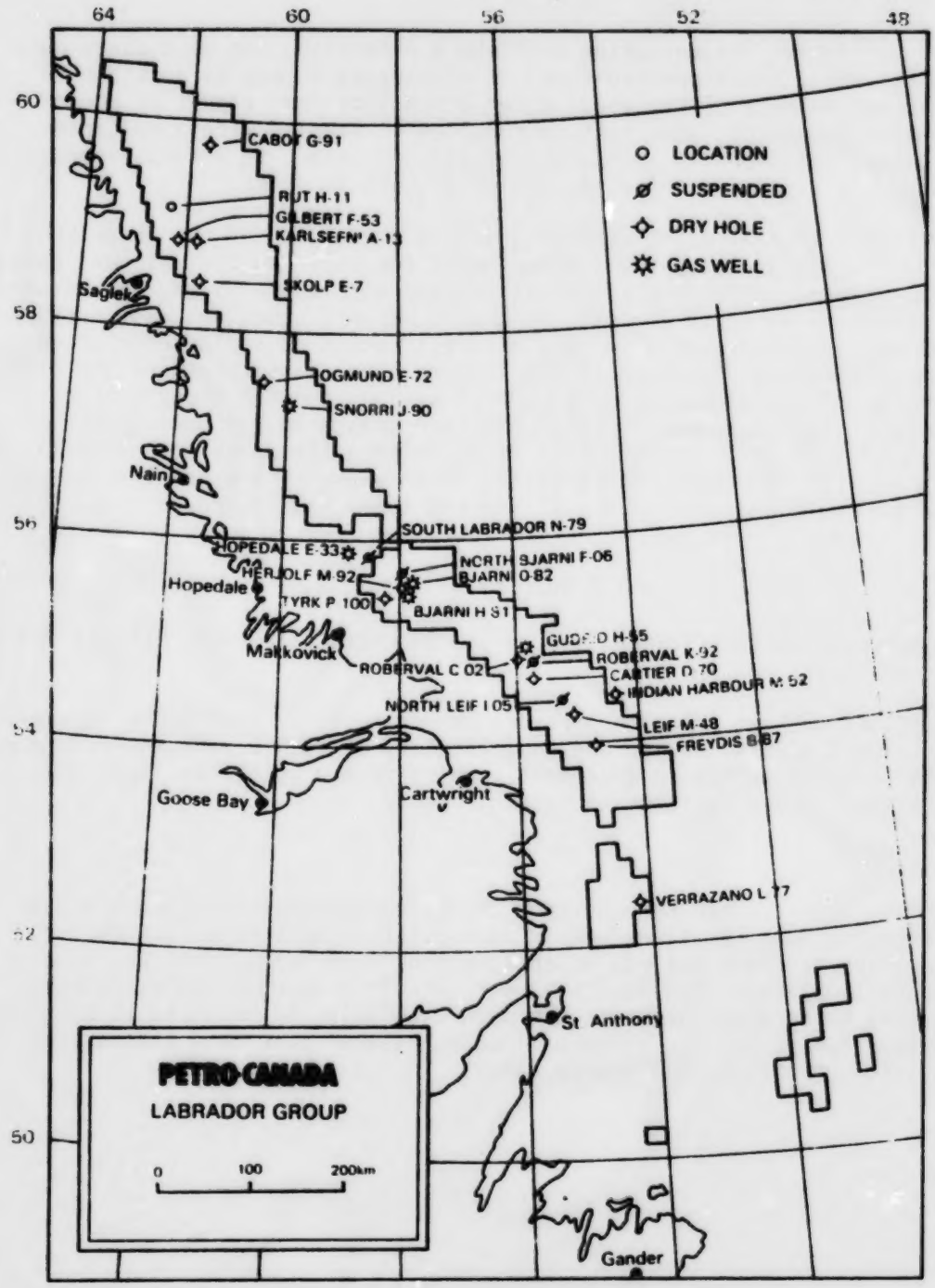

WELL LOCATION MAP

FIGURE 1

RIG ICEBERG OBSERVATIONS
FREQUENCY DISTRIBUTION(%)
LENGTH

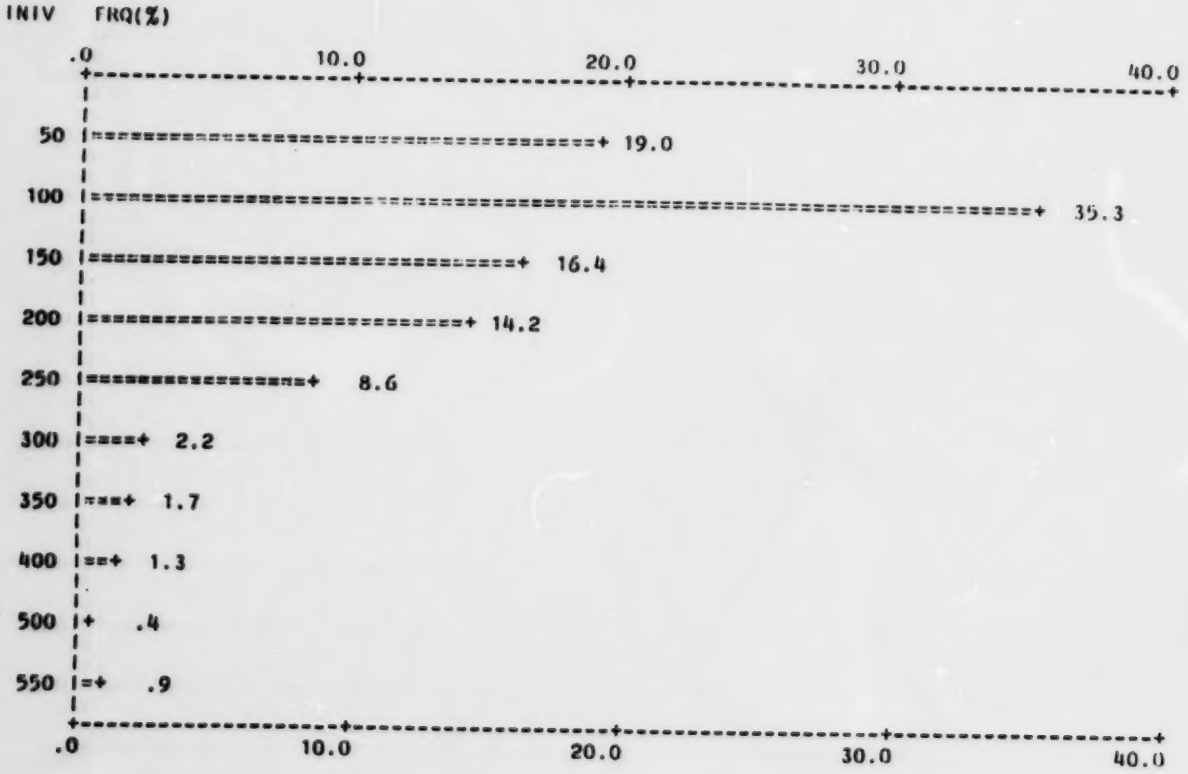

LENGTH INTVL	#OBS	%FRQ
50	44	19.0
100	82	35.3
150	38	16.4
200	33	14.2
250	20	8.6
300	5	2.2
350	4	1.7
400	3	1.3
500	1	.4
550	2	.9
TOTAL	232	100.0

FIGURE 2

RIG ICEBERG OBSERVATIONS
FREQUENCY DISTRIBUTION(%)
WIDTH

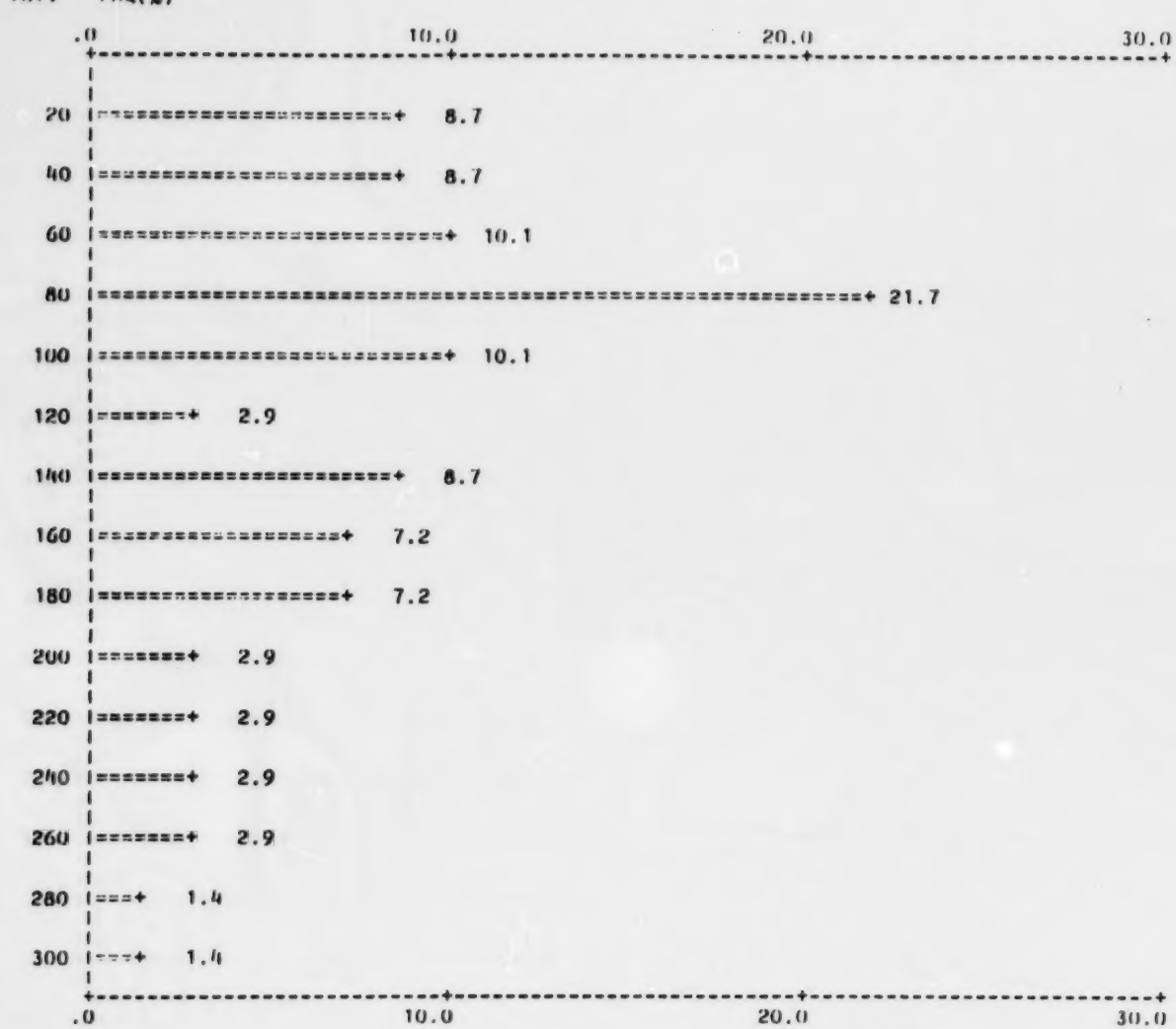

WIDTH INTVL	#OBS	%FRQ
20	6	8.7
40	6	8.7
60	7	10.1
80	15	21.7
100	7	10.1
120	2	2.9
140	6	8.7
160	5	7.2
180	5	7.2
200	2	2.9
220	2	2.9
240	2	2.9
260	2	2.9
280	1	1.4
300	1	1.4
TOTAL	69	100.0

FIGURE 3

RIG ICEBERG OBSERVATIONS
FREQUENCY DISTRIBUTION(%)
HEIGHT

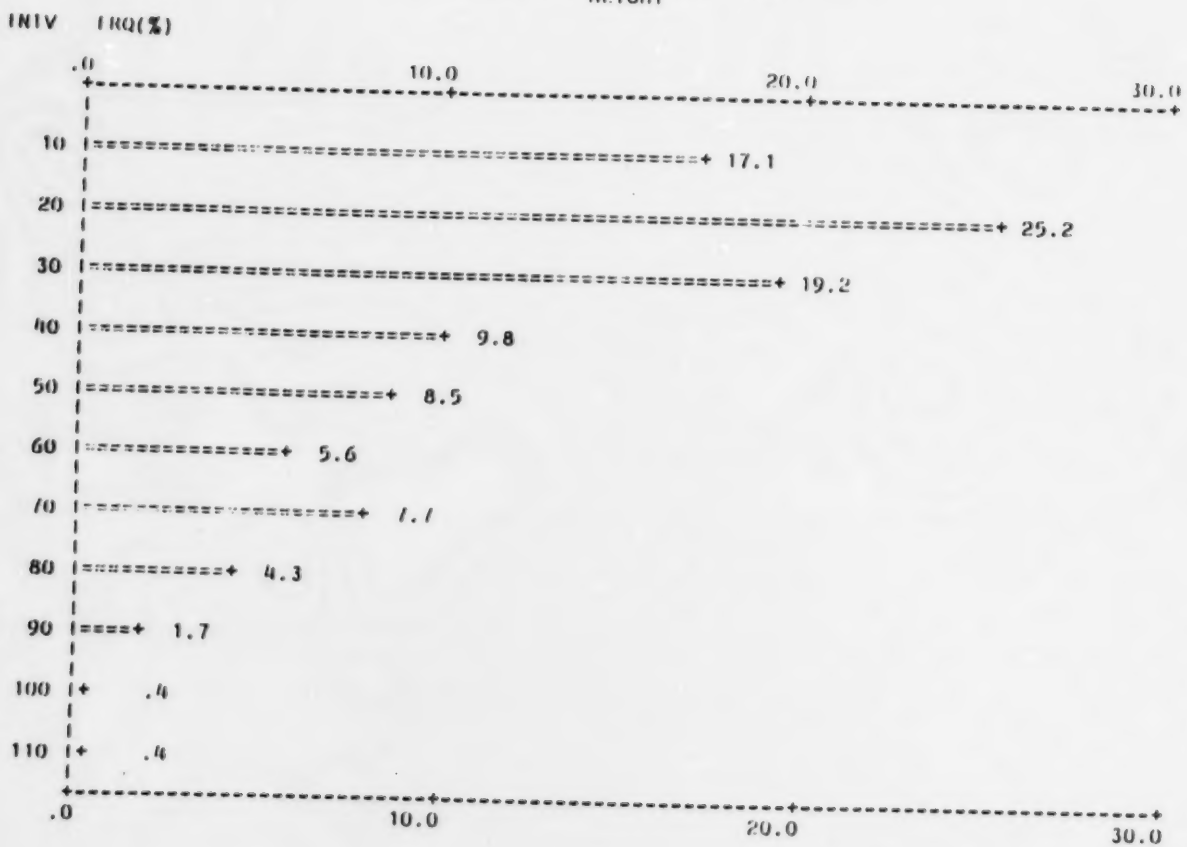

HEIGHT INIVL	#OBS	%FRQ
10	40	17.1
20	59	25.2
30	45	19.2
40	23	9.8
50	20	8.5
60	13	5.6
70	18	7.7
80	10	4.3
90	4	1.7
100	1	.4
110	1	.4
TOTAL	234	100.0

FIGURE 4

RIG ICEBERG OBSERVATIONS
FREQUENCY DISTRIBUTION(%)
DRAFT

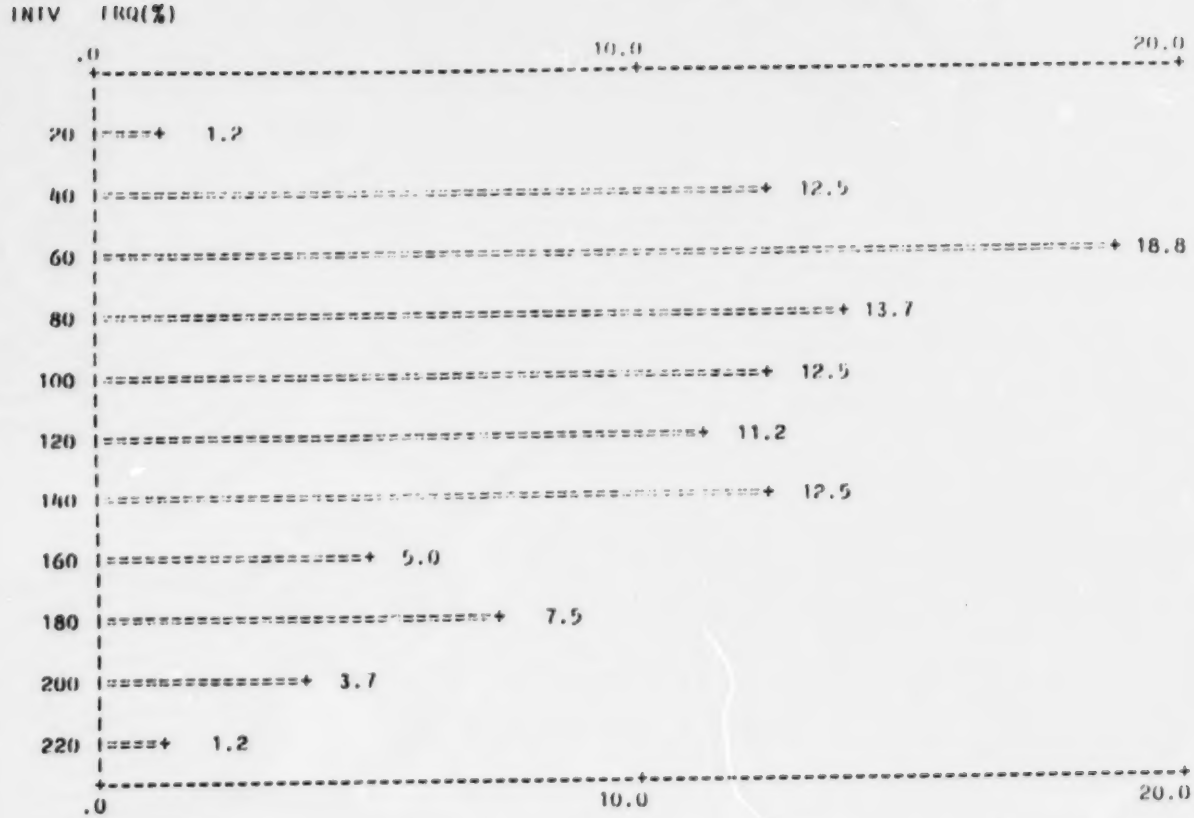

DRAFT INTVL	#OBS	%FRQ
20	1	1.2
40	10	12.5
60	15	18.8
80	11	13.7
100	10	12.5
120	9	11.2
140	10	12.5
160	4	5.0
180	6	7.5
200	3	3.7
220	1	1.2
TOTAL	80	100.0

FIGURE 5

RIG ICEBERG OBSERVATIONS
FREQUENCY DISTRIBUTION(%)
MASS

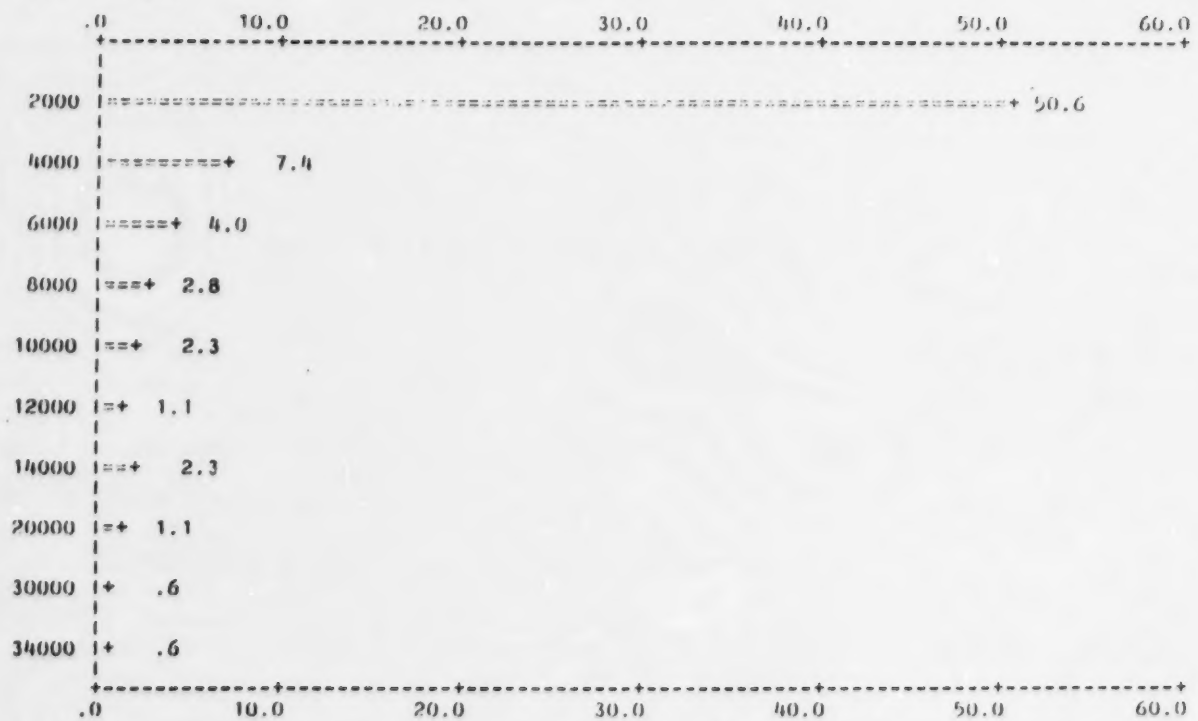

MASS INTVL	#OBS	%FRQ
2000	137	77.8
4000	13	7.4
6000	7	4.0
8000	5	2.8
10000	4	2.3
12000	2	1.1
14000	4	2.3
20000	2	1.1
30000	1	.6
34000	1	.6
TOTAL	176	100.0

Units = Kilotons

FIGURE 6

TABLE 1: STATISTICS OF RIG ICEBERG PARAMETERS

	MEAN	MODE	MEDIAN	STANDARD DEVIATION	RANGE	MAXIMUM	MINIMUM	NUMBER OF OBSERVATIONS
LENGTH	120.0	65.	94.0	90.0	545.0	550.0	5.0	232
WIDTH	105.7	65.	85.0	69.4	294.0	296.0	2.0	69
HEIGHT	30.7	15.	23.3	22.3	101.5	103.0	1.5	234
DRAFT	94.6	35.	88.5	47.5	182.0	202.0	20.0	80
MASS	2184.2	50.	387.5	4698.1	32839.0	32840.0	1.0	176

UNITS: METRES (1-4) AND THOUSANDS OF TONS (5)

TABLE 2

FUNCTIONAL RELATIONSHIPS BETWEEN

ICEBERG DIMENSION PARAMETERS

$$Y = A(X)^B$$

Y,X : ICEBERG PARAMETERS

A,B : REGRESSION EQUATION PARAMETERS

N : NUMBER OF DATA PAIRS

R : CORRELATION COEFFICIENT

TYPE	Y	X	N	R	A	B
ALL	DRAFT	LENGTH	75	.74	3.781E0	0.63
	WIDTH	LENGTH	67	.94	7.118E-1	1.00
	HEIGHT	LENGTH	230	.83	4.025E-1	0.89
	MASS	LENGTH	168	.90	2.009E-3	2.68
	MASS	DRAFT	55	.78	1.470E-2	2.50
TABULAR	DRAFT	LENGTH	19	.64	1.552E0	0.79
	WIDTH	LENGTH	11	.94	3.104E-1	1.19
	HEIGHT	LENGTH	41	.77	1.142E-1	1.12
	MASS	LENGTH	34	.93	1.000E-4	3.38
	MASS	DRAFT	15	.82	5.961E-2	2.16
DOMED	DRAFT	LENGTH	6	.76	6.958E0	0.48
	WIDTH	LENGTH	5	.16	4.126E1	0.16
	HEIGHT	LENGTH	22	.73	2.752E-1	0.92
	MASS	LENGTH	18	.79	1.125E-3	2.68
	MASS	DRAFT	3	.68	2.491E-1	1.70
PINNACL	DRAFT	LENGTH	23	.55	1.091E1	0.43
	WIDTH	LENGTH	20	.93	1.600E0	0.85
	HEIGHT	LENGTH	56	.86	6.570E-1	0.83
	MASS	LENGTH	37	.91	1.026E-2	2.31
	MASS	DRAFT	18	.65	5.961E-2	2.23
BLOCKY	DRAFT	LENGTH	5	.83	1.644E1	0.39
	WIDTH	LENGTH	1			
	HEIGHT	LENGTH	6	.72	1.000E0	0.66
	MASS	LENGTH	1			
	MASS	DRAFT	1			
DRYDOCK	DRAFT	LENGTH	10	.68	2.638E0	0.71
	WIDTH	LENGTH	11	.91	5.067E-1	1.04
	HEIGHT	LENGTH	25	.85	3.946E-1	0.90
	MASS	LENGTH	14	.85	1.046E-2	2.23
	MASS	DRAFT	7	.54	4.527E0	1.04

RELATIONSHIPS BETWEEN MEASURED ICEBERG DIMENSIONS

I. S. Hotzel
Environmental Analyst - Ice
Petro-Canada Exploration Inc.

J. D. Miller
Senior Environmental Analyst - Ice
Petro-Canada Exploration Inc.

1. INTRODUCTION

Iceberg morphometry is an important consideration in both the modelling and operational support aspects of ice scouring. The safe design and operation of bottom founded offshore structures particularly requires accurate estimates of draft distribution. Of the commonly measured iceberg dimensions, draft determination is the most difficult, time consuming and costly. Owing to these problems, therefore, draft measurements have not been collected as frequently as iceberg above water dimensions. In order to evaluate the distributions of draft researchers have in the past attempted to relate selected above water dimensions to the draft. Robe (1975) described the relationship of height to draft as a power curve. More recently Brooks (1981) determined, that a fairly good relationship exists between waterline length and draft and that it is unusual to find drafts larger than the waterline length. The present study shows the relationships between the various length parameters and to a limited degree indicates their applicability. Data used in the analysis were assembled from data collected at drilling rigs operating during the operating seasons (June to October) of 1971-1978. Only simple relationships between draft, width, length and mass are considered. The data were not broken down by iceberg type classification.

2. DATA ANALYSIS

2.1 WIDTH TO LENGTH

Figures 1 and 2 show that iceberg width is approximately 85% of the length. This result is not surprising as the longest waterline dimension is normally designated as the length. It follows, therefore, width would be smaller. Width in this data is taken to be the maximum extent of the iceberg prependicular to the iceberg length.

2.2 DRAFT TO LENGTH

The iceberg sample shows that draft is approximately 70% of the waterline length. In this particular sample of 75 iecbergs only 6 had drafts greater than waterline length. This would tend to confirm the observation by Brooks (1981) that waterline length gives a good first approximation of iceberg draft. Of the icebergs which showed bigger drafts than waterline lengths, three had drafts within 20% of the waterline length, two drafts with 50% of the length, and one iceberg had a draft 2.24 times the length. These icebergs ranged in mass from 6.5×10^4 to 1.9×10^6 metric tonnes with four of the six icebergs being less than $6. \times 10^5$ tonnes. Figures 1 and 3 illustrate this relationship.

2.3 HEIGHT TO LENGTH AND HEIGHT TO WIDTH

The ratio of height to length shown in figures 1 and 4 shows that iceberg height is approximately one third of the waterline length (WL) although this may range from as low 10% to as high as 50% of WL. The ratio of height to width is similar to the height to length ratio, this is expected given the noted similarity of length and width (See figures 1 and 10).

2.4 MASS TO LENGTH

Mass to length ratios are illustrated in figures 1 and 5. Perhaps the most interesting aspect of this relationship is the correspondence between the modal ratios of mass to draft and mass to width, giving further corrobration to the observation that draft, length and width are normally quite closely related. As a predictive tool this ratio appears to have some limited value. Ratios of mass to width are similar to those calculated for mass to length. Once again this is attributable to the similarity of width and length measurements.

2.5 HEIGHT TO DRAFT

Height to draft ratios are shown in figures 1 and 6. The bulk of the data shows ratios from 0.3 to 0.6. It is the author's belief that the variability in height to draft ratios even in quite small size classes precludes its use for prediction of draft.

2.6 DRAFT TO WIDTH

Given the observation that the width of an iceberg is usually smaller than its length and that draft is usually smaller than waterline length it is not surprising that there is a good relationship between iceberg width and draft. The statistics are shown in figures 1 and 7.

2.7 MASS TO DRAFT AND MASS TO WIDTH

The relationships of mass to draft are encouraging as a means of providing first approximations of iceberg drafts. Taking the relationships identified in figure 1 and applying it to the Grand Banks where the iceberg data necessary to perform platform designs is sparse one could estimate that, if the water depth is estimated as 100 metres, the range of iceberg sizes which might move into the area would be from 500,000 tonnes to 1.2 million tonnes. These estimates are derived using the ratios of mass to draft shown in figure 1. The modal value indicates that the ratio between these parameters is 5,000 tonnes mass per metre draft and the median value indicates a ratio of 11,400 tonnes per metre draft. The histogram of ratio's is shown in figure 8.

Some authors (see Lewis et al 1981, for example) have suggested that icebergs greater than 10 million tonnes will not pass over the Grand Banks because of excessive draft. Although on average, the ratio data presented tends to support this contention it should be noted that one iceberg with a mass of nine million tonnes and a draft of $\pm$ 100 m has been measured in Labrador.

Examination of the ratio data showed that the relationship between mass and draft is nonlinear, with the ratio increasing as mass increases. Using the mass to draft ratios calc lated for Labrador and adjusted by mass the accuracy of this technique for estimating draft was tested on 49 icebergs collected by the Danish Hydraulic Institute (1978). For the example shown here only tabular and pinnacle type icebergs were used. Calculated drafts were also made using a derived power curve equation ($14.6 \times \text{mass}^{.253}$). Figures 11 and 12 show that both techniques are reasonably accurate with the power curve data showing less scatter and the ratio data producing more data points close to the best fit line but also in some areas, greater scatter. Given the measurement inaccuracies these results are encouraging. Mass to width ratios show similar attributes as those of mass to draft (figure 9).

Conclusion

Ratios calculated between different iceberg dimensions can be used to a limited degree to calculate other iceberg dimensions. Of particular interest to those working in the field of iceberg scour are those ratios which might be used to calculate iceberg drafts. The Labrador data indicates that waterline length or width can be used to give fairly good estimates of draft and that mass to draft ratios used with some caution can also be used to give estimates of iceberg draft.

This paper has not attempted to demonstrate the accuracy of these ratios in any depth, however, it is hoped that the data may prove useful to those working in the field of ice scour.

REFERENCES

Brooks L.D.; 1981; Another Hypothesis About Iceberg Drafts Proc. 6th International Conference on Ports and Ocean Engineering under Artic Conditions; Vol 2.

Lewis J. and Benedict C.P.; 1981 Icebergs on the Grand Banks: Oil and Gas Considerations World Oil; January.

Robe, R.Q.; 1975; Height to Draft Ratios of Icebergs, Proc. 3rd International Conference on Ports and Oceans Engineering under Arctic Conditions; Vol. 1.

Danish Hydraulic Institute; 1979; Environmental Conditions Offshore West Greenland; Vol. IV Icebergs for Greenland Technical Organization.

FIGURE 1

STATISTICS FOR RIC ICEBERG PARAMETER RATIO DATA

W/L : WIDTH/LENGTH
H/L : HEIGHT/LENGTH
D/W : DRAFT/WIDTH
M/W : MASS/WIDTH
M/D : MASS/DRAFT
D/L : DRAFT/LENGTH
M/L : MASS/LENGTH
H/W : HEIGHT/WIDTH
H/D : HEIGHT/DRAFT

===	MEAN	MODE	MEDN	STDV	RANG	MAXI	MINI	#OBS	MNSQ
W/L	.74	0.85	0.77	.21	1.17	1.45	.29	67	.60
D/L	.67	0.70	0.63	.32	2.04	2.24	.19	75	.55
H/L	.28	0.30	0.32	.18	2.26	2.29	.02	230	.11
M/L	10.81	5.00	4.29	17.15	130.43	130.43	.01	168	410.92
D/W	.93	0.70	0.81	.42	2.20	2.59	.39	48	1.04
H/W	.36	0.35	0.32	.16	.96	1.08	.12	68	.15
M/W	17.61	5.00	8.20	27.00	166.57	166.67	.10	66	1039.15
H/D	.41	0.35	0.35	0.18	.93	0.97	.04	75	.20
M/D	25.10	5.00	11.40	34.32	166.13	166.67	.54	55	1807.95

FIGURE 2

RIG ICEBERG OBSERVATIONS
RATIO FREQUENCY DISTRIBUTION(%)
LD=WIDTH/LENGTH

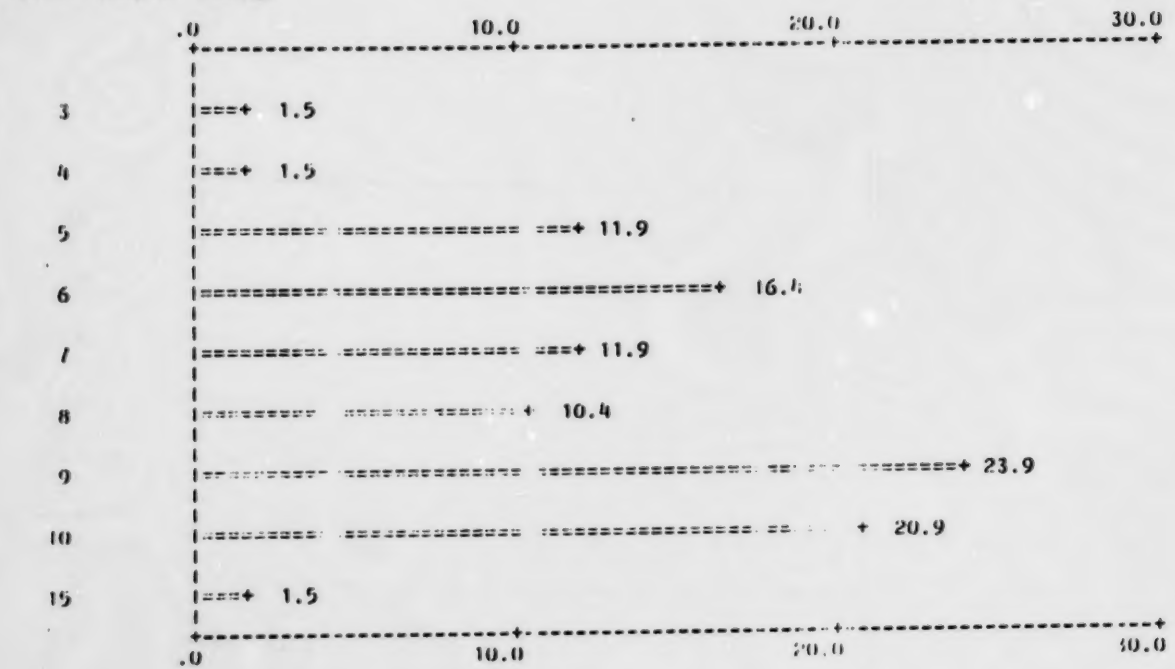

INTVL = VAL/10	FRQ(%)	COUNT
3	1.5	1
4	1.5	1
5	11.9	8
6	16.4	11
7	11.9	8
8	10.4	7
9	23.9	16
10	20.9	14
15	1.5	1
	TOTAL	67

FIGURE 3

RIG ICEBERG OBSERVATIONS
RATIO FREQUENCY DISTRIBUTION(%)
D=DRAFT/LENGTH

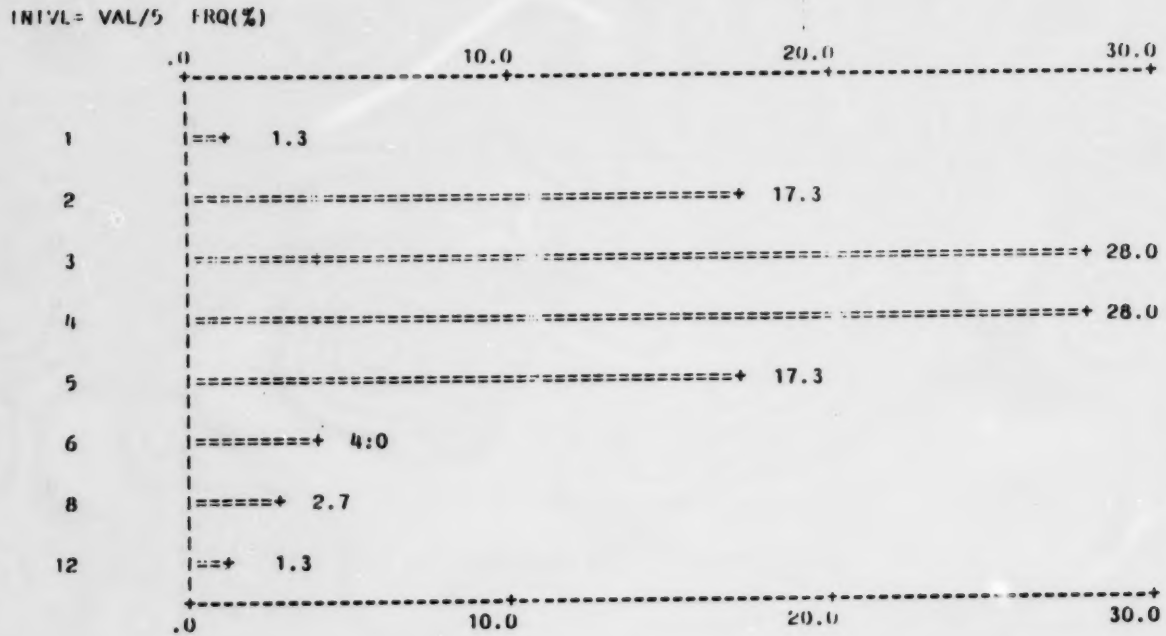

INTVL VAL/5	FRQ(%)	COUNT
1	1.3	1
2	17.3	13
3	28.0	21
4	28.0	21
5	17.3	13
6	4.0	3
8	2.7	2
12	1.3	1
	TOTAL	75

FIGURE 4

RIG ICEBERG OBSERVATIONS
RATIO FREQUENCY DISTRIBUTION(%)
HD=HEIGHT/LENGTH

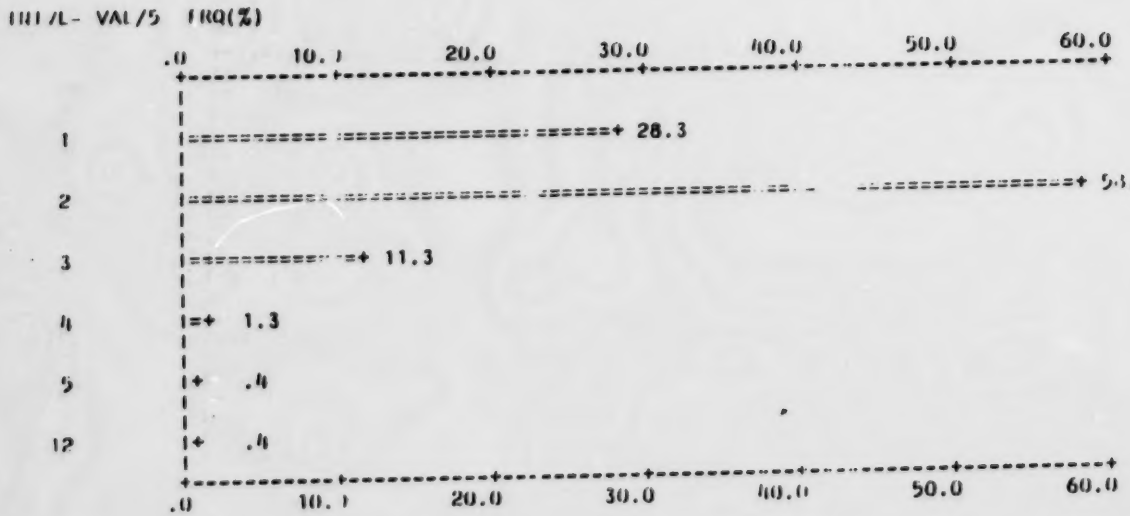

INTVL-VAL/S	FRQ(%)	COUNT
1	28.3	65
2	58.3	134
3	11.3	26
4	1.3	3
5	.4	1
12	.4	1
TOTAL		230

FIGURE 5

RIG ICEBERG OBSERVATIONS
RATIO FREQUENCY DISTRIBUTION(%)
DD=MASS/LENGTH

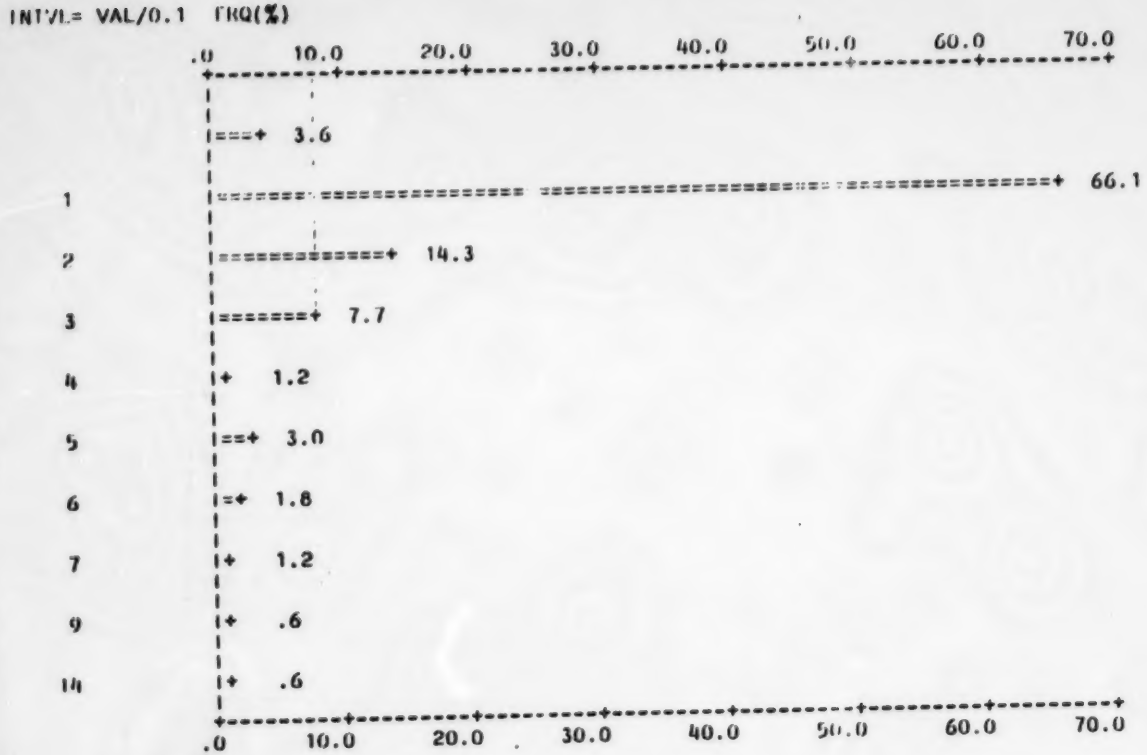

INTVL= VAL/0.1	FRQ(%)	COUNT
	3.6	6
1	66.1	111
2	14.3	24
3	7.7	13
4	1.2	2
5	3.0	5
6	1.8	3
7	1.2	2
9	.6	1
14	.6	1
TOTAL		168

FIGURE 6

RIG ICEBERG OBSERVATIONS
RATIO FREQUENCY DISTRIBUTION(%)
HD=HEIGHT/DRAFT

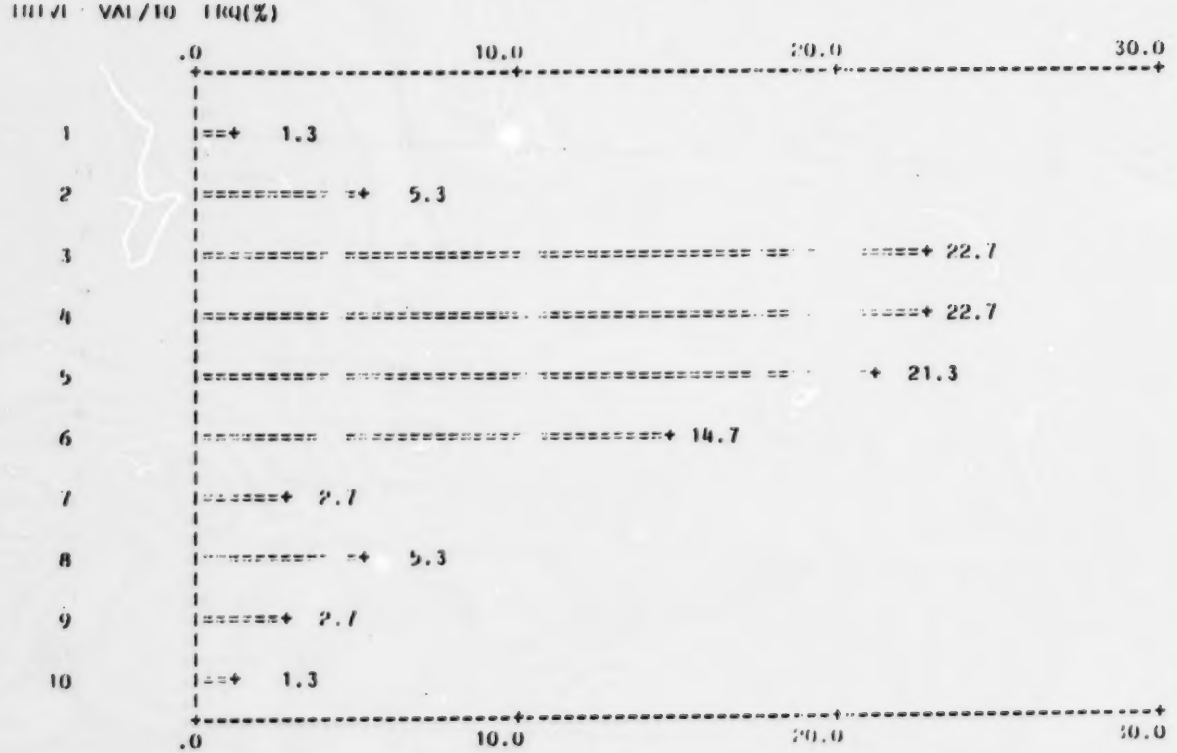

INTVL VAL/10	FRQ(%)	COUNT
1	1.3	1
2	5.3	4
3	22.7	17
4	22.7	17
5	21.3	16
6	14.7	11
7	2.7	2
8	5.3	4
9	2.7	2
10	1.3	1
TOTAL		75

FIGURE 7

RIG ICEBERG OBSERVATIONS
RATIO FREQUENCY DISTRIBUTION(%)
DD=DRAFT/WIDTH

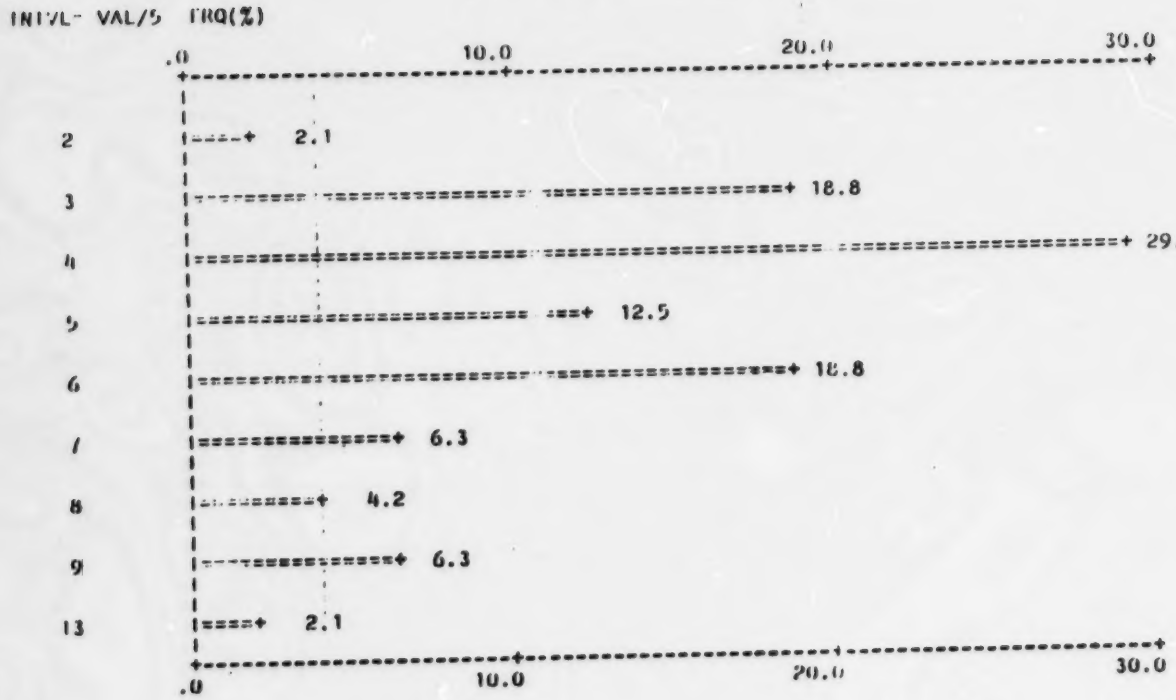

INTVL-VAL/S	FRQ(%)	COUNT
2	2.1	1
3	18.8	9
4	29.2	14
5	12.5	6
6	18.8	9
7	6.3	3
8	4.2	2
9	6.3	3
13	2.1	1
	TOTAL	48

FIGURE 8

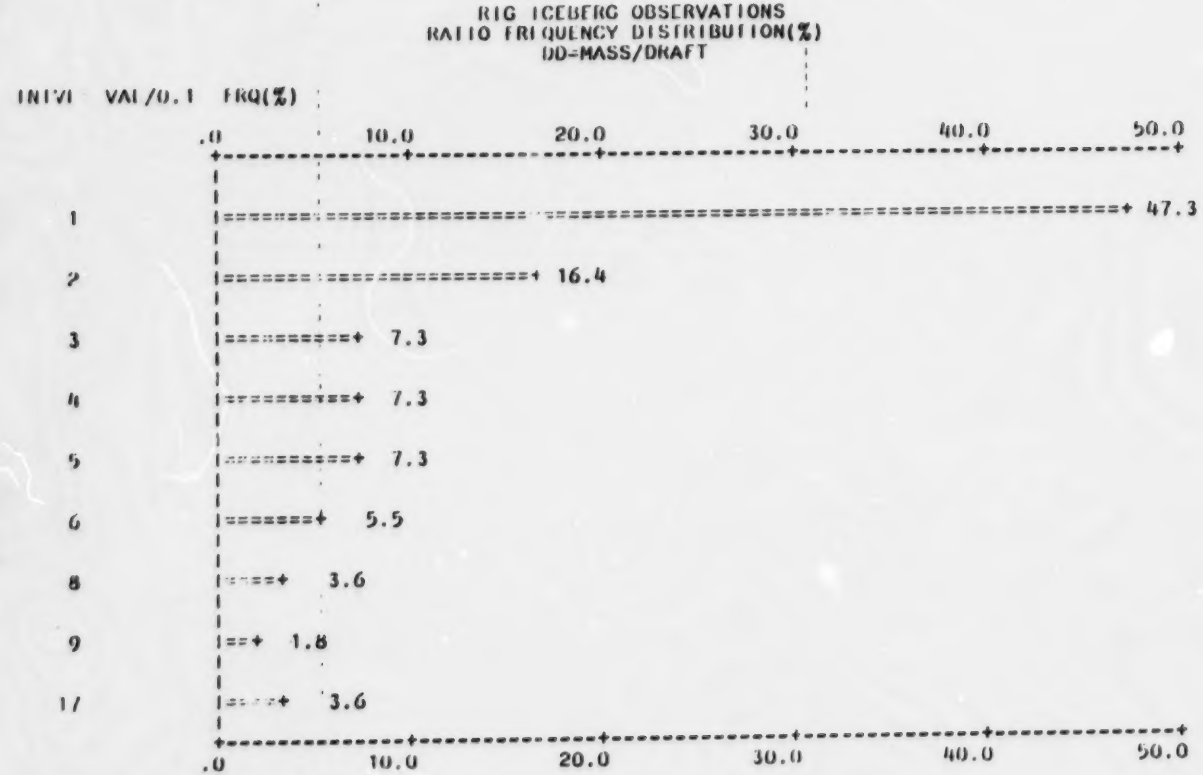

INTVL - VAL/0.1	FRQ(%	COUNT
1	47.3	26
2	16.4	9
3	7.3	4
4	7.3	4
5	7.3	4
6	5.5	3
8	3.6	2
9	1.8	1
17	3.6	2
TOTAL		55

FIGURE 9

RIC ICEBERG OBSERVATIONS
RATIO FREQUENCY DISTRIBUTION(%)
DD=MASS/WIDTH

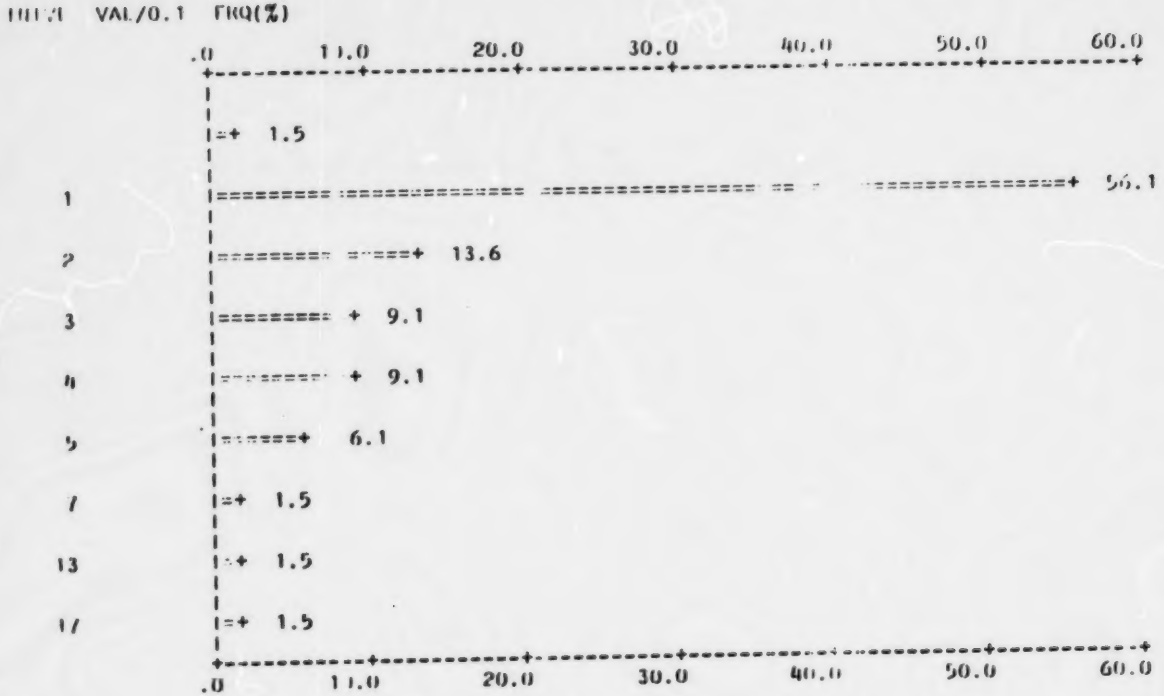

INTVL = VAL/0.1	FRQ(%	COUNT
	1.5	1
1	56.1	37
2	13.6	9
3	9.1	6
4	9.1	6
5	6.1	4
7	1.5	1
13	1.5	1
17	1.5	1
	TOTAL	66

FIGURE 10

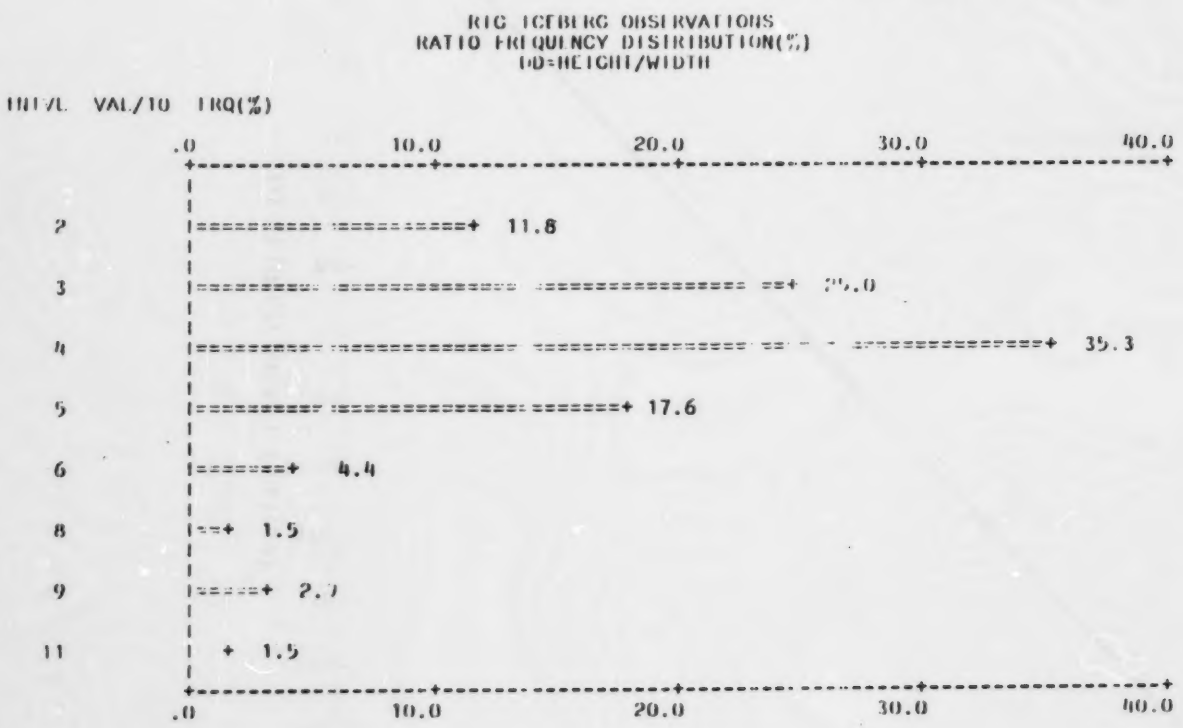

INTVL VAL/10	FRQ(%)	COUNT
2	11.8	8
3	25.0	17
4	35.3	24
5	17.6	12
6	4.4	3
8	1.5	1
9	2.9	2
11	1.5	1
TOTAL		68

FIGURE 11

MEASURED DRAFT VS. CALCULATED DRAFT FOR GREENLAND ICEBERGS* (DHI 1978) USING DRAFT TO ESTIMATED RATIOS

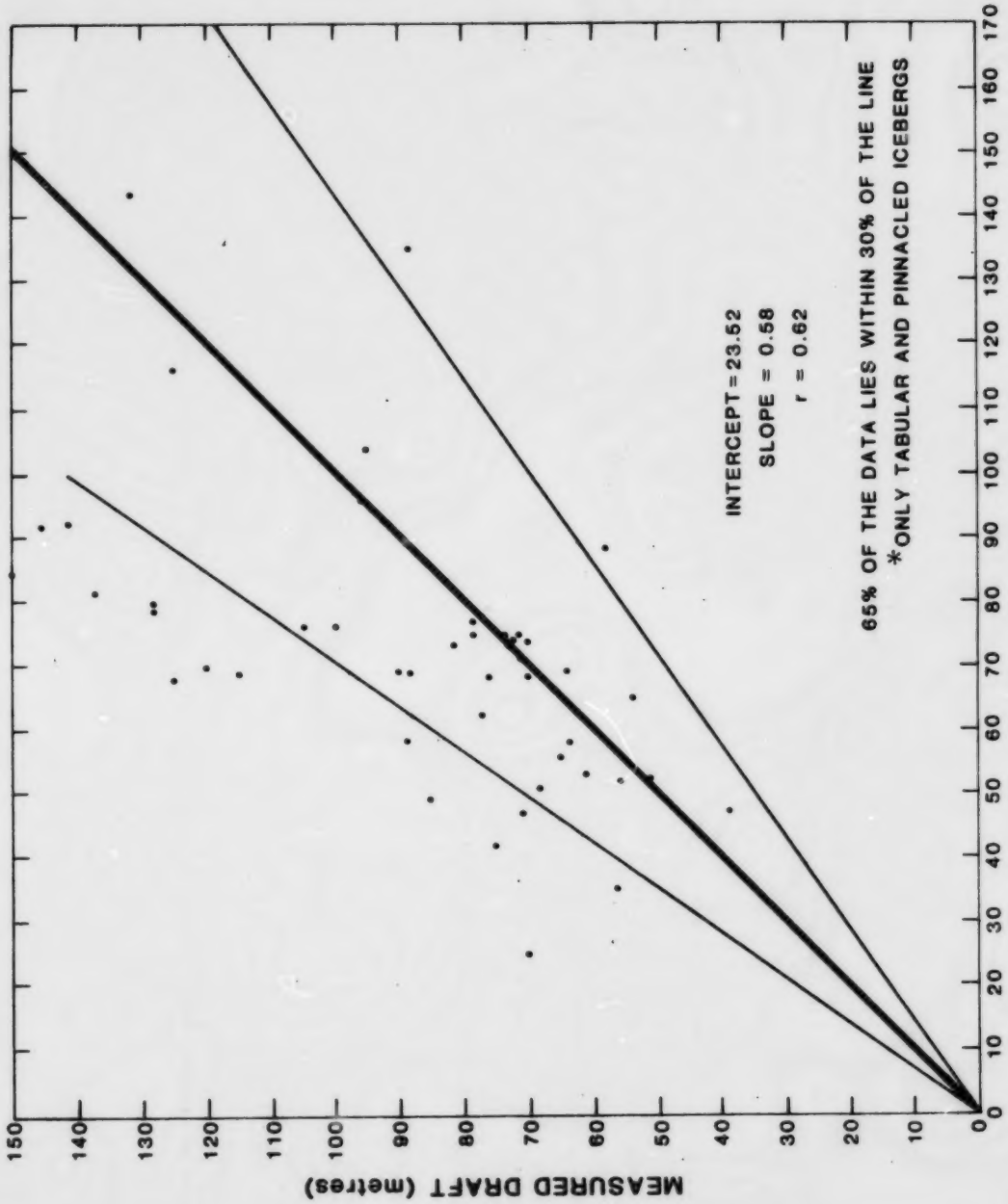

FIGURE 12

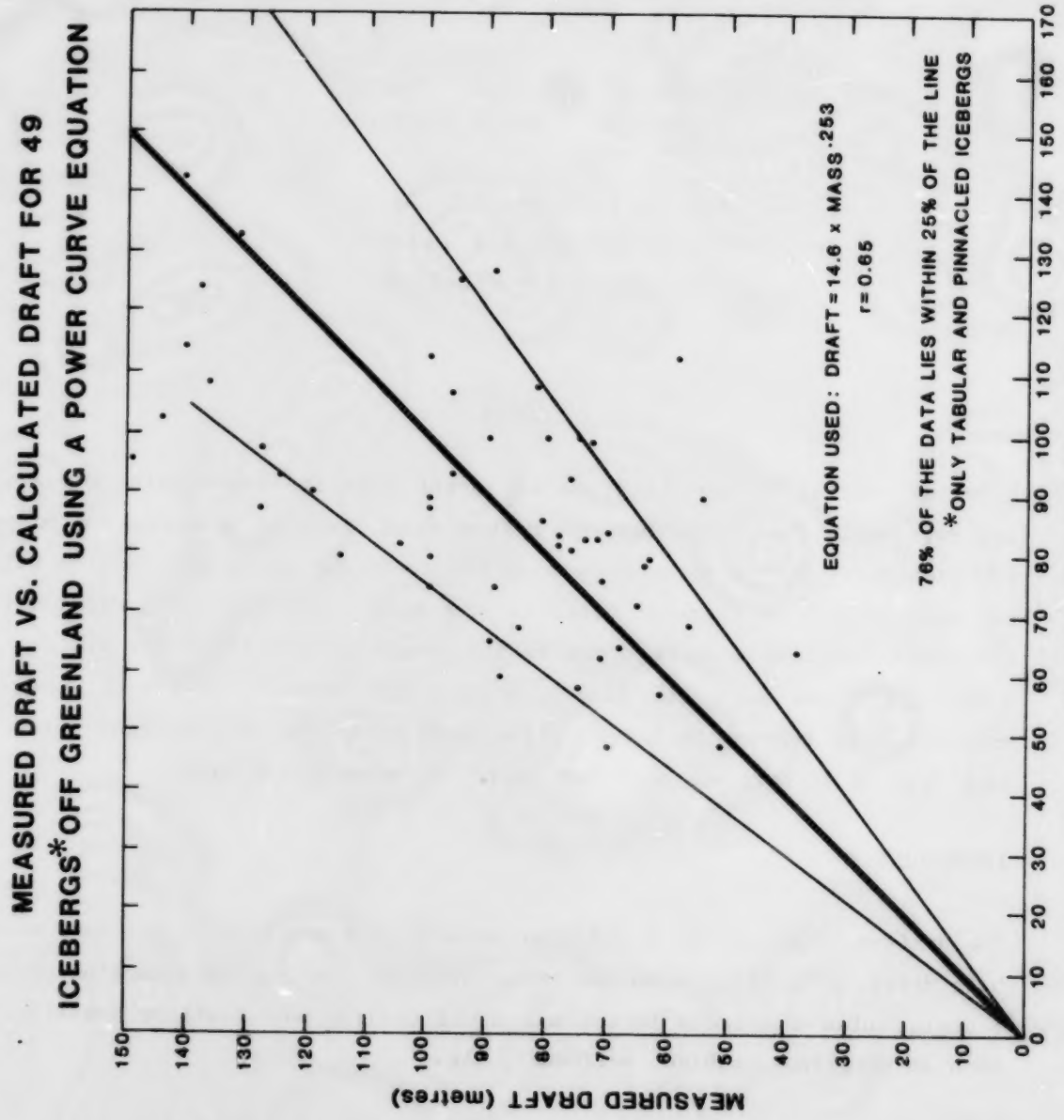
MEASURED DRAFT VS. CALCULATED DRAFT FOR 49
ICEBERGS*OFF GREENLAND USING A POWER CURVE EQUATION
EQUATION USED: DRAFT = 14.6 x MASS·253
r = 0.65
76% OF THE DATA LIES WITHIN 25% OF THE LINE
*ONLY TABULAR AND PINNACLED ICEBERGS
MEASURED DRAFT (metres)
CALCULATED DRAFT (metres)
0
10
20
30
40
50
60
70
80
90
100
110
120
130
140
150
160
170

CORRELATION BETWEEN ICEBERG DRAFT AND ABOVE WATER DIMENSIONS

Mona EL-Tahan and H.L. Davis
Fenco Newfoundland Limited,
St. John's, Newfoundland

ABSTRACT

Previous studies to correlate iceberg draft with its above water dimensions are reviewed. Their findings are tested using data on measurements of over 200 icebergs. The correlation between the draft and the length, width, height and mass of each of these icebergs is presented. The analysis indicated that the upper limit of iceberg draft is its length or 1.5 times the width. The lower limit was 0.25 its length or 0.4 its width. A simple emperical expression to relate the height of an iceberg to its draft/height ratio for each type of iceberg was obtained, based on the measured data.

INTRODUCTION

The draft of icebergs is of interest because of the effect it may have on iceberg drift, grounding, scour and deterioration. During the grounding process, icebergs plow the ocean bottom and could destroy any seafloor installations such as pipelines, cables, wellheads, etc.

Estimates of iceberg draft were made as early as the last decade of the 19th century (15). Attempts to measure iceberg draft continued in the 20th century using different methods with improving degrees of sophistication (Refs. 3, 5, 6, 10,13,14). Robe (13) presented a brief review of the development of the draft measurement methods. Brooks (8) described the different methods used to measure iceberg length and draft.

Above water dimensions of the iceberg can be obtained either by using a range finder and a sextant, or from photos taken from a ship or plane. Iceberg drafts have been estimated from water depth around grounded icebergs, and directly measured with dragline, diver, submarine and sonar.

Two criterian govern the relation between above-water and under-water dimensions of an iceberg: stability and buoyancy. An iceberg seeks a bouyant stable position with seven-eights of its mass submerged.

Few attempts have been made to find some sort of correlation between the above water dimensions (length, width and height) of an iceberg and its draft. These studies generally fall into two categories. In the first category, attempts are made to estimate the maximum possible draft of an iceberg based on its above water dimensions. In the second category, correlation between the draft to height ratio of an iceberg and its draft are sought.

This paper presents a brief review of these studies and an attempt to establish a correlation between an iceberg's draft and its mass, length, width and height.

2.0 DEFINITIONS

Iceberg length is defined as the maximum horizontal dimension of the water plane area of the iceberg.

The width is the maximum horizontal dimension of the water plane area measured in a perpendicular direction to the length.

The height is the vertical distance between water line and the highest point of the iceberg.

The draft is the depth below water line to the deepest point of the iceberg.

3.0 REVIEW OF THE PREVIOUS STUDIES

3.1 Maximum Possible Draft of an Iceberg

Brooks (8) hypothesized that the length of an iceberg is, in general, greater than its draft. In a survey of over 200 icebergs, he found that over 90% of icebergs satisfied this hypothesis. No other relationship could be found between the draft and width, mass or height. Bass (9) examined Brooks' hypothesis and concluded that it had a theoretical foundation based on the stability of the berg, but only when the length was significantly greater than the average width or when the draft was less than or not much greater than average draft.

Magnor and Zorn (11) indicated that the stability of an iceberg is highly dependent on both the width and the draft and that it is independent of the length, and therefore, it seems more physically correct to correlate the draft to the width, than to the length. They provided an estimation of the relationship between the draft (D) and the width (W) as:

$$D_{10} = 1.2\ W + 50 \text{ and } D \leq 230 \text{ m:} \qquad (1)$$

where D_{10} is the draft that only 10% of icebergs exceed. The 230 m limit was provided as the maximum draft of any iceberg with origins in Disko Bay. This value was obtained by studying factors which limit the dimensions of icebergs, such as glacier thickness and topographic factors which cause icebergs to be calved in "small" pieces.

Brooks (9) argued back that while he agrees that it is more correct, physically, to correlate draft with length, than draft with width, the field measurements did not indicate a clear relation between draft and length. Brooks pointed out that Equation (1) indicates a finite draft when width goes to zero and a relationship with an intercept at zero would be more appropriate.

Boe and Benedict (7) pointed out that the apparent violations to Brooks' hypothesis are probably caused by a tendency in understanding the length and plus errors in the draft. They indicated that Brooks' conjecture presented the best currently available "rule of thumb" for estimating an upper bound to the draft.

Another method to calculate the maximum possible draft of an iceberg is presented by Aboul-Azm (1). Based on iceberg statical stability criteria, the maximum possible draft of an iceberg is obtained by:

i) above water volume,
ii) height above water line of the centroid of above water portion,
iii) moment of inertia of water plane area about its major axis, and
iv) constant, k, which depends on the geometry of the underwater portion of the iceberg.

The value of the constant, k, was given as 2 for cylinder and prism and 4 for cone. No value for k was given for other shapes (especially the irregular ones).

The method was tested by comparing the calculated maximum draft with the measured one for a tabular, dome and pinnacled iceberg, using k=2. The measured drafts were within the upper bound in the three cases. For example, the measured draft of a 22.5 million tonne iceberg was about 200 m and the calculated upper limit about 500 m.

The practical application of this method seems very limited since, according to the author, the contours of the above water portions are needed to calculate the position of its centroid. Besides, the value of the maximum draft will depend on k which varies, at least, from 2-4.

We feel, therefore, that it is much easier and more practical to estimate the upper limit of an iceberg's draft using Brooks' hypothesis and imposing the value of 230 m as an upper limit to all the drafts. Brooks' hypothesis will be examined using a set of measurements on more than 200 icebergs (Section 4).

3.2 Draft to Height Ratio

The following paragraph is a summary of the findings of the field studies carried out on the draft to height ratios from 1890 to 1968 (Refs. 10, 12, 14, 15) as presented by Robe (13).

The draft to height ratios obtained by the above studies range from 1 to 10.56. It was found that the draft to height ratio is highly dependent on the shape of the iceberg. The berg floats so that seven-eighths of its mass is submerged and so that the berg is stable. If the berg is tabular (flat top and bottom and vertical sides) a ratio of 7 is expected. If the above water portion is rounded and smooth, while the underwater part is pointed, then a ratio higher than 7 is expected, even as high as 9 or 10. The other extreme is the case where the underside of the berg is rounded and smooth and the above water portion has towering vertical walls. The most pronounced case of this type is the drydock berg where an embayment has been cut out of the centre of the berg leaving only a thin rim of great height and little mass. These can have a draft to height ratio very close to 1.

In a study on iceberg stability, Allaire (2) calculated the draft to height ratio for 14 simple shapes assumed to represent the different classes of icebergs as presented in Table 1. The draft to height ratios ranged from 2.6 to 9 for the tabular icebergs 4.9 to 1.3 for the drydock; 3 to 3.6 for the domed; and 1 to 2.2 for the pinnacled.

Robe (13) studied 30 icebergs measured by the International Ice Patrol near the Davis Strait in an attempt to obtain a relation between an iceberg's height and its draft to height ratio. He concluded that there was no significant difference between iceberg classes with respect to draft to height ratio and that the distribution was not linear, being best represented by the power curve of the form

$$\text{Ratio} = 49.4\ (\text{Height})^{-0.8}$$

Because the number of icebergs used for the study was limited to 30, the above conclusion may not apply to all the icebergs. The findings of Allaire (2) and Robe (13) will be compared to the results of the study carried out (Section 4) on the available data on more than 200 icebergs.

4.0 ANALYSIS OF AVAILABLE DATA

This section presents the analysis of the data available from Fenco Newfoundland Limited computer bank on a total of 214 icebergs measured between latitudes 49°N and 75°N during the period 1973 to 1979. This data set is very large, and has been compiled from a number of sources using several different methods. The possibility of systematic errors resulting from any one measurement technique is minimized. Hence, this data set provides a firm ground on which to base conclusions on the relationship between the draft and height, length, width, and mass as presented in Figures 1 to 4, respectively. The total number of data points vary from one graph to another depending on the availability of information for each parameter. All the measured drafts fall within the 230 m limit.

The draft versus height plot scattered significantly. No relation between draft and height could be established (Figure 1). Essentially ratio vary from 1:1 to 7:1.

Of the 214 icebergs, only 17 had drafts greater than the length and only 2 icebergs had drafts greater than 1.5 times the length. The lower limit of the draft was 1/4 the length (Figure 2).

The draft of icebergs seems to range between 0.4 and 1.5 the width (Figure 3).

The range of the iceberg drafts for a given mass seems to increase considrably for larger icebergs (Figure 4).

Figures 5, 6 and 7 present the relationship between height and draft to height ratio, length and draft to length ratio and width and draft to width ratio, respectively. No significant correlation was found between length and draft to length ratio, or width and draft to width ratio.

However, when the draft to height ratio was plotted against height (Figure 7), it was noticed that there was a general correlation between the height and draft/height ratio (hyperbolic form) with considerable scatter. But there was a definite difference between icebergs dominated by horizontal dimensions (tabular and domed) and those of a more vertical nature

(pinnacled and drydock). Each class of icebergs was therefore plotted in a separate figure (Figures 8 to 11). It became apparent that the draft/height ratios of the pinnacled and drydock icebergs had a small range and seemed independent of height, while those of the domed and tabular icebergs exhibited a greater spread and were more dependent on height values. The ratios for the domed and tabular icebergs decreased as the height increased. However, the relationship was not linear.

The draft to height ratio ranged from 1.0 to 10.5 which are in line with the reported range of 1 to 10.56. The minimum ratio was associated with a pinnacled iceberg and the maximum ratio was associated with a domed iceberg.

In general, the maximum draft to height ratios were associated with the tabular and domed icebergs while the minimum ratios were associated with the drydock and pinnacled icebergs. This can be attributed to the fact that the tabular and domed icebergs have compacted above water portions while the drydock and pinnacled have thin parts with great heights and little mass. These findings generally agree with those of Robe (13).

To check the validity of the theoretical draft/height ratios reported by Allaire (2), the range of theoretical draft/height ratios for each class is compared to the actual range in the following table.

Iceberg Type	Draft/Height Ratio	
	Theoretical	Actual
Tabular	2.6 - 9.0	1.3 - 9.6
Dry Dock	1.3 - 4.9	1.0 - 4.5
Domed	3.0 - 3.6	1.2 -10.6
Pinnacled	1.0 - 2.2	1.0 - 5.0

It can be seen that there is a general agreement between the actual and theoretical ranges of the draft to height ratios of the tabular and drydock icebergs. But this is not the case for the domed and pinnacled icebergs. It seems, therefore, that the simple shapes assumed by Allaire for the domed and pinnacled icebergs cannot represent all the actual shapes of icebergs in these classes.

Using the Least Squares Method of curve fitting, the draft to height ratios for the domed icebergs (Figure 10) was best represented by a power curve of the form

$$\text{Ratio} = 111.04\ (\text{Height})^{-1.111} \qquad (2)$$

and for the tabular icebergs (Figure 11) by a power curve of the form

$$\text{Ratio} = 198\ (\text{Height})^{-1.235} \qquad (3)$$

For the pinnacled and drydock (Figures 8 and 9) icebergs, a mean value of the draft/height ratio of about 2.2 seems to best represent the data for these classes.

The curves given by Equations 2 and 3 are plotted in Figures 10 and 11 respectively. The average value of the draft to height ratio of the pinnacled and drydock icebergs (2.2) is plotted in Figures 8 and 9. The scatter of the actual data around these lines is more evident for the tabular icebergs than for the domed icebergs.

5.0 DISCUSSION

An estimation of the upper limit of an iceberg draft is needed to see if the iceberg has a sufficient draft to pose a threat to any bottom installation. On the other hand, an estimate of the minimum draft is also needed in some other cases to see if the iceberg will be able to drift in certain areas in shallower water. For example, consider an iceberg approaching the Grand Banks area (where water depth is about 80 m). If the minimum value of the draft is estimated to be 100 m, then the iceberg will be grounded before it enters the Grand Banks area.

Therefore, there is a need to estimate the maximum, minimum and the mean value of the draft of a given iceberg. Because iceberg draft is influenced by all the other dimensions, it may be a good idea to estimate iceberg draft (and its limits) using the width, length, height and mass measurements. This can be accomplished as follows:

1. The upper limit of the draft may be taken as the smallest value of:
   10.5 x Height, (Figure 1)
   Length, (Figure 2)
   1.5 x Width, (Figure 3)
   230 m, (Ref. 11)
   or the upper limit of the mass-draft plot (Figure 4).

2. The minimum value of the draft may be taken as the largest value of:
   Height, (Figure 1)
   0.25 x length (Figure 2)
   0.40 x width (Figure 3)
   or, the lower limit of mass-draft plot (Figure 4).

3. An estimate of the draft can be obtained for each type of iceberg from the fitting curves of Figures 8 to 11, or using the corresponding mathematical expressions. The confidence in the draft value (possible error) can be estimated from Figures 14 and 15.

By using the mass, length, width and height values to calculate the range and estimate of the draft value, instead of using one parameter only, the accuracy of the estimated draft is expected to improve.

6.0 CONCLUSION

Based on the above water dimensions of an iceberg, an estimate of iceberg draft and its upper and lower limits can be obtained. The upper and lower limits of an iceberg draft can be estimated, with reasonable accuracy, based on information obtained from the measurements of over 200 icebergs. An estimate of the iceberg draft can be obtained from the graphs or the mathematical expressions obtained emperically, for each type (class) of iceberg. The empirical expressions of the draft and draft/ height ratios can be improved as more data on draft measurements become available.

Acknowledgement

The authors are grateful to Mr. Eric Gray, President, Fenco Newfoundland Limited for his encouragement and support.

Table 1 DRAFT-HEIGHT RATIOS FOR REGULAR SHAPED ICEBERGS (REF. 2)

ICE PATROL CLASSIFICATION	ASSUMED SHAPE	CALCULATED DRAFT - HEIGHT
BLOCKY OR TABULAR	HALF ELLISPSOID	9:1
	RECTANGULAR	7.2:1
	CROSS	4:1
	INVERTED T	3:1
	STAR	2.6:1
DRYDOCK	DEEP DRY DOCK 1	4.9:1
	DEEP DRY DOCK 11	3.3:1
	SHALLOW DRY DOCK 1	3:1
	SHALLOW DRY DOCK 1'	2.5:1
	PINNACLED DRY DOCK	1.3:1
DOMED	ELLIPSOID	3.6:1
	DOMED CYLINDER	3:1
PINNACLED	DIAMOND	2.2:1
	PYRAMID	1:1

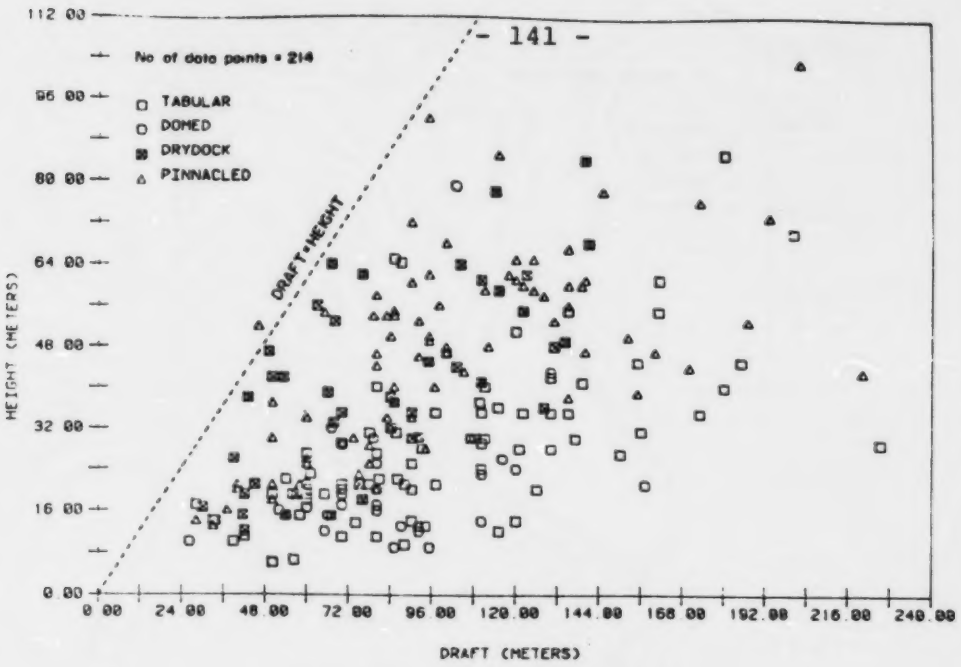

FIG. 1 DRAFT VERSUS ICEBERG HEIGHT FOR DIFFERENT TYPES OF ICEBERGS

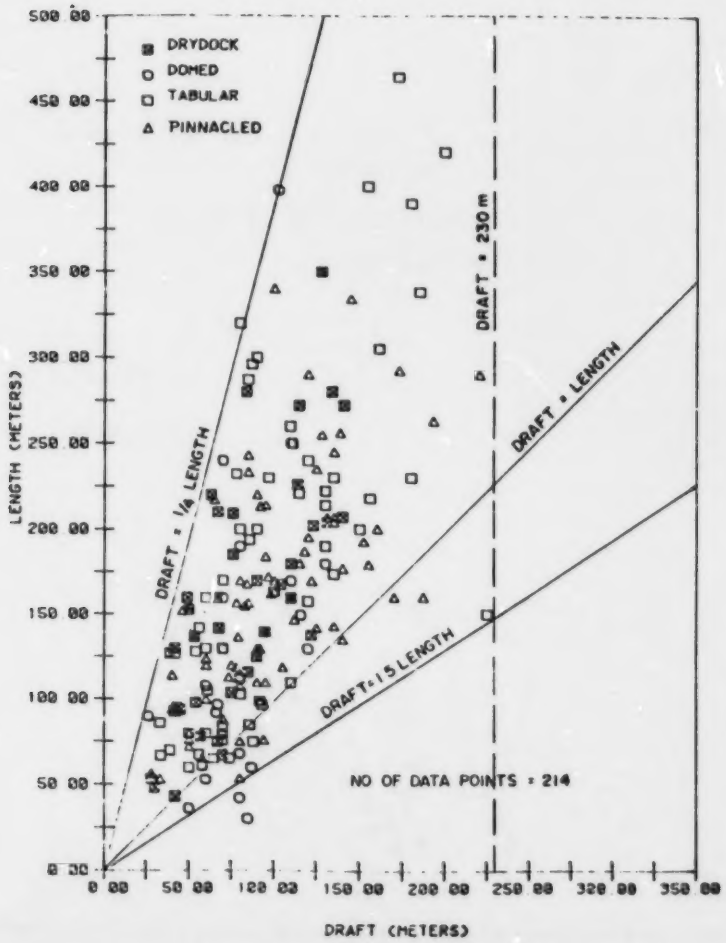

FIG 2 LENGTH VERSUS ICEBERG DRAFT FOR DIFFERENT TYPES OF ICEBERGS

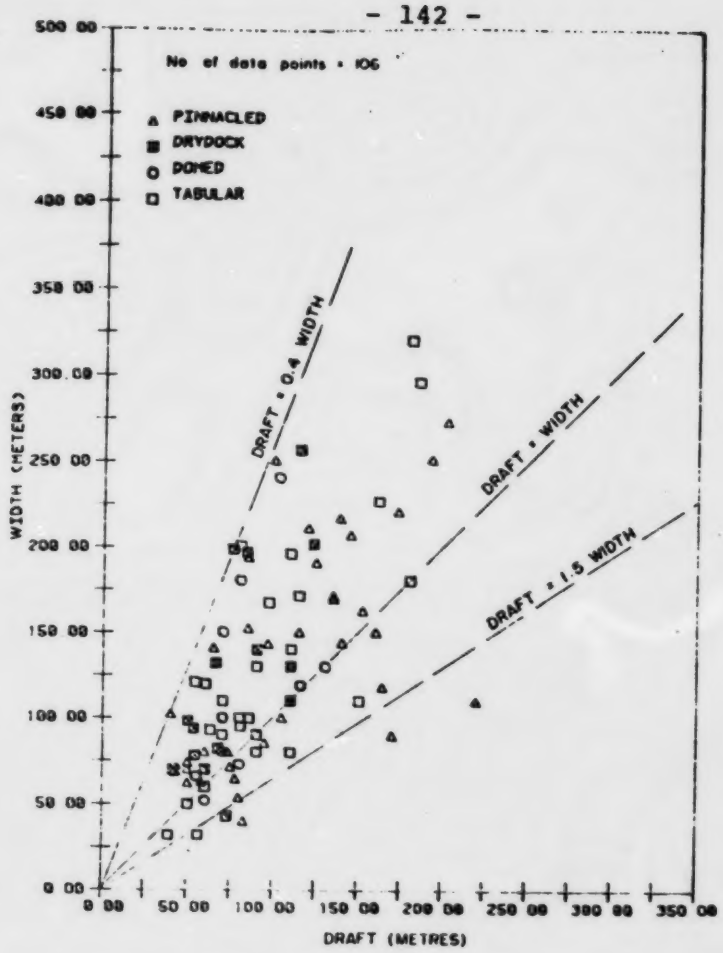

FIG. 3 DRAFT VERSUS WIDTH FOR DIFFERENT TYPES OF ICEBERGS

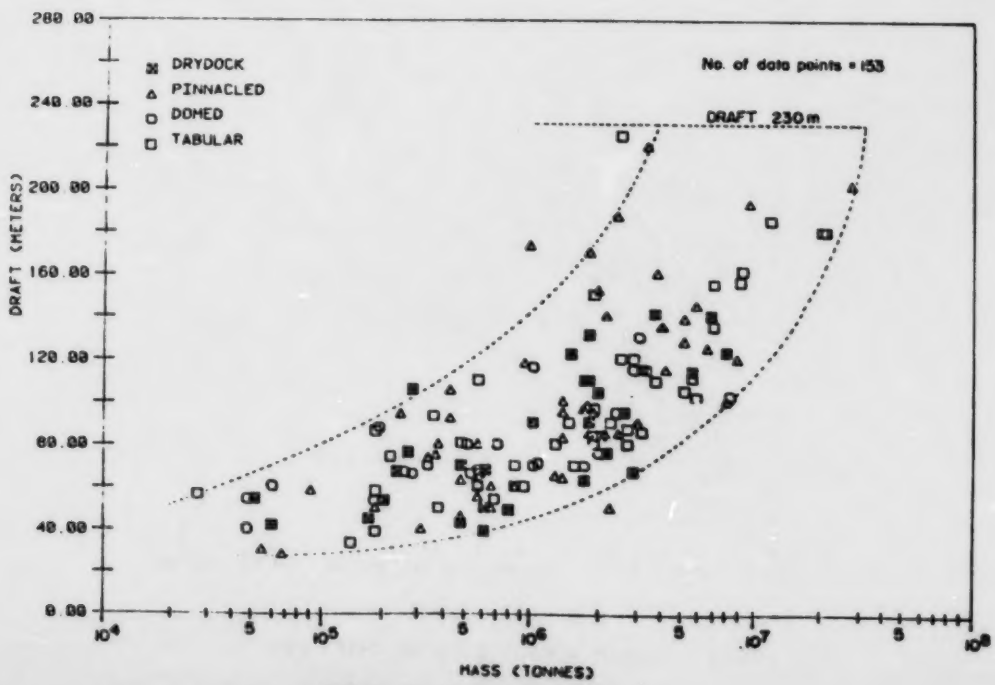

FIG. 4 MASS VS MEASURED DRAFT

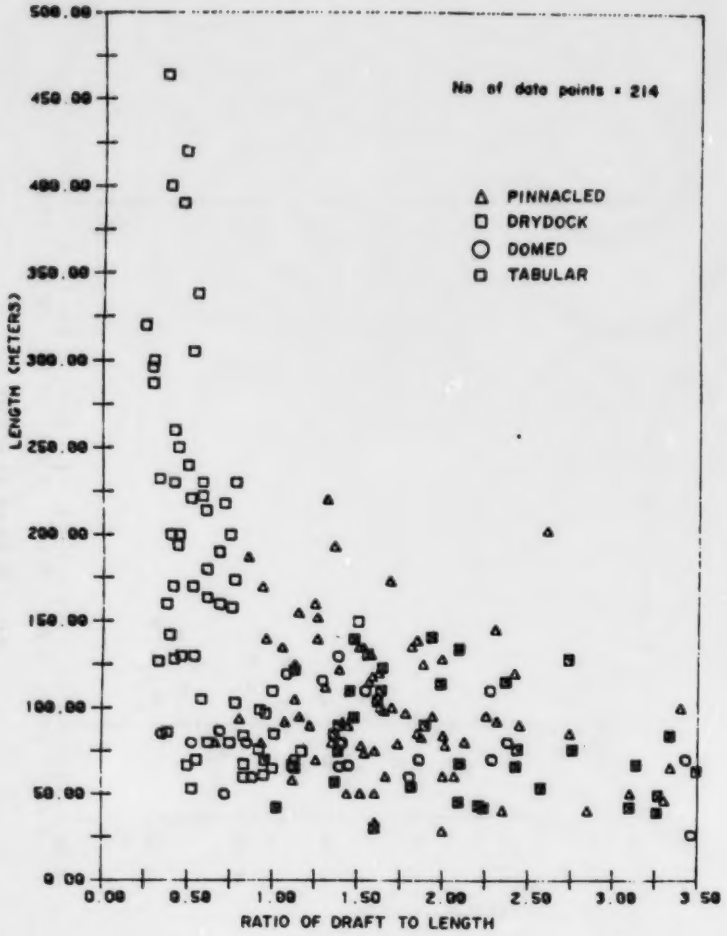

FIG. 5 THE DISTRIBUTION OF DRAFT TO LENGTH RATIO OF DIFFERENT TYPES OF ICEBERGS

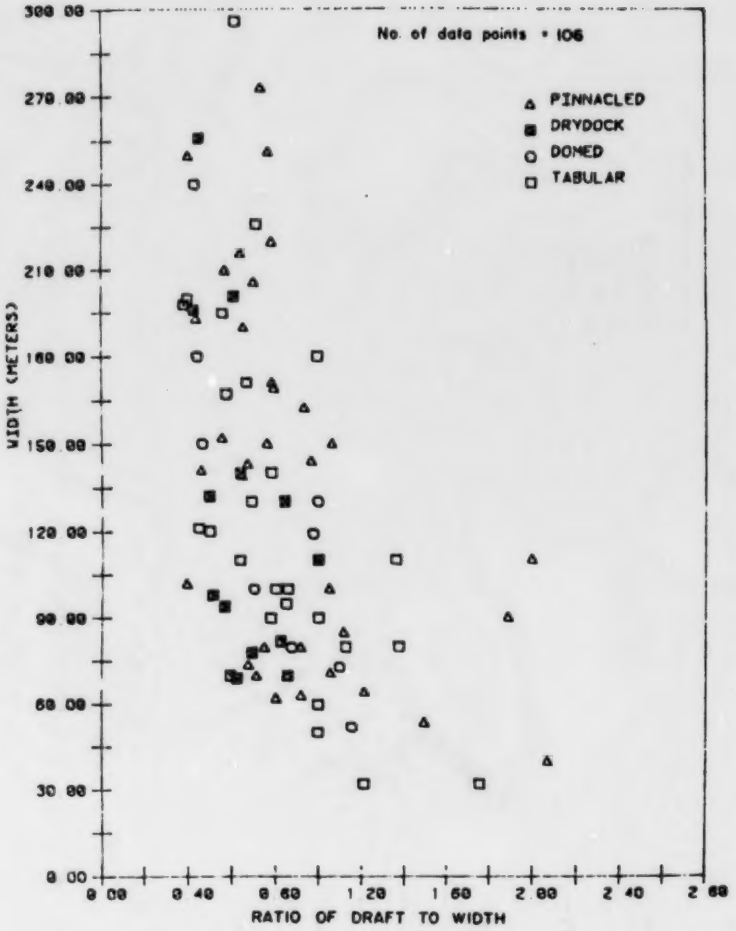

FIG. 6 THE DISTRIBUTION OF DRAFT TO WIDTH RATIOS OF DIFFERENT TYPES OF ICEBERGS

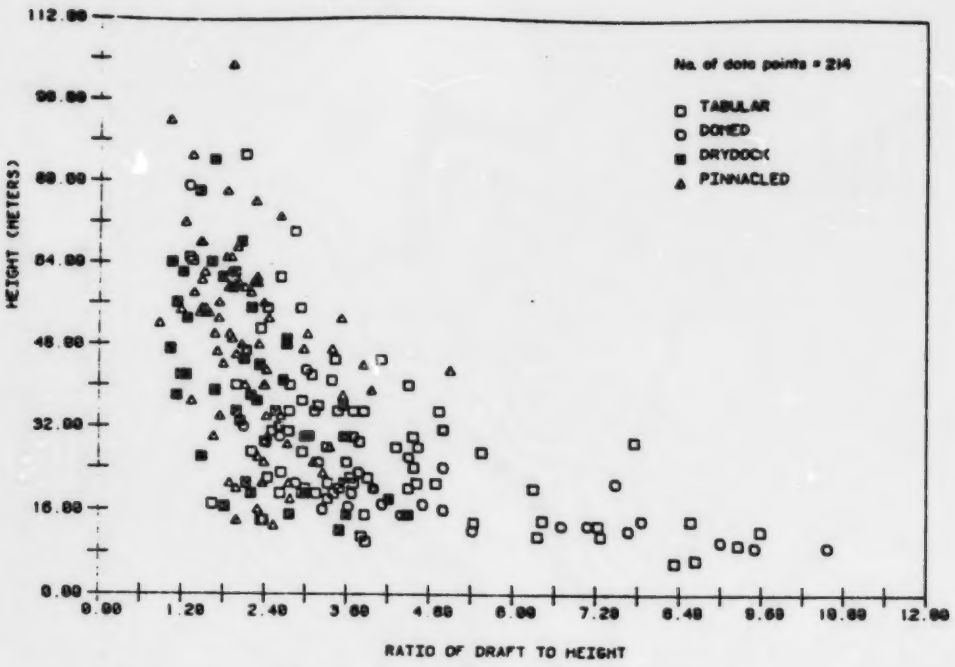

FIG. 7 THE DISTRIBUTION OF DRAFT TO HEIGHT RATIOS OF DIFFERENT TYPES OF ICEBERGS

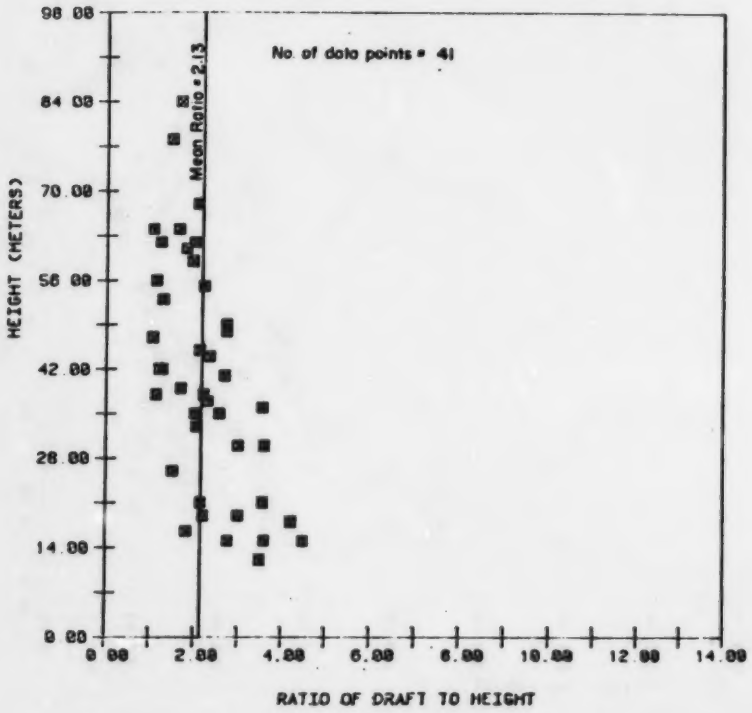

FIG. 8 THE DISTRIBUTION OF DRAFT TO HEIGHT RATIOS OF DRYDOCK ICEBERGS AS A FUNCTION OF ICEBERG HEIGHT

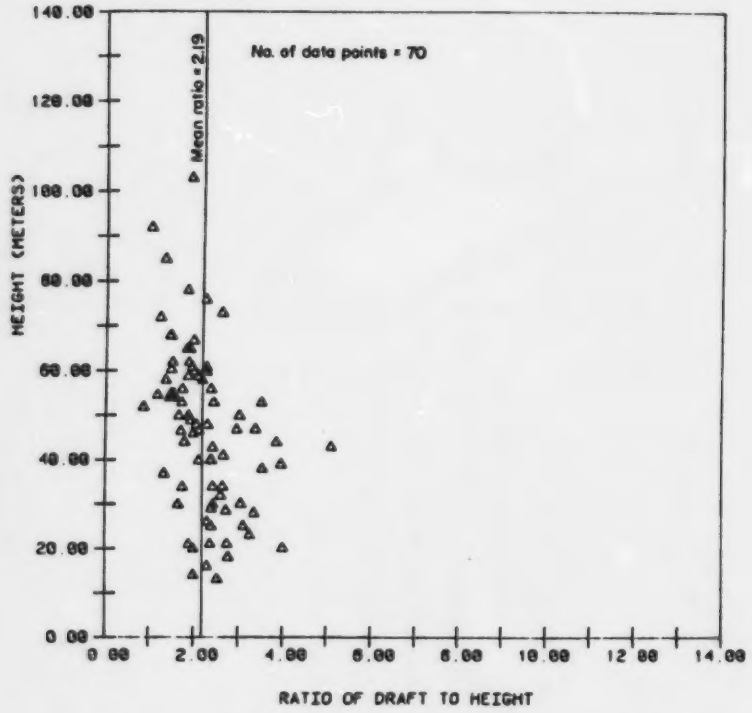

FIG. 9 THE DISTRIBUTION OF DRAFT TO HEIGHT RATIOS OF PINNACLED ICEBERGS AS A FUNCTION OF ICEBERG HEIGHT

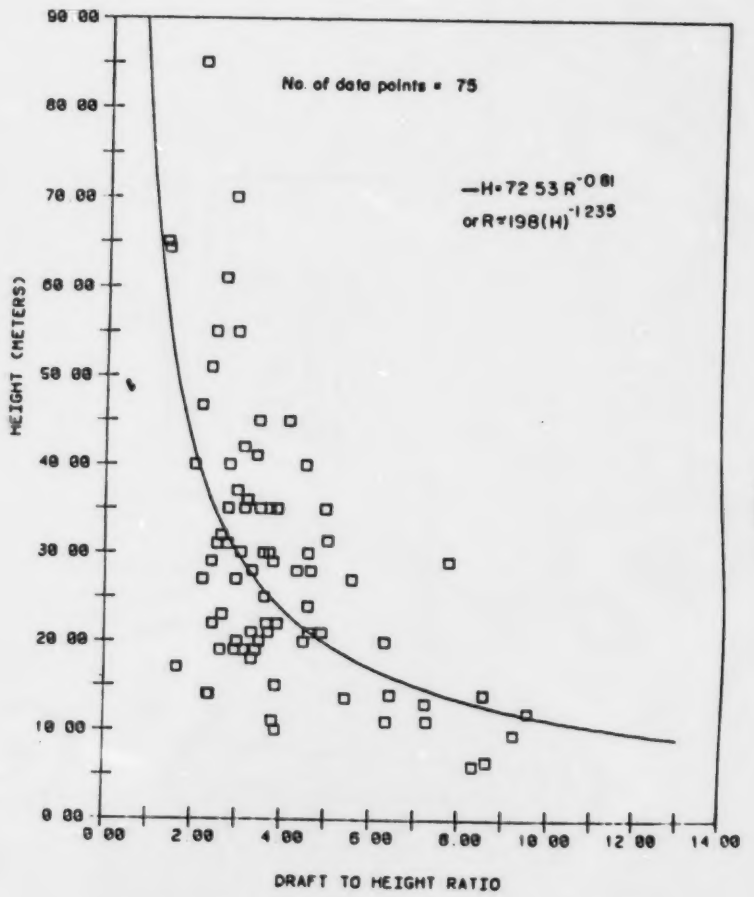

FIG 10 THE DISTRIBUTION OF DRAFT TO HEIGHT RATIOS OF TABULAR ICEBERGS AS A FUNCTION OF ICEBERG HEIGHT

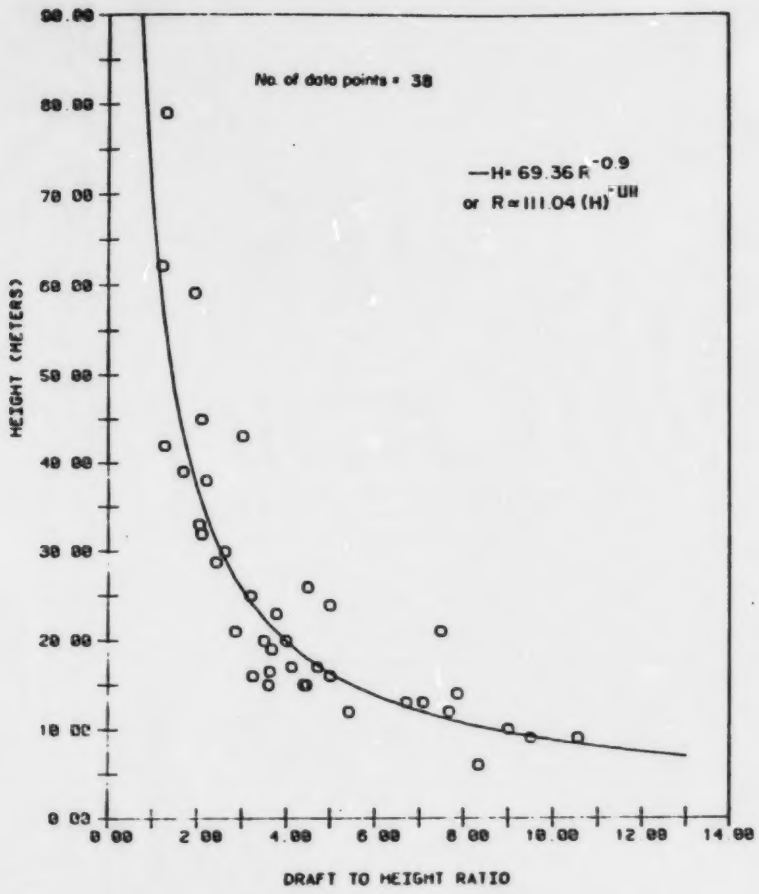

FIG II THE DISTRIBUTION OF DRAFT TO HEIGHT RATIOS OF DOMED ICEBERGS AS A FUNCTION OF ICEBERG HEIGHT

References

1. Aboul-Azam, A.F., (1982), "Estimation of Icebergs Draft Can Be Made From Visible Part", J. Resource Development, Winter 81/82 Edition.

2. Allaire, P.E., (1972), "Stability of Simply Shaped Icebergs", the Journal of Canadian Petroleum Technology, Vol. 11, No. 1.

3. Allen, J.H., (1972), "Iceberg Study, Saglek, Labrador, Including Cruise Report C.S.S. Dawson, August 7-26, 1972", Memorial University of Newfoundland Publication.

4. Bass, D., (1980), "Draft Estimation", Unpublished Report, Memorial University, St. John's, Newfoundland.

5. Benedict, C.P., (1976), "Icebergs and Canadian East Coast Exploration", The 31st Annual Petroleum Mechanical Engineering Conference, Mexico City.

6. Benedict, C.P., (1974), "Underwater Profiling of Icebergs", Proceedings of Second International Conference on Port and Ocean Engineering Under Arctic Conditions, Reykjavik.

7. Boe, B.D. and Benedict, C.P., (1979), Discussion of "Another Hypothesis About Iceberg Draft", Proceedings of International Conference on Port and Ocean Engineering Under Arctic Conditions.

8. Brooks, L.D., (1979), "Another Hypothesis About Iceberg Draft", Proceedings of International Conference on Port and Ocean Engineering Under Arctic Conditions.

9. Brooks, L.D., (1979), "Another's Reply on the Discussion by Mogner and Zorn and Another Hypothesus About Iceberg Draft", Proceedings of International Conference on Port and Ocean Engineering Under Arctic Conditions.

10. Budinger, T.F., (1960), "Wind Effect on Icebergs", U.S. Coast Guard.

11. Mognor, K., and Zorn, R., (1979), "Discussion of "Another Hypothesis About Iceberg Draft", Proceedings of Third International Conference on Port and Ocean Engineering Under Arctic Conditions, Fairbanks.

12. Murray, J.E., (1968), "The Drift, Deterioration and Distribution of Iceberg in the North Atlantic Oceans", Ice Seminar, Calgary, Alberta.

13. Robe, R.Q., (1976), "Height to Draft Ratios of Icebergs", Proceedings of Third International Conference on Port and Ocean Engineering Under Arctic Conditions, Fairbanks.

14. Smith, E.H., (1925), "International Ice Patrol", The Meteorological Magazine, The Meteorological Committee, Air Ministry, Vol. 60, No. 718.

15. Steenstrup, K.J.V., "1893 Bidrag til Kjendskab til Bracerne og Braelsen I Nord-Gronland", Meddelelser om Gronaland, Vol. 4, p 71-112.

ICEBERG DIMENSIONS

Larry D. Brooks
Chevron Oil Company

Background

An iceberg's maximum horizontal dimension in the waterline is defined here as "length", and its draft as the depth below the waterline to its deepest point. Obviously, as an iceberg deteriorates and rolls to new equilibrium positions, its length and draft constantly change. Iceberg lengths have been readily determined by measuring the distance to the iceberg with a rangefinder (radar or optical) and the included angle with a sextant. Iceberg drafts have been inferred from above-water dimensions, assumed from water depth around grounded icebergs, and directly measured with dragline, diver, radar, and sonar. The quantity of these direct measurements is quite limited, and many are not in the public domain.

Because of the relative difficulty and uncertainty in measuring iceberg draft, a simple relationship between maximum possible draft (not necessarily actual draft) and above-water dimensions was sought. The application of this relationship was intended solely for operational situations and not for scientific or engineering purposes.

Measured Data Analysis

Of the many physical parameters of icebergs, only mass below water and total mass have a definite relationship (i.e., Archimedes' Principle). However, this relationship is very difficult to apply in the field because of the irregular, and for the underwater portion unknown, shape. Even if the underwater mass could be determined there is no direct relationship between it and draft. Many investigators have sought a relationship between iceberg draft and height. However, again there is no physical basis for this relationship, and the results have yielded ratios varying from 1:1 to 1:10.56. Wadhams has had reasonable success with Antarctic tabular icebergs which generally have a very rectangular solid shape.[1] This is not the case for the "picturesque" Greenland icebergs, and a more reliable relationship was sought.

The principles of naval architecture relate buoyant stability directly to the moment of inertia of the waterplane area and inversely to the displacement. Moment of inertia is linearly dependent on a waterplane dimension parallel to the axis of roll and dependent on the cube of a dimension normal to that axis. This relationship between stability and moment of inertia assumes the moment of inertia remains constant through small angles of roll (i.e., near vertical sides at the waterline). Applying these principles to icebergs, it appeared that a relationship between maximum possible draft, as a function of displacement, and dimensions of the waterplane area could be developed.

All available measured data were collected, and plots were made of height vs. draft, length vs. draft, width vs. draft, estimated mass (displacement) vs. draft, and the product of height, length, and width vs. draft. Each of the above plots was generally constructed for all data combined and for each

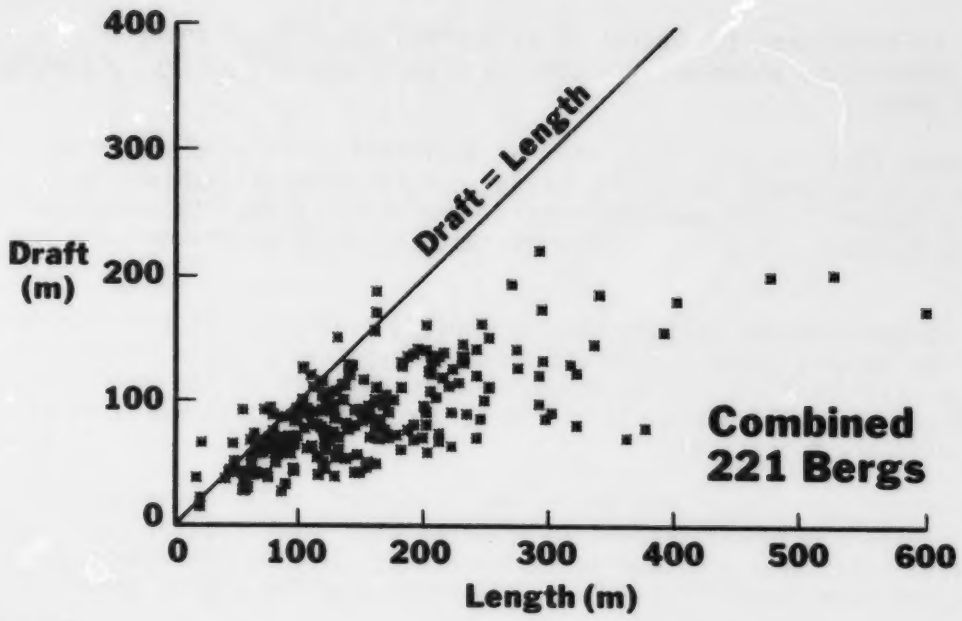

Figure 1

Icebergs With Draft > Length

221 Icebergs	All	Tabular	Blocky	Dry Dock	Pinnacle	Dome
No. Bergs D > L	18	3	3	0	6	6
Mean Overage (m)	17	7	18	—	14	26
Min/Max Overage	1/45	1/12	10/24	—	2/27	10/45
Mean $\left(\frac{\text{Overage}}{\text{Length}}\right)$	0.367	0.085	0.175	—	0.146	0.825

Figure 2

of the five International Ice Patrol (IIP) iceberg classifications (IIP classifies icebergs by above-water shape, as either tabular, blocky, pinnacle, drydock, or dome).

Analysis showed that the only plots with a consistent trend were length vs. draft. The plot of length vs. draft for all classifications combined is presented in Figure 1. The measured drafts were almost always less than or equal to the lengths. Thus the hypothesis that the draft should not exceed the length.

All of the larger icebergs satisfy the hypothesis, regardless of IIP classification. The largest iceberg that violates the hypothesis has a length of 160 m. and a draft of 187 m. (The approximate mean length of the total data base is 160 m.) Generally it would be the larger icebergs that would be of concern in offshore operations.

Of the 221 icebergs with measured drafts and "lengths", only 18 violate the hypothesis. Figure 2 summarizes the 18 icebergs with draft greater than length. A characteristic of these 18 icebergs is that their IIP classifications are mostly the more deteriorated types (i.e., 12 of 18 are pinnacle or dome).

Some of the "length" measurements may not be the maximum dimensions, and therefore the actual length-to-draft ratios may be greater than calculated. The maximum horizontal dimension in the waterplane was not specifically requested from all field investigators. They generally obtained two orthogonal measurements in the waterline plane. Obviously the largest dimension thus measured would always be less than or equal to the "length".

The error associated with the method (as opposed to choice, as discussed above) of length measurement is assumed to be symmetrical, plus and minus, and dependent on the method.

The error associated with the draft measurement is assumed to be unsymmetrical, more plus than minus, and very dependent on the equipment and operator.

Stability Analysis

The purpose of this analysis was to find simple theoretical iceberg shapes that are hydrodynamically stable and have drafts greater than lengths.

The theoretical icebergs were mathematically modeled and their centers of gravity (CG), centers of buoyancy (CB), and metacenters (CM) were determined. This was done with a two-dimensional cross section of the iceberg and a vertical axis of symmetry. Therefore, CG, CB, and CM all lay on this axis. CG is defined as the centroid of the cross section of the berg; CB, as the centroid of the underwater cross section; and CM, as the center of rotation for the CB's as the iceberg rolls through small angles from the vertical axis.

To compare icebergs of similar shapes (e.g., rectangles of various length-to-draft ratios) an indicator of stability is defined here as the ratio of the heights of CM to CG, both measured from the deepest point of the iceberg. If this stability ratio is less than one, the iceberg is unstable.

For rectangular cross sections, the stability ratio decreases with decreasing length-to-draft ratio (Figures 3, 4, 5, 6). When the length-to-draft ratio is decreased to one (Figure 5), the berg is still stable; however, there is a more stable position with the iceberg rotated 90° (the iceberg in Figure 4 is the same iceberg as in Figure 5 but rotated 90°). This implies that this iceberg would remain in the former position until ocean waves, for example, cause it to roll to the more stable position. The above rectangular cross sections would be classified by IIP as tabular icebergs.

The other IIP classifications were also investigated. The Figure 7 configuration is a stable blocky iceberg, with length equal to draft. Figure 8 is an example of an unstable pinnacle iceberg with draft greater than length. It will roll 45° to a stable position. Figure 9 is an example of an unstable drydock iceberg with length equal to draft, and Figure 10 is an example of a dome iceberg.

Many other theoretical shapes were modeled. In some cases the draft exceeded the length; however, in most of these a more stable position was possible for that shape. In Figure 7 the length to draft ratio is unity, and the stability ratio is greater than unity. This implies that the length-to-draft ratio could be reduced to less than unity and the shape would still be stable.

The stable orientations of a shape can be determined by finding the orientations with minimum gravitational potential energy.[2] Potential energy is proportional to the vertical distance between CB and CG. A plot of potential energy vs. orientation is presented as Figure 11 for the Figure 7 shape. The orientation as shown in Figure 7 is at 0° (and 360°), and this orientation does occur at a local minimum in the energy plot. However, there is another minimum in the energy plot at approximately 113° orientation (and 247°), and this orientation yields a lower potential energy than the 0° orientation. Therefore, although the shape is stable at 0° there is a more stable orientation at 113°. If the Figure 7 shape is rolled beyond the maximum energy point at about 53°, it will then continue rolling to the more stable orientation at about 113° (Figure 12). At this orientation the length-to-draft ratio is greater than 1.0, and the shape does not violate the hypothesis.

Epilogue

The measured data base was recently expanded to 296 icebergs, and only 25 violate the hypothesis. The mathematical stability analysis has been improved, and now models non-symmetrical shapes. Interesting shapes have been modeled that increase draft when rolled to an orientation with lower potential energy; however, these shapes still satisfied the hypothesis in the new orientation. These additional measured data and the improved mathematical model results lend more credibility to the hypothesis that an iceberg's draft should not exceed its length.

References

1. Wadhams, P.; personal communication (1982).

2. Benedict, C. P.; personal communication (1978).

Length/Draft = 2.26
Stability = 1.55

Figure 3

Length/Draft = 1.29
Stability = 1.10

Figure 4

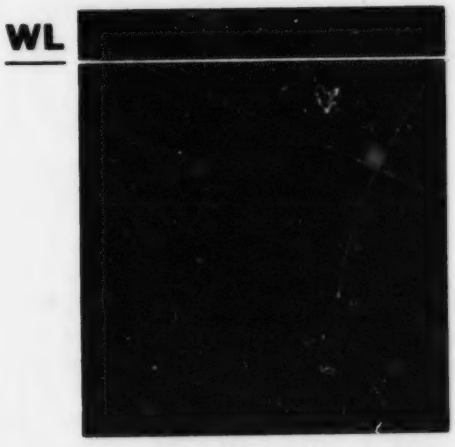

Length/Draft = 1.00
Stability = 1.01

Figure 5

Length/Draft = 0.57
Stability = 0.92

Figure 6

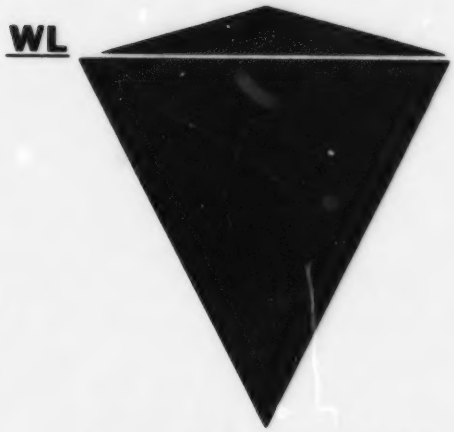

Length/Draft = 1.00
Stability = 1.15

Figure 7

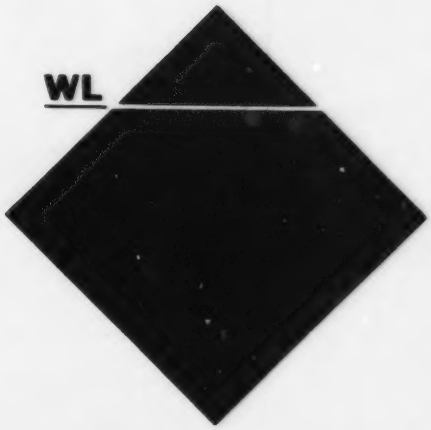

Length/Draft = 0.65
Stability = 0.95

Figure 8

Length/Draft = 1.00
Stability = 0.98

Figure 9

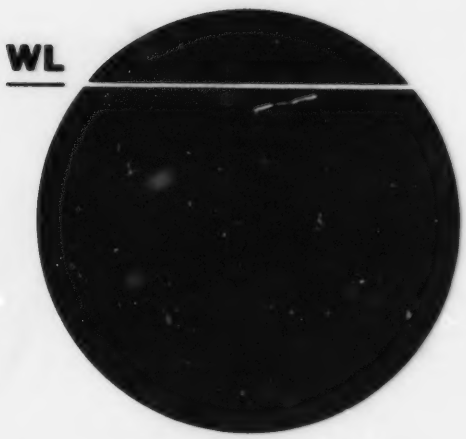

Length/Draft = 0.92
Stability = 1.00

Figure 10

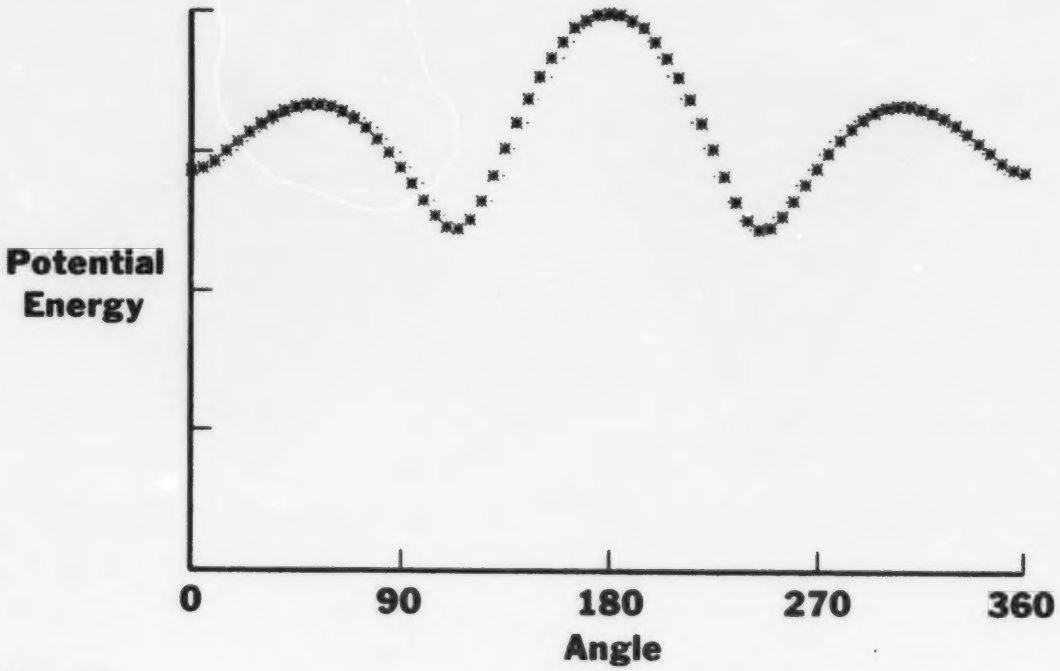

Figure 11

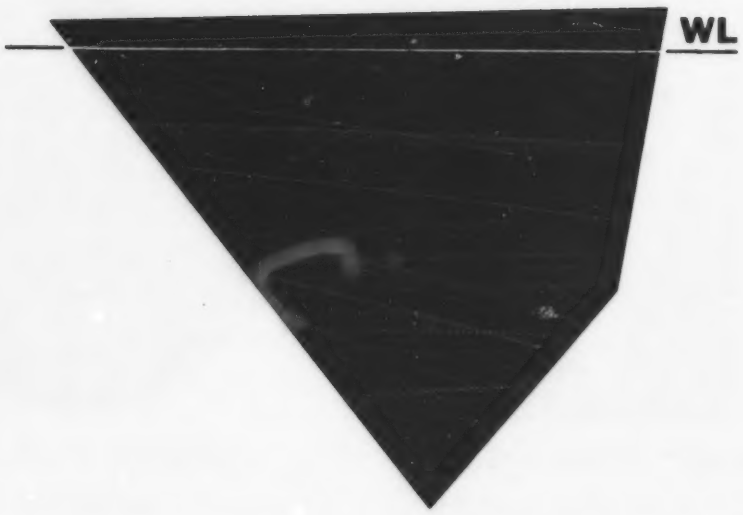

Length/Draft = 1.29 **Stability = 1.24**

Figure 12

REVIEW OF DEEP WATER SCOURS IN THE DAVIS STRAIT AND ITS RELEVANCE TO PRESENT DAY ACTIVITY

J.Y. Guigne[1], D.I. Ross[1] and H. Westergard[2]

ABSTRACT

In July 1980, Geonautics Limited carried out a Sidescan Sonar survey in 350-400 metres water depth in the Davis Strait area for Aquitaine Company of Canada, operator for the Baffin Labrador Group of companies. A major objective of the study was to evaluate the extent and nature of iceberg scouring in the area. The deep water and strong currents required a careful assessment of each line to evaluate layback and side movement corrections for the towed fish. The high illustrative quality of the sonograms provided an excellent record of the nature of scouring around the Hekja Wellsite. Of the 281 scours interpreted 48.4 percent were longer than 500 metres, 63.0 percent were deeper than 1.5 metres and 59.5 percent had widths in the range of 20 to 30 metres. The dominant orientation was NE - SW, concordant to the currents.

The sonograms provided a surprisingly wide catalogue of distinct iceberg scour marks which suggested at least initially, a range of ages from relict to recent time. However, the absence of observed icebergs with keel depths capable of scouring in these water depths raises serious questions on the relevance of using the physical characteristics of iceberg scours in assessing the question of age. This also questions the reliability of interpreting the relative age of scours found in the shallower areas of the Eastern Canadian seaboard based solely on scour characteristics as interpreted off Sidescan Sonar data.

[1]NORDCO/Geonautics, P.O. Box 8833, St. John's, Nfld.
[2]Canterra Energy Ltd., P.O. Box 1051, Calgary, Alberta

INTRODUCTION

During the summer of 1980, Geonautics Limited was involved in the acquisition and interpretation of Sidescan Sonar records in 350 - 400 metres water depth in the Davis Strait area for Aquitaine Company of Canada, operator for the Baffin Labrador Group of companies (refer to Figure 1-Location map; Geonautics Ltd. 1980).

A major objective of the study was to evaluate the extent and nature of iceberg scouring in the area. The sonograms provided a surprisingly wide catalogue of distinct iceberg scour marks which suggested at least initally a range of ages from relict to recent time. This paper is a review of the scour interpretations made for the Hekja Wellsite and vicinity with an account on the relevance of these scours to present day scour activity.

SIDESCAN SONAR ANALYSIS AND INTERPRETATION

The scanning positions of the ORE sonar fish were dramatically controlled by the strong tidal currents which exist in the deep waters of the Davis Strait. To correct for the large layback angle and distance distortions, each survey line had to be carefully interpreted for matching sets of corresponding marks. These sets of marks were then referenced against two known locations on the seabed; an abandon well attempt and the Hekja A-72 wellhead. Where other distinctive traces were noticed an attempt was made to cross correlate the features against adjacent lines. This also took into consideration the effects of the prevailing currents and tidal streams as well as variations in ship heading. The combined result of all the interpreted sonograms produced a good coverage grid. The relative positioning of the iceberg scours mapped are considered precise. (refer to Figure 2-Corrected Layback Tracks).

Scour depths were measured from the base of the berm to the deepest part of the scour. Scour widths were determined after the orientation of the scours were known from the sonogram analyses. The width of a scour was measured as the distance between the centre of the two berms. This is indicated in Figure 3 as "$\dot{w}$" the apparent width. These apparent width measurements were then corrected for distortions resulting from the difference in scale perpendicular and parallel to the Sidescan sonograms.

RESULTS

A chart illustration of the iceberg scour interpretation for the vicinity of the Hekja wellsite is presented in Figure 4. The iceberg scours featured on the sonograms are straight, meandering and curvilinear with berms on one or both sides of their furrow. A few iceberg pits are also present and are oblong in plan view.

Contrary to the theories and assumptions which have been used in past hypothesizes concerning the nature of scour of the more northerly sites (sites in water depths exceeding 300 metres), the Hekja site is seen to be surrounded by prominent linear scours. Over an area 7 km by 4 km in the immediate vicinity of Hekja, 281 scours were measured. Of these 281 scours, 48.4% have gouges which are longer than 500 meters, 27.0% exceed 1 km, and 4.6% are greater than 3 km. These scours are remarkably linear and traverse smoothly across the area. Of further significance are the scour depths observed. For instance 63.0% of the furrows are deeper than 1.5 metres, 17.5% are greater than 2.5 metres and 9.3% exceed 3.5 metres. This latter percent of 9.3% is an important engineering criteria to be considered in the development of protection systems for well heads and other seafloor structures.

The widths recorded are also remarkable. Scour widths in the range of 20 to 30 metres make up 59.5%. However, this is slightly misleading; the breakdown between the width categories of 15 to 40 metres tend to be uniformly distributed as follows:

Widths:
- 11 to 15 metres - 10.5%
- 16 to 20 metres - 22.1%
- 21 to 25 metres - 23.5%
- 26 to 30 metres - 13.9%
- 31 to 35 metres - 9.5%
- 36 to 40 metres - 13.2%

Also of interest to note, only 4% were 10 metres wide or smaller and 1.1% were greater than 60 metres. The widest scour measured was 70 to 80 metres while the smallest was 5 metres. The average scour in the Hekja site could be categorized as 1.5 metres deep or less, 25 metres wide and approximately 500 metres in length.

A further significant factor is the strong NE-SW scour orientation. Most of the scours were linear, traversing concordantly along the perimeter of a rising slope. This is particularly observed on the south east and east portion of Figure 4. Further west a more northerly orientation occurs. This however, is not observed as a distinct change of direction but rather a gradual smooth transition. Since the strong currents which exist here are the dominant forces in this area, these scour marks are predominantly the result of this influence. The interaction of the seabed slope with an iceberg keel is secondary, though present.

Clear examples of icebergs that have grounded leaving oval shaped depressions have been recorded. An outstanding example of a broad iceberg coming to a halt possibly tilting and at a later stage escaping is observed on one of the sonograms and is impressive in structure. (refer to Figure 4 - Indicator A).

CONCLUSIONS

Iceberg scours on the HEKJA site are dominantly linear with a few which illustrate meandering patterns. This reflects the trend of the strong currents in the area with a primary scour orientation in the NE-SW direction. Bathymetry has an influence on scouring even though secondary to the currents. The most striking statistic is the near continuous length of the scours (48.4% longer than 500 metres). These long scours are consistent with the physical nature of the massive bergs which would be needed to scour in water depths of 350 metres. The large number of scours with depths in excess of 3 metres is also an indication of the massive iceberg sizes. Considering the dynamic state of the area, the potential for post scour sedimentation and slumping of low cohesive sands into the scours, the scour depths observed are thus significant factors. Levees or shoulders of old or relict scours tend to be low in reflectivity, rounded or eroded in appearance. However, the scours seen in this site do not all appear like this. Some scours recorded have distinct features such as high levees and/or clear furrows (refer to Figure 5). Since movement of sediments is recognized, e.g. sand waves have been observed on the sidescan records, infilling of the scours would be expected to occur over a hundred year period. Therefore on first observation, it would appear unlikely that all the scours recorded are relict of a past glaciation. In actual fact, the nature of these seabed gouges are not characteristic of glacial or post glacial activities (e.g. fluvio-glacial erosion) but rather of direct iceberg encounters. This is not to say that the scours are of a recent origin but rather that there are some scours which have forms, depth and overall continuous lengths that would suggest scouring in the last century.

In order to correctly answer such questions as, age of scours, effect of mass size, and distribution of current icebergs, as well as effects of bathymetry in deflecting scours, an appreciation for the origin of the present day iceberg is required. Firstly, if we examine the bathymetric control of 350 meters, there are not too many sources or passages from which icebergs having a draft of 350 meters or greater can leave Greenland and strike the vicinity of the Hekja site.

Secondly, and possibly of greater significance, is the mass that would be associated with a draft of 350 meters. From past studies and involvement in iceberg scour models, iceberg drafts of about 200 meters corresponding to a mass of 20 to 50 million tons represent the upper limit of known measurements occuring in the Labrador Sea. Thus extrapolating further for a draft of 350 meters, the calculations suggest a hypothesized mass in the order of 120 to 150 million tons. An iceberg having a mass of 50 to 80 million tons, although very high is a possibility for the Davis Strait. Masses beyond 100 million tons would definitely be of rare occurrence. It is to be understood that the limits of the present statements are based on iceberg draft measurements which do not exceed 200 meters. Since regression curves are only reliable within the limits of the data, no draft to mass relations can be reliably utilized beyond the data boundaries. However, extraploation for a draft of 350 metres, 120 to 150 million tons may be considered as an initial approximation for discussion purposes.

The largest number of large icebergs is formed by the glaciers of the West Greenland Coast flowing into Melville Bight and into Disko and other bays facing the transverse Greenland trough. Since few glaciers come directly into fiords of the required water depth off northern Ellesmere Island or north West Greenland, it would appear unlikely that large icebergs could reach the Hekja site. Nevertheless isolated reports have been published referring to cases where bergs were reported grounded in extreme water depths. A Milne (1969) mentions damage to a bottom mounted hydrophone system by an iceberg in 427 metres of water. Very high berg sail heights are mentioned by Ye Ye Shvede (1966) in which he quoted authors Zubov (1945) and Fabricius (1965) of observing heights 149 and even 225 m above the sea surface. This would yield draft sizes greater than 450 meters.

Based on the available data it is impossible to rule out recent scouring in these water depths. The probability, however, seems small in relation to the density of scouring observed at Hekja. Such a conclusion places in question the traditional classification of iceberg scours as recent or relict based on distinct differences in physical characteristics of the scours. Similarly the use of physical characteristics to develop models of relative age of scour may need careful reassessment in some east coast areas.

REFERENCES

Fabricius, O. On the floating ice in the northern waters. Geogr. Rev. 45, No. 3, 1965.

Geonautics Limited. Side Scan Sonar Survey Hekja Site and Vicinity - Report for Aquitaine Company of Canada Ltd. October 1980 - File No.: 80-1002 Geonautics.

Milne, A. 1969. Underwater acoustics in ice-covered seas. Man in Cold Water Conf., Montreal, Que., May, 1969. Dep. of Industry, Trade and Commerce, Canada. Oceanology Series 1: 37-42.

Shvede, Ye Ye. Icebergs of the Northwest Atlantic. Oceanology, v. 6 (1966). Pg. 499.

Zubov, N.N. L'dy Arktiki (Arctic Ice). Izd. Glavsevmorputi, 1945.

FIGURE 1. LOCATION MAP

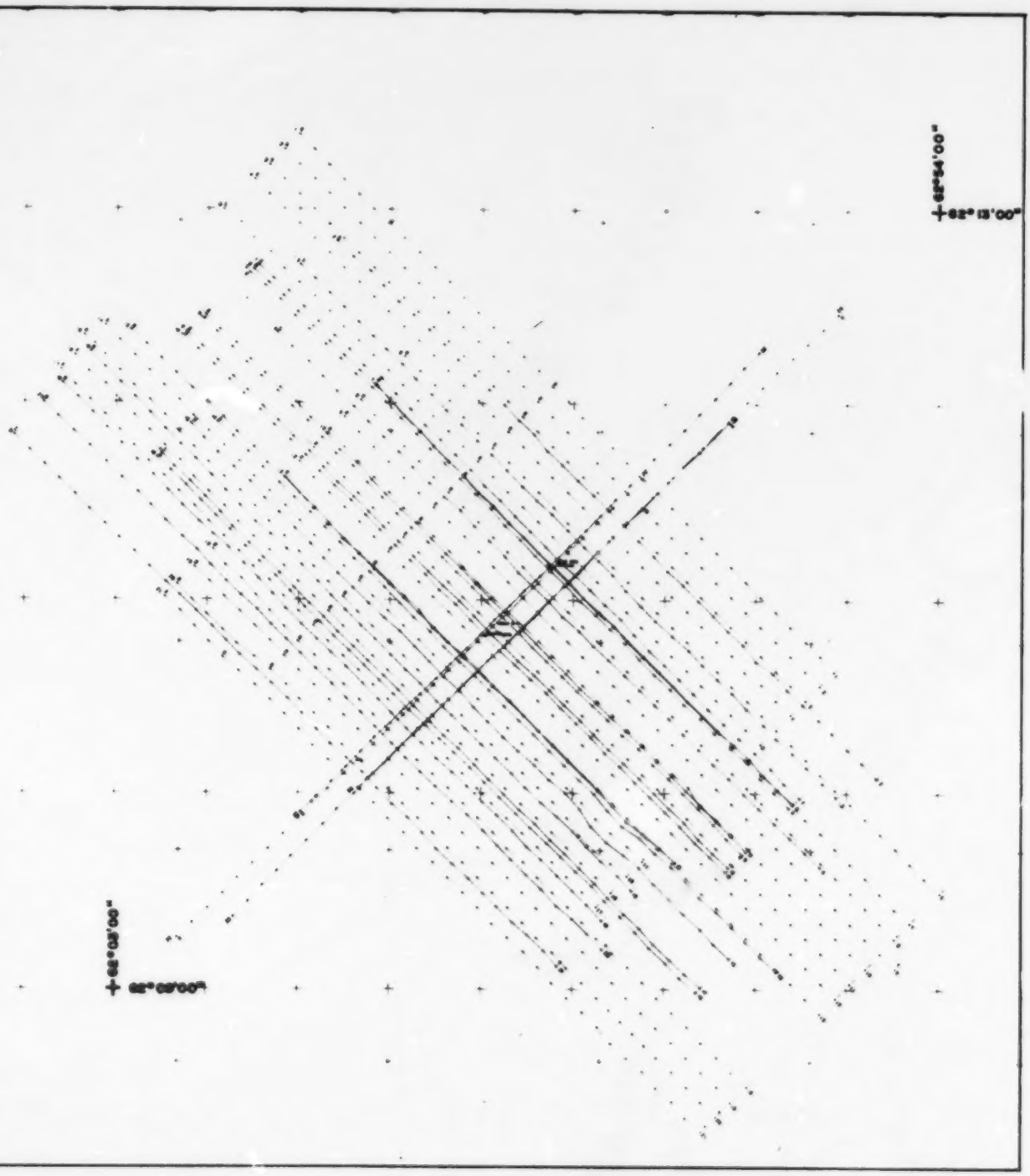

FIGURE 2. CORRECTED LAYBACK TRACKS

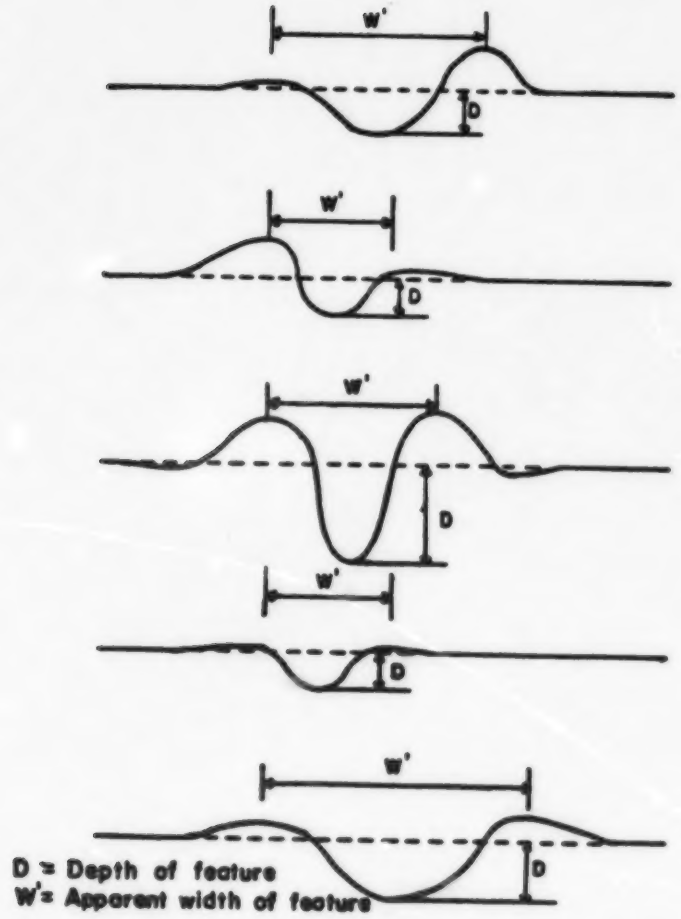

Scour and Pit Depth and Apparent Width

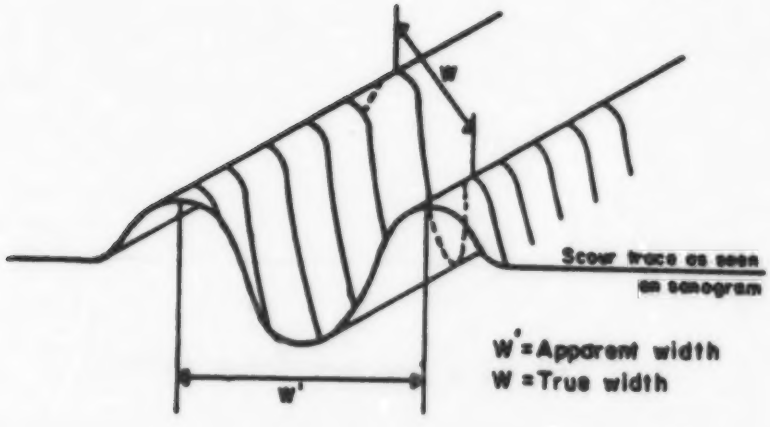

FIGURE 3

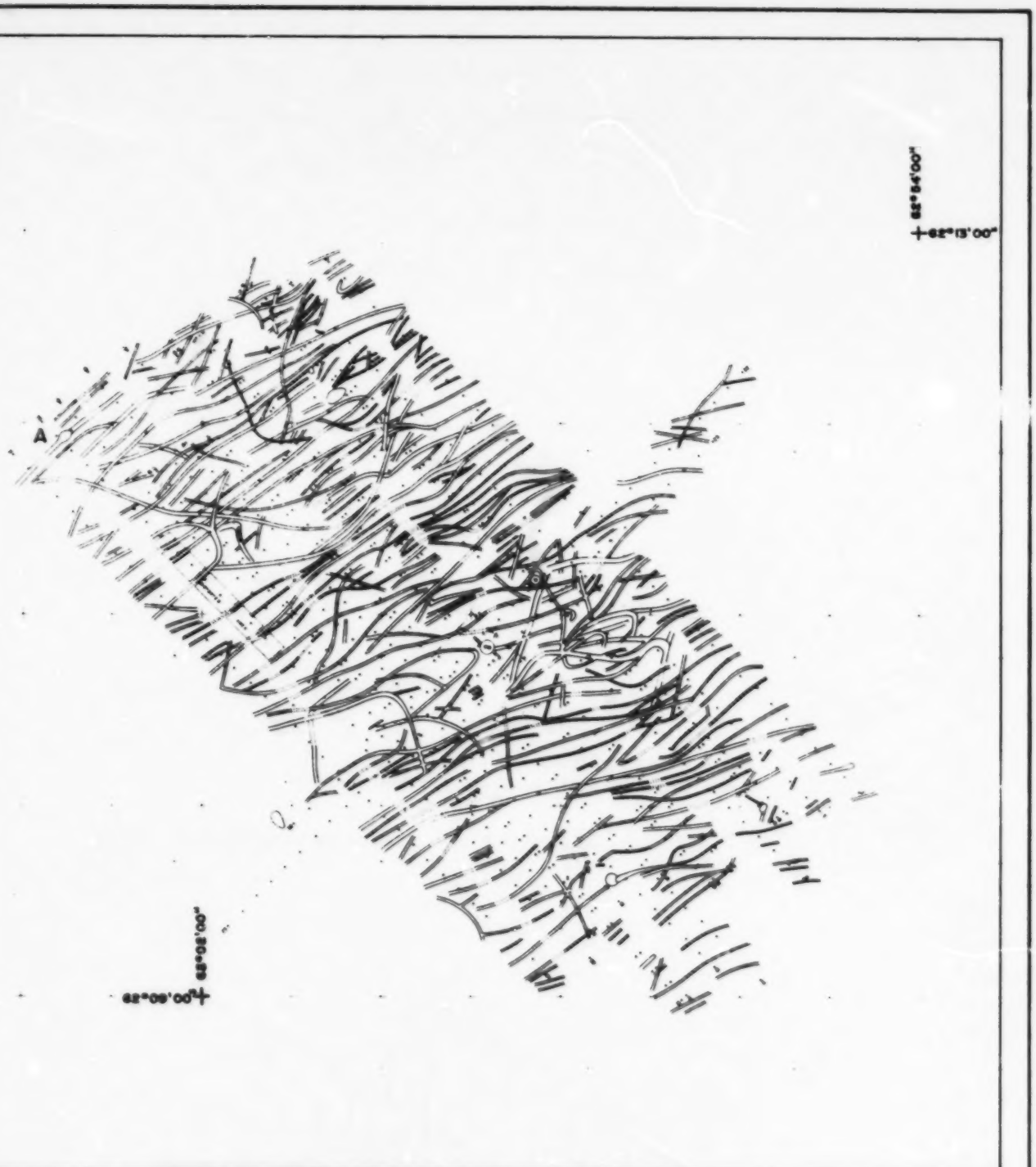

FIGURE 4. ICEBERG SCOUR CHART

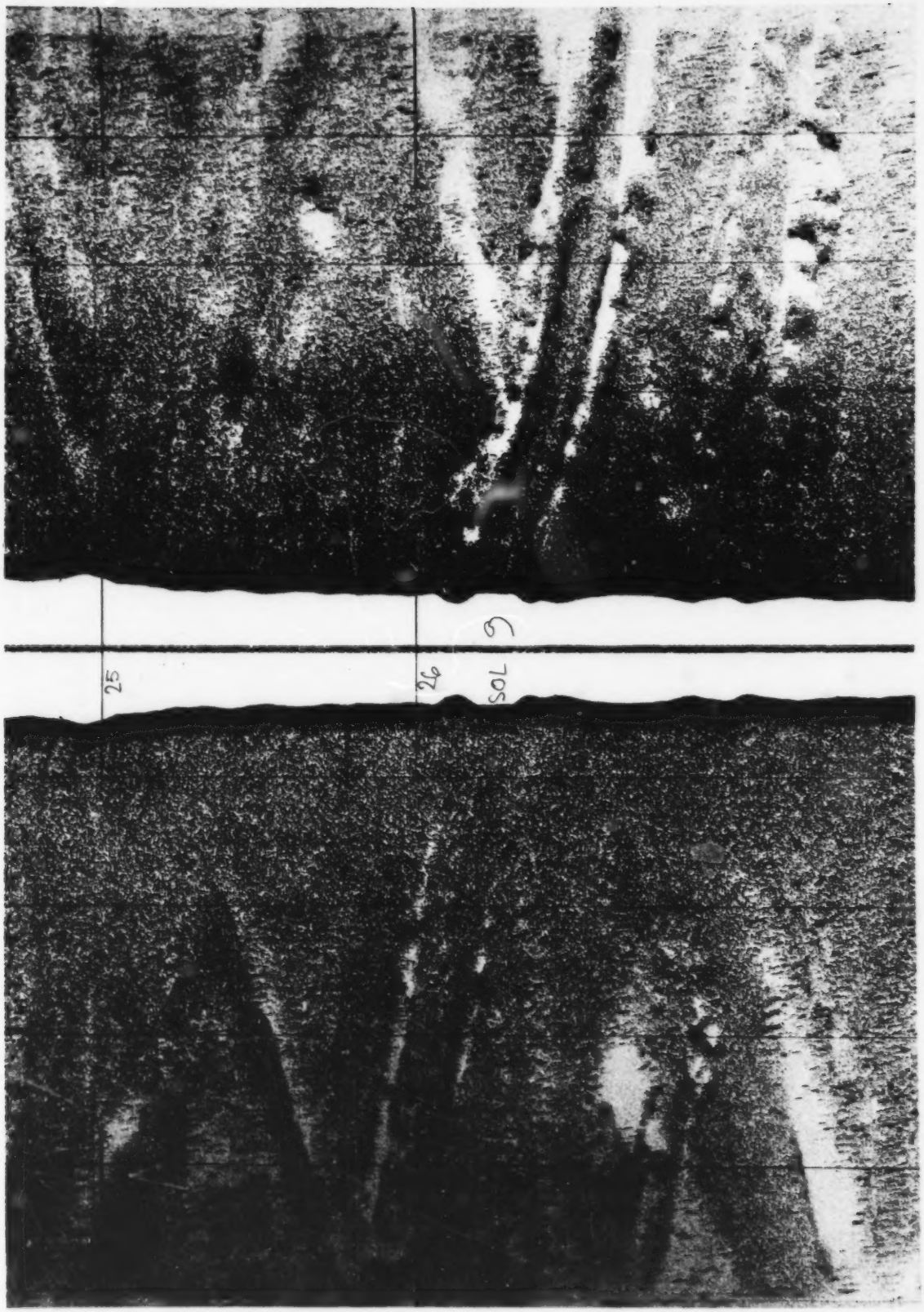

FIGURE 5

Use of Draft Distribution for Evaluating Iceberg Incursion Probability

J. Lewis and P. Benedict
Ice Engineering, P.O. Box 6082
St. Johns, Newfoundland

Before offshore hydrocarbon deposits can be developed commercially, the probability of iceberg scouring and incursion into subsea production facilities must be evaluated. Such information is an essential component in specifying the design parameters related to the platforms and/or subsea systems to be used in recovery of oil and gas.

This paper presents a method for describing analytically the distribution of iceberg drafts at a particular latitude, and of combining this with site bathymetry and iceberg flux data to calculate iceberg incursion probabilities and mean times between incursions as a function of site design parameters.

CORRELATION BETWEEN AN ICE RIDGE AND SEA BED GEOLOGIC BOUNDARY

Peter W. Barnes

C. Robin Ross

Erk Reimnitz

U.S. Geological Survey

Pacific-Arctic Branch of Marine Geology

345 Middlefield Road, MS 99

Menlo Park, CA 94025

Prepared for presentation at National Research Council of Canada's Ice Scour Workshop,

Montebello, Quebec, February 15-19, 1982

ABSTRACT

During the summer of 1979 a series of three precisely navigated side-scan sonar and bathymetry lines were run along well-located ice ridges observed in the spring of the same year. No obvious set of gouges lead up to the location of the ridge nor were gouges associated with the existing remnants of the ice ridges observed in summer. However, the innermost ice ridge of the stamukhi zone appears to correlate with a break in bottom slope and a marked change in gouge character. Gouging is more intense seaward in the stamukhi zone although gouge orientations are essentially the same. The bottom profile is marked by a 1 to 2 m high bench. Diver observations coupled with vibracore sample data indicate that there is a decrease in the compactness of the surficial gravelly mud sediments on the seaward side of the bench. The cause and effect relationship between the ice zonation and the seabed character is well established; however the mechanisms for the abrupt nature of the break are unsure.

INTRODUCTION

Reimnitz and Barnes (1974) noted a small break in slope and an associated change in sediment character. The change in sediment character also correlates with a change in sedimentary structures (Barnes and Reimnitz, 1974) and was later tied into the ice zonation on the inner shelf (Reimnitz et al, 1978). Correlation of in ice-gouge character with this boundry has been alluded to but never clearly established (Brooks, 1974; Barnes et al., 1978, Rearic et al, 1982).

During the spring of 1979 we became aware of data on the exact location of ice ridges at the inner edge of the stamukhi zone (Reimnitz et al., 1978) These data, from an area north of Narwhal Island (Fig. 1), were gathered from

aerial photography, and were kindly provided to us by researchers of the Shell Development Company of Houston, Texas. During August, 1979 open-water and grounded ridge remnants were present in the area of the ice-ridge data. Utilizing a precision navigation system, the remnant grounded ice features and the seabed in the vicinity of the ice ridges located the previous spring were studied. This report is a preliminary interpretation of the relationships that were observed between spring ice ridges, grounded ridge remnants, seabed topography, and ice-gouge character.

METHODS

The innermost ridge of the stamukhi zone and ridges further seaward, along with major rubble piles, were located utilizing aerial photography. The accuracy of these locations is unknown but believed to be within 50 m. These positions were transferred to a UTM projection at a scale of 1:20,000 with a precision of $\pm$20 m. Summer navigation aboard the R/V KARLUK utilized a range-range navigation instrument giving positional accuracy to better than $\pm$10 m. Judging by the location of a major rubble field reported on by Hanson and Metzner (1979), whose position is unlikely to have changed from spring to summer, due to being heavily grounded, we believe our summer positions were within 20 m of the ridges located in the spring aerial photography.

In addition to the navigational data, the following information was gathered. The location of many but not all grounded ice remnants was determined from shipboard navigation and a hand-held range finder. Bathymetry was obtained using a fathometer with a resolution of 20 cm, while seabed morphology was studied from sonographs obtained with a 105 Khz side-scan sonar on a 250-m-scan width. The particulars of these systems are given in Reimnitz and Barnes, 1974 and Barnes et al., 1978.

OBSERVATIONS-COMMENTS

Grounded ice remnants:

As shown in figure 2, observations of grounded ice along trackline 81 indicated that ice ridge remnants were present in August for 5-10 percent of ridge length. Open water was extensive inshore and seaward of these ridge remnants indicating that they were grounded. However, most of the remnants observed extended less than 3 m above sea level. Given ridge to keel ratios of 1:3 to 1:9 (Aug. 1:4.5) (Kovacs and Mellor, 1974), and water depths of 18 to 20 m, these remnants should not have been heavily grounded at the time of observation. We do not have information on ridge height prior to the melt season.

These observations indicate that winter ridges are grounded and suggest that a small percentage of the ridge are resting on the seabed in winter. This data also documents the persistence of these grounded features well into the open-water season.

Bathymetry:

Maximum incision depths for ice gouges were taken from fathograms for 250-m segments of the three tracklines surveyed. The maximum observed gouge incision was 1.4 m. The most striking observation regarding these data is the abrupt change in maximum incision depths as one proceeds seaward along the tracklines. Associated with the increase in incision depths is a break in the bottom slope, which takes the form of a steepening of the slope at about 18 m down to about 20 m.

Ice-gouge morphology (sonographs):

The general character of seabed morphology was examined on the sonographs and found to have undergone a marked change associated with the change in bathymetry. Gouges become much crisper, clearer, on the seaward side of the observed bathymetric boundary (Figure 3). Inshore of the break in slope the number of gouges is similar but the seafloor morphology is much subdued.

The orientations of the dominant gouge trend were determined for 250-m segments on either side of the boundary, using techniques given in Barnes et al. (1978). The trends in both areas are essentially the same; parallel to the trend of the coastline and the bathymetric contours. There is an inconclusive suggestion that the gouges inshore of the break in slope are less randomly oriented than the gouges seaward. These relationships are summarized in figure 4.

Sediment character:

Vibracores from both sides of the break in slope indicate an extremely cohesive, stiff seabed. Of four attempts to vibracore in 1978, only one 50 cm core was recovered from the seaward side of the break in slope (Barnes et al., 1979). The core consisted of a poorly sorted mixture of gravel- to clay-sized material, highly compacted. Two attempts to vibracore in 1979 were also unsuccessful in penetratng or recovering cores in the vicinity of the break in slope.

Diver observations confirm and amplify the coring results. Two dives were made by one of the authors (E.R.) also in 1979, one inside and one seaward of the boundary in the general area of this study. The dive on the higher inshore part of the bench revealed a smooth undulating surface of compacted gravelly muds with clasts to at least 10-cm diameter. There was no

evidence of any recent ice gouging. Furthermore, hydroids and other seabed critters were common. On the seaward side of the bench the seabed was less consolidated and more recently disrupted, although blocks, slabs, and outcrops of highly consolidated material were common. The sediments were also gravelly muds indicating that the sediments on both sides of the boundary are the same.

The ice distribution observed during the period of these dives presented an enigma as high concentrations of grounded ice features including ridge fragments tens of meters long occurred inshore of the break in slope, while seaward of the break was essentially ice free.

DISCUSSION

The principal question to be discussed is whether or not the seabed morphology is more than coincidently related to sea-ice ridging. The observatons are suggestive but inconclusive at present.

Reimnitz et al. (1978) proposed an ice zonation of the inner Beaufort Sea shelf that includes the accretionary grounded ridge system, of the stamukhi zone. The inner boundary of this zone occurs at the approximate position of the observed change in seabed character. Thus the inner ridges observed in the spring of 1979 and those grounded ridge remnants noted during the present survey represent parts of the stamukhi zone. If the location of the stamukhi zone were reasonably repetitive over tens or hundreds of years, as is suggested by the controlling mechanism of coastal promontories (Reimnitz et al., 1978), the seabed under this zone should be more intensely reworked due to the abundance of ridges and grounded features associated with this zone. If this were the case then the reworked and deeply scoured and eroded area seaward of the break in slope would represent an area where repetitive ice keels of the stamukhi zone had bulldozed, resuspended, reworked and eroded sediments to a greater extent than in the area onshore from this zone.

The 1979 observations are inconclusive with regard to the above hypothesis. Indeed, the major ridging, as outlined in the aerial photographic survey, is oriented approximately parallel to the break in slope-gouge character, but in reality cuts obliquely across the boundary (Figs. 1 and 2). Similarly, the grounded ridge fragments noted in summer also cut across this boundary (Fig. 2). This would suggest that the boundary should be less pronounced than observed as the inner edge of the stamukhi is not clearly associated with the seabed boundary. The location of the grounded ice ridge fragments further suggests modern ice gouging should be clearly present inside of this boundary. Neither the sonographs nor the diving observations suggest a gradational boundary nor well-defined modern gouges inside the boundry. Futhermore the summer distribution of grounded ridge features--at least in 1979--was clearly dominated by grounded features inside of this boundary, whereas the hypothesis would be better served if the major grounded features were further seaward, as in the case of the inner ice ridges of the stamukhi zone at Stamukhi Shoal (Reimnitz and Maurer, 1978).

CONCLUSIONS

1) A series of ice ridges grounded during the winter and spring of 1979 north of Narwhal Island. Five to ten percent of these ridges were encountered as grounded remnants in August 1979, suggesting a minimal value for the amount of grounding of the inner edge of the stamukhi zone in winter.

2) The ridging is associated with a marked change in seabed topography and character, and ice-gouge morphology. A 1- to 3-m-high break in slope separates an onshore area of subdued and shallow gouge incisions in a compact gravelly mud from an offshore area of crisp, deeply incised gouges cut into soft to compact gravelly muds. Gouges in both areas are essentially coast-parallel.

3) A hypothesis suggesting a direct association of the ice ridging with the abrupt change in seabed character is hindered by the observation that the the winter location of the 1979 ice ridges cuts across this boundary, as does the summer 1979 distribution of grounded ice features.

4) The similarity of seabed sediments, the orientation of the gouges as well as the intensity of the gouges on the seaward side of the boundary strongly suggest that slope break and seabed character are the result of ice gouging. The boundary also appears to be closely related to the location of the stamukhi zone. However, the factors causing the boundary to be abrupt and well-defined remain an enigma.

REFERENCES

Barnes, P.W., and Reimnitz, Erk, 1974, Sedimentary processes on arctic shelves off the northern coast of Alaska, in: Reed, J.C., and Sater, J.E., (eds.), The Coast and Shelf of the Beaufort Sea, Arctic Institute of North America, Arlington, Va., p. 439-576.

Barnes, P.W., McDowell, David, and Reimnitz, Erk, 1978, Ice gouging characteristics: their changing patterns from 1975-1977, Beaufort Sea, Alaska, U.S. Geological Survey Open-File Report 78-730, 40 p.

Barnes, P.W., Reimnitz, Erk, Toimil, Larry, Maurer, Douglas, and McDowell, David, 1979, Core descriptions and preliminary observations of vibracores from the Alaskan Beaufort Sea shelf, U.S. Geological Survey Open-File Report 79-351, 71 p.

Brooks, L.D., 1974, Ice scour on northern continental shelf of Alaska, in: Reed, J.C., and Sater, J.E., (eds.), The Coast and Shelf of the Beaufort Sea, Arctic Institute of North America, Arlington, Va., p. 355-366.

Hanson, Arnold and Metzner, Ronald, 1979, Forty-meter ice pile in the proposed Beaufort Sea lease area, Abs. Alaska Science Congress, 1979.

Kovacs, A. and Mellor, M., 1974, Sea Ice Morphology and Ice as a geologic agent in the southern Beaufort Sea, in: Reed, J. C., and Sater, J. E., (Eds.) The Coast and Shelf of the Beaufort Sea, Arctic Institute of North America, Arlington, VA, p. 113-161.

Rearic, D.M., Barnes, P.W., and Reimnitz, Erk, 1982, Ice gouge data, Beaufort Sea Alaska, 1972-1980, U.S. Geological Survey Open-file Report, 81-950.

Reimnitz, Erk, and Barnes, P.W., 1974, Sea ice as a geologic agent on the Beaufort Sea shelf of Alaska: in: Reed, J.C., and Sater, J.E., (eds.), The Coast and Shelf of the Beaufort Sea, Arctic Institute of North America, Arlington, Va., p. 355-366.

Reimnitz, Erk, and Maurer, D.K., 1978, Stamukhi shoals of the arctic--some observations from the Beaufort Sea, U.S. Geological Survey Open-File Report 78-666, 17 p.

Reimnitz, Erk, Toimil, L.J., and Barnes, Peter, 1978, Arctic continental shelf morphology related to sea-ice zonation, Beaufort Sea, Alaska, Marine Geology, v. 28, p. 179-210.

FIGURES

Figure 1. Ice gouge character along lines 79, 80, and 81. Maximum gouge incisions are taken from fathograms. Dominant and subordinate gouge orientations were measured on the sonograph from trackline 81. The change in gouge character was determined from both sonographs and fathograms. Photographs from sections of the sonograph from Line 81 are represented by letters and are shown in figure 3.

Figure 2. Map of same area as figure 1. Grounded ice remnants were located in August, 1979. These compare with ice ridges drawn using data obtained from Shell Development Company. Depth contours were determined from 1979 fathograms.

Figure 3. Sonographs of seabed morphology along trackline 81. A and B are taken of the seabed seaward of the boundary. C and D illustrate the subdued seabed character typical of the bench area inshore from the boundary.

Figure 4. Dominant orientations of gouges measured north and south of the change in gouge character. Bar shows the percent of the total number of gouge orientations in 30° segments.

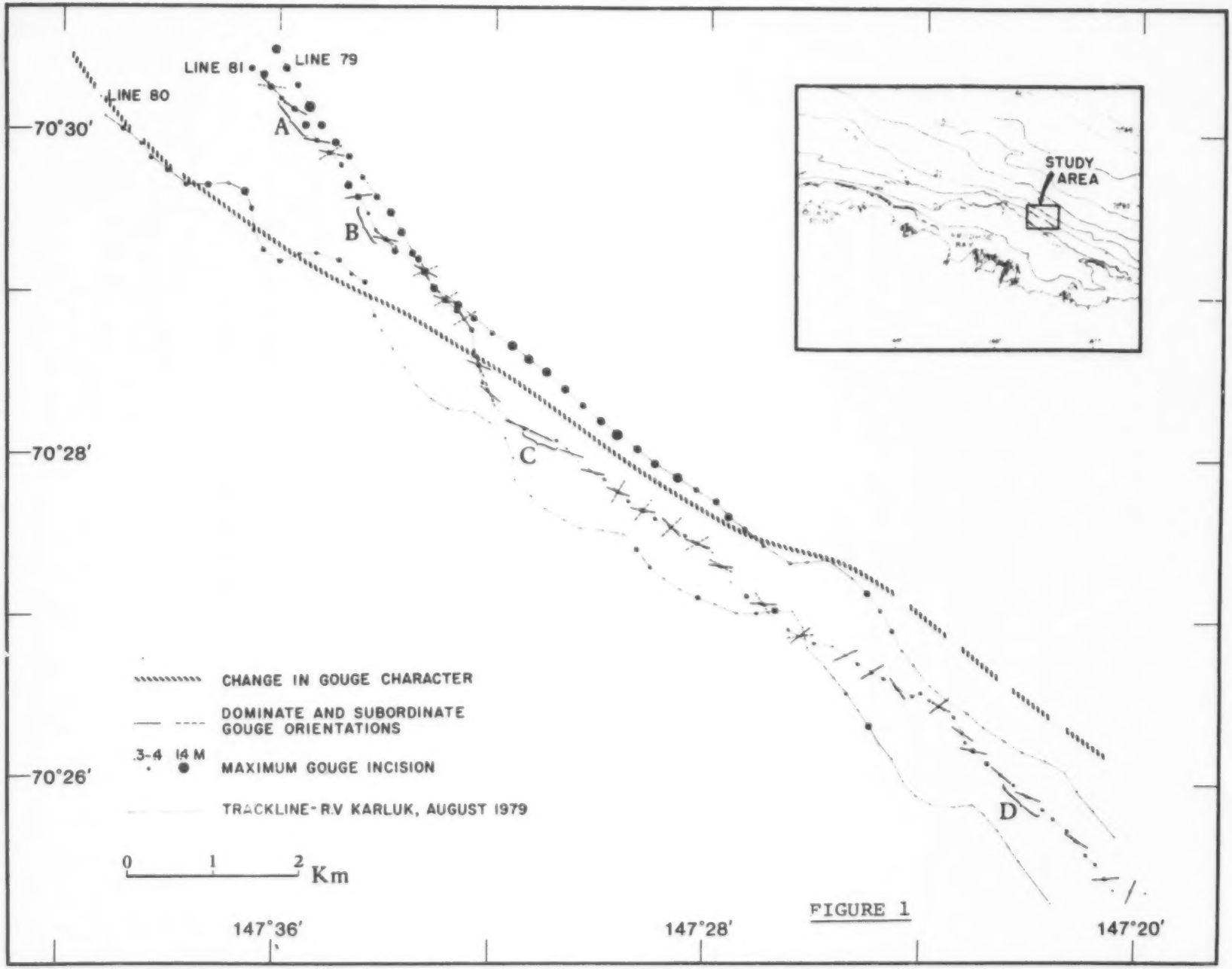
LINE 81
LINE 79
LINE 80
70°30'
70°28'
70°26'
A
B
C
D
STUDY AREA
CHANGE IN GOUGE CHARACTER
DOMINATE AND SUBORDINATE GOUGE ORIENTATIONS
3-4
14 M
MAXIMUM GOUGE INCISION
TRACKLINE-R.V KARLUK, AUGUST 1979
0
1
2
Km
147°36'
147°28'
147°20'

FIGURE 1

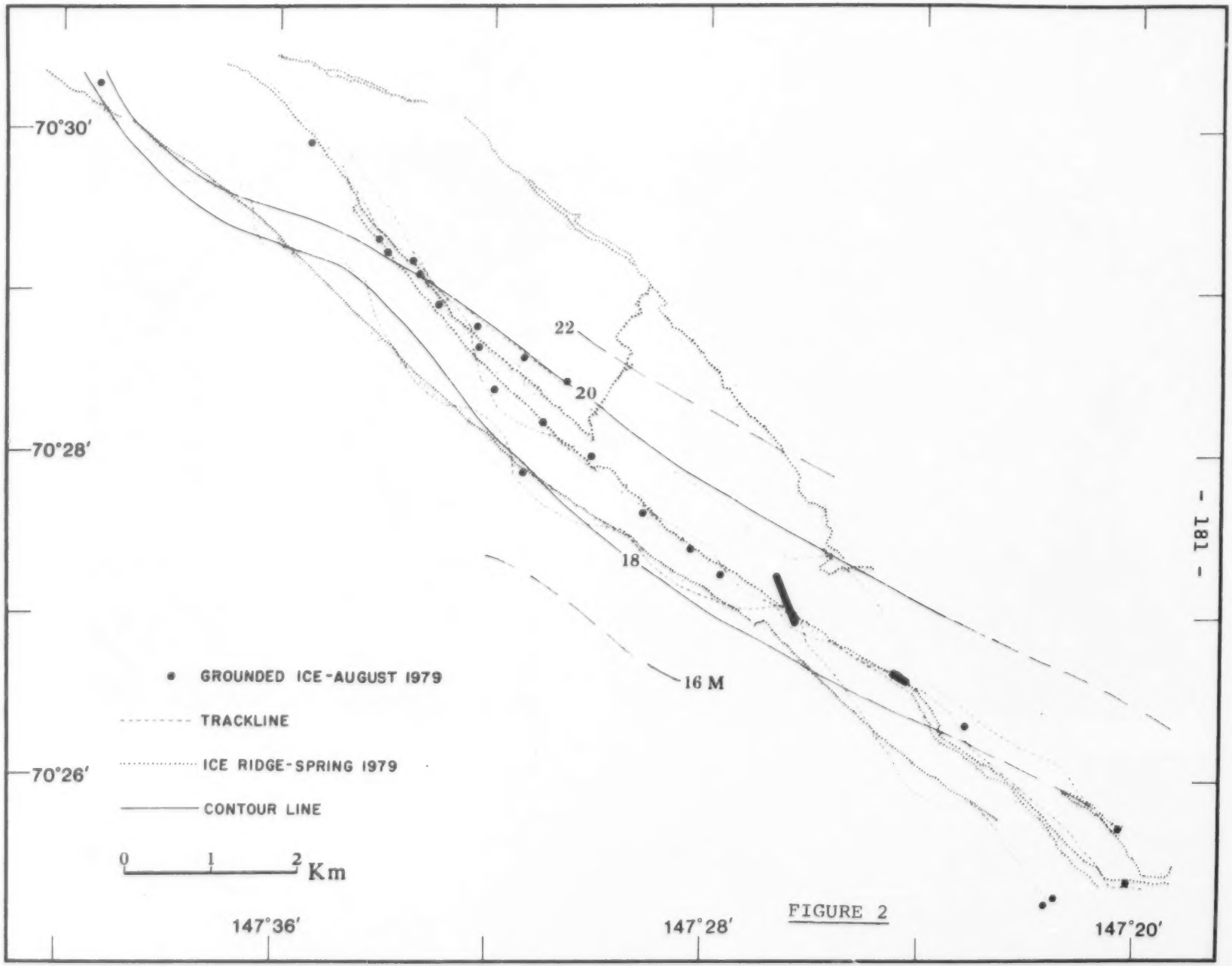
70°30′
70°28′
70°26′
147°36′
147°28′
147°20′
22
20
18
16 M
GROUNDED ICE-AUGUST 1979
TRACKLINE
ICE RIDGE-SPRING 1979
CONTOUR LINE
0 1 2 Km

FIGURE 2

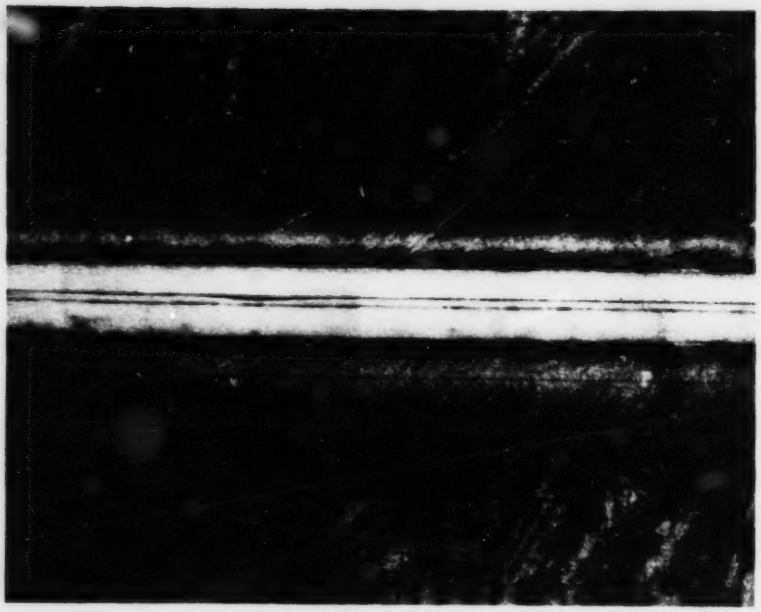

A

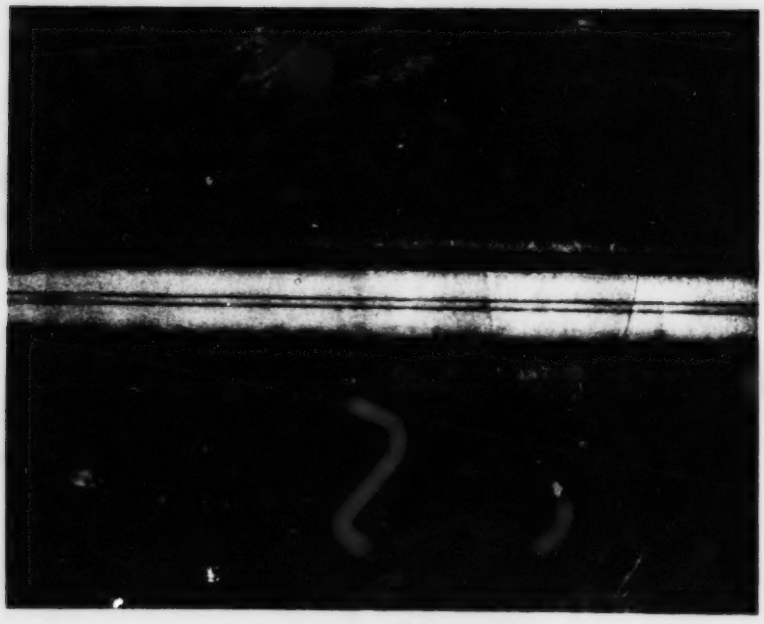

B

FIGURE 3

C

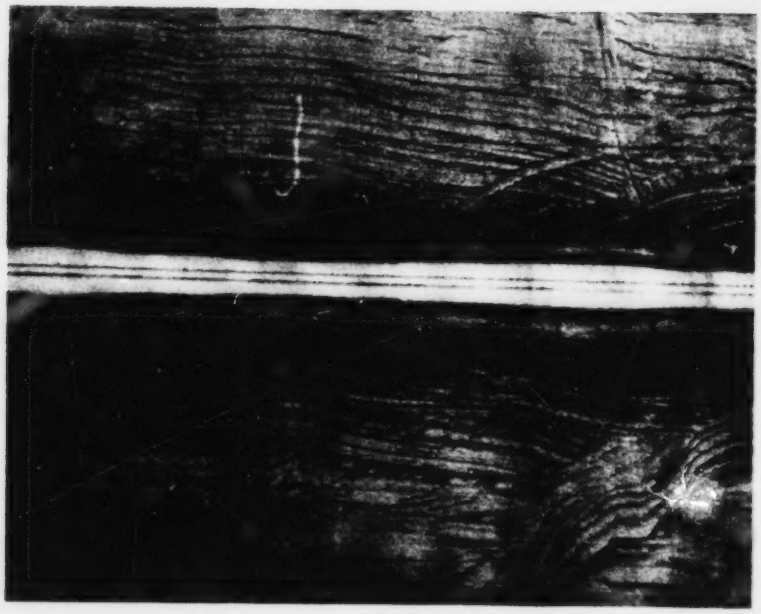

D

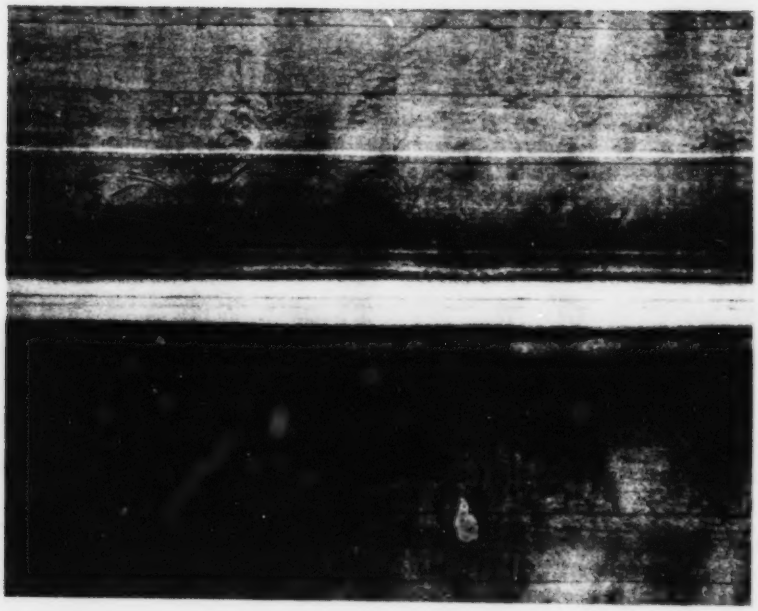

FIGURE 3 (CONTINUED)

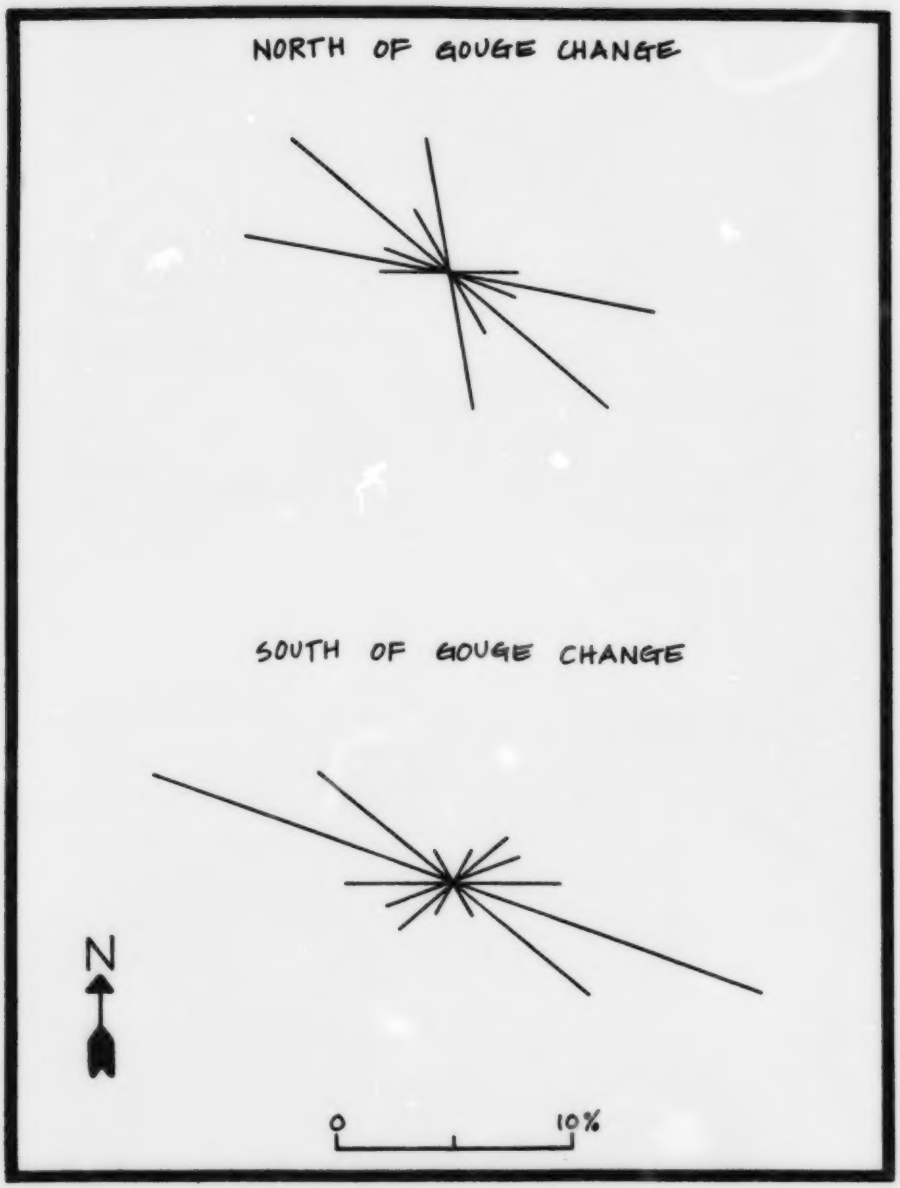

Figure 4. Dominant orientations of gouges measured north and south of the change in gouge character. Bar shows the percent of the total number of gouge orientations in 30° segments.

Ice Gouge Characteristics Related to Sea-Ice Zonation, Beaufort Sea, Alaska

Peter W. Barnes
Erk Reimnitz
Douglas M. Rearic

U.S. Geological Survey
Pacific-Arctic Branch of Marine Geology
345 Middlefield Road, MS-99
Menlo Park, CA 94025

Prepared for presentation at National Research Council of Canada's Ice Scour Workshop,
Montebello, Quebec, February 15-19, 1982

INTRODUCTION

Gouging of the sea floor by ice is an ongoing process that disrupts and modifies the seabed, affecting sedimentologic processes, ice zonation, and petroleum development activities. The sea ice off northern Alaska is not smooth but broken by ridges of ice on its surface, expressed as keels below the surface. Gouging occurs where these keels come into contact with, and plow into, the seafloor. Sediments are disrupted, atmospheric and oceanic energy is absorbed, ice movement is arrested, stabilizing the ice and affecting ice zonation. Development activities that place pipelines and subsea structures on the sea floor are affected by the plowing and forces involved in ice gouging.

In this report we summarize 8 years of bathymetric and side-scan sonar data regarding the character and variability of ice gouging on the shelf of the Beaufort Sea off northern Alaska. A description of the character of ice gouging is presented to describe the regional character of gouging on the shelf without regard to yearly variability. Regional and process-related variability are then discussed to show general ice, seabed-sediment relationships in a reassessment and updating of our earlier work (Reimnitz and Barnes, 1974).

BACKGROUND

The Beaufort Sea shelf can be characterized as a broad shallow shelf (shelf break less than 100 m) extending 60 to 100 km offshore from a coastline of low tundra bluffs (Fig. 1). The major bathymetric features are a broad 2-m bench off major rivers, sand and gravel island chains en echelon from east to west, and a series of sand and gravel shoals in water 10 to 20 m deep. The surficial sediments are characterized by extreme variability and patchiness over short-lateral distances (Barnes and others, 1980). In nearshore areas (water depths to 15 m) surficial sediments are reworked to depths of tens of centimeters by episodic storm waves and currents (Barnes and Reimnitz, 1979). In water depths of 15-40 m the entire sea floor is reworked by ice gouging. Exposures of stiff, overconsolidated silty clay are common on the inner and central part of the shelf (Reimnitz and others, 1980).

Ice Regime

In the fall landfast ice grows seaward from the coast. As winter progresses lateral ice motions inside the barrier islands and in shallow water (less than 2 m) are small, while at the seaward boundary of the fast ice, incursions of the polar pack repeatedly build massive grounded ridges forming a stamukhi zone. The stamukhi zone is formed by a series of grounded ice ridges in water depths of 13-35 m, strung from promontory to promontory or shoal to shoal along the inner shelf (Reimnitz and others, 1978). In Harrison Bay two zones of pronounced ice ridging occur in winter (Stringer, 1978; Reimnitz and others, 1978). An inshore stamukhi zone occurs near the 8-12 m isobaths. Further offshore a major stamukhi zone is controlled by the shoals in the northeast part of Harrison Bay and elsewhere, generally along the 15-20 m isobaths. The onset of melting in spring deteriorates and disseminates the fast-ice canopy, although remnants of ice ridges may persist through the summer open-water period. After breakup in the spring, arctic rivers flood the nearshore sea ice. As the sea ice melts and the pack ice retreats during

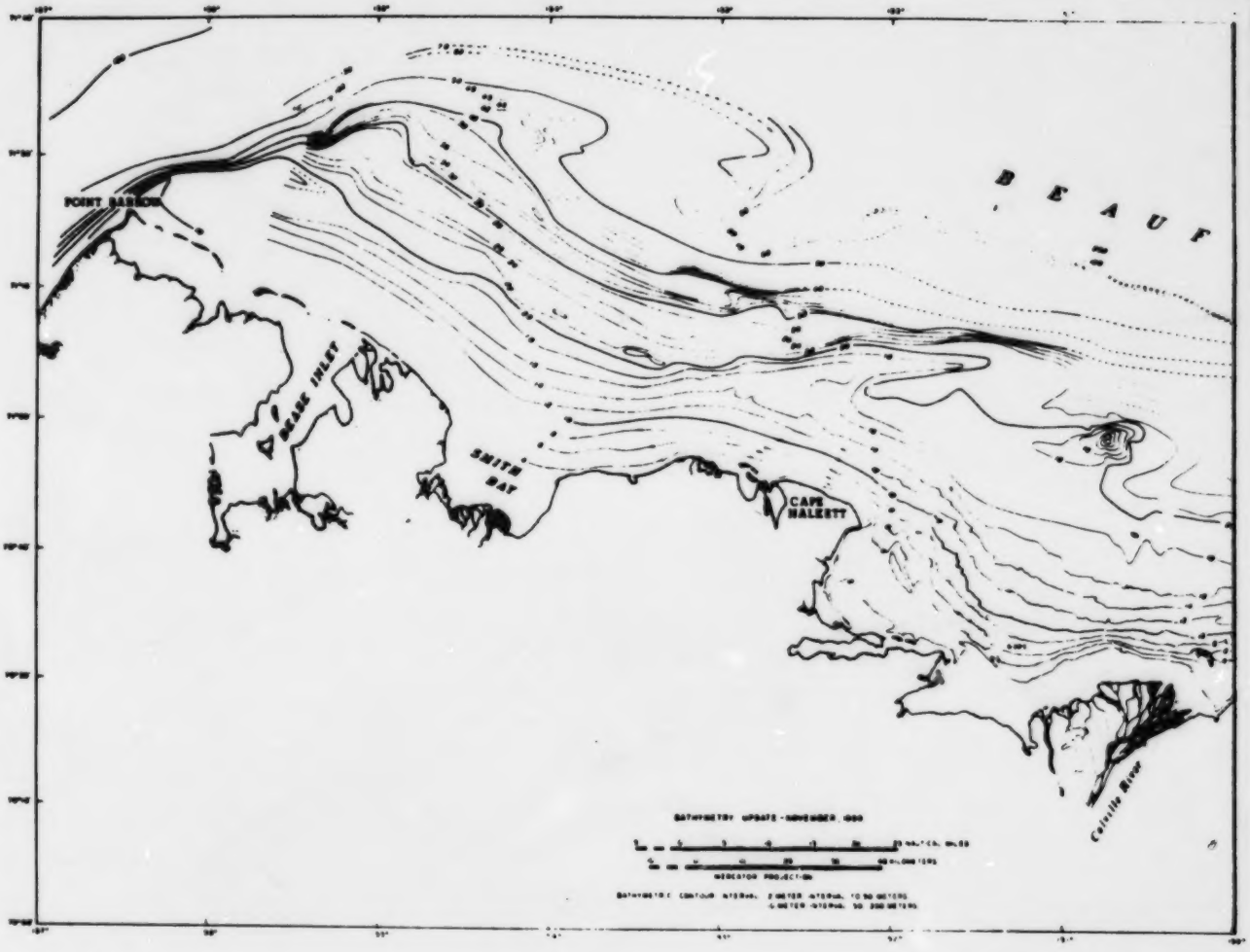

Figure 1. Location map and inner shelf bathymetry of the Alaskan Beaufort Coast. Harrison Bay is the large embayment between Oliktok Point and Cape Halkett in the center of the map. Note the shoals in the vicinity of the 20-m contour north of Oliktok Point.

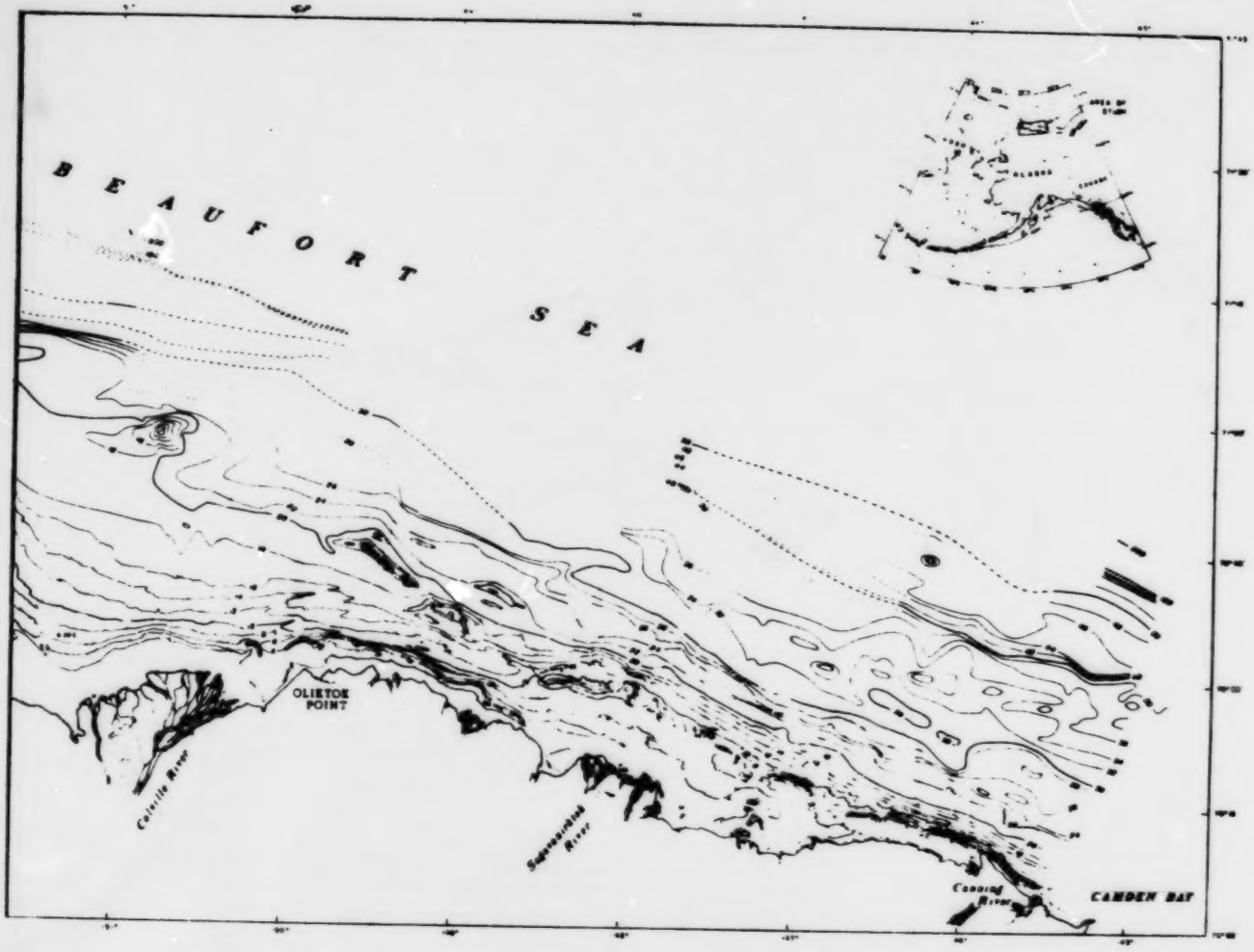

Continuation of Figure 1

Table I - Summary Statistics of Counted Gouges

(Values for 1-km-trackline segment)

Type Measure	Maximum	Minimum	Mean (includes '0' values)	Std. Deviation
Individual Gouges				
Water depth	125.0 m	1.2 m	16.8	
Distance from coast	42.7 km	0.2 km	12.9 km	
Gouge density	490/trackline-km	0.0	63.0	70.1
Dominant orientation			90°T	29.7
Subdominant orientation			87°T	42.7
Max. incision depth	5.5 m(4.0)	less than 0.2 m	0.5 m	0.6
Max. incision width	62.0 m	less than 1 m	7.5 m	8.0
Max. ridge height	2.7 m	less than 0.2 m	0.4 m	0.5
Multiple Incision Gouges				
No. multiple gouge events	15/trackline-km	0.0	1.6	2.3
Max. no. incisions per event	27	2	4.8	3.7
Max. multi-incision disruption width	150.0 m	2.0 m	28 m	
Dominant multi-incision orientation			162°T	0 - 180°I

summer, the wave and current regimes intensify as more water surface is exposed to wind stress. Maximum open water generally occurs in September and early October and corresponds to the period of most intense storms. The waves and currents produced by these storms cause active reworking of sediment, particularly in shallow water areas.

METHODS

The data in this report are a result of the examination (by D.R.) of over 2000 km of trackline segments containing about 100,000 ice gouges (Rearic and others, 1981). The bulk of the data were extracted from high-precision fathograms with a resolution of 10 cm and from side-scan sonar-generated sonographs of the sea floor. The details and methods involved in extracting information from these records is given in Barnes and others, 1978, and in Rearic and others, 1980. These data were compiled by computer and used to generate the scattergrams and figures of this report.

A glossary of terms used in this report can be found in Appendix I. It is of import to note that ice gouge (this report), ice scour (Lewis, 1978) iceberg plow marks (Belderson and Wilson, 1973), and ice score (Kovacs, 1972) have all been used to describe the same morphologic seabed feature. We have chosen to use the term ice gouge to describe these features as the first descriptions of the seafloor micro-relief in the arctic related to sea ice (Rex, 1955) uses gouge to describe the process forming these features. Gouge --groove made by digging and forcing with a tool--appears to define the ice/sediment interaction most precisely. Scour implies hydraulic interaction of a surficial rubbing of a less bold nature than the process we are considering. The definition of score implies a singular event creating a mark, while ice often interacts with the bottom in multiple events. As a word, score also has many other unique uses, as in hockey.

RESULTS

Average Gouge

From computer summarization of the gouge data, the average ice gouge on the Beaufort shelf was determined. These data are misleading in that there are regional and physical relationships controlling ice gouge distribution and our data set is dominated by observations made in water less than 20 m deep. However the "average gouge" is representative of our data set. The "gouge" would occur in water depths of about 17 m at a distance of 13 km from the coast and would be incised into the bottom a distance of 50 cm with ridges on the gouge side of 40 cm and thus present a total relief of almost 1 m (Table I). The gouge would have a width of 7.5 meters and be oriented east-west, slightly onshore from the coastline and isobath orientation of 105-285° (Fig. 1).

Ice Gouge Variability Versus Depth

Scattergrams were prepared to show the variability of gouge parameters versus water depth. The numbers on these figures are plot points where one or more observations are plotted (9 = 9 or more observations at point).

Gouge density: The number of gouges observed for each kilometer of trackline data expressed as gouge densities, shows the highest values in water between 15 and 30 m deep, generally being more than 100 gouges per kilometer of trackline. Lowest values occur in water less than 5 m deep or more than 45 m deep (Fig. 2). In water 20 to 40 m deep low gouge densities are almost nonexistent, indicating pervasive gouging at these depths.

Maximum incision depth: The maximum incision depth of gouges in the seabed follows a pattern similar to gouge densities; being greatest in water 18 to 35 m deep (Fig. 3). These incisions are commonly over 1 m deep, and often more than 2 m deep. In water less than 10 m deep and over 45 m deep, maximum incision depths are less than 1 m. As in the case of gouge density, maximum gouge depths observed in water 20 to 40 m deep show an absence of low values, with few incisions less than 0.5 m deep.

Maximum incision width: The maximum single incision widths show a less clear pattern (Fig. 4). Generally, the maximum incision widths increase with increasing water depth for single-incision gouges. This trend can be characterized by gouges about 5 m wide, in water less than 10 m deep, to over 50 m wide in water 20 to 30 m deep, although the bulk of the gouges are less than 20 m wide.

Maximum ridge height: The sediment ridge piled up by a single plowing ice keel is highest in water 18 to 40 m deep with ridges over 1 to 2 m common (Fig. 5). In shallower and deeper water maximum ridge heights are usually less than 60 cm.

Gouge orientation: The dominant orientation of ice gouging in trackline segments is clustered around the average 090° (Fig. 6, Table I). With increasing water depth the trend becomes more pronounced. Subordinant or secondary orientation, although having an average (87°) similar to the average dominant orientation (Table I), does not show any pattern associated with water depth. Instead, subordinant gouge orientation is essentially random regardless of water depths.

Number of multiple incisions: The number of multiple keel incisions caused by pressure ridges (Reimnitz and others 1973) again shows a similar pattern of gouge density, incision depth, and ridge height with the highest values observed in water 15 to 30 m deep. In water greater than 20 m deep (Table I), 8 or more multiple tracks are commonly observed in a 1-km trackline segment (Fig. 7). In water less than 10 m deep and greater than 40 m deep, fewer than 4 multiple incisions are normally encountered in each 1-km trackline segment.

Maximum multiple incision disruption width: The maximum width of seabed disrupted by multiple ice-keel incisions occurs in water 15 to 40 m deep. The maximum width is 62 m and the average width is about 30 m (Table I). In water less than 10 m deep the disruption width is commonly less than 50 m. At water depths greater than 40 m the decrease is less definitive.

Distribution of incision depths: Using fathograms to plot the number of gouges in each trackline segment observed in 0.2-m depth increments provides a distribution of the number of gouges in each incision increment (Fig. 8). As it was not possible to measure incision depths of less than 0.2 m on the fathograms due to lack of instrument resolution, all larger gouges were

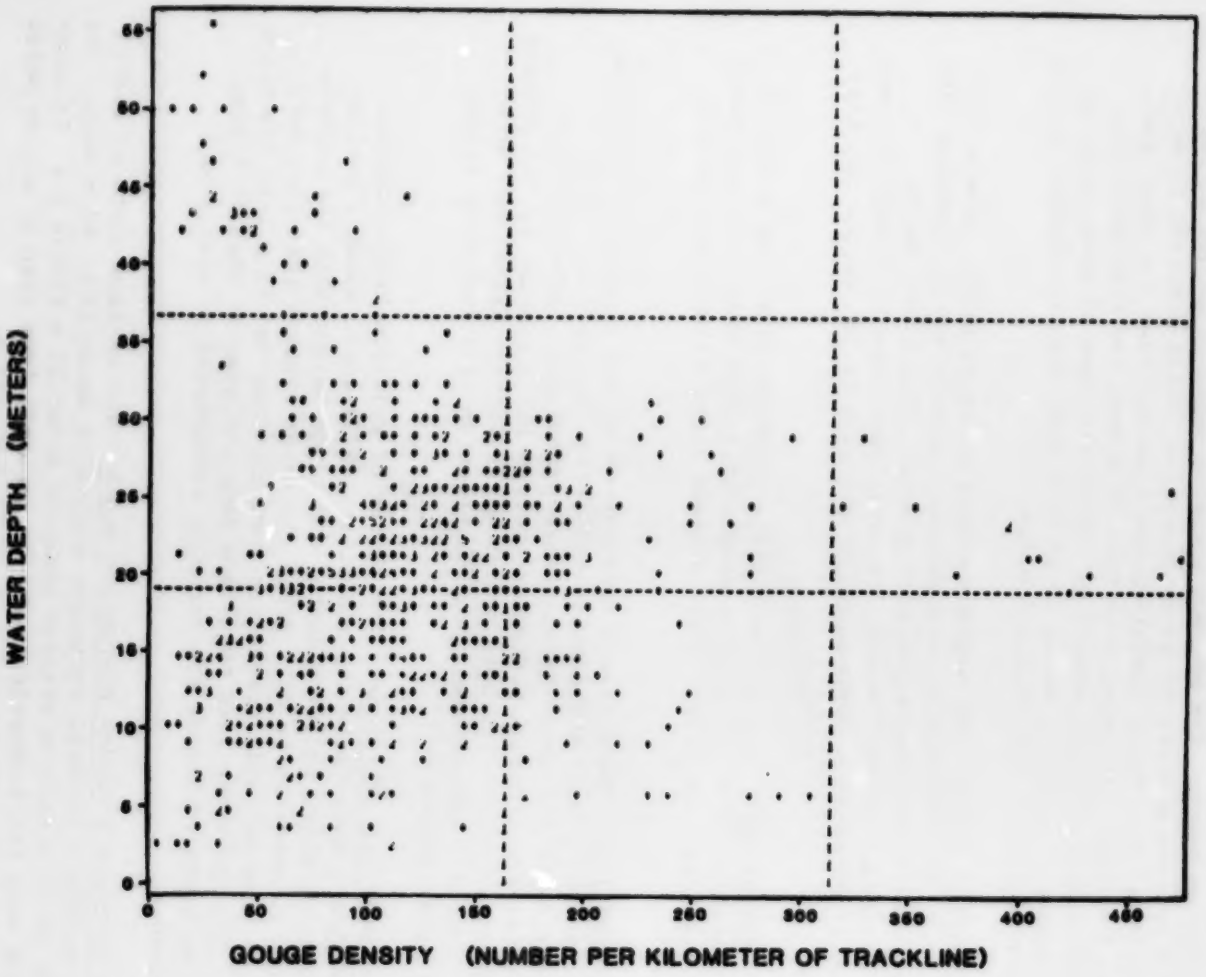

Figure 2. Scattergram of gouge density versus water depth for all gouges on the shelf. The numbers on the scattergram designate plotting points where more than one value is located (9 - 9 or more observations at that point).

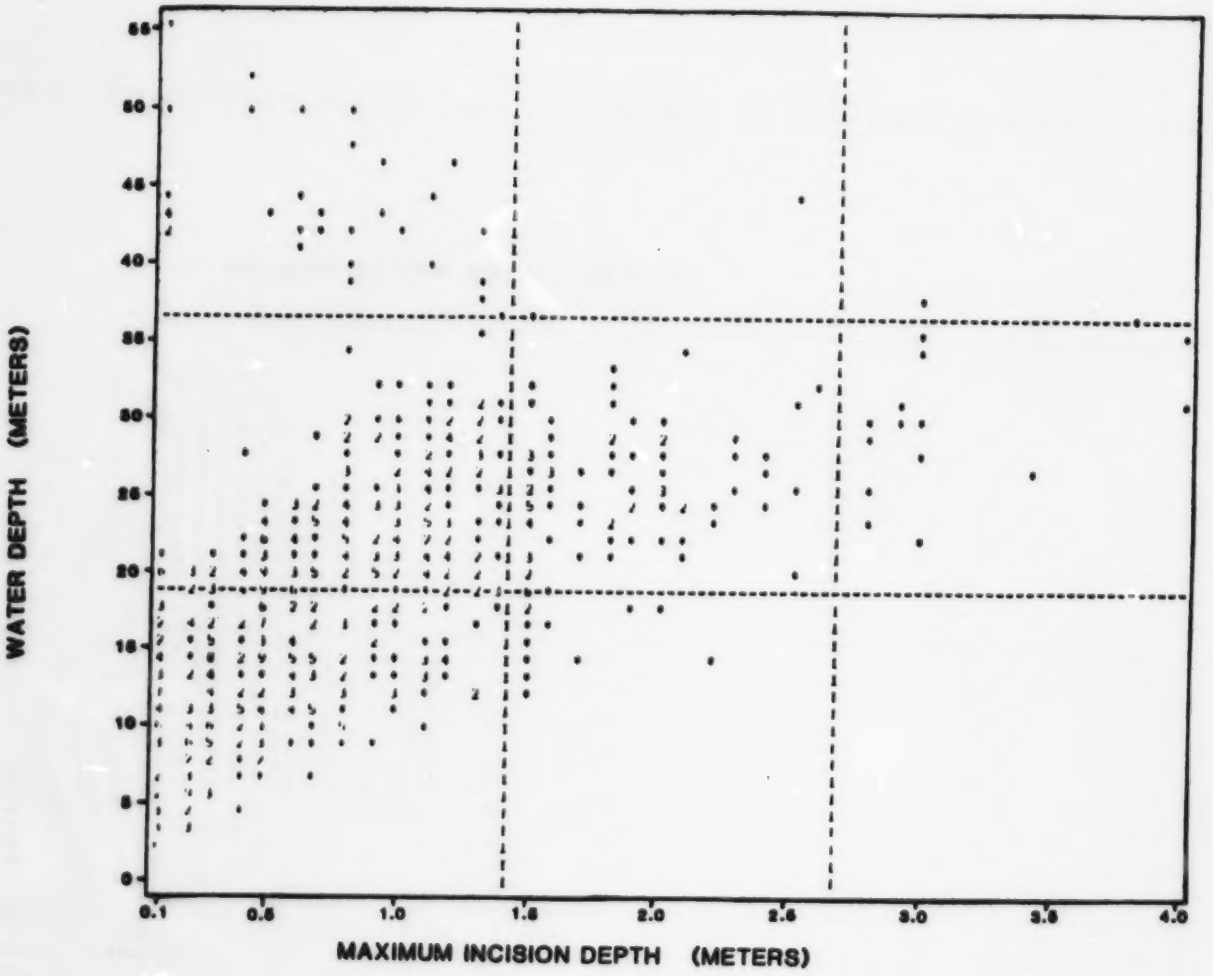

Figure 3. Scattergram of maximum gouge incision depth in each trackline segment versus water depth. Note the absence of low incision values in water depths of 20 to 40 m.

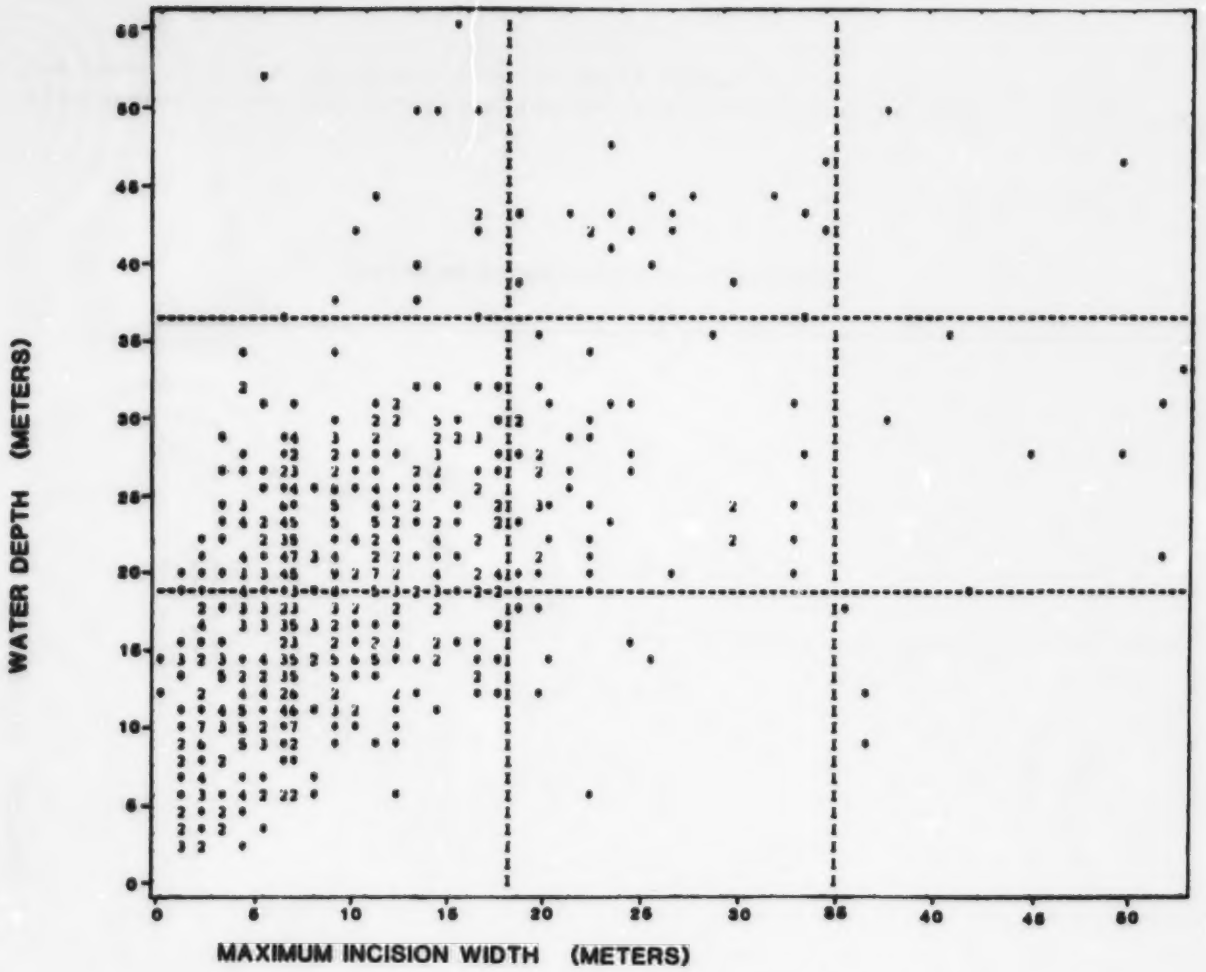

Figure 4. Scattergram of maximum gouge incision width in each trackline segment versus water depth.

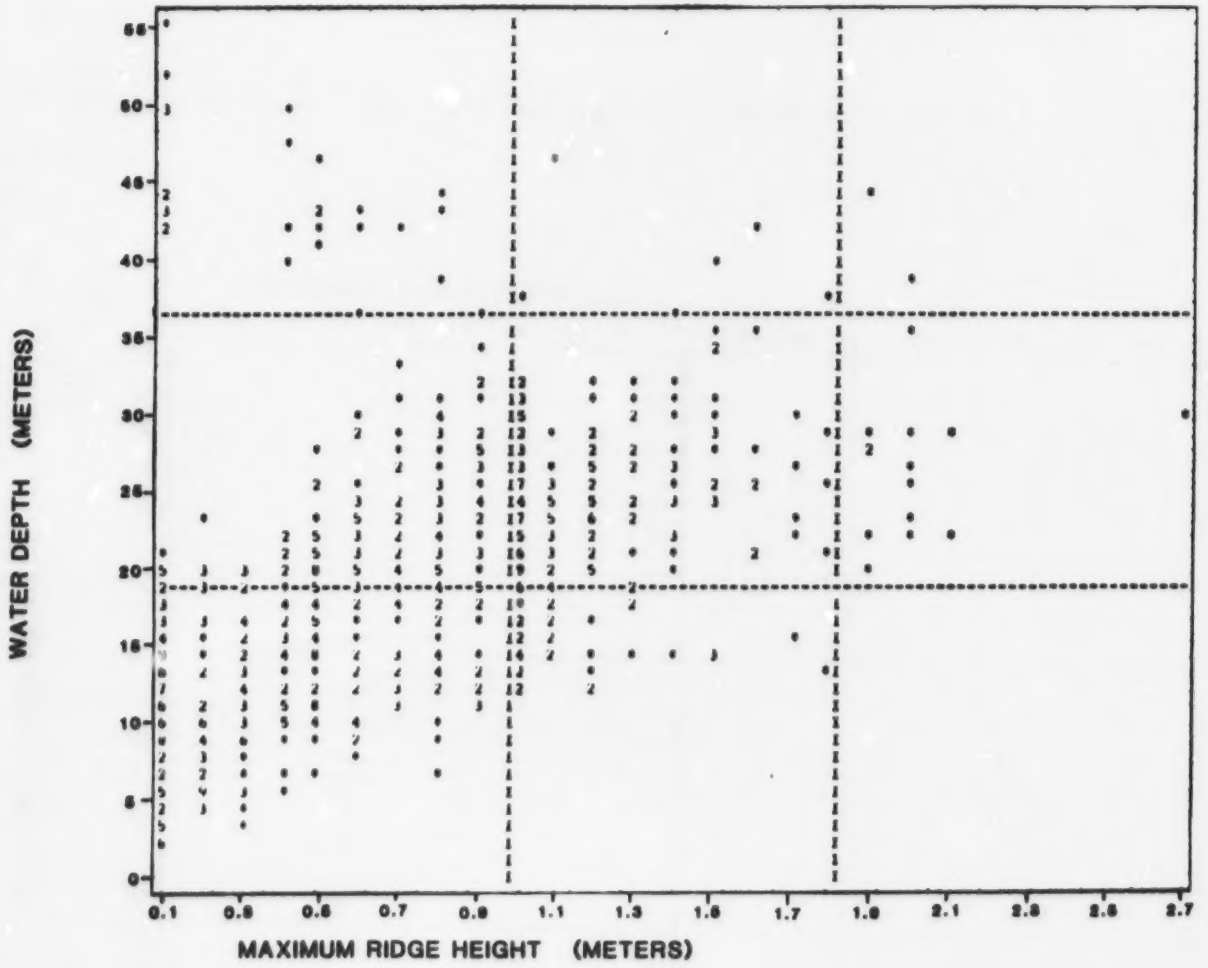

Figure 5. Scattergram of maximum gouge ridge height in each trackline segment versus water depth. Note the absence of low ridge heights in water depths of 20 to 40 m.

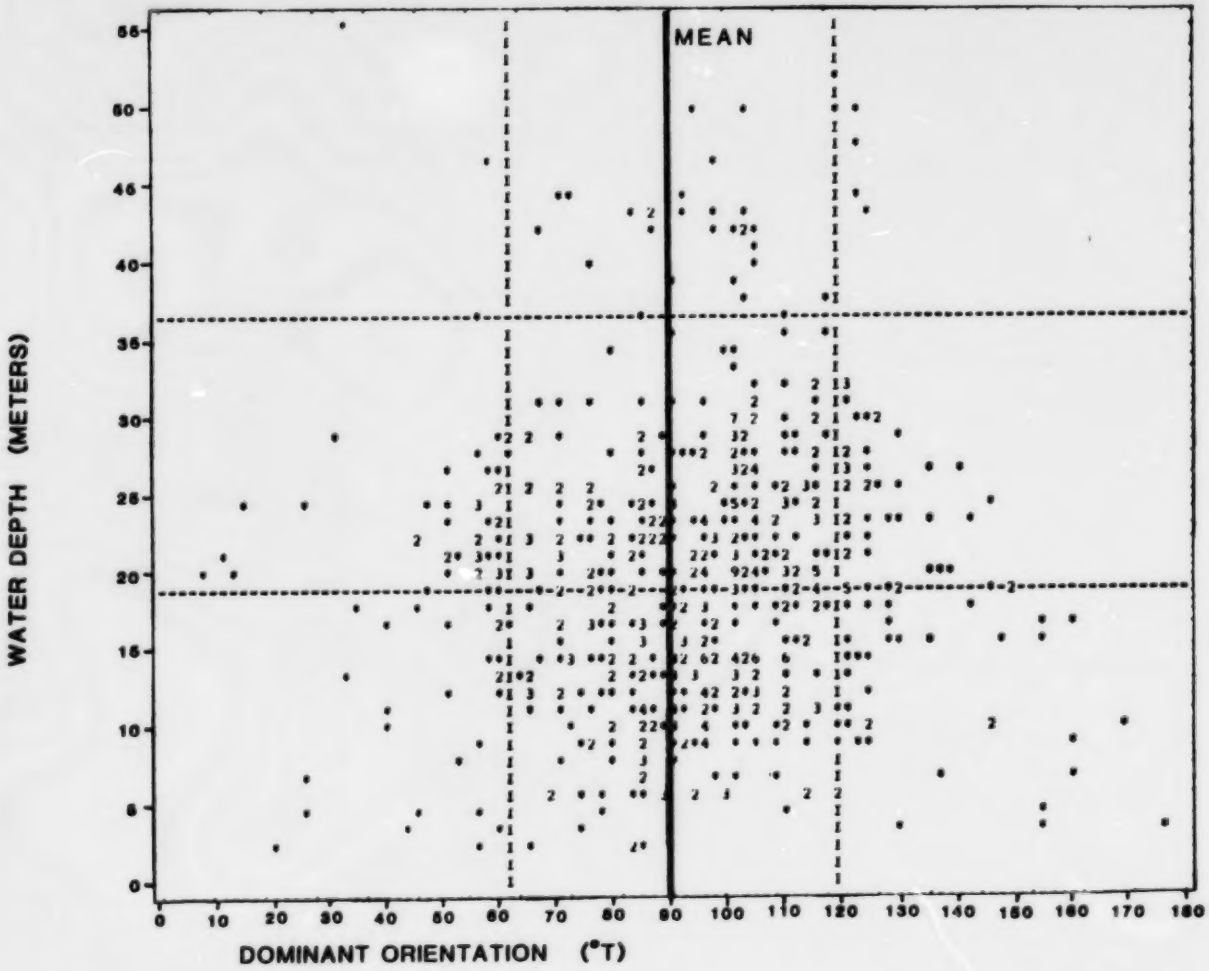

Figure 6. Scattergram of dominant gouge orientation versus water depth. From Table I the average dominant orientation is 090°T.

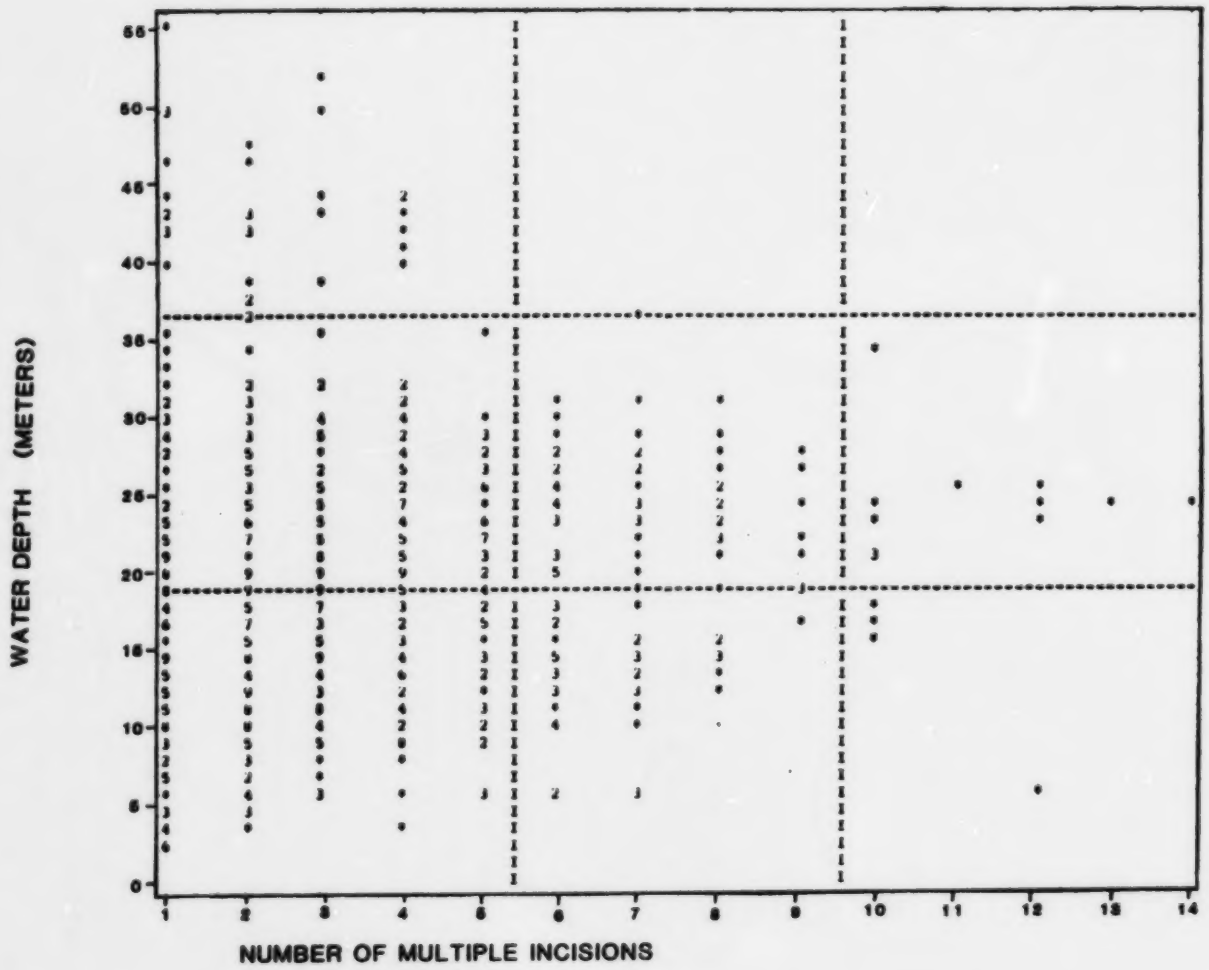

Figure 7. Scattergram of number of multiple incision gouge events observed in each trackline segment versus water depth. Each event may produce many gouges.

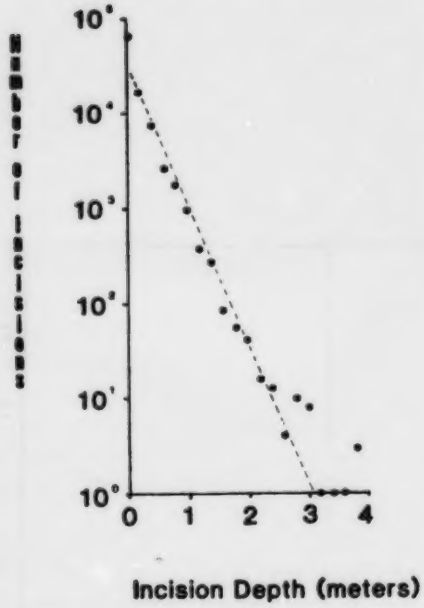

Figure 8. The distribution of the total number of ice gouge incisions observed versus the depth of these incisions.

counted and this total was then subtracted from the total number of gouges observed on the sonograph which commonly resolved the gouges smaller than 0.2 m deep. As not all gouges observed on the sonographs (areal observation) were crossed by the fathometer (linear observation) the number of gouges reported as less than 0.2 m (no measurement possible) is probably somewhat higher for this incision increment than the number would be if measured along the trackline. The plot of all incision values (Fig. 8) shows a logarithmic distribution from the shallowest gouges to gouges 2.5 m deep. The large incisions that have been measured do not follow the same distribution, perhaps due to the small number counted.

Character of Maximum Gouging

A maximum gouge density of 490 gouges per trackline kilometer were encountered on the Beaufort Sea shelf in water 20 m deep (Fig. 2). Maximum incision depth of 5.5 m was found in water 39 m deep north of Smith Bay (Reimnitz and Barnes, 1974). Poor fathometer records due to rough weather precluded enumeration of gouges on this segment except for this large one; therefore this gouge does not show in our routine statistics. Other large incisions (4 m deep) were observed northeast of Cape Halkett in water 31 to 37 m deep (Fig. 3). A maximum incision width of 62 m was found in water 34 m

deep and gouge widths exceeding 50 m were found in water 20 to 33 m deep (Table I and Fig. 4). A maximum ridge height of 2.7 m was encountered northeast of Cape Halkett in water 30 m deep. Thus maximum seabed incisions occur in water over 30 m deep where seabed relief (incision depth plus ridge height) of more than 8 m may be found. Where the bottom is saturated with gouges, fewer large gouges can be accommodated in any kilometer of trackline segment than is the case where gouges are small. Thus the highest density gouging does not correspond with the biggest gouge. The most dense gouging occurs in shallower water, about 20 m deep.

Gouge Densities Related to Other Parameters

Gouge density was plotted against other parameters which suggested correlations might exist. A plot of gouge density versus maximum gouge incision depth shows that maximum incisions do not occur where maximum densities are encountered. Maximum incisions (over 2 m) are found where gouge densities are between 50 and 200 gouges per trackline kilometer (Fig. 9), while maximum densities are associated with incisions of less than 2 m.

Maximum incision widths decrease with increasing gouge density (Fig. 10). Gouges 40 m wide are frequently encountered where density is less than 150 gouges per trackline kilometer but gouge widths decrease to less than 20 m where density of more than 200 gouges per kilometer of trackline is found. In part this represents the fact that increasing gouge density is limited by the greater number of gouges in a highly gouged area of the sea floor.

As is the case with gouge incision width, maximum ridge heights are not associated with highest gouge density. The maximum values of ridge heights (over 1.5 m) are associated with areas where there are 50 to 200 gouges per trackline mile. Maximum gouge densities occur where ridge heights are 1 m and less.

Orientation is most varied where densities are low and become less varied and closer to the average orientatioin of 90°T as gouge density increases (Fig. 11, Table I). However, even where gouge density is low, the major orientation is between 60° and 120°.

Maximum Incision Depth Relationships

Maximum gouge incision depths show a strong relationship to ridge heights. Increasing maximum ridge heights are found together with increased incision depths. Relief is commonly over 3 m and maximum relief is over 7 m. This follows, as the deepest gouge events must displace more sediment causing buildup of higher ridges (Fig. 12).

Regional Distribution of Ice Gouge Character

Gouge density: Gouge densities were plotted along the trackline and contoured (Figure 13). Both show low densities inshore and at the seaward edges of the tracklines. Highest densities of gouges are found on the inner slopes of the shelf, seaward of the stamukhi zone in water 20-30 m deep, as off the Colville delta, and to the west. Low values are encountered in the lee of the coastal islands and to the southwest of the offshore shoals which also form a lee for the east-to-west ice motion. The central portion of Harrison Bay also has relatively low gouge densities.

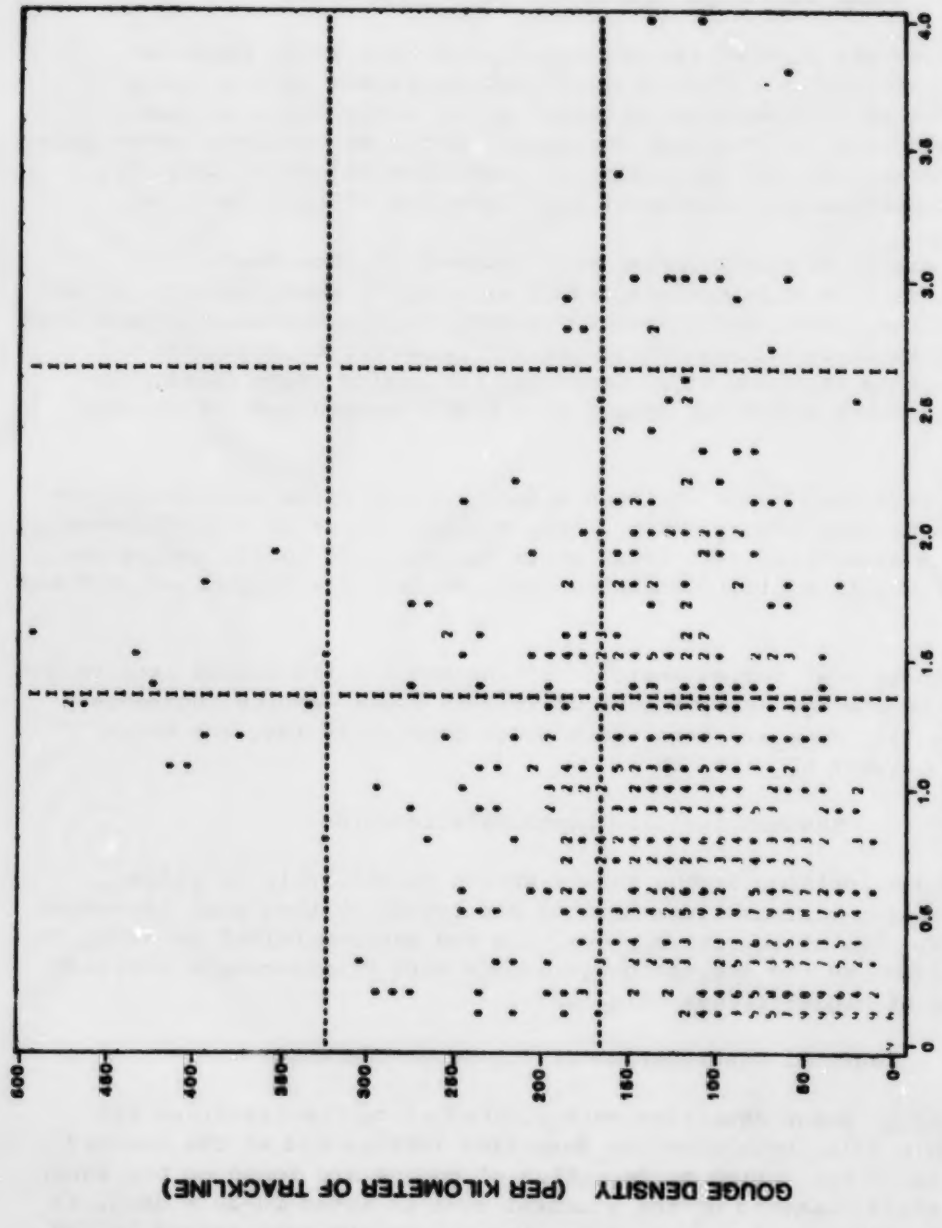

Figure 9. Scattergram of maximum gouge incision depths in each trackline segment versus the density of gouges in that segment. Note the lack of correlation with high densities and deep incision depths.

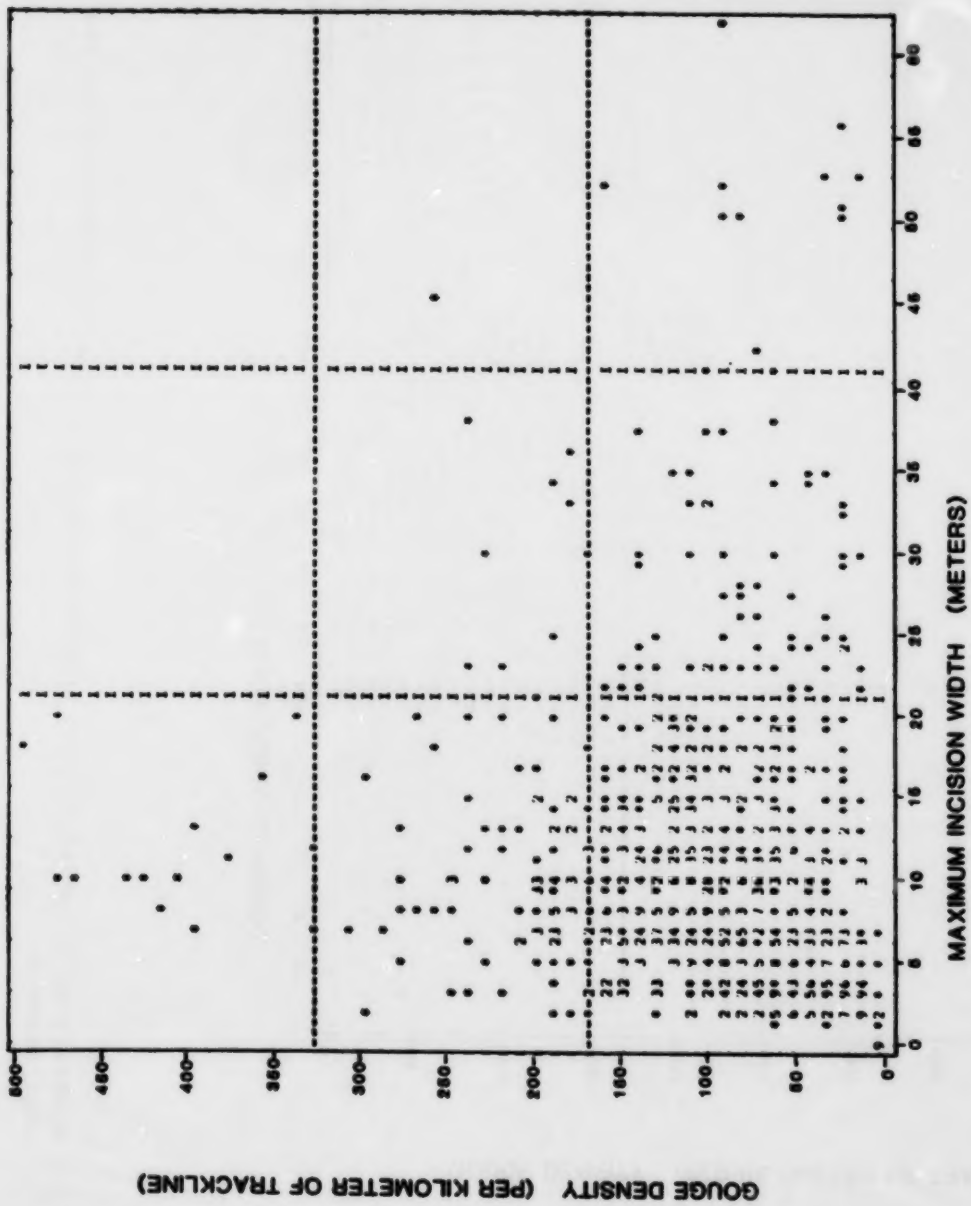

Figure 10. Scattergram of maximum gouge incision width in each trackline segment plotted against gouge density. Again note the disparity between maximal incision widths and maximal densities.

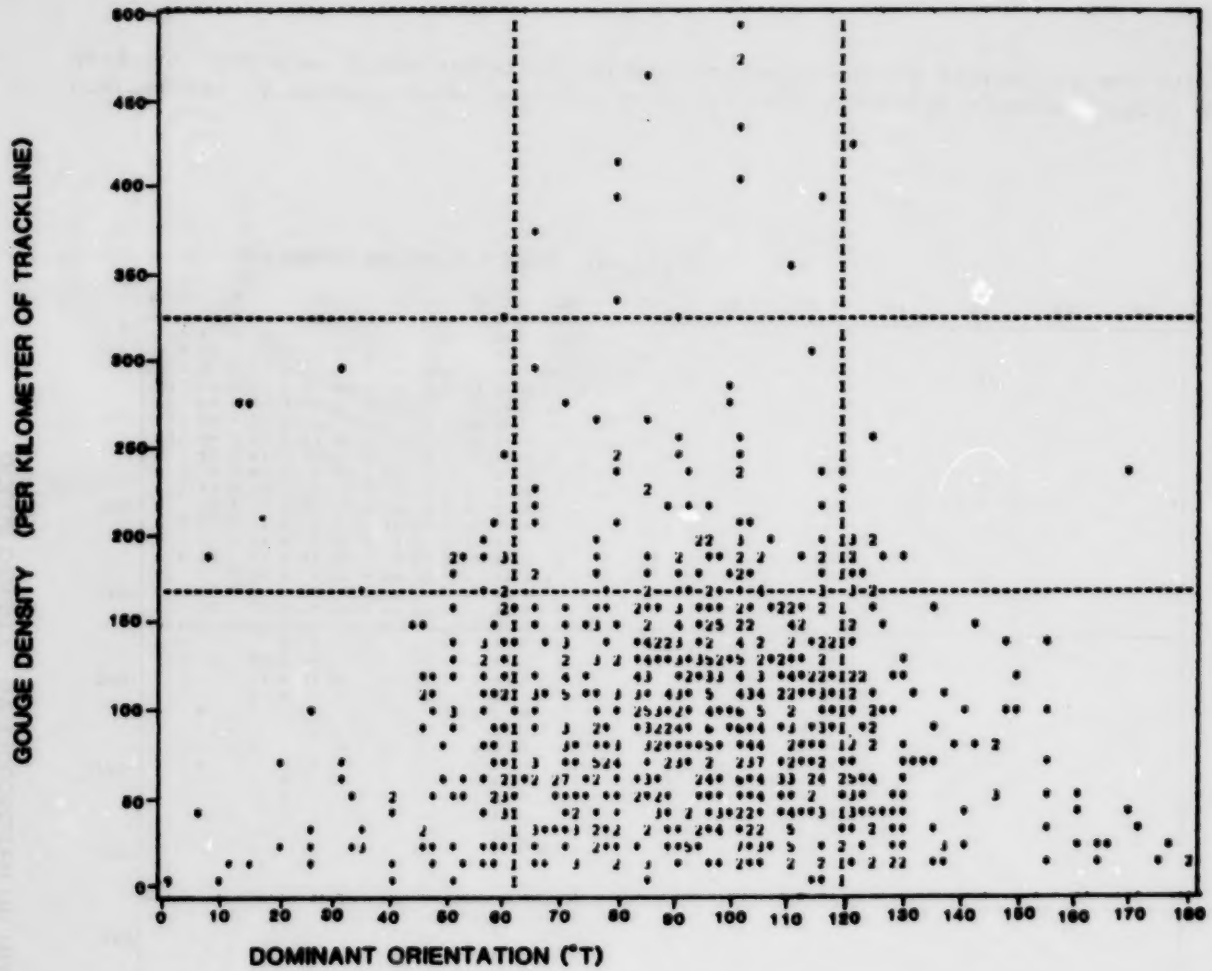

Figure 11. Scattergram of dominant gouge orientation in each trackline segment versus the gouge density in that segment.

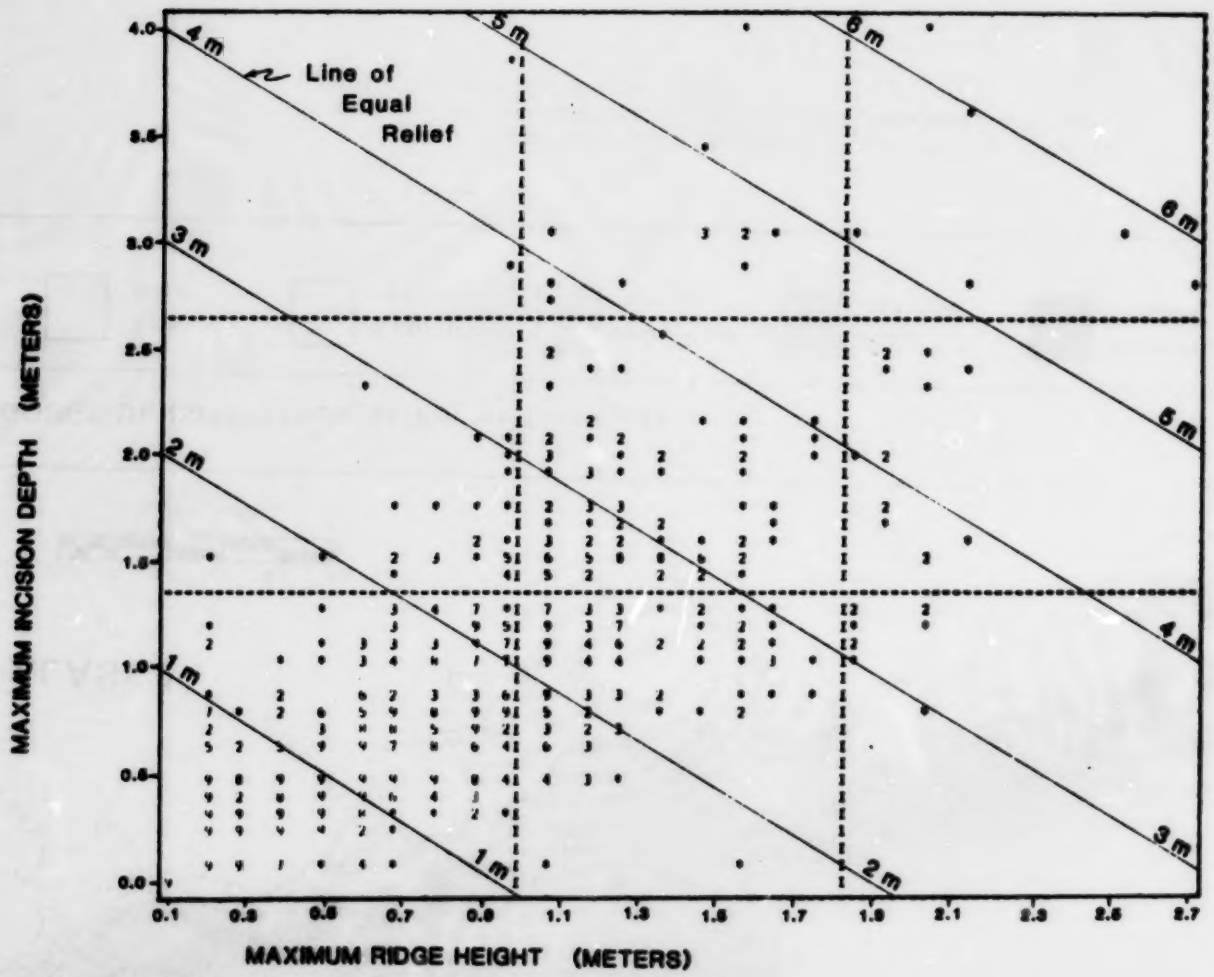

Figure 12. Scattergram of maximum ridge heights observed in each trackline segment plotted against the maximum incision depth noted in that same segment. Relief - as incision depth plus ridge height - is represented by the diagonal grid.

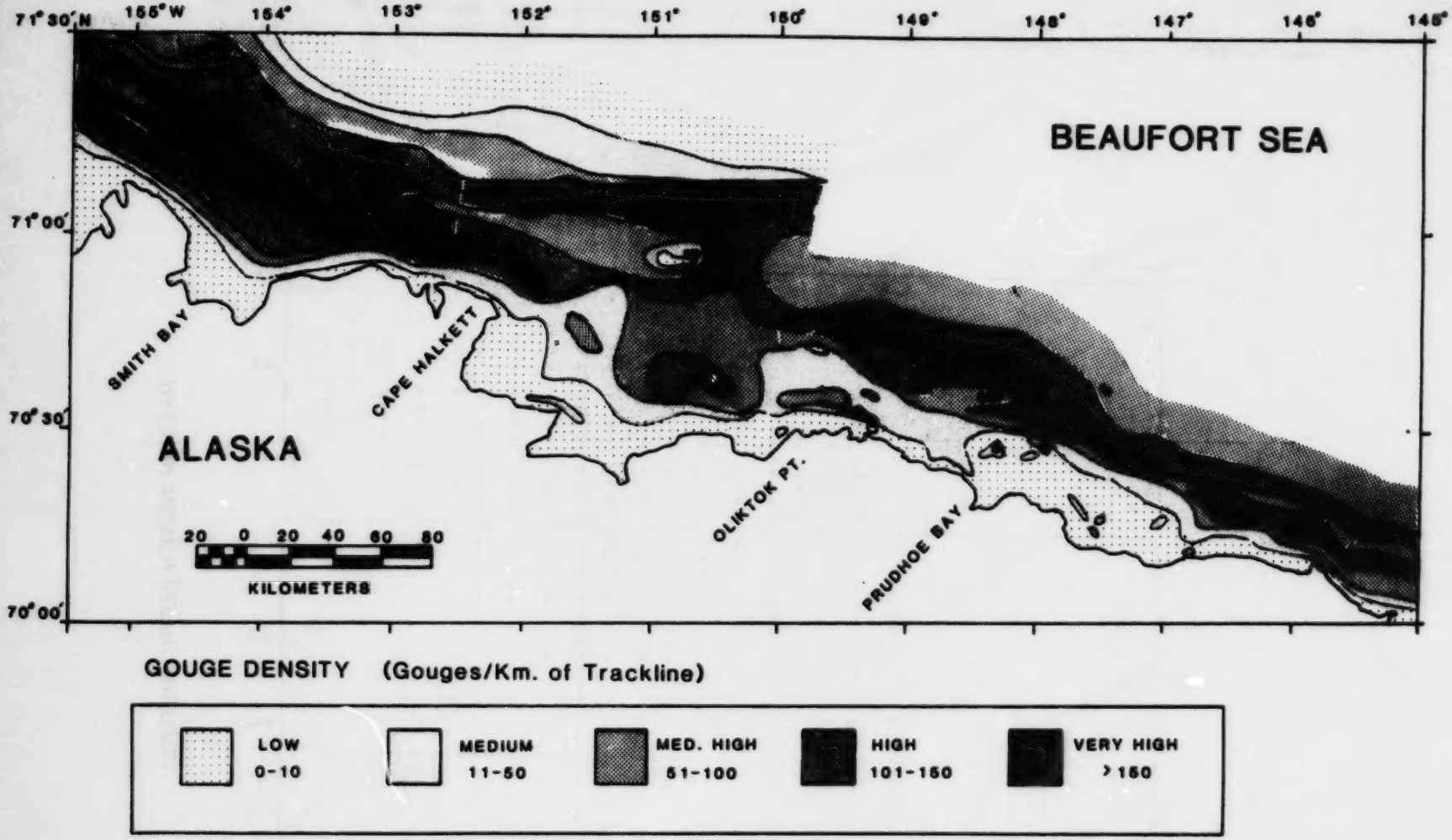

Figure 13. Contours of gouge density on the Beaufort Sea shelf. Note low densities on the inner shelf and around shoals and the high densities near the stamukhi zone.

Maximum incision depth: The maximum gouge incision depth in each trackline segment is contoured in Figure 14. Maximum incision depths generally increase with increasing water depth, at least to the depth where our data become sparse, as on the westernmost trackline beyond the 30-m isobath. North of Cape Halkett, where we have obtained data to the shelf edge, the maximum incision depths decrease beyond about 45 m. In contrast to the density values, maximum incision depths are concentrated in deeper water, whereas maximum densities are found in shallow water, i.e., the inner parts of Harrison Bay and Smith Bay (Figs. 2, 3, and 13).

Dominant gouge orientation: The summary plot of dominant gouge orientations shown in Figure 15 illustrates the general coast-parallel trend of gouging, but with considerable scatter and local variation. The dominant orientation in the sounds, lagoons, and shallows of western Harrison Bay are particularly variable. Offshore, the orientation between the 20- and 40-m countours appears to be essentially all coast-parallel and slightly onshore. Another trend which needs further study occurs on several onshore-offshore transects. Gouge orientations trend onshore more and more frequently as they approach the coast. This is noticeable on the westernmost transect, off Cape Halkett, and north and northwest of Oliktok Point. This trend is not apparently depth related (Fig. 6). Onshore-offshore trends to the east of Oliktok Point are unclear at the present time.

DISCUSSION

When all factors are considered, it is apparent that the most intense gouging is concentrated in water between 15 and 35 m deep. Gouge density, incision depth, ridge height, maximum incision width, and number of multiple incisions are all at a maximum in these water depths (Figs. 2, 3, 4, 5, and 7). We consider intensity of gouging to be a function of the intensity in number of ice-seabed impacts, recurrence rate, and amount of bottom area disrupted by these impacts. Bottom disruption is expressed by the maximum incision depths, ridge heights, and incision widths. High density values do not alone show intense gouging, as high values may simply represent shallow, small, short gouges as observed in the uniform area counted on the sonograph.

Reimnitz and others, 1978, show that the most intense ridging occurs in water 15 to 40 m deep, at the shear zone between the polar pack and the fast ice. They named this intensely ridged area the stamukhi zone and demonstrated that shoals, islands, and coastal promontories controlled the location of this zone. Furthermore, they suggested that much of this stamukhi zone was intensely gouged due to the grounding of ice keels as indicated by stability after formation and during the open-water season. In addition, the shelf of the Beaufort Sea is known to be an area of energy dissipation for pack ice forces (Thomas and Pritchard, 1980). As this would be a zone where polar pack ice forces would be expended on the seabed and where sediment disruption might be at a maximum (Barnes and Reimnitz, 1974). Box cores in this zone show no horizontal laminations while seaward of 45 m and landward of 18 m these current related laminations are common (Barnes and Reimnitz, 1974 and Barnes, unpublished data). We have postulated that the stamukhi zone should be an area of intense ice gouging (Barnes and others 1978; Reimnitz and others 1978). The data presented here strongly support these earlier observations. However, the recurrence rates of gouges, a factor in determining gouge intensity, are not known in these depths from direct evidence. We have used maximum incision

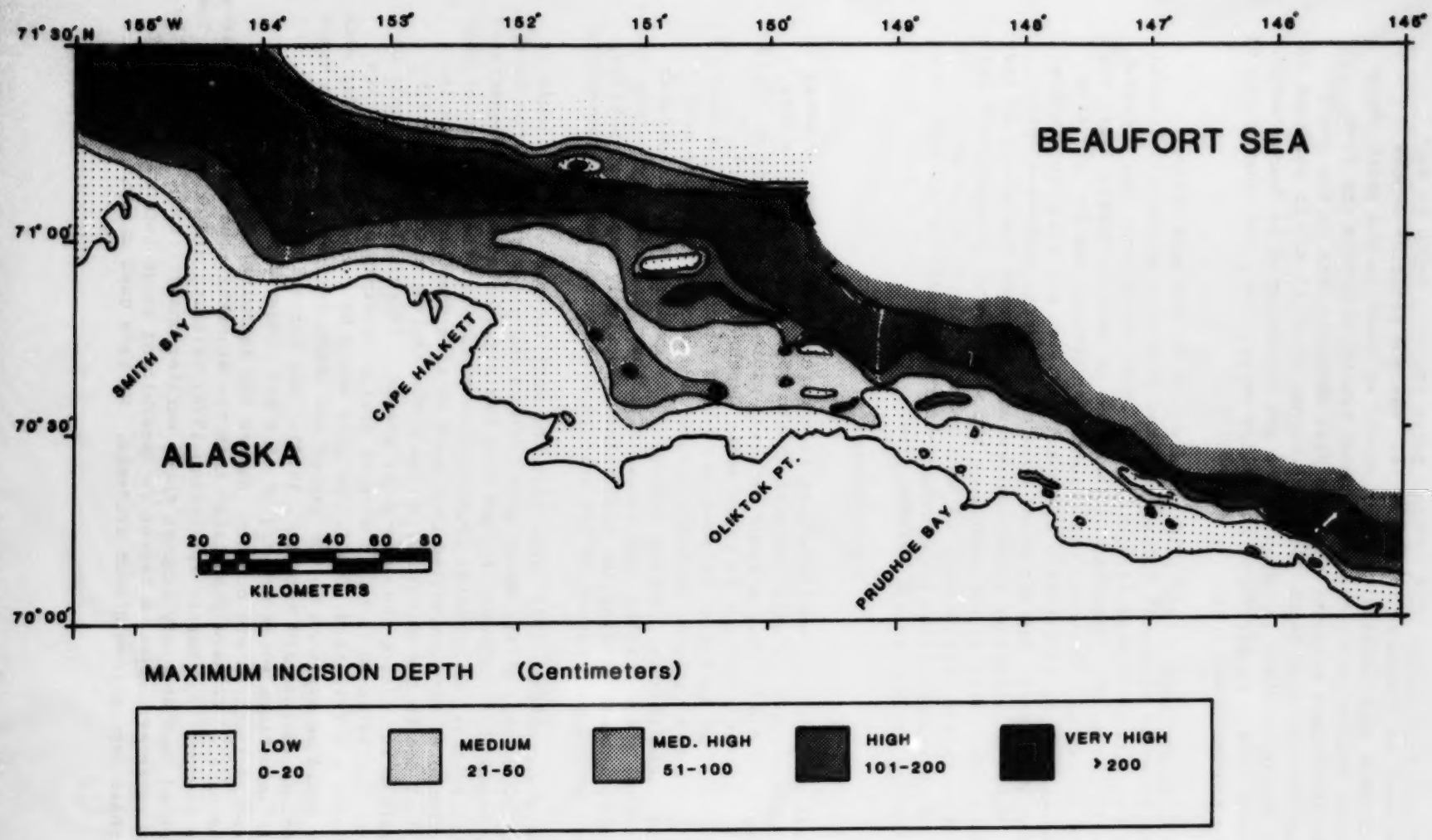

MAXIMUM INCISION DEPTH (Centimeters)

LOW	MEDIUM	MED. HIGH	HIGH	VERY HIGH
0-20	21-50	51-100	101-200	> 200

Figure 14. Contours of maximum gouge incision depth of the Beaufort Sea shelf. Note the low values on the inner shelf and on the shoals, and the higher values at and just seaward of the stamukhi zone.

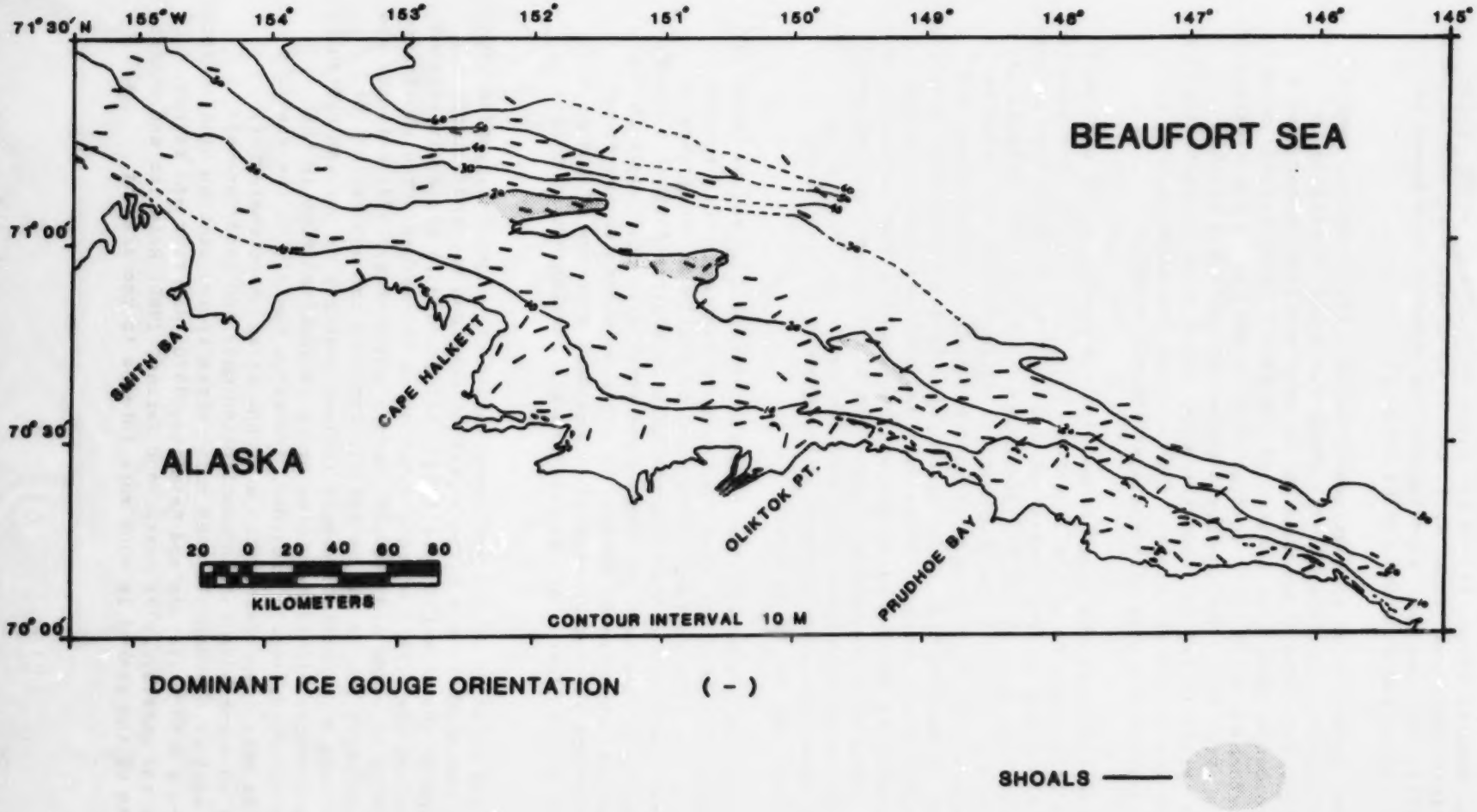

Figure 15. Dominant gouge orientations on the shelf of the Beaufort Sea from 1972-1980 data. Note the gouging seaward of the islands on the central shelf is parallel to the isobath or oriented slightly onshore. Also note the varied orientation of gouging in the lagoons and on the inner shelf.

depths and gouge density (Figs. 13 and 14) along with data on width, ridge height and multiple incisions (Figs. 4, 5, and 7) to create a subjective gouge intensity map (Fig. 16). We then superimposed the stamukhi zone based on Reimnitz et al. (1978) and Stringer (1978) (Fig. 17).

Harrison Bay demonstrates a relationship between ice zonation, seabed morphology, and gouging. Stringer (1978) shows two zones of ridging in Harrison Bay (Fig. 17). One ridge zone occurs near the 10-m isobath and a second, more pronounced zone runs seaward of the shoals (Reimnitz and others, 1978) in the northeastern and outer central part of the bay in the vicinity of the 20-m isobath (Fig. 18). The contoured gouge densities and maximum incision depths (Figs. 13 and 14) show these two areas to be characterized by higher densities and deeper incisions. This association suggests that the most intense gouging correlates with the most intense ridging.

Gouge orientations for the inner ridge zone are predominantly east-west, parallel to slightly onshore, of the isobaths (Fig. 15). In the area seaward of the shoals, the trend is less persistent but might be characterized as more onshore in the eastern part of the bay and more parallel to the isobaths in the western portion. Assuming the dominant ice motions along the Beaufort coast in winter are from east to west (Kovacs and Mellor, 1974; Thomas and Pritchard, 1980) we believe that gouge orientation is associated with slightly onshore components of ice motion. These west and southwest motion reults in less intense gouging in the lee of shoals and the stamukhi zone (Reimnitz and Barnes, 1974). This is a reasonable observation since intense gouging would be most likely to occur when keels plow into the seabed and move uphill. Thus gouging will be more intense on steeper rather than on gradual slopes, although the gouges may not be as long.

When orientations are broken down by water depth and by region (Fig. 19) a trend is evident that does not show when orientation is plotted against water depth (Fig. 6). The regions inshore and in shallower water show orientations that are directed more onshore than in regions farther seaward. We have also observed this onshore turning characteristic for gouges in the Barrow area (Barnes, unpublished data). We offer no mechanism except to suggest the long-term ice motion related to boundary stresses of the polar pack on the ice of the inner shelf may lead to the development of this pattern.

Areas of low incision depths and lower values of gouge density associated with shoals in the northern and eastern part of Harrison Bay and outside the islands, but inside the stamukhi zone (Figs. 13, 14, and 1) are again related to ice zonation and the effect of this zonation on the seabed. The shoals are composed primarily of sands and gravels (Barnes and others, 1979; Reimnitz and Maurer, 1978) on which gouges may be readily infilled through failure of noncohesive sediments to maintain deeply incised features or through hydraulic reworking of sediments, either by storms or by intensified flow in the vicinity of grounded, or nearly grounded, ice-ridge keels. To the east the stamukhi zone is often associated with a change in sediment character. Seaward of the zone cohesive but unconsolidated muds and muddy gravels offshore abut against overconsolidated muds, often in association with a bench or a shoal 1 to 2 m high (Barnes and Reimnitz, 1978; Reimnitz and Barnes, 1978; Reimnitz and others, 1978; Rearic and Barnes, 1980; Reimnitz and others 1980). Gouging of the seabed is much more intense in the area of

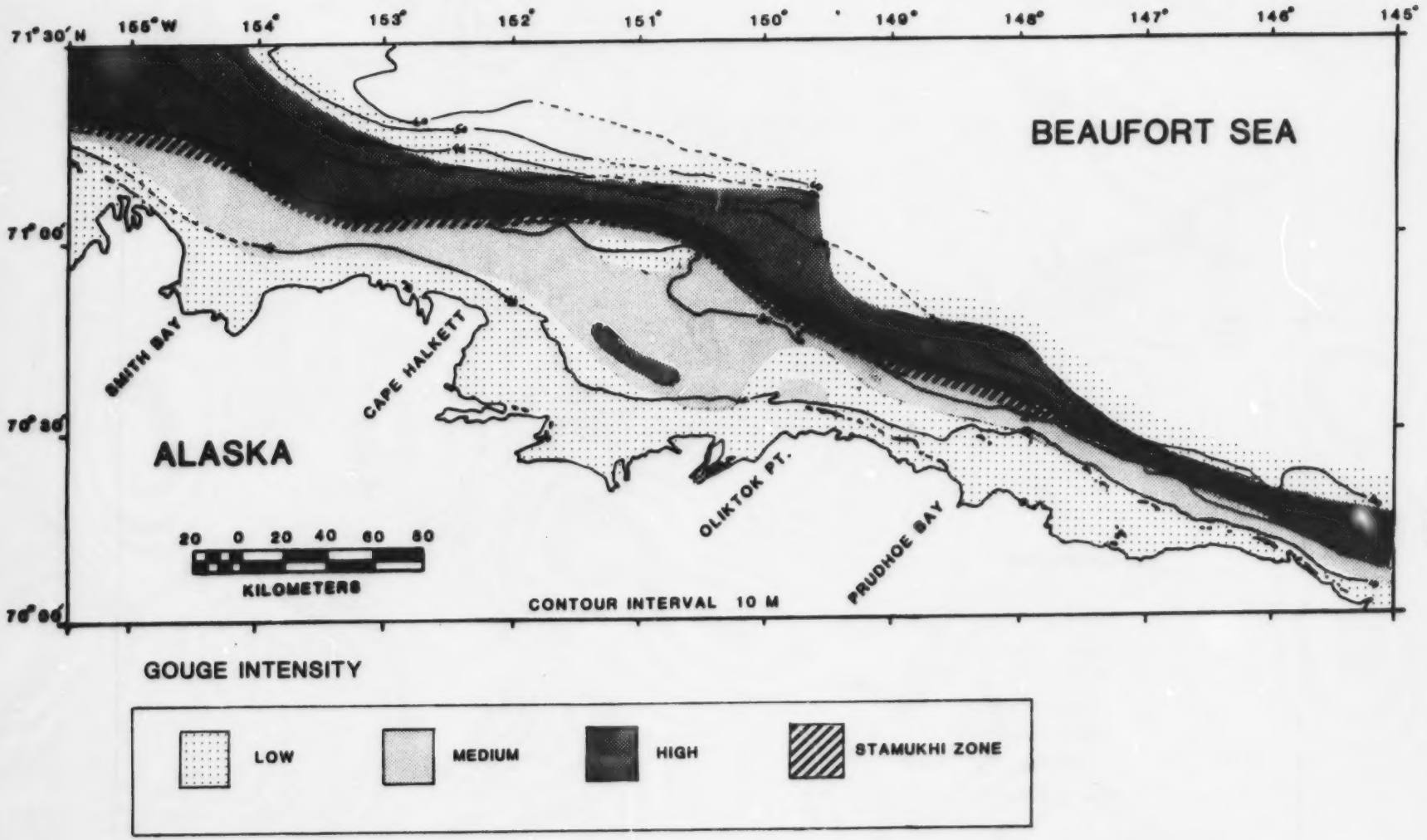

Figure 16. Interpretive map of ice gouge intensity on the Beaufort Sea shelf based on gouge density, maximum incision depths, and ice ridge intensities.

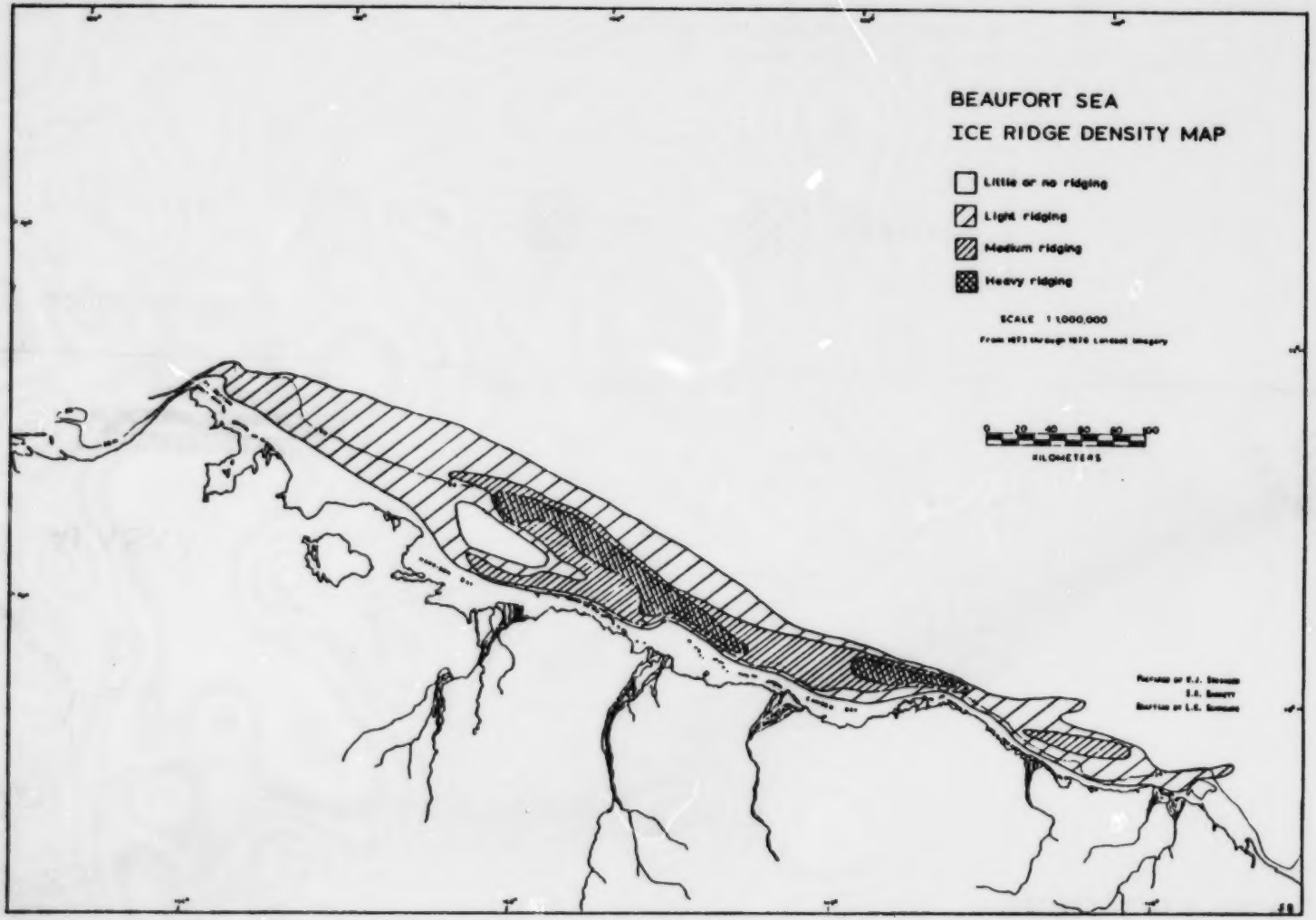

Figure 17. Map of ice ridge density compiled by Stringer and others (1978).

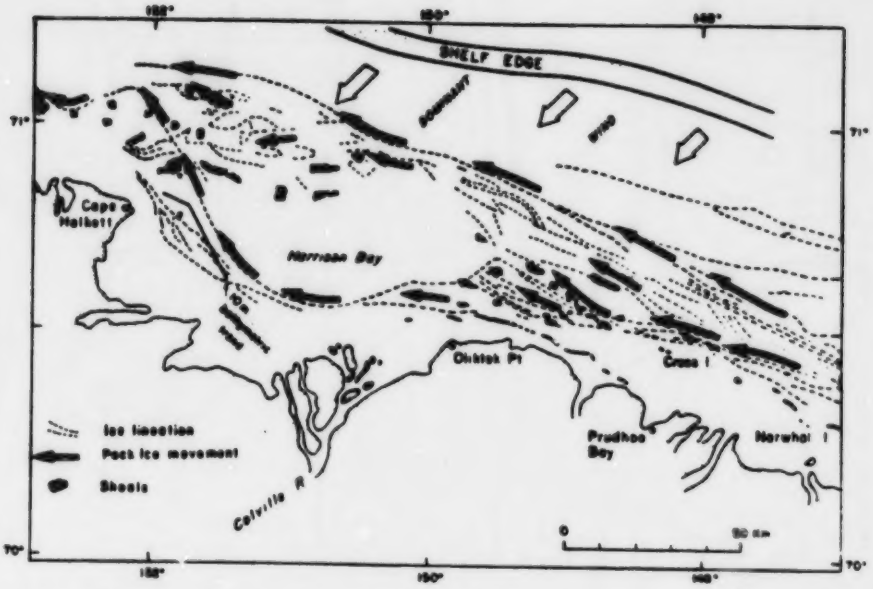

Figure 18. Generalized model of ice drift in Harrison Bay (after Reimnitz et al., 1978), showing the control of shoals on ice ridging patterns and the two zones of ridging at about 10 and 20 m in Harrison Bay.

unconsolidated sediment within, and just seaward of, the stamukhi zone (Barnes and Ross, 1980) (Figs. 13, 14 and 20). We are uncertain as to the origin of the unconsolidated sediments but believe they may be the result of freeze/thaw processes (Chamberlain et al., 1978) during the Holocene transgression or they may be caused by dynamic vertical, and perhaps more importantly, horizontal forces associated with the intense ice-seabed interacton in the stamukhi zone.

CONCLUSIONS

The most intense gouging on the Beaufort Sea shelf is associated with the major ridging of the stamukhi zone. This gouging generally occurs in water between 15 and 35 m deep, can result in gouges as deep as 4 m or more,, and may have relief of 7 m or more. Both inshore and seaward from this zone gouging tends to decrease in intensity. Gouging itensity is further controlled by the presence of shoals and the sedimentologic character of the seabed and can vary greatly over short distances.

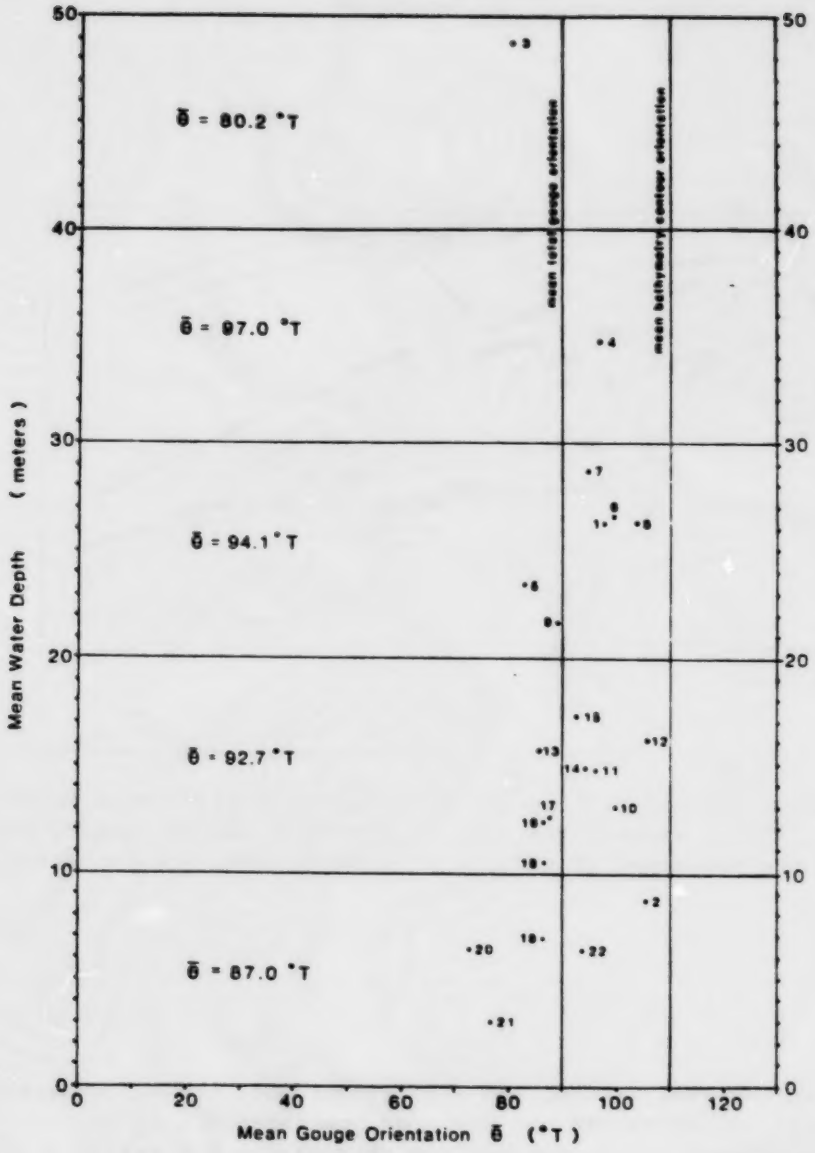

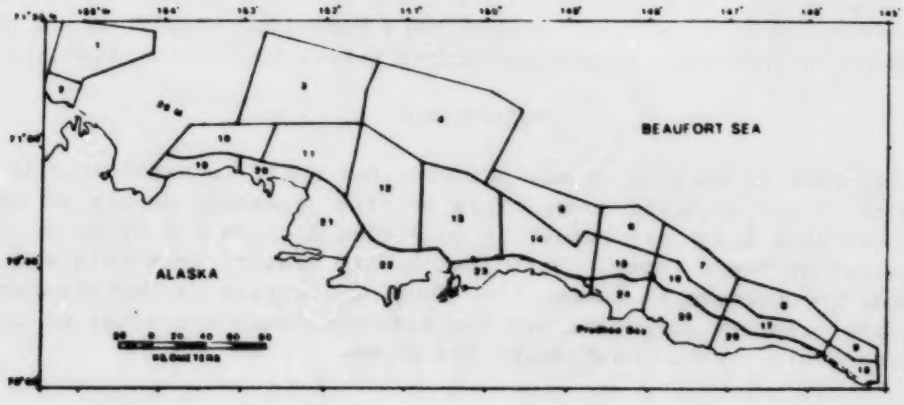

Figure 19. Mean gouge orientations arranged by water depth and shelf area.

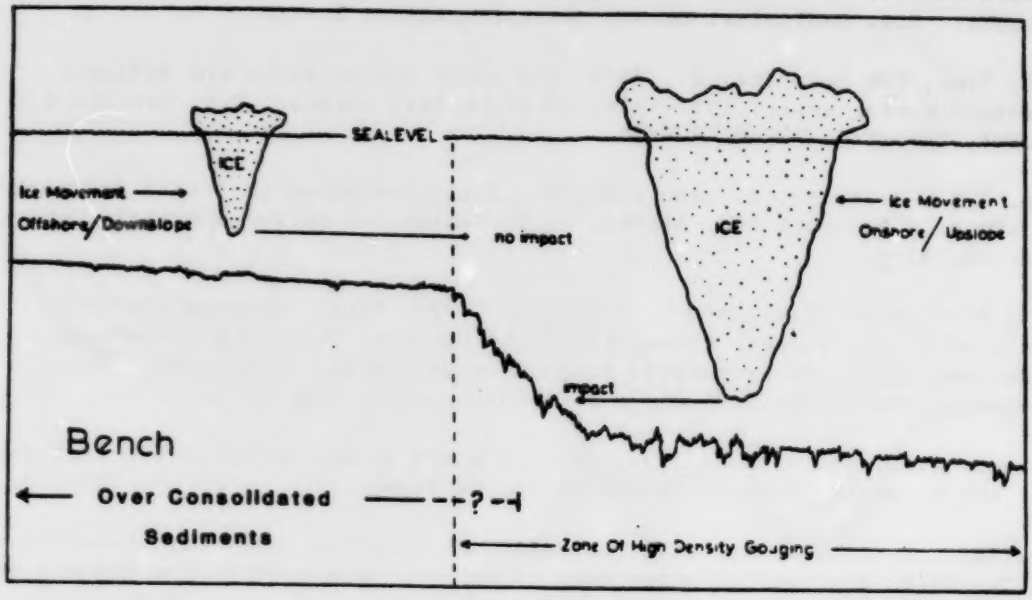

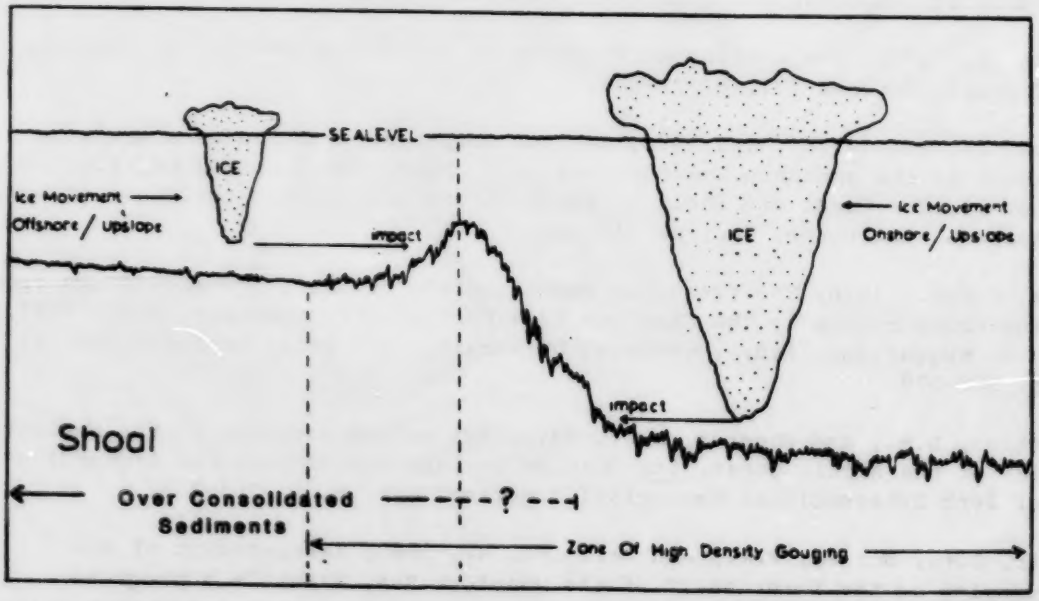

Figure 20. Ice gouge character change as it relates to bench, shoal, and unconsolidated sediments.

REFERENCES

Barnes, P.W., McDowell, D.M., and Reimnitz, E., 1978, Ice gouging characteristics: their changing patterns from 1975-1977, Beaufort Sea, Alaska: U.S. Geological Survey Open-File Report 78-730.

Barnes, P.W., and Reimnitz, E., 1979, Ice gouge obliteration and sediment redistribution event; 1977-1978, Beaufort Sea, Alaska: U.S. Geological Survey Open-File Report 79-848.

Barnes, P.W., Reimnitz, E., and Ross, R., 1980, Nearshore surficial sediment textures - Beaufort Sea, Alaska: U.S. Geological Survey Open-File Report 80-196, 41 p.

Barnes, P.W., Ross, C.R., and Reimnitz, E., 1980, Break in gouge character related to ice ridges, Annual Report to National Oceanic and Atmospheric Administration, Environmental Assessment of Alaskan Continental Shelf; Principal Investigators' Reports, 1980, Attachment E, 11 p.

Belderson, R.H., and Wilson, J.B., 1973, Icegerg plough marks in the vicinity of the Norwegian Trough: Norsk Geologisk Tidssdrift, v. 53, p. 323-328.

Chamberlain, E.J., Sellman, P.V., Blouin, S.E., Hopkins, D.M., and Lewellen, R.I., 1978, Engineering properties of subsea permafrost in the Prudhoe Bay region of the Beaufort Sea, Third International Conference on Permafrost, Edmonton, Alberta, Canada, p. 629-635.

Kovacs, A., 1972, Ice scoring marks floor of the arctic shelf: Oil and Gas Journal (October 23), p. 92-106.

Kovacs, A., and Mellor, M., 1974, Sea ice morphology and ice as a geologic agent in the southern Beaufort Sea, in: Reed, J.C., and Sater, J.E. (eds.), The Coast and Shelf of the Beaufort Sea, Arctic Institute of North America, Arlington, Va., p. 113-161.

Lewis, C.F.M., 1978, The frequency and magnitude of drift ice groundings from ice-scour tracks in the Canadian BVeaufort Sea, Proceedings, POAC, 1977, D.B. Muggeridge, (ed.), Memorial University, St. Johns Newfoundland, v. 1, p. 568-579.

Pelletier, B.R., and Shearer, J.M., 1972, Sea bottom scouring in the Beaufort Sea of the Arctic Ocean, in: Marine Geology and Geophysics, Proceedings of 24th International Geological Congress, Sec. 8, p. 251-261.

Rearic, D.M., Barnes, P.W., and Reimnitz, E., 1980, Reassessment of ice gouging on the inner shelf of the Beaufort Sea, Alaska - a progress report, Annual Report to National Oceanic and Atmospheric Administration, Environmental Assessment of Alaskan Continental Shelf; Principal Investigators' Reports, March 1980, Attachment D, 15 p.

Rearic, D.M., Barnes, P.W., and Reimnitz, E., 1981, Ice gouge data, Beaufort Sea, Alaska, 1972-1980: U.S. Geological Survey Open-File Report 81-950, 22 p.

Reimnitz, E., Barnes, P.W., and Alpha, T.R., 1973, Bottom features and processes related to drifting ice on the arctic shelf, Alaska: U.S. Geological Survey Miscellaneous Field Studies Map, MF-532.

Reimnitz, E., and Barnes, P.W., 1974, Sea ice as a geologic agent on the Beaufort Sea shelf of Alaska, in: Reed, J.C., and Sater, J.E. (eds.), The Coast and Shelf of the Beaufort Sea, Arctic Institute of North America, Arlington, Va., p. 301-353.

Reimnitz, E., Kempem, E.W., Ross, C.R., and Minkler, P.W., 1980, Overconsolidated surficial deposits on the Beaufort Sea shelf, Annual Report to National Oceanic and Atmospheric Administration, Environmental Assessment of Alaskan Continental Shelf; Principal Investigators' Annual Reports, 1980, Attachment B, 29 p.

Reimnitz, E., and Maurer, D.K., 1980, Stamukhi shoals of the arctic, some observations from the Beaufort Sea, Annual Report to National Oceanic and Atmospheric Administration, Environmental Assessment of Alaskan Continental Shelf; Principal Investigators' Reports, 1979, Attachment D, 10 p.

Reimnitz, E., Toimil, L.J., and Barnes, 1978, Arctic continental shelf morphology related to sea-ice zonation, Beaufort Sea, Alaska: Marine Geology, v. 28, p. 179-210.

Rex, R.W., 1955, Microrelief produced by sea ice grounding in the Chukchi Sea near Barrow, Alaska: Arctic, v. 8, p. 177-186.

Stringer, W.J., 1978, Morphology of Beaufort, Chukchi, and Bering Seas nearshore ice conditions by means of satellite and aerial remote sensing, Geophysical Inst., University of Alaska, Fairbanks, v. 2, 794 p.

Thomas, D.R., and Pritchard, R.S., 1980, Beaufort Sea ice mechanical energy budget, 1975-76, Flow Research Company, Kent, Washington, Report no. 165, 34 p.

Thorndike, A.S., and Colony, R., 1980, Large scale ice motion in the Beaufort Sea, in: Pritchard, R.S. (ed.), Sea Ice Processes and Models, University of Washington Press, Seattle, Wa. p. 249-26.

Weeks, W.F., Barnes, P.W., Rearic, D.M., and Remnitz, E., 1980, Statistical aspects of ice gouging on the Alaskan shelf of the Beaufort Sea, Draft Report, U.S. Army Cold Regions Research Laboratory, Hanover, New Hampshire.

Appendix I - Glossary of Terms

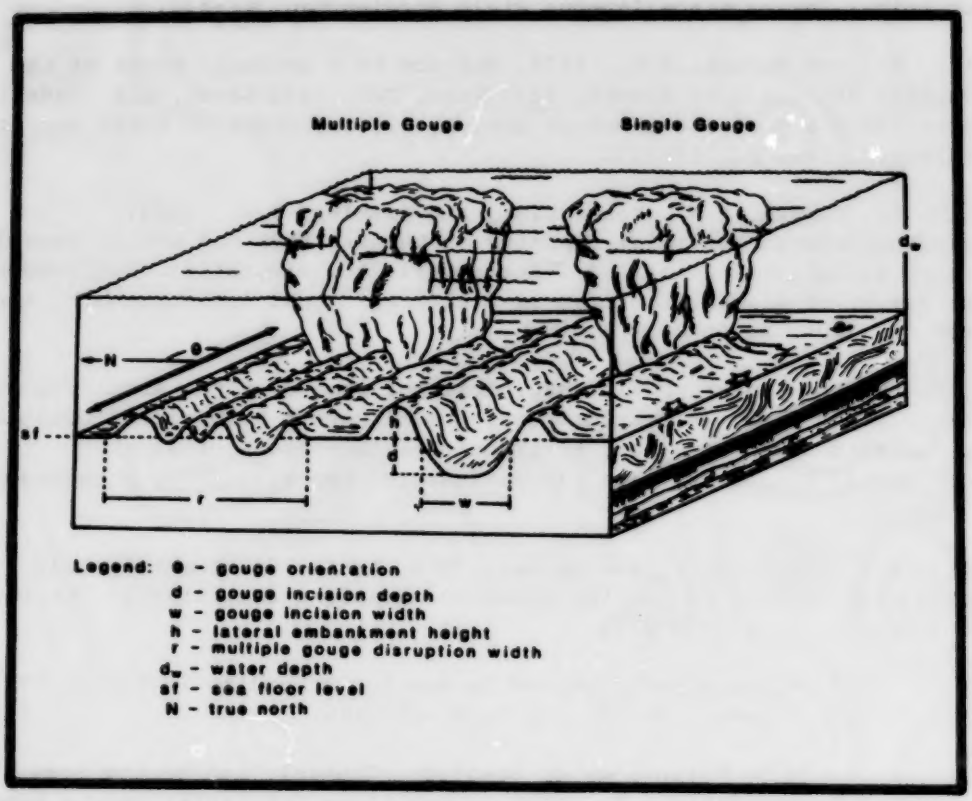

Figure 1. Diagram of the typical gouge measurements made from side scan sonar and fathometer records.

Water depth (dw).- Depth to sea floor subjectively smoothing and averaging ice gouge relief.

Observed Number of Gouges (sonographs).- Each individual gouge lineation was counted from sonar records and recorded for each segment.

Gouge Density.- In order to make comparisons between segments, the gouge density normal to the trackline was determined using a correction factor and gouge orientation (Barnes and others, 1978, Reimnitz and Barnes, 1974). The normalizing of the gouges in each segment allows us to compare segments on an equal basis and also consider a number per unit area value for that segment. The normalizing assumes all gouges are parallel and infinitely long. Other investigators have counted only those gouges crossed over by the ship (Lewis, 1978). We count all gouges on a sonograph segment, yet gouge length is often short and orientation varies. The estimates of density we obtain from this technique may be high.

Gouge Depth (d).- The depth of penetration ("Gouge Incision Depth," Barnes and others, 1978) of ice keels into the seabed (see Fig. 1) was measured along the trackline from fathograms and enumerated in 20-cm increments for each segment. The maximum incision depth was also recorded. In a few cases the resolution of the fathograms was not good enough to accomplish this enumeration. In areas of considerable seafloor relief it was often necessary to subjectively estimate the level of the sea floor due to the abundance of ice gouge ridges and troughs. Gouges less than 20 cm in depth or those that were observed on the sonar but not on the fathogram were also counted.

Orientations (θ)- All orientations were measured to the nearest five degrees relative to the trackline by constructed templates (Fig. 1). Using the ship's course, these relative orientations were converted to True orientations between 0 - 180°T. As the sense of ice motion is unknown, the orientations are not vectors. They can be represented as either bidirectional or unidirectional, as can the strike of a bed. That is, a gouge with a "measured" orientation of 270°T is also oriented along a line 090° or is oriented 270°-090°.

Maximum Ridge Height (h).- A measurement was made of the highest ridge in each segment from the fathograms. The measurement was made from the adjacent seafloor depth to the highest point of the ridge (Fig. 1). Summing the maximum ridge height and maximum gouge depth in each segment gives the maximum seabed relief from ice gouging in each segment.

Maximum Gouge Incision Width (w).- A measurement of the maximum width of a single gouge in each segment was made from the sonographs (Fig. 1). The gouge incision was measured from inside the bounding ridges at seafloor depth, as opposed to disruption width (Barnes and others, 1973) which would include the width of the bounding ridges. As with orientation, width measurements are distorted by horizontal exaggeration on most records and must be corrected.

Multiple Gouge Incisions.- When pressure ridge keels rake the bottom, parallel multiple gouges are formed (Reimnitz and others, 1973). (1) The number of multiple incision gouges (Fig. 1) in each segment was noted along with (2) the maximum number of incisions formed by any one event. (3) The maximum disruption width (y) for the widest multiple gouge was measured across the gouge from the furthest edge of the disrupted sediments outside the bounding ridges. (4) The dominant orientation for multiple gouge incisions in each segment may be different than for single incisions and was therefore measured independent of the single incisions.

DISCUSSION

B. Marcellus

You mentioned that in 1977 the ice scour signatures took on a completely new appearance. You have mentioned that scours up to 2 m deep have been infilled in a previous publication. Could you expand on the change in general appearance of the seabed over the whole shelf both before and after the 1977 storm.

E. Reimnitz

In two different reports, we dealt with infilling and obliteration of gouges. Reimnitz and Barnes (1974)* discussed the effects of a storm on an area resurveyed and showed that data from two different years cannot be combined in one contour map. Barnes and Reimnitz (1979)**demonstrated with the aid of accurately repeated surveys that almost all gouges on the inner shelf disappeared from 1977 to 1978, and were replaced by large, hydraulic bedforms. The Fall of 1977 was not unusually stormy but had no ice on the shelf and long fetches for wave generation.

*Reimnitz, Erk and Barnes, P.W. 1974 - Sea ice as a geologic agent on the Beaufort Sea Shelf of Alaska in Reed, J.C. and Sater, J.E. (eds.) The Coast and Shelf of the Beaufort Sea. Proceedings of the Arctic Institute of North America Symposium on Beaufort Sea Coast and Shelf Research, Arlington, VA., Arctic Institute of North America, pp. 301-353.

**Barnes, P.W., and Reimnitz, Erk, 1979 - Ice gouge obliteration and redistribution event; 1977-1978, Beaufort Sea, Alaska: U.S. Geological Survey Open-File Report 79-648, 27 p.

DISCUSSION

M.J. O'Connor

Are the sand waves parallel to the shoreline or are they aligned seaward, i.e. perpendicular to the shore?

E. Reimnitz

The sand waves off Pingok Island are about 2 m high, spaced 500 m apart, trend normal to the beach, and are seaward appendages to a well developed shore-parallel bar.

THE FREQUENCY OF ICE SCOURING OF THE NORTHEASTERN GRAND BANKS OF NEWFOUNDLAND USING THE INTERRELATIONSHIP OF SCOURS AND BEDFORM MIGRATION

C.L. Amos
Geological Survey of Canada
Bedford Institute of Oceanography
and
J.V. Barrie
Centre for Cold Ocean Resources Engineering (C-CORE)
Memorial University of Newfoundland

There are several lines of evidence to suggest that the seabed in the vicinity of the Hibernia discovery is mobile under certain conditions. High resolution sidescan records have revealed sand ribbons, sand ridges, sand waves and two and three-dimensional megaripples (Lewis and Barrie, 1981). These features can only be generated by unidirectional flows at velocities of between 60-120 cm/sec. Sequential photography reveal asymmetrical, wave-formed oscillatory ripple marks after severe storms, above 110 m, which are subsequently degraded by browsing echinoderms and bivalves. The inference is that the smaller bedforms observed on the sidescan records are modern and migrate periodically across the shelf, presumably during periods of intense storms. The migration of these bedforms tend to cover older features, such as ice scours, with the result that an area may appear free of scouring.

Recent high resolution sidescan records collected in May 1981 show fields of megaripples (5 m length) that appear to be migrating across otter broad trawl marks left by recent fishing operations (Barrie et al., 1983). These marks were created by the modern dragging fleet which has been active in the region for perhaps twenty years. The conclusion is that the megaripples were active since that time. However, no motion has been measured over the last two years. A re-examination of the records showed that a number of the ice scours appear to have been transgressed by the megaripple fields, while others cut through these fields. It is considered, applying the Law of Superposition, that the ice scours cutting the megaripple fields were formed since the last event which lead to bedform migration.

There are between 10 and 20 scours which appear to cut megaripple fields over a survey area of 30 x 60 km. These scours are, on average, 20 m wide and 500 m long. The frequency of ice scouring can be determined, provided the frequency of bedform migration is known, using the following relationship:

Scour frequency = scour number x bedform migration frequency, for any given area. The scour number is the total sum of scours which appear to cut megaripple fields over the area of interest. A conservative estimate of 0.5/year is obtained assuming a bedform migration rate of 20 years, and that 10 scours cut through megaripple fields. Biasing the selection of alternatives to the maximum scour numbers, we arrive at a frequency of 10/year. The results indicate that the seabed would be totally scoured in a period of approximately 6000 years, assuming no overlap in scouring. This same approach can be used in relating iceberg scours and the otter board trawl marks.

REFERENCES

Barrie, J.V., Lewis, C.F.M. and Fader, G.B., 1983. Seabed processes on the northeastern Grand Banks of Newfoundland; Modern reworking of relict sediments. Marine Geology, Aspects of Sedimentation on High Latitude Continental Shelves. (in press).

Lewis, C.F.M. and Barrie, J.V. 1981. Geological evidence of iceberg groundings and related seafloor processes in the Hibernia discovery area of Grand Banks, Newfoundland. In: Symposium on Production and Transportation Systems for the Hibernia Discovery, St. John's, Newfoundland. pp. 146-177.

SEA BOTTOM SCOURING IN THE CANADIAN BEAUFORT SEA

J. Hnatiuk and B.D. Wright
Gulf Canada Resources Inc.

(This paper was presented at the 15th Annual Offshore Technology Conference in Houston, Texas, May 2-5, 1983. OTC 4584).

ABSTRACT

Echo sounding, side scan sonar and seismic profiling records have shown that the continental shelf of the Canadian Beaufort Sea has been subjected to extensive scouring by ice features. The scouring phenomena is extremely important in the design and protection of offshore wells and future pipelines. Analyses of records collected by industry and government in the early 1970's and reported by Hnatiuk and Brown in 1977 have been refined with the inclusion of additional data collected by industry and government in 1975 and 1976. Here, the results of the information synthesis are presented in terms of regional maps showing relevant scouring parameters and their variation with location and water depth. A quantitative evaluation of scour return period is also presented on the basis of sedimentation assumptions. This information is compared with a recent analysis of sidescan scour mosaics collected repetitively over four areas ranging in water depths from 45 to 150 feet and with time intervals ranging from 2 to 7 years between the repetitive seafloor maps. The rate of addition of new scours determined from the repetitive mosaic approach supports the regional assessment of Beaufort Sea scour but suggests more episodic and areally frequent scour events along with more active scouring in water depths approaching 150 feet. This information is discussed in terms of the Beaufort Sea ice regime.

SHORE-ZONE ICE SCOUR STATISTICS: IMPLICATIONS TO COASTAL DEVELOPMENT

John R. Harper
Woodward-Clyde Consultants
1 Walnut Creek Center
100 Pringle Avenue
Walnut Creek, California 94596
U.S.A.

ABSTRACT

Shore-zone ice-scour statistics are available for some sections of the arctic coast, and these statistics provide some preliminary design constraints for coastal development in areas of ice infested waters. The statistics suggest that ice override and associated ice scour may be a process occurring frequently enough to dictate minimum set back distances of coastal structures; the risk of damage by scouring to buried structures, such as pipelines or cables, appears to be of comparable magnitude to other hazards such as coastal erosion, thaw settlement, storm surge, strudel scour and ice "wallowing". These hazards may pose more serious design problems.

INTRODUCTION

Ice override with its associated scouring, is a process occurring along coasts of ice-infested waters. Ice override, which is the process of sea or lake ice penetrating substantial distances into the backshore (greater than 20 m), represents a potential hazard to coastal shore structures. Ice push, which

is a similar ice-shore interaction, is limited to areas seaward of the high water line (i.e., the zone normally reworked by wave action). Scouring of the shore-zone may accompany both ice push and ice override and poses a hazard to buried structures such as pipelines or cables. Statistics on shore-zone ice scour provide a means estimating the level or risk associated with such a hazard and also provide a way of comparing the risk of override to other natural hazards.

This paper summarizes previously published information on ice overrides and ice push and qualitatively evaluates the potential risk associated with ice scour in comparison to other coastal zone hazards.

ICE PUSH, ICE OVERRIDE AND SHORE-ZONE ICE SCOUR

Numerous descriptions of overrides occur within the published literature (Kovacs and Sodhi, 1979; 1980). Overrides of particular note include: (1) an event on Somerset Island (N.W.T., Canada) which penetrated as much as 185 m from the shore and scoured beach sediments to a depth of approximately 1 m (Taylor, 1978), (2) an override event on Tapkaluk Island (Alaska) where the alongshore distance of the override exceeded 500 m and also included neighboring islands (Hanson et. al., 1978) and (3) observations by Alestalo and Haikio (1976) that documented override penetrations of up to 100 m of thin ice (less than 30 cm in thickness). Kovacs and Sodhi (1980) provide an exhaustive review of reported override events, and their work should be consulted for further detail.

Harper and Owens (1981; also Harper, 1980) reviewed aerial photographs to estimate the frequency of ice override events and to quantify the risk associated with ice override as an environmental hazard. Summary results are presented in Table 1

and suggest that ice override and associated scouring are relatively rare along the Chukchi and Beaufort Sea coasts of Alaska. The results are biased to some extent in that the analysis only evaluated override features and associated ice scours that were visible on aerial photographs (i.e., large events) and smaller events may have gone undetected. The data probably provide a realistic estimate of the frequency of severe events that are potentially damaging to shore structures.

Table 1. Summary of Ice-Override Events From the Alaskan Chukchi and Beaufort Sea Coasts (After Harper and Owens, 1981).

	Length of Shoreline Surveyed	Number of Events Observed	Number of Severe Events Observed
Beaufort Sea Coast	611 km	11	4
Chukchi Sea Coast	970 km	9	6
TOTAL	1,581 km	20	10

There are no systematic statistics on shore-zone scour depths, but observations of the author suggest that 1 m is probably a maximum scour depth. Overrides that occur between fall freeze-up and spring break-up are unlikely to cause significant scours because beach sediments are frozen below the surface. Even during summer months, backshore areas along arctic coasts have a permafrost table close to 1 m below the beach surface (Owens and Harper 1978).

DISCUSSION OF SHORE-ZONE ICE SCOUR STATISTICS

Statistics for shore-zone ice scour, based on results from an ice override study, provide a preliminary basis for evaluating the frequency of ice scouring in the shore-zone. Ice push, which is much more common than override, also causes shore-zone ice scour, but, unfortunately, there is no quantitative information on the frequency of occurrence of ice push.

The statistics suggest that shore-zone ice scour due to override along a given 500-m long section of coast is relatively rare with a probable return period of 100-200 years and greater than 300 years for the most severe events (Harper, 1980). It should be recognized, however, that consideration of ice push events would reduce the probable return periods by an unknown factor. On the other hand, pipelines are substantially less than 500 m in width and if one assumes a shore-zone pipeline crossing width of 10 to 20 m, then probable return periods would increase due to the smaller alongshore length of the shore-zone considered.

The frequency of shore-zone scouring has been evaluated only for the Chukchi and Beaufort Sea coasts of Alaska. The statistics are probably applicable to the Beaufort Sea coast of Canada, but recent observations along the Northwest Passage of the Canadian archipelago (Owens and Harper, in press) suggest that shore-zone scour may be more common along some segments of Amundsen Gulf, Viscount Melville Sound, and Lancaster Sound Coasts.

SHORE-ZONE ICE SCOUR IN COMPARISON TO OTHER NATURAL HAZARDS

Preliminary assessment of shore-zone ice scour statistics suggests that significant scour events occur relatively infre-

quently. Although these events may be important geologically (McLaren, 1982), the analysis suggests that shore-zone ice scour may not pose a significant coastal design problem, particularly when compared with other coastal hazards.

The relationship of scour limits to other natural features of an arctic beach system is schematically illustrated in Figure 1 (the scour limit is assumed to be 1 m below the beach surface). Significant additional hazards and their zone of influence are also illustrated. Coastal erosion, which is typically high along many arctic coasts (up to 10 m/yr), but usually 1-2 m/yr, would represent a signiricant concern over the probable lifetime of a buried pipeline. Over a 25 year period, for example, coastline retreat in the order of 25-50 m might be expected. As permafrost melts during coastal retreat, thaw settlement of the nearshore area may occur, and, in areas of ice-rich sediments, may be as much as 1-2 m. Seasonal beach changes of several meters have been documented in the arctic, and provide an additional constraint to structures crossing the shore zone. Ice wallowing, a process where large ice blocks are pushed through nearshore sediments (Reimnitz and Kempema, 1982), may scour to depths at least as great as 1 m, and therefore represents a comparable hazard to shore-zone ice scour. Strudel scour has been identified as a potential hazard to nearshore structures, but is most active in areas seaward of the 2-m water depth (Figure 1).

Summary

An analysis of ice override events from the Alaskan arctic coast suggests that ice override and associated scour events are relatively rare; return periods for potentially damaging scour events, based on this data set, are estimated to be greater than 100 years. The consideration of ice push, which

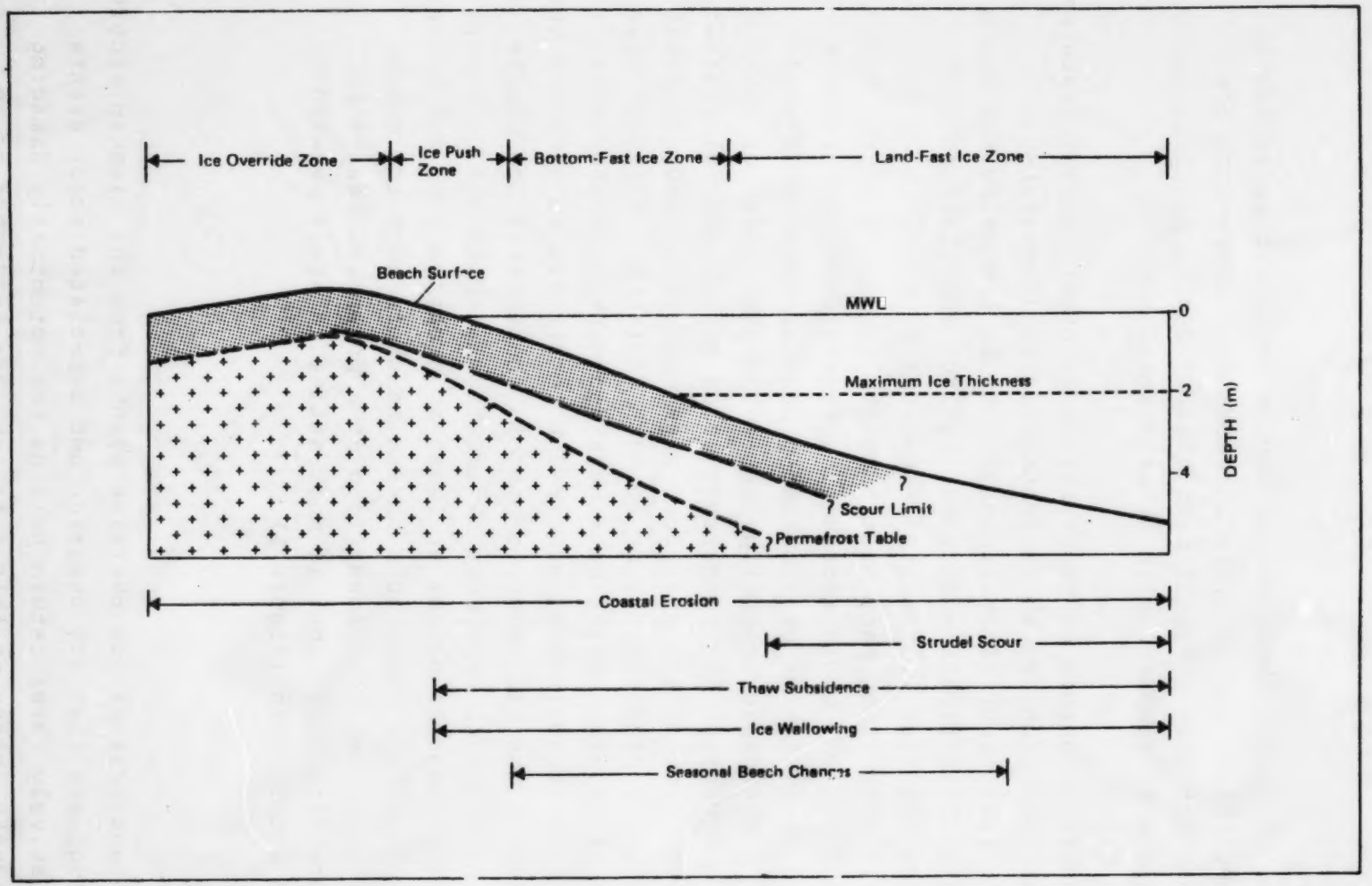

Figure 1. Schematic cross-section of Arctic beach illustrating estimated scour limits in relation to the permafrost table, the beach surface, and other natural hazards

was not included in the analysis, would have the effect of reducing the estimated return period as ice push is more common than ice override. On the other hand, pipeline corridors are narrower than the wide corridors (500 m) considered in the override analysis, and consideration of the narrower corridor would effectively increase estimated return periods. An additional limitation to these scour statistics, is the representativeness of the data, which were collected from a relatively small section of the arctic. Recent observations indicate that shore-zone ice scour is more intensive in the Canadian arctic than along the Chukchi and Beaufort Sea Coasts.

A qualitative comparison of shore-zone ice scour to other natural coastal hazards in the arctic suggests that in certain areas of the arctic coastal erosion rates, ice wallowing, seasonal beach changes, and thaw settlement will probably pose more significant design constraints for buried structures than will shore-zone ice scour.

REFERENCES

Hanson, A., Metzner, R., and Shapiro, L., 1978. Ice shove in the Point Barrow area. Arctic Project Bulletin #22, OCSEAP, p. 4-8.

Harper, J.D., 1980. Analysis of ice override potential along the Beaufort Sea coast of Alaska. Unpublished proprietary report prepared for Chevron USA (San Francisco) by Woodward-Clyde Consultants (Victoria, B.C.), 114 pp.

Harper, J.R. and Owens, E.N., 1981. Analysis of ice override potential along the Beaufort Sea Coast of Alaska. Proceedings of Port and Ocean Engineering under Arctic Conditions (POAC 1981), Quebec City, Quebec, p. 974-984.

Kovacs, A., and Sodhi, D., 1979. Shore ice pile-up and ride-up, field observations, models, theoretical analyses; O.N.R. Workshop on Problems of the Seasonal Sea Ice Zone, Naval Postgraduate School, Monterey, Calif., 84 pp.

_____, 1980. Shore ice pile-up and ride-up, field observations, models, theoretical analyses. Cold Regions Science and Technology 2:209-288.

McLaren, P., 1982. The coastal geomorphology, sedimentology and processes of eastern Melville and western Byam Martin Islands, Canadian Arctic Archipelago. Geological Survey of Canada, Ottawa, Bulletin 333, 39 pp.

Owens, E.H. and Harper, J.R., 1977. Frost-table and thaw depths in the littoral zone near Peard Bay, Alaska. Arctic, 30(3):155-168.

Reimnitz, E., and Kempema, E., 1982. Dynamic ice wallow relief of Northern Alaska's nearshore. Jour. Sed. Pet. 52(2):451-461.

Taylor, R.B., 1977. The occurrence of grounded ice ridges and shore ice piling along the northern coast of Somerset Island, N.W.T.. Arctic, 31(2), p. 133-149.

RISK ASSESSMENT & PIPELINE TRENCH DEPTHS
(DISCUSSION SUMMARY)

Many of the talks at the workshop covered methods of calculating pipeline trench depths; this paper reviews these talks.

The methods can be divided into three general categories involving:

- measurements or observations of the seabed soils
- ice keels statistics
- ice scour statistics

1. METHODS OF DETERMINING PIPELINE TRENCH DEPTHS

1.1 Scour Dating

The pipeline trench depth corresponding to a given return period can be determined if we know the age of all scours on the seafloor, and in particular the age of the deepest scours. A study has recently been conducted by Petrocan (Haider 1981) discussing these techniques and methods of collecting the soil samples.

The usual method requires collection of a soil sample through the bottom of the scour providing both the infill sediment and sediment from the scour bottom. The age of the bottom layer of infill sediment is the age of the scour. This sample is best collected by a diver. The two most promising methods of dating the sediment are carbon 14 and pollen. Carbon 14 requires identification of some organic matter (shell, piece of wood) within the sample, preferably in the lower zone. This organic matter must also have been fresh when it fell into the scour. Pollen dating requires identification of the ratio of various pollens in the sample, and this ratio can be tied back into other onshore samples that have been dated by other means. In principle the methods are feasible, but in practice it is found that most

of the infill sediment originates from other scours on the seafloor and consequently no consistent dates will be found.

The method would be useful to date the occasional deep scour in deep water where scouring is infrequent. There, most of the scour infill sediment probably originates from the water column and not from reworking of the sea floor.

In summary, the method will not work in areas of frequent scouring, but would be useful for the occasional deep scour in deep water. However, it is not recommended as it is extremely expensive to get even one sample, let alone a statistically significant sample, and it is not guaranteed to be successful.

1.2 Seabed Dating

An alternative method that appears promising for scour dating in deep water was discovered at the workshop (Blasco). The method is applicable to deep water areas where scouring is infrequent. Shallow seismic records indicate the individual filled-in scours in the upper layers of the seabed. From these records the number of scours that have occurred over a distance of several kilometers and in the top, say, 2 meters of seabed can be determined. If we can determine the age of the top 2 m of seabed, then we know how many scours occurred per thousand years per kilometer, from which we can find a return period for scouring. This method is only useful in areas where scouring is infrequent, permitting one to count individual scours in the shallow seismic records, and in regions of cohesive soils, as non-cohesive soils do not retain scour signatures. An initial quick look at this technique suggests that scouring has been sufficiently infrequent in 60 m water depths that pipeline burial is not necessary, as was also indicated by the keel statistics method discussed later.

1.3 Comparative Scour Ages 1

By comparing the overlapping of scours it is possible to determine their relative age (Barry, this workshop). However, it is impossible to say if all the scours occurred during the same year or over many years. Such an analysis should be done prior to actual scour dating, so that one dates, say, the oldest scour in an area. As scour dating appears to be of limited use, it is unlikely that this comparative dating will yield any results useful for engineering design. This method is felt to be useful for comparative purposes.

1.4 Comparative Scour Ages 2

Shearer (1982), after reviewing scours on the sea floor at 60 m in the Beaufort Sea, suggested that some scours were "very recent" (evidence of clear cuts), "old", and "very old" (evidence of infill erosion). No ages could be placed on these scours and it is not known if the "very recent" scours had occurred within the past few years as might be indicated by repetitive mapping.

This method is useful for comparative purposes.

1.5 Saturated Scour Zone (SSZ) Method

As mentioned above shallow seismic records in cohesive sediments retain a print of scours that have occurred over the years. Examination of these records show a zone of no stratification, due to extensive scouring, underlain by a zone of stratification indicative of the pre-transgression zone. Clearly, placing a pipeline into this stratified zone would ensure that it would not be hit by ice.

This method is only useful in zones of cohesive sediments (non-cohesive sediments don't retain scour signatures) and in water depths of less than about 10 m, for which the transgression occurred within the last

5000 or so years. In most areas in the delta, the sedimentation rate has been so high that scours over the past 1000 years or so have not penetrated as deeply as the transgression zone, and so trenching below this zone is too conservative. However, in areas where the base of the SSZ is less than about 3 to 4 m, the depth can be safely used unless there is good reason to choose an even shallower depth.

1.6 Repetitive Mapping

The most reliable method of obtaining current scouring frequency is to generate a mosaic of the seafloor and repeat the mosaic one or more years later to reveal any new scours. This method indicates the number of scours per km of track per year in the particular area of interest; it naturally indicates if an area is particularly exposed to scouring (shoal) or is protected (area behind a shoal or dip in seabed).

Baseline mosaics are now available for many areas, but more are required for other possible sites. Once an initial mosaic has been run, the area can be resurveyed at any time and the number of scours occurring in the intervening time determined. It is extremely important that initial mosaics are conducted for all possible pipeline corridors.

The following relationship can be used to estimate the number of scours that have depths greater or equal to it:

$$\frac{n}{N} = e^{-kd} \qquad (1)$$

n = expected no. of scours greater than d
N = total no. of scours
k = inverse of mean scour depth (m^{-1})
d = scour depth (m)

$$N = \bar{g}\, TL \qquad (2)$$

$\bar{g}$ = average number of scours/km/year
$\bar{T}$ = return period (years)
L = Length of pipeline

Substituting equation (2) into equation (1) and solving for depth (d).

$$d = -\frac{1}{k} \ln \frac{n}{g\bar{T}L}$$

or

$$d = \frac{1}{k} \ln (\bar{g}\bar{T}L) \text{ for } n = 1$$

Weeks et al (1983) and others have used this method to calculate pipeline burial depth*. However, due to the sparity of data, the mosaicing data has to be supplemented with ice keel statistics data (see section 2) to obtain the decrease in number of seafloor impacts with water depth.

With modern survey techniques it should be possible to use any recent, single side scan sonar tracks for repetitive mapping.

1.7 Scour Fill-in Rate Method

If one assumes that the number of scours on the seafloor is constant and the scour fill-in rate is known, it is possible to calculate the scour frequency (Lewis, 1977). Lewis used this method to determine pipeline trench depths. However, the method depends critically on the fill-in rate and this is not known. Scour fill-in is due to bottom trans

* This should be interpreted as top-of-pipeline depth. "Burial" implies covering the pipe with soil and the desirability of this has not been established.

port of sediment reworked by scouring or in shallow locations by sediment reworked by extreme waves. Infact, the majority of fill-in probably occurs during episodic events and so very difficult if not impossible to measure reliably with sediment traps over the short term.

1.8 Deepest Scour

It is generally assumed that burial of a pipeline below the deepest scour in an area will provide adequate protection against scouring. This is totally erroneous. It is extremely unlikely that the 1000 year or even 100 year scour is presently on the sea floor in areas of frequent scouring.

Calculations using other methods discussed here (see section 1.6) suggest that the pipe must be buried several metres below the deepest scour in water depths where there is active scouring. However, in deep water where scours fill in slowly, it appears (see Pilkington and Marcellus, 1981) that the deepest scour exceeds the trench depth required.

In general it is felt that the deepest scour is useful for comparative purposes only.

1.9 Comparison with other Sea Bed Phenomenon

It has been suggested by Amos and Barrie (this workshop) that it might be possible to judge the age of scours by comparing them to other sea bed phenomenon, such as a sand or silt bar over an area of scouring, or scours in a sand or silt bar where the sand or silt bar can be dated.

This method could be very useful if unambiguous, interpretable results can be obtained.

1.10 Scour Depth and Soil Strength

Based on intuition one would expect that scours in soft sediments will be deeper than those in harder sediments, and infact one sees this in the east-west variation of scour depths across the Beaufort Sea. One might expect to find a relationship between scour depth and the soil strength, such that for some soil strengths there are essentially no scours, and so a pipeline within such a layer would not be subject to scouring.

Such a study would require scour depths and soil strengths from the same location. There may not be soils in the Beaufort Sea that are strong enough to prevent scouring, but as the ice driving force varies as does the strength of ice keels one would expect to find a statistical variation of scour depth or number with soil strength. Thus one should expect a correlation between the scour depth distribution constant, K (see 1.6) and soil strength, and indeed this correlation may allow extrapolation of scour depth distribution results into areas where only limited scour data are available, based on soil characteristics. It is recommended that a mean value of K be obtained by averaging all data for similar type soils.

1.11 Keel Statistic Methods

These methods are based on the statistics of ice keel depths that might impact the seafloor in a given water depth per year. Thus knowing the ice keel distribution, which is usually of the form:

$$n = n_o \, e^{-D/Do} \qquad \text{keels/m/km}$$

where n_o and D_o are constant
n is number of keels of depth D
and e is the base of the natural log

The number of keels hitting the seabed in Dm water depth is

$$= \int_{D}^{D+\delta} n_o \, e^{-D/Do} dD$$

Where δ is the maximum expected scour for the particular water depth (about 8m).

The number obtained is in keels/km of track or if we know the mean ice velocity, km/year, we can obtain the number of keels/year impacting the seabed. We need to convert this to keels/km/year and this conversion is discussed by Wadham's in his paper in this workshop.

The keel distribution data can be taken from various sources: upward looking ice keel profiler, submarines, Laser data, or stereo surveys. However, one must be careful to ensure that the data being used can be extrapolated to the area of interest. Infact the keel statistics data should be compared to and normalized to repetitive mosaic data where possible, then the keel data can be used to calculate seabed impacts in deeper water. A recent confidential study by Gulf Canada Resources Inc. indicates that seabed impacts calculated from keel statistics and repetitive mosaic data are within each others data set variations.

Once the seabed impact rate has been determined, return periods are calculated as discussed in 1.6.

2. PIPELINE TRENCH DEPTHS

2.1 Pipeline Trench Depth Philosophy

The philosophy of risk as applied to pipeline trench depths was discussed briefly. The dilemma here is that one pipeline may be buried to a depth corresponding to, say, a 1000 year return period. A second pipe buried to with the same criteria gives the combination a 500 year return period, 10 such pipes reduces the total risk to 100 year, which might be considered unacceptable. However, if this risk philosophy is permitted for buildings in a city - each building may be designed to a 100 year storm, if there are 1000 buildings, 10 will fall down every year! Of course this doesn't happen because the 100 year storm only occurs every 100 years, at which time we might expect that most of the buildings will suffer damage.

It has been suggested (Wadhams, this workshop) that if n pipes are to be built in the Beaufort Sea, each should be buried to a depth corresponding to an n x 1000 year return period. This is contrary to all construction risks that are used, and not recommended. Ed Phifer of Shell has developed a routine for optimizing pipeline burial for a pileline going through different risk zones, such that the risk for the entire line is T years.

2.2 Cost Optimization

One method of determining a suitable burial depth using available statistics is to minimize the cost. With this method burial depth ceases to be function of pipeline length and becomes a function of cost of pipe, cost of burial to depth d, risk, cost of failure etc. (see Pilkington and Marcellus, 1981).

It is recommended that this approach be applied, and if the recommended depth corresponds to a burial depth of greater than the desired return period, then the results can be used. If the burial depth by this method is less than that corresponding to the desired return period, the

return period method should probably be applied (some things are political rather than economical!).

2.3 Acceptable Risk

Acceptable risk levels were discussed. Several engineers implied that they were satisfied with a 100 year return period, as this is the standard return period applied to most engineering structures where only limited life risk is involved. Others generally favoured a higher return period, possibly, 1000 years. The philosophy here was that the chance of damage to the pipeline should be about 2% or less over the 25 year life of the line. Also, the limited reliability of the data was considered.

In most engineering design a 100 year return period is used plus a safety factor that may increase the return period by a factor of 10. Or one can take a much higher level of risk and drop the safety factor. Different damage levels should also be considered; for example impact of a pipeline by a first year keel may be permissible as this would probably not cause rupture.

3. PIPELINE PROTECTION vs BURIAL

This was discussed briefly (Marcellus, this workshop). It was felt to be unlikely to be considered as any protection against scouring would be massive and very expensive.

4. TRANSMISSION OF SOIL PRESSURES

A scouring ice keel causes pressure to be transmitted through the soil which could result in damage to a pipeline below. This problem has been stuided by Shell Oil and Chari at the Memorial University, Newfoundland. The problem can be resolved by trenching deeper and/or not covering up the pipeline in the trench.

5. MATHEMATICAL MODELS

Math models have been developed by Kivisild et al (1980), Chari (this workshop) and others. Most of the models assume a retangular block of ice with square corners being pushed into a sloping beach. Passive pressure on the front, soil reaction on the base and friction on the sides are considered. The soil pushed up ahead of the block is usually assumed to reside infront of the block and increase the passive soil pressure. Different approaches are used. Chari considers icebergs and assumes that they penetrate horizontally into the slope and lose their Kinetic energy as work done against the soil forces. Kivisild et al (1980) describe several models most of which allow the block to lift. The models included a "least resistance" approach, and one in which the equations of motion of the ice block were solved by numerical solution. Recently Marcellus and Croasdale (1981) describe a math model in which the ice block has a rounded front edge.

These models are extremely useful for gaining an understanding of the scouring process and some idea of maximum scour depth for given conditions. The parameters needed for the models are urgently required at this time. However, it is expected that models will identify critical parameters and subsequent measurements will give the parameters for input into the models.

6. PHYSICAL MODELS

Physical models were described by Abdelnour and Chari (this workshop). Most of these models involved moving indenters of different shapes into beaches of different slopes and soils in a test tank. Measurements of forces on the indenter, soils pressures etc. are made and compared to theory.

7. AVOIDANCE

This is clearly the most satisfactory way of resolving the scour problem but not necessarily the cheapest.

A cable from Newfoundland to Greenland was damaged frequently by icebergs until it was placed on the lee side of natural rises on the sea-floor. It was placed to the south side of the rises on the west side of the channel, and to the north side on the east side as icebergs drift south on the west side then north on the east side of the Labrador Strait. Since this change it is believed that no further damage has occurred.

In the high arctic it is planned to tunnel pipelines to below the level of current scouring for pipe lines crossing the Viscount Melville Sound.

In the Arctic Islands calculation of pipeline trench depths are very difficult as the seabed does not retain scour signatures due to its very soft nature. Panarctic froze the pipeline area at their shore approach at Drake.

In the Beaufort Sea the possibility of running pipelines out to deep waters along submarine river valleys, where they could then be layed directly on the sea floor or placed in very shallow trenches was considered. Here it was not economical as the cost of the pipe was considerably higher than the cost of burial (unlike the cable situation described above) and so the most direct route was cheapest. Also close examination of the submarine valleys indicated scouring on the valley floors.

References

Haider, S. (1981), A Review of Scour Dating Techniques, Petrocan Report.

Kivisild, H., G.R. Pilkington and H. Iyer (1980), Mathematical Models for Ice Scouring, ASME, , Jan, 1980.

Lewis, C.F.M. (1977), Bottom Scour by Sea Ice in the Southern Beaufort Sea. Dept. of Fisheries and Envt., Ottawa, Beaufort Sea Project Tech. Rept. 23.

Marcellus, R.W., and K.R. Croasdale (1981), Ice Forces on Large Marine Structures, IAHA, Quebec City, 1981.

Shearer, J. (1982), Comparative Ages of Scours. Confidential Report to Dome Petroleum.

Weeks, W.F., W.B. Tukker III, M. Frank and S. Fungcharoen (1980), in R.S. Pritchard (ed.), Sea Ice Processes and Models, U. of Washington Press, Seattle, pp. 300-312.

PANEL DISCUSSION

PANEL

Vaughn Barrie Mike Lewis Drew Allan	East Coast
Steve Blasco Brian Wright	Beaufort Sea
Peter Barnes or Erk Reimnitz Ed Phifer	U.S. Beaufort Sea
Peter Wadhams	Cam River

PLEASE COMMENT ON THE FOLLOWING

1. Present data quality and reliability for your area.
2. Data quantity and distribution for your area.
3. What are the important parameters needed for calculations of burial depth?
4. Do you feel more data are needed? What type of data?
5. Should we be studying the ice keels or the seabed?
6. Methods to use to collect data. Do we need new methods?
7. Which do you feel are the most reliable methods of calculating burial depth?
8. Do you see any merit in mathematical and physical models for your area?
9. Other comments.

PANEL DISCUSSIONS

Q. What do the Panel feel about the quality, quantity and reliability of data in their locations?

A. There is a large amount of scour data available but more site specific data are required covering prospective routes. For these routes we need detailed information on the geomorphology, geology, scour depth, etc. When we get into this work we will be pushing technology to the limit and very likely have to improve technology or adopt new technology.

Q. How accurately are we measuring scour depths? Are the different types of equipment consistent in terms of number and depths of scours.

A. Yes the data obtained are consistent for reconnaissance, but we now recognize that for more accurate work the equipment is limited, for example, scour depth. This is an extremely important factor which we need to measure accurately and determine if there is infilling, or a zone of deformation.

We have recognized what is needed and now have to concentrate on areas of critical concern and improve technology as necessary, such as higher resolution sonars and subbottom profiles.

Q. What does the Panel feel about the currently used methods of calculating pipeline burial depths?

A. The Beaufort Sea, East Coast and High Arctic have quite different ice regimes. The techniques used in one area for calculating pipeline burial depths may not be applicable to the other areas although I would think that some of the statistical approaches may apply. In fact statistical approaches used in one area of the Beaufort may not be relevant to other areas. Certainly the high Arctic is a very difficult

problem because of the ice regime and also the sea bed does not retain scour information. In fact in the high Arctic the plan is to tunnel through the shoreline to water depths below the zone of active scouring. This method may work in other areas.

One gap is the availability of iceberg profiles. One can take an ice bottom profile with a submarine or a top profile with a laser and obtain a substantial record. However, for icebergs it is much more difficult. After several years we have only profiled maybe 300 bergs, which is rather a small number. We need some rapid technique for profiling bergs to provide an adequate statistical sample. Unfortunately impulse radars are not a proven technique yet. I gather some work will be conducted on this this year at C-Core or Memorial University.

(Vaugn Barrie) I agree with the above. Clearly the technology of side scan sonar, sonar measurements of icebergs, etc., is a closed subject. There are a lot of problems for which acoustic methods have not been considered. Most icebergs are measured by the traditional side scan methods because the work boats are there, available and essentially free. The alternative method of impulse radar or a submarine provides a much larger data set very quickly but is far more expensive (even if the impulse radar method does work). We also need to calibrate the different draught measuring systems against each other.

Q. What are the important parameters needed in the calculation of burial depth.

(Steve Blasco) cost of trenching is probably the most important parameter. We should look at the geology of the area and the cost of trenching the particular conditions. If it is relatively cheap to trench and only marginally more expensive to go deeper, then maybe we can bury the pipeline much deeper than we need and forget about it. Of course it will always be more expensive to bury deeper so if we can confidently reduce burial depths there will be worthwhile cost saving.

Clearly cost saving and change in level of confidence with burial depth go hand in hand. If, for example, the dredged soil may be needed for island building or the dredge has been leased for 12 months to do a 2 month trenching project, then the cost of trenching to 5 m may be the same as going to 10 m.

Q. Are there other processes that we do not understand - such as ice wallowing? This process and others may be of much greater risk than the other mechanisms that we think we understand.

A. We do not understand the ridge building process itself and how the ridge impacts the seafloor. Do we get high currents, and the resulting hydraulic scour, as a result of the constriction caused by pressure ridge keels. There is evidence of shoals which have no scours on them most probably due to hydraulic reworking, and gravel areas that show sand waves. The system of ridges grounding along a number of shoals can be a fairly effective dam to oceanographic circulation. In fact, there is some evidence that nearshore water level rises in 1972 and 76 were due to this damming effect further offshore.

Another aspect involving risk is the probability of a leak occurring from a pipeline if a keel contacts it, and what size the leak might be. We really do not understand this mechanism or its consequences, and surely the amount of spill must be included in any pipe burial calculations.

We also need more information on orientation of scours relative to the pipeline and the magnitude of scour loads transmitted below the scour. Near surface permafrost also will affect scouring and pipeline burial.

We must understand the scour mechanism to evaluate the effectiveness of any protection we may devise, and this is best done by scour observations and physical modelling.

(Mike Lewis BIO) I agree we ought to make actual scour observations and we could probably do this as we are very flexible in our operation, provided the event is reported to us. Maybe we should attempt to monitor infilling of scours, possibly using traps.

Q. Do you feel there is enough data in your area for a determination of trench depths and should we be studying the keel or the seabed.

A. The consensus of this group is that we should continue to look at both the keels, seabed and geology of the area. There are a variety of techniques being used at present and hopefully our answers will converge.

For a regional or reconnaisance scale, I feel that probably enough information exists in the Canadian Beaufort Sea for feasibility studies. We still need site specific data along potential pipeline routes and gathering system corridors.

There should be an interaction between all methods - i.e. keel, seabed, geology and mathematical and physical models. Each method will compliment and help the others.

If it is a matter of budget, I feel looking at the seafloor or lake bed is most important. After all, if a keel impacts the seafloor it leaves a scour for a considerable length of time.

(Vaugn Barrie) We have not yet looked at the iceberg scouring mechanism in winter; we feel it is a different mechanism. This agrees with earlier comments that understanding the mechanism of scouring is very important. We have been studying both iceberg statistics and seabed on the east coast but have not brought the information together yet, basically due to a lack of data. We need to correlate iceberg draft and dynamics, soil and scour for the same event.

Q. Mike Lewis - do you feel that by the time you may want to put a pipe on the seafloor, say 5 years time, enough scour statistics will be available to provide acceptable burial depths.

A. We must continue to pursue all available methods and look for convergence in the results (and of course explain any discrepancies). Answering your question, yes, I think that we could have enough information within a few years, but interpretation may be a problem. In the Grand Banks area we need a full understanding of what's going on, but for now we need initial burial depths for evaluating which way to go (i.e., tankers or pipelines). Management must be made to realize the time scale to collect the required data. We have to collect a lot of data, then interpret the data and finally put it into engineering calculations and this all takes time. Will we be ready for development?

We must be very careful how we use the information we collect, particularly the statistical information. We can use data and a statistical method and get a trench depth number, but how realistic or meaningful is this number both in general or for a specific area? We must be very careful.

As there is a limited amount of data it is imperative that we all co-operate and pool our data. This emphasises the need for a consistent data bank. We must overcome the confidentiality problem in industry possibly by entering the data as flagged. We also need a data management system.

AES is setting up a data bank of iceberg keel statistics but the Government's interest stops at number, size and location; this is a serious problem.

I do not think that we need to study keels as it is improbable that we will see the scour occurring and we are interested in the scour that is left. Also, the major events that we are really interested in are rare

and we are unlikely to catch this extreme keel scouring during a storm. In fact, we need a method of measuring scours as they are being made. Possibly, some acoustic system to indicate that a feature is scouring, which would then initiate a field program.

This technique could be very useful as it could provide location, time, energy expenditure, etc. and identification of the scour afterwards would allow measurements of scour depth and soil types.

We discussed the possibility of towing a small ice feature into a scour. This has a lot of merit as we can document forces involved and also instrument the ice floe.

We should also be looking at sacrificial structures on the seafloor - such as a piece of instrumented pipe buried in an area where scouring usually occurs. However, this might be expensive.

I think we need a large number of upward looking ice keel sonars. A method of measuring from above right through the ice might even be better.

Data on the coherence length of the crest of a sail is extremely important.

Q. What do the Panel feel are the most reliable methods of calculating pipeline trench depths?

A. We have considered a variety of methods and convergence of the methods is extremely important. We need some short term answers to decide if pipelines are indeed viable. It is, however, dangerous and unwise to claim that the trench depths we are presently talking about are correct considering our data base.

Q. Do you see any merit in mathematical and physical models for your area?

A. (Erik Reimnitz) The USGS has made little use of models to date but I don't think the state-of-the-art allows us to get design numbers at present as we do not have a good knowledge of the parameters required. But I feel that soon such models may be very useful.

I feel that models allow us to determine what we do, in fact need to measure. The models should help us to tie together ice keel and seabed data, but they haven't done that yet.

(Mike Lewis) Models are vital to test and improve our level of understanding of the scouring phenomenon. It indicates the sensitivity of scouring to different parameters.

Q. Is enough information available to consider the feasibility of pipelines?

A. I think we can put enough information together to study at least the feasibility of pipelines. But then considerably more work is needed. Although we have to make management aware of the reliability of the results they are getting and the cost of the necessary conservation. However, once a design number has been provided, if it is acceptable, management will question the need for further work. We clearly have to present research costs and operational savings to management.

APPENDIX "A"

ICE SCOUR WORKSHOP

PROGRAM

MONDAY, FEBRUARY 15, 1982

08:00 - 09:00	Registration	
09:00 - 09:30	Introduction	R. Pilkington L.W. Gold
09:30 - 10:00	Nomenclature	R. Marcellus
10:00 - 10:30	Coffee	
LAKES		
10:30 - 11:00	Lake Erie Cable Crossing Ice Scour Study	J.D. Grass
11:00 - 11:30	Subaerial Expressions of Relict Ice Scour Signatures in Different Environments on Mainland Canada	J. Mollard
11:30 - 12:00		
12:00 - 03:00	Lunch	
BEAUFORT SEA		
03:00 - 03:30	The Geomorphology and Sedimentology Resulting from Ice Scour	P. McLaren
03:30 - 04:00	Evidence for Differing Scour Ages in the Beaufort Sea	J. Shearer & M. Gajtani
04:00 - 04:30	Dating of Soil Samples in the Beaufort Sea	R. Pilkington & M. Marcellus
04:30 - 05:00	Dynamic Ice Wallow Relief of Northern Alaska's Near-shore	E. Reimnitz & E. Kempema
05:00 - 05:30	Coffee	
05:30 - 06:00	Prediction of Extreme Keel Depths from Submarine Sonar	P. Wadhams

MONDAY, FEBRUARY 15, 1982 (Continued)

SHORES

06:00 - 06:30	Shore P9le Ups	J. Harper
06:30 - 07:00		
07:00 - 07:30	Drake Shore Crossing	M. Van Ieperien

TUESDAY, FEBRUARY 16, 1982

EAST COAST

08:00 - 08:15	Introduction	M. Lewis
08:15 - 08:30	Scour Cross Cutting Analysis	C. Lynas
08:30 - 09:15	Effects of Icebergs on Eastern Canadian Continental Shelf as Seen by Submersible	H. Josenhaus
09:15 - 09:45	Hibernia Sufficial Geology and Iceberg Scouring	M. Lewis
09:45 - 10:30	Coffee	
10:45 - 11:15	Iceberg "Harrowing" as Opposed to Iceberg "Ploughing"	A. Ruffman
11:15 - 11:30	Evidence of Iceberg Rotation	L. Brooks
11:30 - 12:00	A New Type of Lineation Seen on the Ocean Floor in Lancaster Sound N.W.T. - Possible Glacial Fluting	A. Ruffman & L. Lee
12:00 - 03:00	Lunch	
03:00 - 03:30	Physical Dimensions of Icebergs in the Labrador Sea	J. D. Miller & I. S. Hotzel
03:30 - 04:00	Labrador Sea Iceberg Physical Dimension Data in Non-Dimensional Form	I. S. Hotzel & J. D. Miller
04:00 - 04:30	Iceberg Size Statistics	L. Brooks
04:30 - 05:00	Correlation Between Iceberg Draft and Above Water Deminsions	M. El-Tahan & H. L. Davis
05:00 - 05:30	Coffee	
05:30 - 06:00	Review of Deep Water Scours in the Davis Strait and Its Relevance to Present Day Activity	J. Guigne, D. Ross & H. Westergard
06:00 - 06:30	Use of Draft Distribution for Evaluating Iceberg Incursion Probability	J. Lewis & P. Benedict
06:30 - 07:00	Lake Erie Ice Scour Investigation	G. Comfort et al. (B. Graham)

WEDNESDAY, FEBRUARY 17, 1982

08:00 - 08:15	Introduction	R. Pilkington
GENERAL AND MEASUREMENT TECHNIQUES		
08:15 - 09:00	Ice Type/Scour Signatures	E. Reimnitz
09:00 - 10:00	Geological Processes During and After Scoring	V. Barrie
STATISTICS		
10:30 - 11:00	Canadian Beaufort Sea	B. Wright
11:00 - 11:30	U.S. Beaufort Sea	E. Reimnitz & P. Barnes
11:30 - 12:00	East Coast	C. F. M. Lewis
12:00 - 03:00	Lunch	
03:00 - 03:20	Shores	J. Harper
03:20 - 03:40	Lakes	J. Grass
03:40 - 04:00	Discussion	
PROPOSED DEVELOPMENT, DESIGN CRITERIA REQUIREMENTS, AND TIMING		
04:00 - 04:30	Canadian Beaufort Sea	B. Wright
04:30 - 05:00	East Coast	A. Allan
05:00 - 05:30	Coffee	
06:30 - 07:30	Instrumentation Developments and Techniques	S. Blasco
07:30 - 08:00	The Canadian Government Perspective on Ice Scour	T. Starr

THURSDAY, FEBRUARY 18, 1982

RISK ASSESSMENT

08:00 - 08:20	The Pipeline Burial Criteria Dilemma	E. Phifer
08:20 - 08:40	Cost Optimization Approach	R. Pilkington
08:40 - 09:00	Burial Vs. Protection	R. Marcellus
09:00 - 09:30	The Need to Backfill	R. Marcellus
09:30 - 10:00	Coffee	

MODELLING

10:00 - 10:30	Physical Modelling	R. Abdelnour
10:30 - 11:30	Physical Modelling	T. Chari
11:30 - 12:00	Trajectory Modelling	J. Lewis
12:00 - 03:00	Lunch	
03:00 - 03:30	Mathematical Modelling	R. Pilkington
03:30 - 04:00	Some Notes on Iceberg Grounding	P. Sabatini
04:00 - 04:30	Coffee	

ICE FEATURE METHODS

04:30 - 08:00	Flux Models	S. Hotzel
	Icebergs Beaufort Sea Ice	P. Wadhams
	Lineal to Areal Ridge Statistics	P. Wadhams
	Ice/Scour Statistics Method	R. Marcellus
	Ice Trajectories and Bathemetry	

SCORE ANALYSIS METHODS

	Repetitive Mosaicing	J. Shearer
	Deepest Score in Area	R. Pilkington
	Overscouring	V. Barrie
	Inter Relationship with Other Events	

THURSDAY, FEBRUARY 18, 1982 (Continued)

SCORE ANALYSIS METHODS (Continued)

Sedimentation Rate Method	M. Lewis
SSZ Method & Geological Processes	M. O'Connor
Scour Dating	R. Pilkington

FRIDAY, FEBRUARY 19, 1982

08:00 - 10:00	Risk Assessment and Design Criteria for Ice Scoring - A Panel Discussion (Panel to be Announced)	
10:00 - 10:30	Coffee	
10:30 - 11:30	Present and Future Research	
11:30 - 12:00	Closing Remarks	R. Pilkington

LIST OF PARTICIPANTS

APPENDIX "B"

A.I. Allan
Petro Canada Exploration Inc.
P.O. Box 2844
Calgary, Alberta
T2P 3E3

Vaughn Barrie
C-Core
Memorial University
St. John's, Newfoundland
A1B 3X5

Jacques Benoit
Mobil Oil
330 - 5th Avenue S.W.
Calgary, Alberta
T2P 2J7

Steve Blasco
Bedford Institute of Oceanography
P.O. Box 1006
Dartmouth, Nova Scotia
B2Y 4A2

Larry Brooks
Chevron Oilfield Research Co.
P.O. Box 446
LaHabra, California
USA, 90631

Tuppal Chari
Faculty of Engineering
Memorial University
St. John's, Newfoundland
A1B 3X5

Ian Cookson
McElhanney Surveying and Engineering Ltd.
#450, 999 - 8th Street S.W.
Calgary, Alberta
T2R 1J5

Dave Danyluk
McElhanney Surveying and Engineering
#450, 999 - 8th Street S.W.
Calgary, Alberta
T2R 1J5

Mona El-Tahn
McLaren Plansearch
P.O. Box 13250, Station "A"
St. John's, Newfoundland
A1B 4A5

Bob Frederking
National Research Council
Division of Building Research
Ottawa, Ontario
K1A 0R6

Muharrem Gajtani
Dome Petroleum Ltd.
P.O. Box 200
Calgary, Alberta
T2P 2H8

Bruce Graham
Arctec Canada Limited
#16, 6325 - 11th Street S.E.
Calgary, Alberta
T2H 2L6

Nicholas Grande
SNC

Jim Grass
Ontario Hydro
700 University Avenue
Toronto, Ontario
M5G 1X6

Jacques Guigne
Nordco
P.O. Box 8833
St. John's, Newfoundland
A1B 3T2

John Harper
Woodward-Clyde Consultants
16 Bastion Square
Victoria, B.C.
V8W 1H9

Stuart Hotzel
Petro Canada Exploration Inc.
P.O. Box 2844
Calgary, Alberta
T2P 3E3

Orrie Johnston
Ontario Hydro
700 University Avenue
Toronto, Ontario
M5G 1X6

Heiner Josenhans
Atlantic Geoscience Centre
Bedford Institute of Oceanography
P.O. Box 1006
Dartmouth, Nova Scotia
B2Y 4A2

Hans Kivisild
Lavalin
c/o Shawinigan Engineering
808 - 4th Avenue S.W.
Calgary, Alberta
T2P 3E8

John Lewis
Ice Engineering
P.O. Box 6082
St. John's, Newfoundland

Mike Lewis
Bedford Institute of Oceanography
P.O. Box 1006
Dartmouth, Nova Scotia
B2Y 4A2

Steven Lord
COGLA
355 River Road
Ottawa, Ontario
K1A 4L4

Chris Lynas
C-Core
Memorial University
St. John's, Newfoundland
A1B 3X5

Brian MacLean
Atlantic Geoscience Centre
Bedford Institute of Oceanography
P.O. Box 1006
Dartmouth, Nova Scotia
B2Y 4A2

Bob Marcellus
Canada Marine Engineering Ltd.
924 Cantabrian Drive S.W.
Calgary, Alberta
T2W 1L7

Patrick McLaren
Institute of Oceanographic Sciences
P.O. Box 6000
Sidney, B.C.
V8L 4B2

John Miller
Petro Canada Exploration Inc.
P.O. Box 2844
Calgary, Alberta
T2P 3E3

J.D. Mollard
Mollard & Associates
801 McCallum-Hill Building
Regina, Saskatchewan

Linda Nicks
Nordco
P.O. Box 8833
St. John's, Newfoundland
A1B 3T2

Mike O'Connor
O'Connor & Associates
#101, 4712 - 13th Street N.E.
Calgary, Alberta
T2E 6P1

Bernie Pelletier
Geological Survey of Canada
Ottawa, Ontario
K1A 0E8

Ed Phifer
Shell Development Company
P.O. Box 1380
Houston, Texas
USA, 77001

Roger Pilkington
Gulf Canada Resources Inc.
P.O. Box 130
Calgary, Alberta
T2P 2H7

Daniel Plasse
Geomarine Associates Ltd.
P.O. Box 41, Station "M"
Halifax, Nova Scotia
B3J 2L4

Rick Quinn
Geoterrex
9865 West Saanich Road
R.R.2
Sidney, B.C.
V8L 3S1

Allan Ruffman
Geomarine Associates Ltd.
P.O. Box 41, Station "M"
Halifax, Nova Scotia
B3J 2L4

Paul Sabatini
Petro Canada Exploration Inc.
P.O. Box 2844
Calgary, Alberta
T2P 3E3

Jim Shearer
26 Second Avenue
Ottawa, Ontario

Walt Spring
Mobil Research and Development
P.O. Box 900 (FRL)
Dallas, Texas
USA, 75221

Ted Starr
COGLA
355 River Road
Ottawa, Ontario
K1A 4L4

Martin Van Iperen
Panarctic Oils
P.O. Box 190
Calgary, Alberta
T2P 2H8

Paul Vandall Jr.
COGLA
355 River Road
Ottawa, Ontario
K1A 0E4

Howard Westergard
Canterra Energy Ltd.
P.O. Box 1051
Calgary, Alberta

Brian Wright
Gulf Canada Resources
P.O. Box 130
Calgary, Alberta
T2P 2H7